Development of Needle Trap Devices for Particle Entrapment

by

Shakiba Zeinali

A thesis

presented to the University of Waterloo

in fulfillment of the

thesis requirement for the degree of

Doctor of Philosophy

in

Chemistry

Waterloo, Ontario, Canada, 2022

Examining Committee Membership

The following served on the Examining Committee for this thesis. The decision of the Examining Committee is by majority vote.

External Examiner:	NAME: Prof. Torsten C. Schmidt Title: Chair of Instrumental Analytical Chemistry and Centre for Water and Environmental Research, Department of Chemistry, University of Duisburg-Essen
Supervisors:	NAME: Prof. Janusz Pawliszyn Title: Professor and Canada Research Chair Department of Chemistry, University of Waterloo
Internal Examiner:	NAME: Prof. Michael Chong Title: Professor, Department of Chemistry, University of Waterloo
Internal Examiner:	NAME: Prof. Scott Hopkins Title: Associate Professor, Department of Chemistry, University of Waterloo
Internal-external Examiner:	NAME: Prof. Carol Ptacek Title: Professor and University Research Chair in Earth & Environmental Sciences, Earth and Environmental Sciences, University of Waterloo

Author's Declaration

This thesis consists of material all of which I authored or co-authored: see Statement of Contributions included in the thesis. This is a true copy of the thesis, including any required final revisions, as accepted by examiners.

I understand that my thesis may be made electronically available to the public.

Statement of Contributions

I hereby declare that I am the sole author of this thesis. Chapter one contains sections that will be published as an article in TrAC, Trends in Analytical Chemistry. Most subchapters are included in the article entitled "*The evolution of needle-trap devices with focus on aerosol investigation"* by Shakiba Zeinali, Mehrdad Khalilzadeh and Janusz Pawliszyn, 153, 2022, 116643. The main parts have been written and revised by the author of this thesis, Mehrdad Khalilzadeh helped on conceptions and revisions.

Chapter 4 contains sections that was published as an article in Food Chemistry. All subchapters are included in the article entitled "*Free versus droplet-bound aroma compounds in sparkling beverages"* by Shakiba Zeinali, Martyna Natalia Wieczorek and Janusz Pawliszyn, *Food Chemistry,* 378, 2022, 131985–131991. In all cases, experimental planning and design, experimental work conducted in the laboratory, data analysis, interpretation, and writing were performed by the author of the thesis and the resulting manuscript was co-authored/supervised by J. Pawliszyn. Martyna Natalia Wieczorek provided scientific input and helped with writing and revision of the paper.

Chapter 5 contains sections that was published as three articles in Analytica Chimica Acta and Analytical and Bioanalytical Chemistry. Subchapter 5.2 is included in the article entitled "*Simultaneous determination of exhaled breath vapor and exhaled breath aerosol using filter-incorporated needle-trap devices: A comparison of gas-phase and droplet-bound components"* by Shakiba Zeinali, Chiranjit Ghosh and Janusz Pawliszyn, *Analytica Chimica Acta*, 1203, 2022, 339671-339682. Experimental planning and design, experimental work conducted in the laboratory, data analysis, interpretation, and writing were performed by the

author of the thesis and the resulting manuscript was co-authored/supervised by J. Pawliszyn and Chiranjit Ghosh provided scientific input and helped with writing and revision of the paper. Subchapter 5.3 is included in a communication article entitled "*On-site microextraction technologies for the comprehensive investigation of breath composition in lung cancer patients"* by Shakiba Zeinali, Mersedeh Pourkar, Khaleeq Khan, Devalben Patel, Janusz Pawliszyn, *Green Analytical Chemistry*, 2022. Experimental planning and design, experimental work conducted in the laboratory, data analysis, interpretation, and writing were performed by the author of the thesis and the resulting manuscript was co-authored/supervised by J. Pawliszyn. The access to patients was granted by Dr. Liu and UHN staff collaborated on consent from patients and provided access during sampling and extraction. Subchapter 5.4 is included in the article entitled "*Effect of household air pollutants on the composition of exhaled breath characterized by solid-phase microextraction and needle-trap devices components"* by Shakiba Zeinali and Janusz Pawliszyn, *Analytical and Bioanalytical Chemistry*, special issue" Promising Early-Career (Bio)Analytical Researchers", 2022, 1-11. In this case, experimental planning and design, experimental work conducted in the laboratory, data analysis, interpretation, and writing were performed by the author of the thesis and the resulting manuscript was co-authored/supervised by J. Pawliszyn.

Abstract

The importance of studying particle-bound components in aerosol samples has been highlighted during the COVID-19 pandemic, when people tried to stop the spread of droplet-bound viruses by wearing face masks. While the importance of these droplet/particle-bound analytes is well-known, their study has been hampered by the lack of a proper device for sampling and detection of these compounds. All these reasons explain the need for development of an extraction device that, not only traps droplet/particles from aerosol samples, but also preconcentrates free and gaseous analytes to enable comprehensive analysis of aerosol samples.

Among various microextraction methods, the needle-trap device (NTD) is the best candidate for entrapment and investigation of particle or droplet-bound compounds. The dynamic sampling and packed design can improve the role of NTD as a trapping device. Still, the filtration efficiency of NTD packed with commercial sorbent particles is limited due to the large diameter of packing material and can be improved by addition of an appropriate filter into the NTD. To this end, in this thesis, initially the filter with required criteria was developed and optimized. Then, the filter was packed inside the needle, in addition to the commercial sorbent particles to trap droplets/particles and extract gaseous compounds, respectively. The prepared NTD was then applied to study the aerosol sample including breath, air pollutants, sprays and sparkling beverages. To compare total and free (gas-phase) concentrations, the results from filter-incorporated NTD was compared to the results of solid-phase microextraction (SPME) methods.

After device development, free (from SPME results) versus total (from NTD results) concentration of fragrance compounds in different types of sprays was studied. In this study, the trend of concentration of fragrances over a time span after administration and the effect of air circulation with fan on air pollution was studied and reported. It was shown that the actual exposure concentration to fragrances during application of sprays can be much higher than gas-phase concentration. In another study, the concentration of aroma compounds in real consumer experience condition from sparkling beverages was studied and it was shown that the type and extent of carbonation and the physiochemical properties of aroma compounds plays influential roles on the distribution of these components between gas and droplet phase.

The next sections were dedicated to study of the most critical aerosol sample: breath samples and air pollutions. Based on the importance of these samples, various breath samples were studied from lung cancer patients or volunteers exposed to indoor air pollutants. The results showed that polar compounds have high tendencies to remain inside breath droplets, which mean during studying only gas-phase breath this type of information can be lost. For air pollution samples, it was revealed that less-volatile compounds such as large PAHs can be attached on the surface of smoke particles and carried to various locations by wind.

As the conclusion, it was shown that the developed NTD device is efficient and green for comprehensive study of aerosol samples. Among various potential applications, breath and air pollution provided the most critical and vital information, opening a new window to a novel type of information which was missing in previous studies in this area. The device is cheap and re-usable which highlights its environmental friendliness. While initial studies provided promising results, the application of NTD for aerosol samples is in its initial stages and there is a wide window of opportunities for future studies. The type and characteristics of

filter can be varied and other types of samples can be studied. In the field of breath analysis, the application of studying droplet-bound compounds for diagnostic and treatments can be an opportunity for non-invasive and fast sampling.

Acknowledgments

I would like to express my gratitude to my supervisor, Professor Janusz Pawliszyn, for providing me the opportunity to work in his research group. Thanks for his valuable ideas, support and encouragement. I would also like to thank my committee members, Dr. Chong, Dr. Hopkins, Dr. Schimdt and Dr. Ptacek for their insightful comments and ideas to improve this thesis.

I also acknowledge all my friends and lab members who helped me during the projects. I would like to thank my family members for their support that facilitate the whole process.

Dedication

I dedicate this thesis to

My caring husband,

My beloved parents and my dearest siblings

Table of Contents

List of Figures

List of Tables

List of Symbols

α	Solidity of the packing bed
Δp	hydrostatic pressure difference
A	Needle cross–sectional area
C_0	Initial concentration of analyte in sample
C_f	Concentration of analyte in fiber
C_s	Concentration of analyte in sample
D	apparent diffusion constant
D_0	Diffusion constant
D_m	diffusion constant of analytes into the sorbent bed
dP	Particle diameter
E	Filtration efficiency
K_{fs} or K_{es}	distribution coefficient of the analyte between the fiber (or extraction phase) and the sample matrix
K_p	permeability of sorbent packing
L	Sorbent bed length
n	amount of analyte extracted to the fiber
Ø	Porosity
P	penetration
Q	Volumetric flow rate
T	tortuosity of the sorbent bed
t_b	Breakthrough time
t_e	Equilibrium time

t_S	Sampling time
u	linear gas velocity
V_b	Breakthrough volume
V_f or V_e	Volume of fiber or extractive phase
V_s	Volume of sample
V_v	Void volume
ε	Single fiber collection efficiency
η	Viscosity of the sample
μ	viscosity
σ	root mean square dispersion of the front

List of Abbreviations

TWA	Time–weighted averaging
CAR	Carboxen
DI–SPME	Direct–immersion solid–phase microextraction
DVB	Divinyl benzene
GC	Gas chromatography
GC–MS	Gas chromatography–mass spectrometry
HS–SPME	Head–space solid–phase microextraction
LLE	Liquid–liquid extraction
NTD	Needle–trap devices
NTE	Needle–trap extraction
PDMS	Poly dimethylsiloxane
SMPS	Scanning Mobility Particle Sizer
SPE	Solid–phase extraction
SPME	Solid–phase microextraction
TWA	Time–weighted averaging
VOC	Volatile organic compounds

Introduction and Fundamentals

1.1 Preamble

This chapter contains sections that have already published as an article in Trends in Analytical Chemistry (TrAC). Most subchapters are included in the article entitled *the evolution of needle-trap devices with focus on aerosol investigation* by Shakiba Zeinali, Mehrdad Khalilzadeh and Janusz Pawliszyn, 153, 2022, 116643. The contents of the articles are herein being reprinted with permission of Elsevier, in compliance with both publisher's and the University of Waterloo policies.

1.2 Sampling and sample preparation

An analytical procedure comprised of different steps including sampling, sample preparation, quantitative/qualitative analysis, data acquisition and conclusion. Among these different steps, sampling and sample preparation are the most time consuming and critical steps for obtaining reliable data [1]. The main goals of sample preparation are representative sampling, isolation of target compounds from unclean samples and changing the concentration range and sample condition to make them suitable for instrumental analysis.

Despite the advances in separation and quantification methods, sample preparation and extraction methods are mostly traditional, costly, time–consuming and require large volumes of organic solvent. It is worth mentioning that due to an increase in people's awareness of environmental pollution, there is an interest for environmentally friendly, simple, fast and miniaturized sample preparation methods. All of these reasons lead us to the importance of an extraction method to tackle the above–mentioned limitations.

The advent of microextraction techniques revolutionized sample preparation methods by combining the clean-up, sampling and preconcentration steps into one miniaturized device. Solid and liquid phase microextraction techniques are sensitive, environmentally friendly, fast, reliable and portable for on-site analysis. In the following, some of the sample preparation methods applied in this thesis and their fundamentals are explained in more details.

1.3 Solid–phase microextraction (SPME)

Solid–phase microextraction (SPME) was introduced in 1989 by Pawliszyn and coworkers [2] to resolve some of the previously mentioned problems in conventional sample preparation methods. SPME is a solvent–free technique, combining sampling and sample preparation into one step. Additionally, SPME is fast and environmentally–friendly with the possibility to eliminate matrix interferences.

In SPME devices, a fused–silica fiber is coated with a known amount of extraction phase. The proper coating should have specific properties, such as thermal resistance, high extraction capacity, high surface area and chemical stability. There are hundreds of different reports on the development of various extraction phases for SPME [3–5], among them polydimethylsiloxane (PDMS), Carboxen (CAR) and divinylbenzene (DVB) are some of the most commonly used ones. As a result of the development of various fibers, the application of SPME method covers a wide range of samples from environmental [6,7] and food analysis [8–10], to pharmaceutical and medical analysis [11–13].

Different modes of extraction are possible with SPME-fiber, including direct immersion, head–space and membrane–protected SPME (Figure 1-1). In headspace mode (HS), coated fibers

are exposed to sample head–space for extraction of volatile compounds, while polar and non-volatiles are extracted in direct immersion (DI) modes, either directly from sample matrix or through a membrane protection. After exposure of extraction phase to sample, an equilibrium is established for the distribution of analytes between sample and extraction phase. In the next step, extracted analytes are desorbed and analyzed.

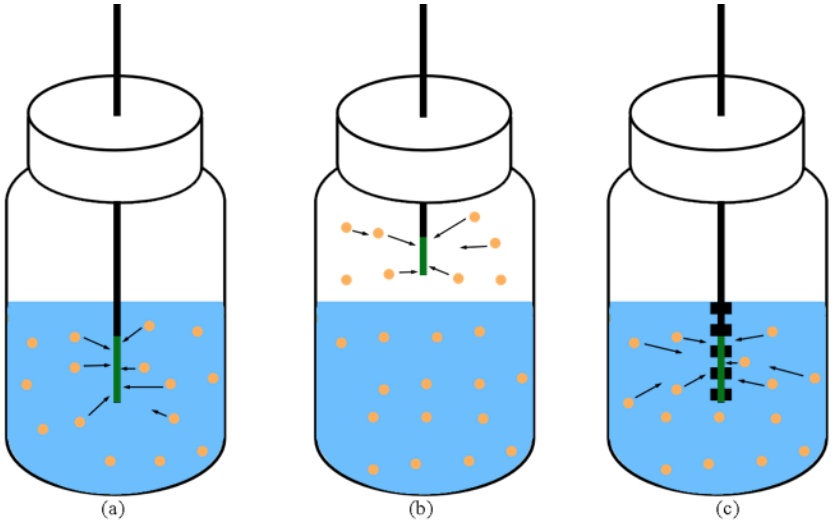

Figure 1-1. Modes of SPME for analysis of compounds from a liquid/solid matrix (a) direct immersion-SPME for non-volatile compounds (b) headspace-SPME for volatile compounds (c) Membrane–protected direct immersion-SPME for extraction from unclean samples [Constructed for this thesis by the author].

1.3.1 Fundamentals of SPME

For SPME, after establishment of equilibrium, we can use Eq. 1-1[14]:

$$K_{fs}=\frac{C_f}{C_s} \qquad \text{Eq. 1-1}$$

K_{fs} is the distribution coefficient of the analyte between the fiber and the sample matrix, C_f is the concentration in fiber (extracted) and C_s is the concentration of analyte in sample.

Considering that the combination of the mole of analyte remained in sample and fiber equals the initial mole of analyte ($C_0V_s=C_sV_s+C_fV_f$ where V_s is sample volume, V_f, is fiber volume and C_0 is the initial concentration) and defining n as the number of moles of analyte extracted ($n= C_fV_f$) we will have Eq. 1-2 [14]:

$$n=C_0 \frac{K_{fs}V_sV_f}{K_{fs}V_f+V_s} \qquad \text{Eq. 1-2}$$

In most cases, the volume of sample is much higher than fiber volume ($V_s>>K_{fs}V_f$), we can mark out $K_{fs}V_f$ in denominator, reaching to Eq. 1-3:

$$n=C_0K_{fs}V_f \qquad \text{Eq. 1-3}$$

Here it can be concluded that the amount of analyte extracted on the fiber (n) is linearly proportional to the initial concentration of analyte in the sample (C_0) [14]. This characteristic is the basis for calibration and quantification of analytes in sample matrix using SPME devices.

In addition, Eq. 1-3 is independent of sample volume, which facilitates the direct analysis of flowing blood and ambient air without requiring to know the exact volume of sample.

From equilibrium point of view, SPME is a non-exhaustive technique, as it only removes a small amount of analyte from the sample matrix, when compared to conventional extraction methods such as liquid-liquid extraction (LLE), solid phase extraction (SPE), and Soxhlet extraction that deplete the sample from analyte. As a result, SPME requires appropriate calibration and control of extraction conditions for accurate quantitative analysis [15]. Accordingly, SPME calibration methods have been developed based on the mass transfer of analytes in multiphase systems. In this regard, several methods such as diffusion-based calibration, kinetic calibration,

exhaustive extraction, and external calibration have been described [15]. The most commonly used calibration method is external calibration that can be used by establishing equilibrium of analytes between the sample matrix and the extraction phase. The fundamental of this method is based on preparation of different standard solutions of known concentration and providing a mathematical relationship between concentration and instrumental signal.

1.4 Thin–film microextraction (TFME)

Thin-film microextraction is similar to SPME from fundamental point of view. In TFME, a larger surface (mostly carbon mesh) is covered with a layer of extraction phase glued with a viscous polymer such as PDMS [16,17]. The extraction process is similar to SPME and depends on surface adsorption, although, the area available for extraction is much larger compared to fiber SPME. Higher extraction surface increases the extraction efficiency and improve sensitivity. After extraction, TFME can be desorbed thermally or by a solvent. Thermal desorption of TFME requires thermal desorption unit (TDU) of GC, which limits its widespread applications. The other advantage of TFME over SPME, is the flexibility of thin-films which decreases the chance of breakage, which is more often for SPME fibers.

1.5 Needle Trap Device (NTD)

1.5.1 Fundamentals and History

The advent of microextraction techniques revolutionized sample preparation by combining clean-up, sampling, and sample-preparation into a single step. Further adding to their appeal, microextraction methods are also sensitive, environmentally friendly, fast, portable, and rather inexpensive.

Of the various available microextraction techniques, needle-based methods are among the most intriguing. In needle-based methods, an extraction phase is immobilized/packed inside a needle, which is then applied for extraction and the subsequent desorption of analytes via direct injection into chromatographic instruments. This section focuses on needle-trap devices (NTD), which consist of a small tube or a needle that is packed with extraction phase for the active or passive extraction of volatile compounds. Theoretically, both gas and liquid samples can be drawn through the needle. However, the application of NTDs for liquid samples has been limited to only a few reports due to flow resistance [18,19]. With the majority of NTD-based studies focusing on gaseous samples (i.e., air) or headspace of liquid samples. While similar sorbent-packed tubing devices have been designed for the dynamic sampling of liquid and biological matrices (e.g., microextraction in packed syringe (MEPS) [20], these devices are beyond the scope of this thesis.

The various NTD designs can be coupled with benchtop or portable GC and automated. The main difference between NTDs and other microextraction techniques is that NTDs enable exhaustive extraction as long as the breakthrough volume (BTV) is not reached. This is significant, as it means that NTD extractions are less sensitive to kinetic and thermodynamic conditions and do not require the extraction conditions to be strictly controlled (i.e., temperature).

Given their exhaustive extraction capabilities, NTD should be compared to other conventional methods such as SPE. Significantly, unlike SPE, NTDs are solventless and fast, in addition to being more sensitive. A schematic showing the mechanism of operation and design of a filter-incorporated multi-bed NTD in dynamic mode for total extraction from an aerosol sample is provided in Figure 1-2.

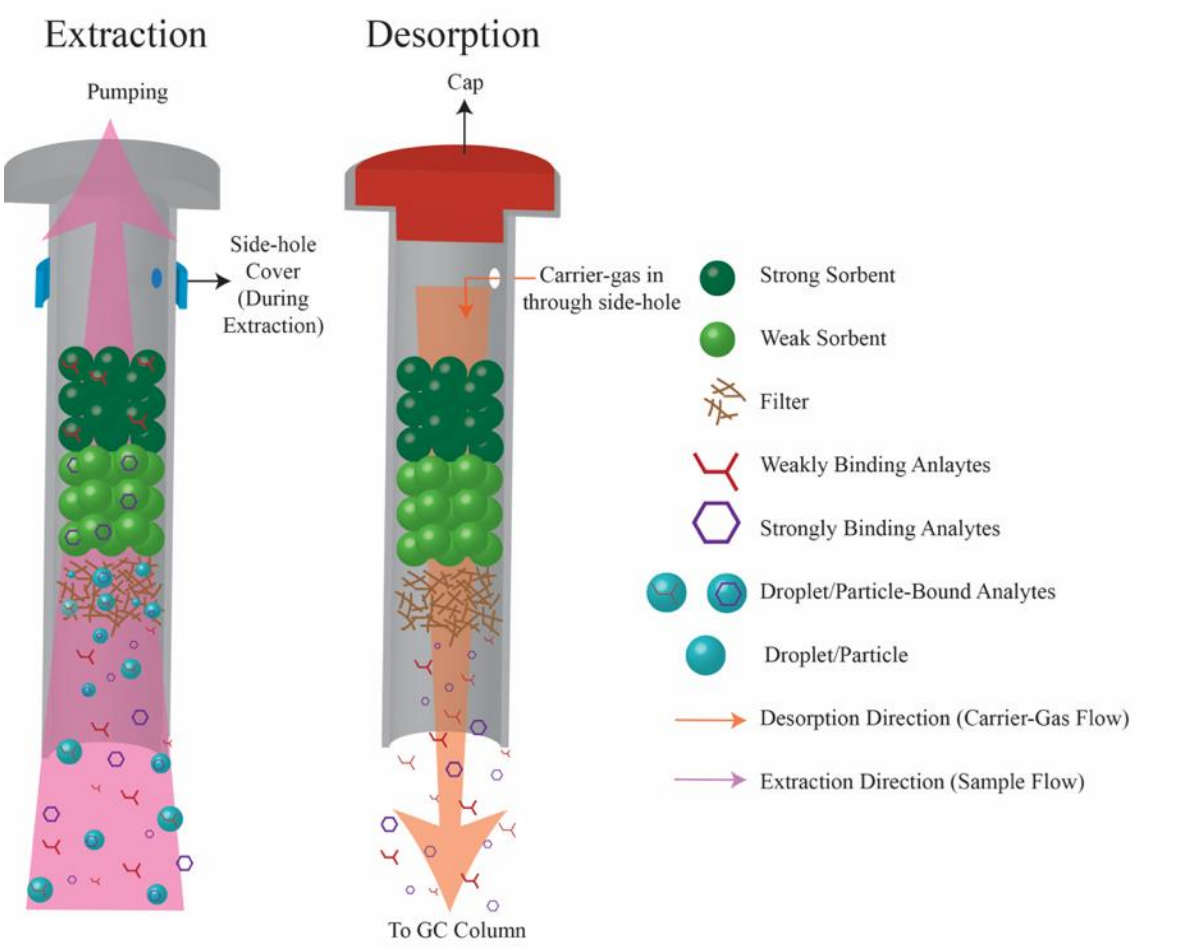

Figure 1-2. Schematic of a needle-trap extraction device for extraction/entrapment from aerosol samples during extraction and thermal desorption steps [with permission from [21]].

NTDs are also simpler to calibrate due to their exhaustive nature of the extraction. Furthermore, before the BTV is reached, the sample concentration (C_0) can be obtained using the extracted amount (n) and the sampled volume (V_S). Eq. 1-4 shows the relationship between the sample volume, the amounts of extracted analytes, and the concentration of analytes in a given sample [22]:

$$n = C_0 V_S \qquad \text{Eq. 1-4}$$

Simple calibration, exhaustive extraction, and a robust design make NTDs ideal for on-site sampling.

The earliest application of a device resembling an NTD dates back to 1978 in a study published by Raschdorf [23] who used a tube packed with Tenax to trap fragrant molecules. Later, in 1997, Qin et al. [24] packed a needle with charcoal and silica-gel for the extraction of VOCs such as methanol, ethanol, acetone, and pentane from human breath samples and ambient air. Although these devices can be cited as the progenitors of the NTD concept, they were difficult to use and could not be coupled with commercial analytical instruments, as their large dimensions, prevented them from being inserted into a standard GC injector.

To address these limitations, a 23-gauge needle for packing sorbents was introduced [22]. The new design was small enough to allow direct introduction into the GC inlet without the need for any modification or additional parts. This innovation was critical in extending the range of applications for NTDs, as the new design was both accessible and affordable for use in a laboratory setting. Currently, most NTD-based studies employ a modified version of this design.

Commercial versions of NTDs have been successfully developed by PAS Technology[1], Shinwa[2], PerkinElmer[3] and CTC analytics[4]. In the commercial NTD developed by Shinwa Chemical Industries, known as NeedlEx, the extractive media is packed inside the needle, which can be attached to the syringe for dynamic extraction. A tri-bed (Tenax TA, Carboxen 1016,

[1] https://www.pas-tec.com/en/analytic-technology/needle-trap
[2] https://shinwa-cpc.co.jp/en/products/needlex/
[3] https://www.perkinelmer.com/product/needle-trap-syringe-blunt-19-ga-pkg-1-ntsc19ntb200
[4] https://pdf.directindustry.com/pdf/ctc-analytics/itex-dynamic-headspace/65926-662936.html

Carboxen 1003) needle trap was also established by PerkinElmer for use with Torion T-9 portable GC-MS which can be applied for on-site sampling.

1.6 NTD Configurations

In the early designs [25], the sorbent was packed in a large cylindrical tube (Figure 1-3-a) or needle micro-concentrator (Figure 1-3-b). Unfortunately, the GC systems for these extraction devices required a modified inlet system. Although the next generation of NTDs was smaller, they still required an auxiliary carrier gas [25,26] for thermal desorption.

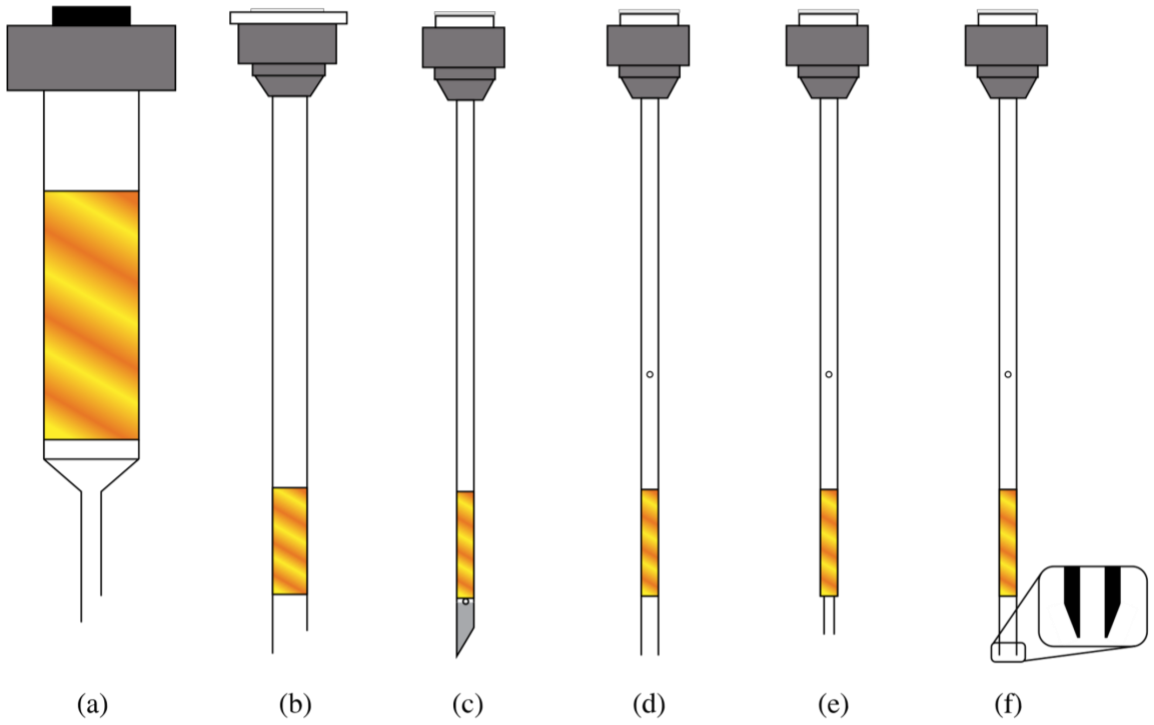

Figure 1-3. Various NTD configurations: (a) cylindrical micro-concentrator, (b) needle micro-concentrator with bevel tip (c) sealed-tip needle with side-hole (d) blunt-tip NTD with side-hole (e) extended-tip NTD with side-hole, and (f) cone-shaped tip NTD with side-hole [with permission from [21]].

In 2001, Koziel et al. [27] developed an NTD consisting of a small stainless-steel needle (23 gauge) packed with glass wool. Significantly, this NTD design was the first to be compatible with

benchtop GC and did not require further inlet modification and/or auxiliary carrier gas (similar to Figure 1-3-d but without the side-hole).

The next evolution in NTD design occurred in 2005, when Wang et al. [28] introduced a sealed-bevel tip with a hole in the side to facilitate packing and the convenient desorption of adsorbed analytes (Figure 1-3-c).

While blunt-tip needles without side holes can be used in NTDs, , the blunt-tip-with-side-hole design introduced by Warren [29] remains the most common NTD design, as it provides the best desorption efficiency (Figure 1-3-d). The reasons why a side hole is necessary in blunt-tip-based designs will be discussed in detail in the Desorption Mechanisms section. The latest developments introduced by researchers are extended-tip (Figure 1-3-e) [30] and cone-shaped (Figure 1-3-f) tip designs which can further improve desorption by blocking the gas flow through the narrow-neck liner.

1.7 Desorption Mechanisms

One of the main challenges associated with NTDs has always been the low efficiency and difficulty of the desorption procedure, which is largely related to the densely packed needles used in these devices. As such, most developments in NTD design have been oriented towards solving these desorption issues.

In almost all NTD designs, a cap is used to seal the needle hub to prevent the escape of compounds during desorption. In initial NTD configurations, compounds were mainly desorbed thermally wherein the needle-trap tube was simply heated to high temperatures. Using this method, Eom et al. [31] were able to achieve low carry over (around 1%) for the desorption of BTEX from

a DVB substrate. Subsequently, researchers have attempted to assist desorption by drawing a certain amount of an auxiliary gas (air, nitrogen, or helium) into a syringe and expelling it into the NTD while heating the needle in an injector (Figure 1-4-a)

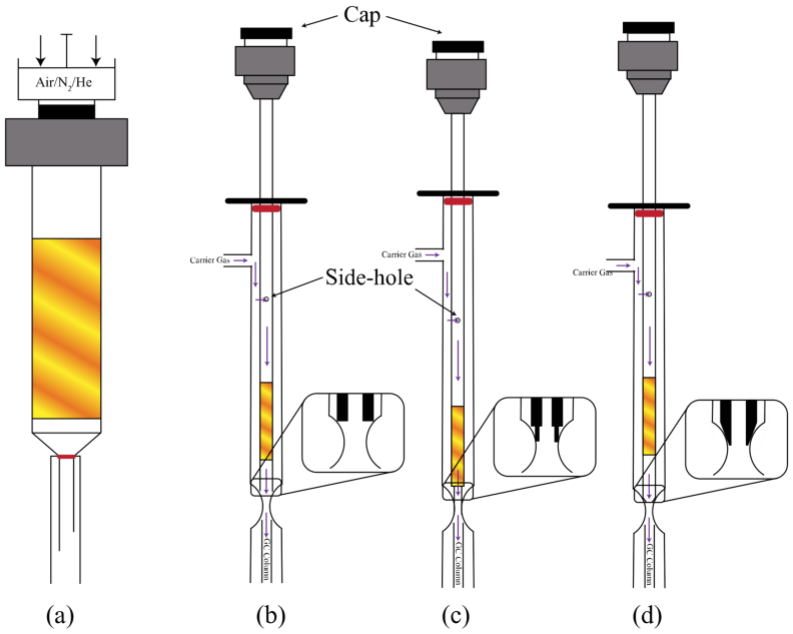

Figure 1-4. Schematic of (a) gas-assisted desorption for a micro-concentrator setup, (b) carrier-gas-assisted desorption setup for a blunt-tip NTD with a side hole, (c) improved desorption with a narrow-neck liner and extended tip, and (d) cone-shaped tip [with permission from [21]].

The auxiliary gas method has been applied to enhance the desorption of compounds from diesel exhaust [27] and breath [32–34] samples. Furthermore, the addition of a small amount of water for flash vaporization and improved desorption has also been investigated [35]. Nonetheless, the above-described desorption methods have some issues, including: carry-over; the need for other devices, such as syringes; and potential damage to analytes or instruments due to the addition of water and oxygen. In some rare examples, solvent desorption has also been applied for thermally sensitive compounds [36].

The most commonly used NTD protocols utilize the final design wherein a combination of a carrier-gas and high temperatures are applied to desorb the compounds [29]. In early designs, the carrier gas was passed through the sorbent tube via a diversion; however, after miniaturizing the needle size, the carrier gas was directed to the sorbent bed through a side hole (Figure 1-4-b). The use of a blunt-tip needle can create a seal that prevents the carrier gas from passing outside the needle, forcing it into the needle tube through the side hole. As a result, commercial GC systems can be used with needle-trap devices without any pre-requisites.

The latest desorption designs utilize either extended-tip (Figure 1-4-c) [30] or conical-tip needles (Figure 1-4-d). In both designs, the main goal is to guarantee the passage of the carrier gas to the sorbent bed by efficiently blocking the narrow-neck liner.

1.8 Packing procedures

Packing the extractive phase inside the needle in a reproducible manner is a challenge in preparing needle–trap devices. Generally, needles in NTD are a 22–gauge size needle with a nominal outer diameter of 0.71 mm and nominal inner diameter of 0.41 mm. With this small size, manual packing is very difficult and different methods are developed to facilitate the procedure. Sorbents can be packed from the side–hole (Figure 1-5) [28]. It is also possible to use a small droplet of glue to keep the extractive phase in its position. The problem here is the possibility of blocking the needle with glue, so a pump draw air during the drying time of glue to maintain porosity [37]. The other alternative method is to use a frit and o–ring inside the needle. To this end, Kubinec et al. [38] employed a stainless–steel tube and two stainless steel o–rings to retain extractive phases between each layer. For the most recent needle designs, namely extended–tips needles, a wire spring is prepared and pushed into the needle, which is positioned in the narrow–

neck part of the needle. This spring helps to keep the sorbents in place, another spring can also be added to the needle after packing is completed [29]. So, the sorbent is sandwiched between two springs. The packing of the NTD using glass wool has also been discussed previously [39].

During packing procedure, it is important to maintain an appropriate porosity of the bed for dynamic sampling. At the time of packing the sorbent, if the materials are pressed so tightly, it can block the needle, losing decent flow rate [28]. If materials are packed loosely, it may lead to channeling. In this case, an air path is made inside the packing material, as a result, the air sample prefers to pass from channeling, rather than packed bed with high pressure and the analytes can escape the sorbent bed.

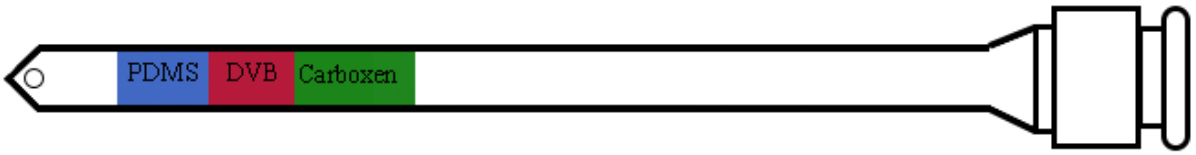

Figure 1-5. Schematic of a multiple bed packed NTD with PDMS, DVB and Carboxen particles. The packing has been performed from side hole [Reconstructed from [28]].

1.9 Criteria for a Suitable Packing for NTD: Extraction Phase and Filter

The NTD should be properly packed to meet important criteria, such as the reproducibility of the packing procedure and extraction results. In addition, the packing material should maintain proper porosity while also avoiding any flow channeling. Regardless of the packing procedure, an efficient packing material should have specific characteristics which will be detailed in the following sub-section.

1.9.1 Extraction/Desorption Behavior

The extraction and desorption behaviors of a packing material are the most important factors to consider when selecting a sorbent for an NTD. Both reproducible behavior and suitable extraction efficiency are vital for accurate and sensitive determinations. The efficiency of the extraction phase depends on the extraction medium's affinity toward the targeted analytes. While high affinity is desired for higher extraction efficiency and better sensitivity, it is also important to consider the need for efficient desorption; if the extraction medium has too high an affinity toward the target analytes, it will not be possible to further analyze the compounds adsorbed onto the surface of the extraction phase via desorption [39]. Therefore, the extraction phase's affinity for the analytes should be kept within an acceptable range.

The affinity between the analytes and the sorbent mainly depends on their respective polarities. As a rule, polar sorbents are better at extracting polar analytes, while non-polar sorbents are more effective for extracting non-polar analytes. Early applications of NTDs mainly utilized conventional sorbents, such as DVB, silica particles, and Carboxen. However, later applications aimed at extracting more polar analytes led to the introduction of more polar sorbents such as poly methylmethacrylate and ethyleneglycoldimethacrylate [40].

For on-site analysis or non-targeted purposes, where the nature of the analytes is not fully understood, it is possible to pack the needle with different sorbents with a wide range of polarities [28]. In such instances, weaker sorbents are packed closer to the tip, which helps prevent "strongly binding analytes" from irreversibly adsorbing onto the stronger sorbents (Figure 1-5). If the compounds are known and selectivity is required, molecularly imprinted polymers (MIP) can be used [41].

NTDs can be packed with a filter in addition to the extraction phase for applications aimed at studying the total concentrations of analytes in aerosol samples. In such cases, it is optimal to utilize a filter that is inert toward analytes. The use of a non-inert filter can increase the standard deviation of extraction, as the filter surface can be occupied by particles or droplets during aerosol sampling, which can cause variations in extraction efficiency.

1.9.2 Packing Material Size

Another important feature of the extraction phase is the packing material size. While decreasing the sorbent particle size can improve extraction efficiency by increasing the surface area, it also increases the pressure drop and decreases the flow rate, which negatively impacts extraction efficiency. Therefore, in optimizing the particle size, it is important to find a balance between the accessible surface area and the pressure drop. Furthermore, pore size and the porosity of the sorbent particles also dramatically influence the extraction capacity of an NTD.

Previous studies have shown that an NTD packed only with sorbent particles can also be used to trap particles in aerosol samples. These findings indicate that the use of a packing material with a smaller diameter will improve trapping efficiency, but limit the flow rate [22]. In addition, findings have shown that, while the trapping efficiency of sorbent-packed NTDs is limited, it can be improved significantly by adding a filter.

In fiber-based filters, the fiber diameter is one of the most significant determinants of the quality factor, and it is also one of the easiest parameters to adjust. Furthermore, it is also important to consider how the fiber diameter influences the pressure drop and filtration efficiency. Figure 1-6 shows the relationship between the fiber diameter, pressure drop, filtration efficiency, and quality

factor. As the data suggest, a smaller fiber diameter results in better filtration efficiency, but it also increases the pressure drop. Therefore, it is important to find the optimum fiber diameter, as doing so will ensure the maximum filter quality factor is achieved.

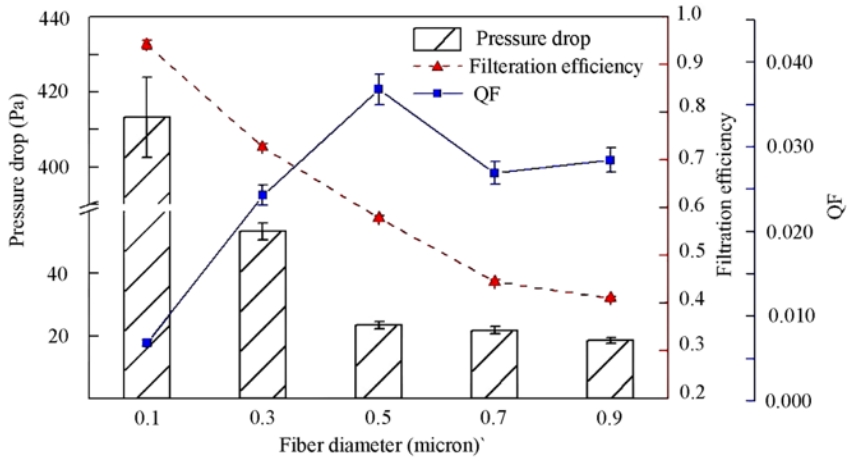

Figure 1-6. Effect of fiber diameter on pressure drop, filtration efficiency and quality factor for air filters.

Similarly, the packing length can also influence the extraction/filtration efficiency and pressure drop. For instance, while longer beds can improve the extraction/filtration efficiency, they also increase the pressure drop. Therefore, the packing length should also be optimized to ensure maximum efficiency.

1.9.3 Other Factors

In addition to extraction/desorption behavior and packing material size, there are other vital criteria to consider when selecting a suitable packing material for an NTD. For instance, the packing material (sorbent and/or filter) should be mechanically and thermally robust to ensure that it is re-usable for multiple extraction cycles and suitable for thermal desorption. Both the sorbent and filter should also be inert towards the sample matrix and analytes, and an inexpensive packing material should be selected to keep experimental costs down.

In general, the final NTD design should provide: exhaustive extraction, negligible breakthrough, reproducible results, and efficient desorption.

1.10 Modes of Sampling

In general, there are two main sampling methods for NTD: active and passive sampling. While active sampling requires the passage of sample through the extraction phase, passive sampling mode is based on the diffusion mechanism.

In passive sampling, the NTD is exposed to the sample for a defined time that is long enough to allow the analytes to diffuse into the needle to reach the extraction phase. This method is also known as the time-weighted average (TWA) method (Figure 1-7-a).

In the active analysis of volatile compounds in the headspace of a liquid sample, the drawing of the sample's headspace can be performed with or without purging. Purging an inert gas into the sample can increase and accelerate the release of analytes into the headspace. In addition, simultaneous purging and drawing can prevent any pressure drop inside the sampling vessel (Figure 1-7-b). The effect of sequential and continuous purging on NTD extractions has been studied in a prior work, with findings showing that sequential purging enhances the headspace extraction efficiency [42].

In the cases where purging is not applied (Figure 1-7-c,d), it is critical to maintain the pressure inside the sample, as drops in pressure inside the sampling vessel can disturb the extraction process. This can be achieved by decreasing the sample volume and maintaining a very small ratio of drawn gas to total sample gas volume. Since decreasing the sampling volume can

result in poor sensitivity, it is suggested to use purging or increase the drawn volume in the case of large samples (i.e., air samples) whenever possible.

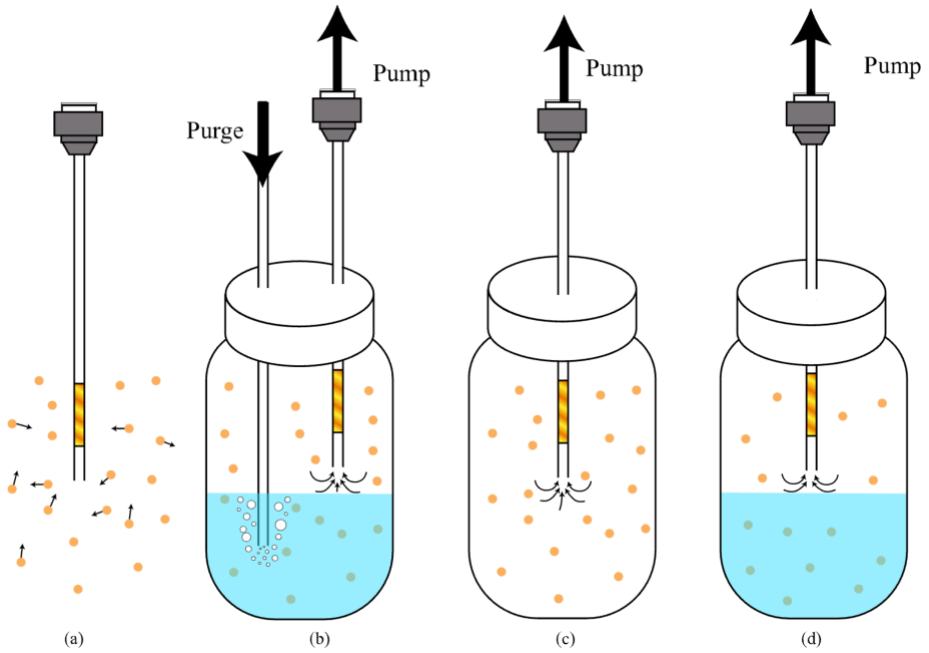

Figure 1-7. Different modes of NTD sampling (a) passive sampling, (b) active sampling with purging (c) active gas extraction, (d) active head-space extraction [with permission from [21]].

1.10.1 Active sampling

As mentioned earlier, in active method, sample is introduced continuously to the sorbent bed, which make this method similar to frontal chromatography. In frontal chromatography, the capacity that determine the maximum injectable sample is an important factor. This column capacity in frontal chromatography is the same as breakthrough volume in NTD. The capacity is affected by several parameters including temperature, humidity, flow rate and packing properties. Frontal chromatography fundamentals can be attributed to the NTD. In an effort to relate column capacity to chromatography parameters by Lovkvist [43] theoretical plate number (N) is defined as Eq. 1-5:

$$N=\frac{uL}{2D} \qquad \text{Eq. 1-5}$$

L is the column length (or sorbent packing length of NTD), D is the apparent diffusion constant and u is the linear gas velocity [43]. D is defined as in Eq. 1-6:

$$D=\frac{1}{T^2}D_0+Td_pu \qquad \text{Eq. 1-6}$$

Here T is tortuosity of the sorbent bed, D_0 is the diffusion constant (including all mechanism of dispersion), d_p is the particle diameter. u can be defined with Eq. 1-7:

$$u=\frac{Q}{A\varphi} \qquad \text{Eq. 1-7}$$

This equation is based on ignoring compressibility of gas and constant flow rate, Q is the volume flow rate, A is cross–sectional area (for needle) and φ is the porosity. Q is related to other factors using Eq. 1-8:

$$Q=\frac{K_pA\Delta p}{\mu L} \qquad \text{Eq. 1-8}$$

Δp is the hydrostatic pressure difference along the packing sorbent bed. μ is the viscosity and K_p is the permeability of sorbent packing [43]. K_p is defined as Eq. 1-9:

$$K_p=\frac{\overline{d_{p2}^2}\emptyset^{5.5}}{5.6K} \qquad \text{Eq. 1-9}$$

d_{p2} is surface average sphere (particle diameter, d_p) and K=1 for spherical particles. According to Eq. 1-8, sampling volumetric flow rate (Q) is dependent on particle size and packing

density (assuming constant pressure drop which is the case when pump is used for sampling). Required time for a complete sampling (t_s) can be calculated by Eq. 1-10 [22]:

$$t_s = \frac{Q_0}{Q} \qquad \text{Eq. 1-10}$$

Where Q_0 is sample volume and Q is the volumetric flow rate.

Considering frontal chromatography principles, concentration of analyte along x-axis with time can be calculated by Eq. 1-11:

$$C_{(x,t)} = \frac{1}{2} C_s \left(1\text{-}\mathrm{erf}\frac{x-\frac{ut}{L(1+k)}}{\sigma L\sqrt{2}}\right) - \frac{1}{2} C_s \times \exp(2n) \times \left(1\text{-}\mathrm{erf}\frac{x-\frac{ut}{L(1+k)}+2}{\sigma L\sqrt{2}}\right) \qquad \text{Eq. 1-11}$$

Here, k is the retention factor. This equation is more suited to small number of theoretical plates values, which is the case for needle–trap systems. k is defined as:

$$k = K_{fs} \frac{V_e}{V_v} \qquad \text{Eq. 1-12}$$

K_{es} is the partition coefficient between sample and extraction phase (fiber) for analyte, V_e is defined as the volume of the extractive phase, and V_v is the void volume (needle volume without sorbent) [22].

1.10.2 Passive sampling

For passive sampling, a sorbent is packed inside the needle with a definite, known distance from the needle tip. Exposure of this packed needle to gas sample leads to time–weighted average (TWA) sampling (Figure 1-8).

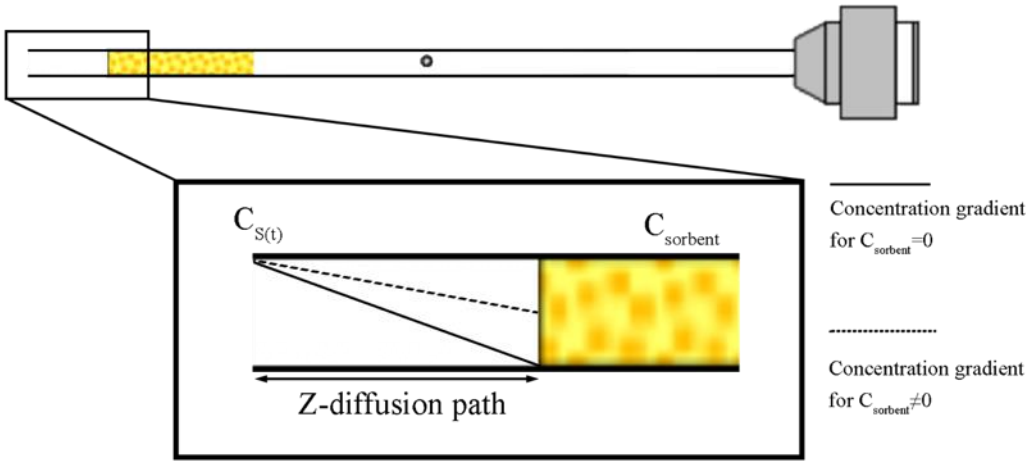

Figure 1-8.Concentration gradient of an analyte produced between the opening of the needle and the position of the sorbent Z. Z: diffusion path; $C_{sorbent}$: concentration near the sorbent interface; $C_{S(t)}$: concentration of the analyte at the needle opening as a function of time [Reconstructed from [22]].

In TWA the only driving force of extraction is the diffusion of analytes into the sorbent bed. In this case, as long as the volume is less than BTV, the sorbent bed acts as a complete sink for the analyte; all analytes stick to the extractive phase, without any analyte escaping the bed. During this process, there is a linear concentration profile between needle entrance point and position of sorbent. Considering Fick's law, we can calculate the amount of extracted analyte (dn) using Eq. 1-13 [22]:

$$dn=AD_m\frac{dc}{dz}dt=AD_m\frac{\Delta C(t)}{Z}dt \qquad \text{Eq. 1-13}$$

Here, D_m is the diffusion coefficient, and Z is the distance between the needle opening and sorbent. In this equation, $\frac{\Delta C(t)}{Z}$ is the concentration gradient between needle opening and position of the sorbent, $\Delta C(t)=C(t)-C_z$ and C(t) is the time-dependent concentration of analyte (at needle opening) and C_z is the concentration of analyte near sorbent bed. For high affinity of sorbent toward

analyte and/or low concentration of analytes, where extractive phase acts as "zero sink", C_z equals or nears zero [22]. The amount of analyte integrated over time is calculated as Eq. 2-1:

$$n=D_m \frac{A}{Z} \int C_s(t)dx \qquad \text{Eq. 1-14}$$

This equation works only for zero sink condition. According to this equation, n or the amount of the extracted analyte is proportional to the diffusion constant of analytes into the sorbent bed (D_m), area of the needle opening (A), integral of the sample concentration over time and inversely proportional to the distance between needle opening and sorbent bed (Z). As long as TWA meets the desired conditions namely zero sink, fast response and continuous exposure of needle to the sample, calibration can be applied like normal methods. For calibration, the total extracted amount is measured and sample concentration is determined using previously determined response factor.

1.11 Breakthrough volume

Breakthrough volume (BTV) is a critical factor affecting the efficacy of NTDs, as NTDs can provide exhaustive sampling as long as the BTV is not reached. Breakthrough volume has been variously defined as "the sample volume which can be loaded on the sorbent bed without the loss of the analytes." or the volume at which "a defined amount exiting the sampling device is typically some fraction (e.g., 1%, 5%, 10%, etc.) of the input amount" [44].

Despite the differences in definitions, it remains the case that the sorbent bed becomes saturated or equilibrated once the breakthrough volume has been surpassed, precluding the further extraction of analytes. In order to obtain a linear relationship between the amount of extracted analytes and the concentration of analytes in the sample, it is important to ensure that the BTV is not reached during the working concentration. The BTV of the sorbent bed is affected by a number

of parameters, including the sorbent bed's characteristics (packing length, density, size), the sorbent/analyte's properties (extraction affinity for specific analytes), and the concentration and sample flow rate of analytes. It is possible to increase the BTV by increasing the packing length, packing density (i.e., decreasing the packing size), the sorbent's affinity for the target analytes, and the surface area. Furthermore, the BTV can also be increased by decreasing the sample concentration and sampling flow rate.

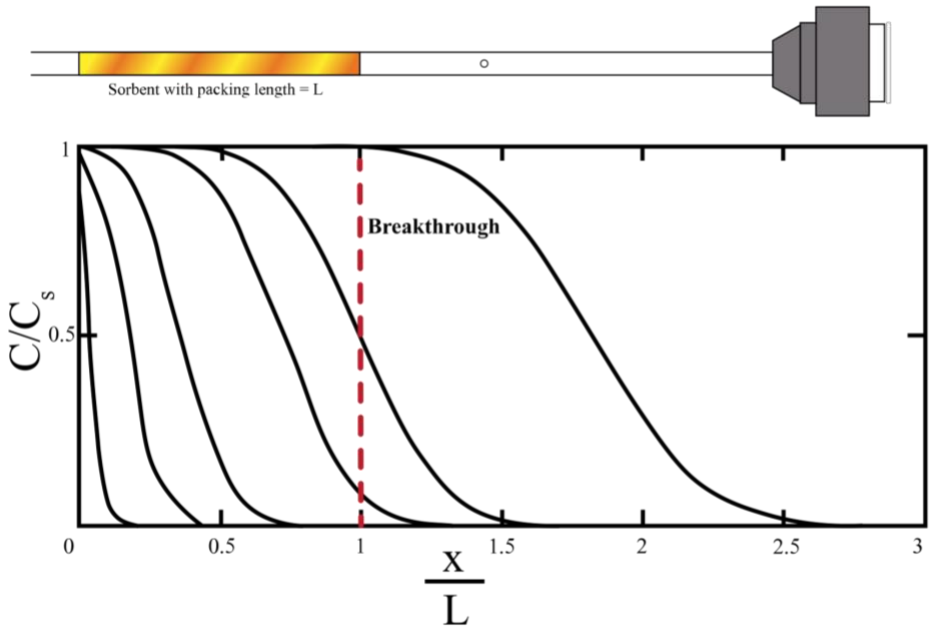

Figure 1-9. Schematic of a packed needle with sorbent length (L) and theoretical concentration profiles in the sorbent bed with sample concentration Cs and x is the relative position along L [with permission from [21]].

Figure 1-9 shows normalized concentration profile in extraction bed according to Eq. 1-11. In right curve, complete breakthrough volume occurs. Equilibration time or the time required to pass this volume of sample is called t_e. This time can be considered the time needed for the center of the front to reach the end of the sorbent.

$$t_e = \frac{L(1+k)}{u} \qquad \text{Eq. 1-15}$$

Before reaching breakthrough volume, extractive phase can extract all analytes being passed through the bed (perfect sink). In this case, analyte loaded into the bed can be described with Eq. 1-16 (when x=0 in Eq. 1-11):

$$n(t) = Au\varphi \int_0^t C(0,t)dt = A\varphi u C_s t = C_s V_s \qquad \text{Eq. 1-16}$$

The breakthrough volume can be defined as the percentage of mass exiting the sorbent bed in comparison to the initial mass entering the sorbent bed with Eq. 1-17:

$$b = \frac{Au\varphi \int_o^t C_{(L,t)}dt}{Au\emptyset C_s t} = \frac{\int_0^t C_{(L,t)}dt}{C_s t} \qquad \text{Eq. 1-17}$$

The approximate solution of this integral can be found in a work by Lovkvist [43], resulting in breakthrough volume after derivation in Eq. 1-18:

$$t_b = \frac{L(1+k)}{u}\left[(1-b)^2 + \frac{a_1}{N} + \frac{a_2}{N^2}\right]^{-1/2} \qquad \text{Eq. 1-18}$$

Where t_b is breakthrough volume time and a_1 and a_2 are a complex function of b and can be found in the previous work by Lovkvist [43].

According to the definition mentioned earlier, breakthrough volume can be defined as the volume of sample in which the extracted analyte is 5% (or more) less than expected (according to the previous data), which occurs when b≥5%. In the case when b=5, we can have a_1=5.360 and a_2=4.603 [45]. With these numbers we can rewrite Eq. 1-18 to Eq. 1-19:

$$t_b = \frac{L(1+k)}{u}\left[0.903 + \frac{5.360}{N} + \frac{4.603}{N^2}\right]^{-1/2} \qquad \text{Eq. 1-19}$$

This breakthrough time can be converted into breakthrough volume:

$$BTV = A\varphi L(1+k)\left[0.903 + \frac{5.360}{N} + \frac{4.603}{N^2}\right]^{-1/2} \qquad \text{Eq. 1-20}$$

Comparing Eq. 1-19 and Eq. 1-15 reveals that for high plate numbers ($n>10$), t_b and t_e are very close to each other. So, Eq. 1-15 can be used to calculate breakthrough time as an approximation [45].

From calculation, it is possible to find a guidance on how to prepare NTD. For higher sampling rate (low analysis time), linear sampling rate should be high, at the same time, for higher capacity, the linear flow rate should not exceed a certain value. Consequently, linear flow rate and porosity needs to be kept in a certain range.

1.11.1 Breakthrough volume measurements

As explained in the previous section, breakthrough volume is defined as the volume at which the extraction phase becomes saturated/equilibrated. It can be assumed that, based on the exhaustive nature of NTD extraction, all analytes will be quantitatively trapped prior to the BTV; however, after this volume, the analytes begin to escape the extraction phase. In this region, the linear relationship between the concentration and amounts of analytes extracted is lost. These characteristics can be used to find the BTV:

i. The breakthrough volume can be calculated using Eq. 1-20. if the theoretical plate number of the NTD and other parameters are known. This equation requires equilibrium

conditions without the saturation of the adsorbent, which means it is suitable for the study of low concentrations of analytes [45].

ii. The other method of finding the BTV entails monitoring the amounts of extracted analytes (or the extraction signal) compared to the sampling volume. As the schematic chart in Figure 1-10 shows, the amount of extracted analytes increases linearly as the sampling volume increases, with a plateau occurring after the BTV is reached. Thus, the BTV can be determined by calculating the volume at which the signal (from the experiment) is 5% lower than the value predicted by the linear equation (this percentage varies depending on the definition of BTV). For simplicity, the plateau volume is roughly estimated as BTV.

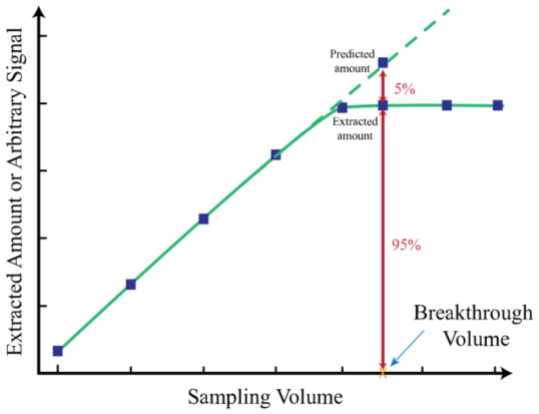

Figure 1-10. Schematic chart showing expected extracted amount/extraction signal vs. sampling volume for finding BTV. Plateau happens when BTV has been reached. [with permission from [21]].

iii. The other method of measuring BTV is to connect two needles in series, and then to draw the sample through both needles (the sample initially passes through first needle and then goes to the second one, as shown in Figure 1-11). Prior to reaching the BTV, all analytes will be trapped in the first needle; as such no peaks for any of the analytes

will be observed during the desorption of the secondary needle. Once the BTV is reached, the analytes begin escaping from the first needle and are captured by the second needle. Thus, the BTV of the first needle can be defined as the sampling volume at which peaks for the targeted analytes begin to appear in the chromatograms for the second needle after desorption.

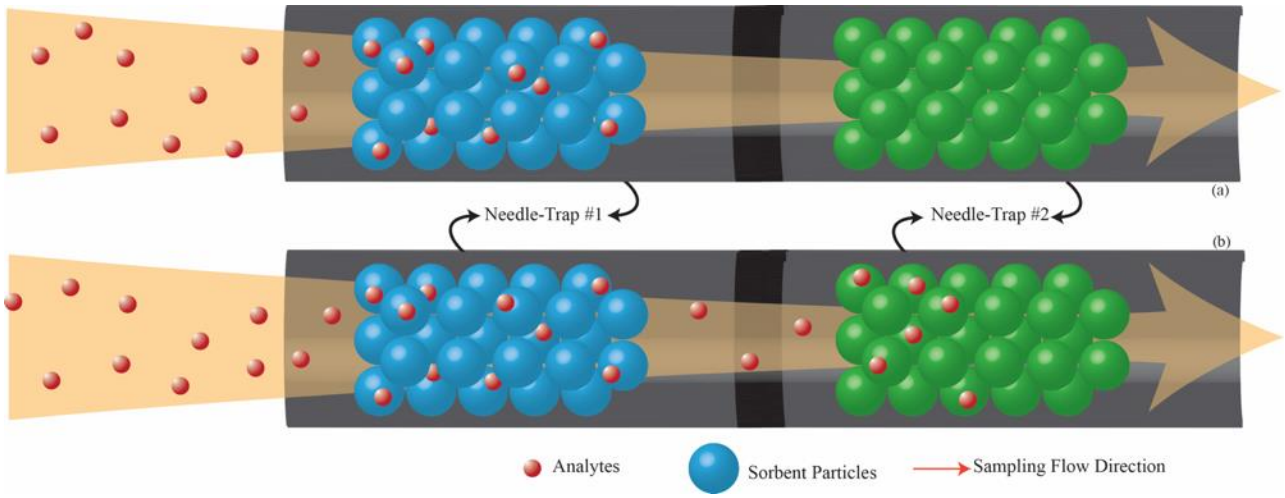

Figure 1-11. Two needles arranged in series to identify the BTV of first needle by monitoring chromatogram peaks during the desorption of the second needle-trap device: (a) before reaching the BTV and needle-trap #1 act as exhaustive sampler and (b) after reaching the BTV when analytes start escaping from needle-trap #1 and extracted by needle-trap #2 [with permission from [21]].

1.12 Total vs. free concentration

The first application of needle-packed devices was for the analysis of volatile organic compounds (VOCs) [23,46]. For a long time, the use of NTDs was limited to the analysis of compounds in the gas phase; however, subsequent research has demonstrated that the packed design of NTDs and dynamic sampling make them suitable for sampling particles and droplets from aerosol samples [27,47].

Aerosols are suspensions of solid particles or liquid droplets in a gas medium. Aerosol particles/droplets are capable of carrying other species such as pollutants, biomarkers, or

microorganisms (e.g., coronavirus, E. coli, etc.). For example, the airborne transmission of respiratory diseases generally occurs via small droplets, which can remain suspended in the air for a long time. These features of aerosols underscore the importance of developing effective methods of analyzing them.

While particle-bound analytes play an important role in aerosol studies, most investigations of aerosol samples are limited to measuring the number, size, and distribution of particles/droplets. Commonly, comprehensive studies of aerosol samples required the use of multiple sample-preparation techniques and instruments, as it was necessary to analyze the gas phase and droplets/particles separately. Thus, such studies were more time consuming and expensive to conduct.

Among the different available microextraction techniques, NTDs are the best candidates for analyzing aerosol samples. The main limiting factor in capturing particles is the low mobility of particles/droplets, which is increased by the dynamic sampling afforded by NTDs. Additionally, the NTD's packed design can act as a filter to trap droplets/particles. During the desorption step, these particle-bound components can be desorbed and studied along with free compounds. By enabling the capture of particles/droplets, the NTD makes it possible to study the gaseous and particle-bound compounds in a sample simultaneously.

Koziel et al. [27] used a glass-wool-packed NTD and SPME to extract PAHs from diesel exhaust. In addition, they also used their NTD to measure the triamcinolone acetonide content in a dose of an aerosolized asthma drug and DEET in an application of insect repellent spray. Their findings confirmed that the designed NTD could be successfully applied to trap droplet/particles in the study of aerosol air samples.

In 2009, Niri et al. [47] used an NTD and SPME to determine the concentrations of allethrin in mosquito coil smoke and in a microwave allethrin generator. In the microwave assisted allethrin generator, which is capable of producing gaseous compounds, the allethrin concentrations determined via NTD and SPME were similar. However, in the case of the mosquito coil smoke, the allethrin concentration measured with the NTD was significantly higher than the concentration detected via SPME. These results confirmed that NTDs are capable of measuring the total concentration of analytes in a sample, even when some of those analytes are bound to particles.

In another study, Grandy et al. [48] applied NTD and SPME to determine formaldehyde content in car exhaust at different temperatures. At low temperatures, the concentrations detected by the NTD (total concentration) and SPME (gaseous concentration) were meaningfully different, indicating that a large proportion of the formaldehyde was bound to particles in the car exhaust. Conversely, the results obtained by these two methods were very similar at higher exhaust temperatures. Thus, it can be concluded that, at high temperatures, particle-bound formaldehyde molecules are mostly desorbed and present in a free state.

While the NTD inherently acts as a filter that traps particles/droplets, its trapping efficiency is limited when it is packed with large commercial sorbent particles (diameter ~ 200 microns). Additionally, the use of large-diameter packing materials increases the probability of channeling and the escape of small sample droplets/particles from the packed bed. However, it is possible to improve filtration efficiency by adding a filter to the NTD packing bed. In preparing a filter for an NTD, it is important to fully understand the filtration mechanism and the criteria of a suitable filter.

1.13 Filters: Types, Mechanisms and Quality Evaluation

Typically, air filters are designed using either fibers or monolithic porous membranes (Figure 1-12). In monolithic membranes, pore size and permeability are the limiting factors with regards to filtration efficiency. While the use of porous membranes in NTDs has been studied previously [49], the findings indicated that these membranes are hampered by high flow resistance and potential channeling due to their physical properties. As such, we will focus on the use of fibrous structures for trapping particles.

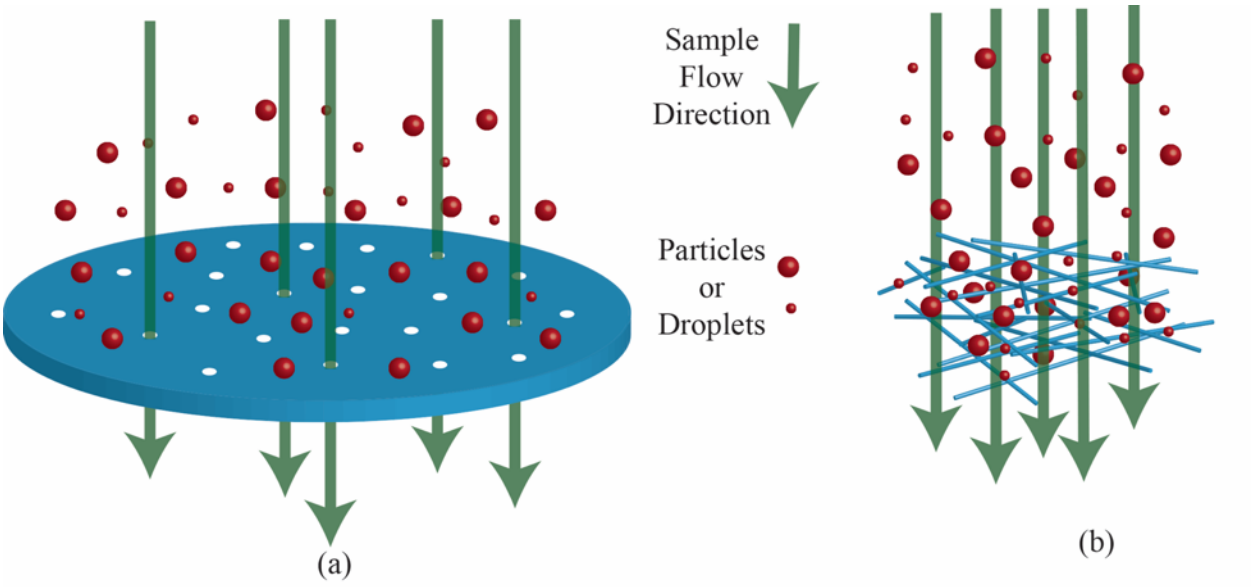

Figure 1-12. Types of air filter: (a) porous membrane and (b) fiber-based [with permission from [21]].

There are three main trapping mechanisms in fiber-based filters: inertial impaction, interception, and diffusion. Inertial impaction occurs when larger particles are unable to maintain airflow direction change, causing them to become deposited on the fibers. This mechanism is related to the ratio of particles to the fiber diameter. Interception takes place when the air pathway

and fibers are close enough that the fiber is able to retain particles via Van der Waals forces. A single fiber's efficiency for interception is proportional to the ratio of particles to the fiber's diameter. Inertial impaction and interception become more prominent as particle size increases [50]. Diffusion results from the Brownian motion of particles, which increases their likelihood of coming into contact with a fiber while traveling past it on a non-intercepting streamline. This mechanism is highly dependent on the linear flow rate and diffusion coefficient of the particles. Furthermore, unlike inertial impaction and interception, diffusion becomes less prevalent as the particle size increases. These filtration mechanisms are illustrated in Figure 1-13. It is worth mentioning that all of these mechanisms are also related to the fiber diameter, packing density, and packing length.

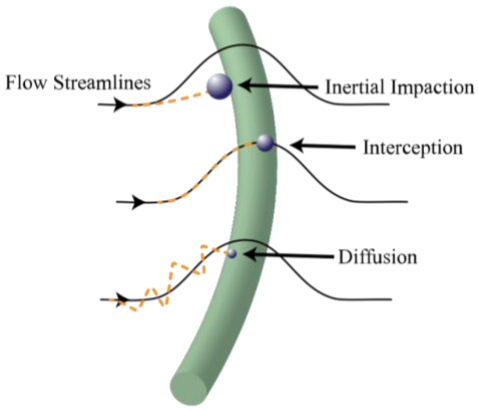

Figure 1-13. Mechanisms of particle filtration [with permission from [21]].

Gravitational settling is another trapping mechanism, but is negligible for the small particles considered in this study. As shown in Figure 1-14 inertial impaction and interception are the dominant mechanisms for larger particles, while diffusion is the main mechanism for smaller particles. Minimum efficiency or breakthrough happens for particles with diameters between 50-

300 nm. In this range, particles are too large for diffusion to be effective and too small for interception and inertial impaction to function adequately (Figure 1-14).

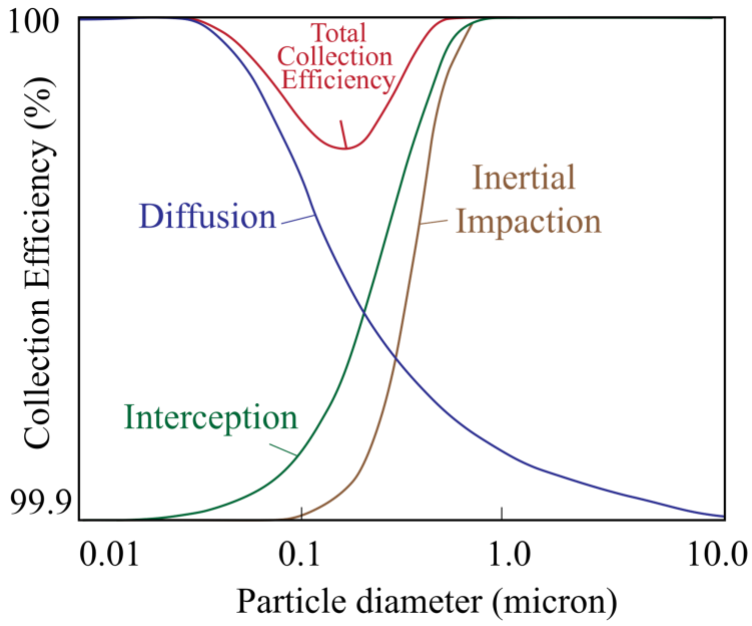

Figure 1-14. (a) Collection efficiency of filter versus particle diameter of HEPA filter [reconstructed from [51]] .

Different filter properties, including the filter structure (fiber size, porosity, permeability, etc.), particle properties (particle size, particle interaction with fiber, etc.), and filtration condition (sampling flow rate, humidity, temperature, etc.), can influence particle collection efficiency. As a result, a criterion is required for comparing different filters and their capacities. In this regard, the quality factor (Q_f) is defined as [52]:

$$Q_f = \frac{-\ln P}{\Delta p} \qquad \text{Eq. 1-21}$$

Here, Δp is the pressure drop along the filter bed and P is the penetrated portion (i.e., escaped particles from the filter). As Eq. 1-21 shows, the quality factor is inversely related to the pressure

drop and penetration; that is, the lower the pressure drop and penetration, the higher the quality factor. The pressure drop depends on the permeability of the structure and can be calculated by Eq. 1-22 [53]:

$$\Delta p = 2C_D \frac{\rho \alpha U^2 L}{D_f} \qquad \text{Eq. 1-22}$$

Where C_D is the drag coefficient, ρ is the air density, α is the solidity of the fiber, U is the air face velocity equal to the ratio of volumetric flow (Q) to the surface area of the filter ($U_0 = \frac{Q}{A}$), L is the packing length and D_f is the filter's diameter. Penetration (P) is also defined as:

$$P = 1 - E = \frac{N}{N_0} \qquad \text{Eq. 1-23}$$

Here, E is the collection efficiency. The ratio of particles passing through the filter (P) added to the ratio of particles trapped in the filter (E) gives us the total portion of particles (=1). N is the number of particles passing through the filter (particles in the filter outlet), while, N_0 is the initial number of particles present in the sample (particles in the filter inlet). We can then rewrite the above equation as:

$$E = \frac{N_0 - N}{N_0} \qquad \text{Eq. 1-24}$$

Normally, this equation is used to calculate the filtration efficiency by counting the particles in the filter inlet and outlet. Single-fiber theory can be also used to study particle trapping ability. After calculations and integrations, the following equation describing the trapping efficiency is obtained [54]:

$$E=\frac{N_0\text{-}N}{N_0}=1\text{-}\exp\left(\frac{-4\alpha L\eta_f}{\pi D_f(1-\alpha)}\right) \quad \text{Eq. 1-25}$$

In this equation, η_f is the single fiber collection efficiency and can be defined as:

$$\eta_f = \eta_I + \eta_R + \eta_D \quad \text{Eq. 1-26}$$

Where η_I, η_R and η_D are the single collector efficiencies for inertial impaction, interception and diffusion, respectively. Different simulations and mathematical models have been developed to predict the impact of each mechanism on total filtration efficiency [54,55].

Along with the quality factor, capacity is a critical parameter in determining the effectiveness of a filter. Filtration is similar to exhaustive sampling, as entrapment continues until the device reaches its full capacity in both processes. In this regard, filter capacity can be considered the equivalent of BTV for an NTD. A filter's capacity determines the maximum amount of sample (or volume) that can be passed through it without particle loss per filter mass.

The equations in the previous section provide guidance on how to prepare an air filter with high filtration efficiency. With regards to the variables that define pressure drop and filtration efficiency, it is very difficult to optimize sample density, solidity, and drag coefficient, as they are inherent characteristics of the sample or fiber. However, face velocity, packing length, and fiber diameter can be optimized to obtain minimum pressure drop and maximum filtration efficiency. The most critical of these variable parameters is fiber diameter, which was discussed in greater detail in the **1.9.2 Packing Material Size** section.

1.14 Scanning Mobility Particle Sizer (SMPS)

As mentioned in previous section, the filtration efficiency can be measured using SMPS instrument. This instrument is designed for analysis of aerosol particles. In SMPS, compressed air is injected into atomizer solution to produce salt particles or oil droplets from solution. These vaporized particles/droplets and the associated humid air, then passes through dryer to remove water. Next, particles of different size enter electrostatic classifier which classifies aerosol particles based on their size (between 5-225 nm). These separated particles enter condensation particle counter (CPC) for counting. Schematic of the SMPS instrument is provided in Figure 1-15. If we insert the filter in this instrument, preferably, before electrostatic classifier, and by comparing the number of particles before and after insertion, the filtration efficiency of the prepared fiber can be determined.

The type of particle output depends on the solution in particle generator. Common solutes for solid particles are sodium chloride, uranine and methylene sucrose in fresh distilled water as solvent. For oil droplets dioctyl phthalate and olive oil in reagent grade alcohol are recommended. Usually, 0.0001 g solute per milliliter of solvent is convenient for most applications.

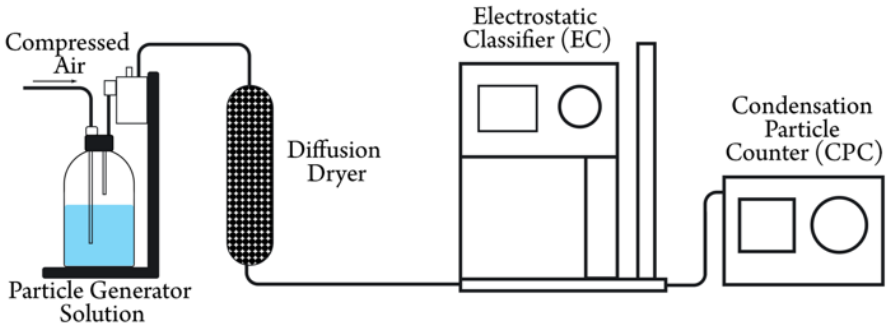

Figure 1-15. Instrumentation of scanning mobility particle sizer (SMPS) for production, sorting and counting particles [the schematic is prepared for this thesis by the author].

1.15 Preparation of fibers

To have a fibrous filter, first step is choosing the basic material appropriate for filtration as well as the packing material of NTD. Next, the chosen material should be prepared in fiber structure. To obtain fiber structure, the material should have specific viscosity, surface tension and other physical properties, as a result, organic polymers dissolved in solvent are among the best candidates for fiber preparations. Different methods of fiber preparation will be discussed in next sections.

1.15.1 Phase separation

One method of fiber preparation is using phase separation method. In this method, initially, polymer is dissolved in a solvent to get a gel structure [56]. Then, a non–solvent is added to exchange with the solvent and force the polymer out of the solution (Figure 1-16). The method is relatively simple but the resulting fiber can be heterogenous in size and mostly large fiber diameter are obtained. The type of solvent and polymer for this method are also limited.

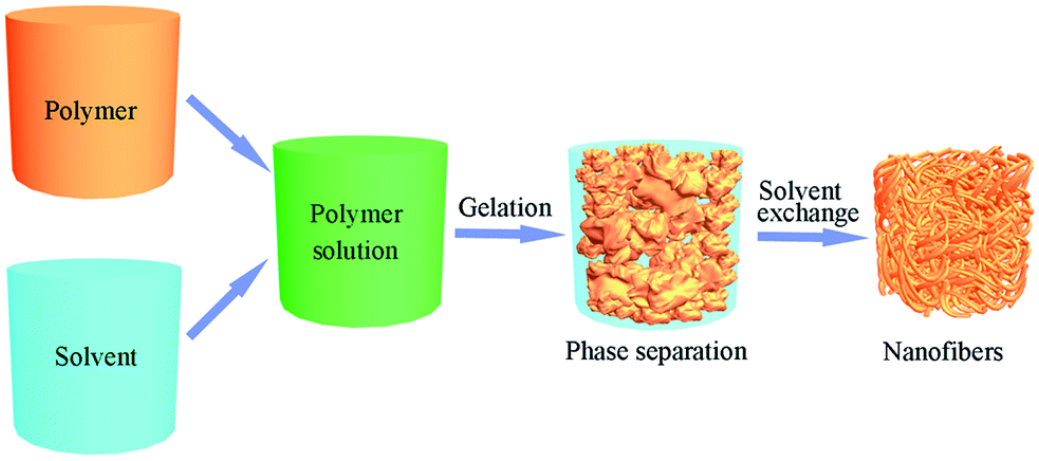

Figure 1-16. Steps in phase separation method for fiber preparation including the mixture of polymer/solvent, gelation and phase separation by solvent exchange steps [with permission from [56]].

1.15.2 Template

It is also possible to apply a template for fiber preparation. In this technique, as the name suggests, a polymer solution is pressed through a template with a known hole diameter is used [57]. The method requires special instrumentation and for small fiber diameter in the range of nanometer, high pressure is needed. A schematic of the process can be found in Figure 1-17 .

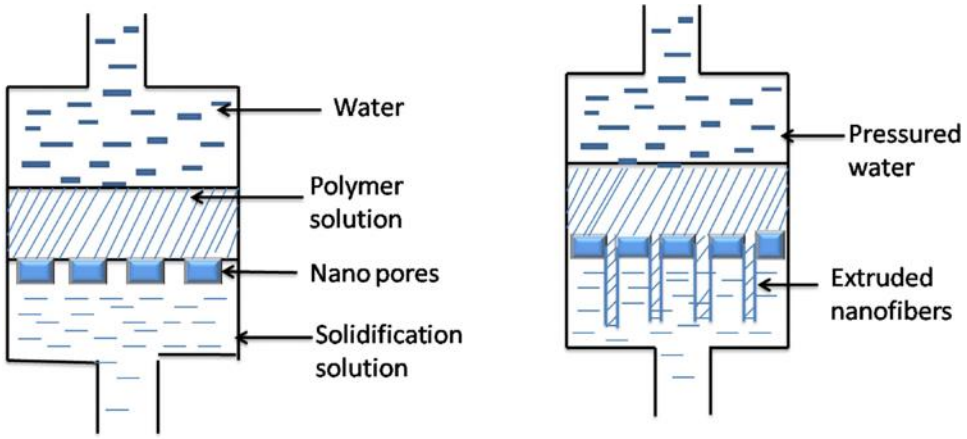

Figure 1-17. Preparation of nanofibers by pressure passing the polymer/solvent gel through nanopores to get nanofibers [with permission from [57]].

1.15.3 Drawing

For polymers solutions with a proper viscosity range, drawing can also be used for fiber preparation. To this end, a polymer solution or melt is drawn with a needle tip. The diameter of the final product severely depends on the physical properties of the solution [58]. In addition, according to physical limitations, it is not easy to prepare lengthy fibers with this method (Figure 1-18).

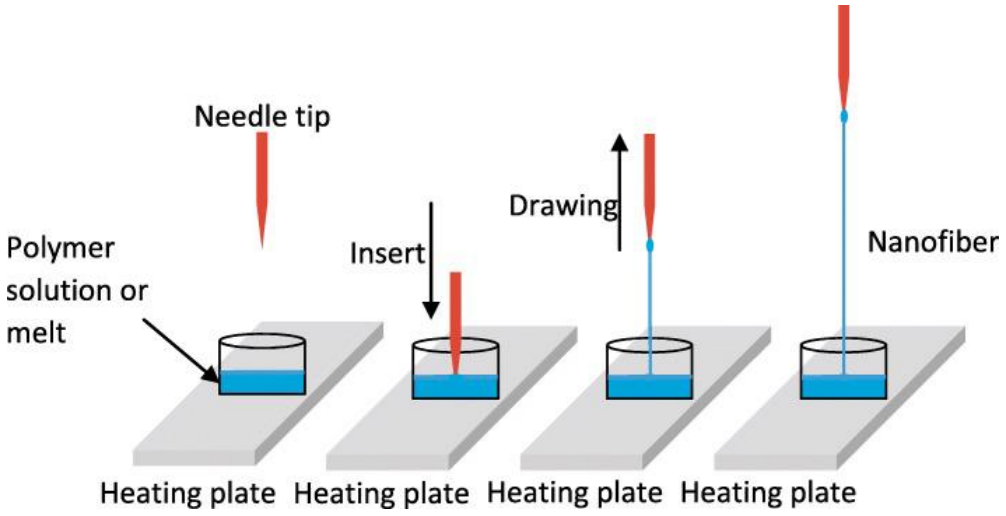

Figure 1-18. Preparation of nanofibers by drawing a polymer/solvent gel using a small needle tip [with permission from [58]].

1.15.4 Electrospinning

In electrospinning method, a high voltage is applied to a polymeric solution in order to induce electrical charge in the solution. The high voltage is applied between needle of the syringe pump (containing polymer solution) and a collector (a conductive surface), while the solution is pushed by syringe pump. After this voltage reaches a threshold value, ejecting fluid from needle leads to the formation of the Taylor cone [59]. When this threshold is reached, the solution is charged, the electrostatic repulsion contracts surface tension, so the droplet is stretched to a fiber, which is stream of solution ejecting from needle. According to the polymer and electrospinning properties, we may have a stream of distinct droplets or a continuous fiber. This ejected solution dries in its way to the collector, while simultaneously elongated by a whipping process caused by electrostatic repulsion at small bends in the fibers [60]. So, as it goes further closer to the collector, solvents are dried, fibers get smaller and solid fiber is obtained (Figure 1-19).

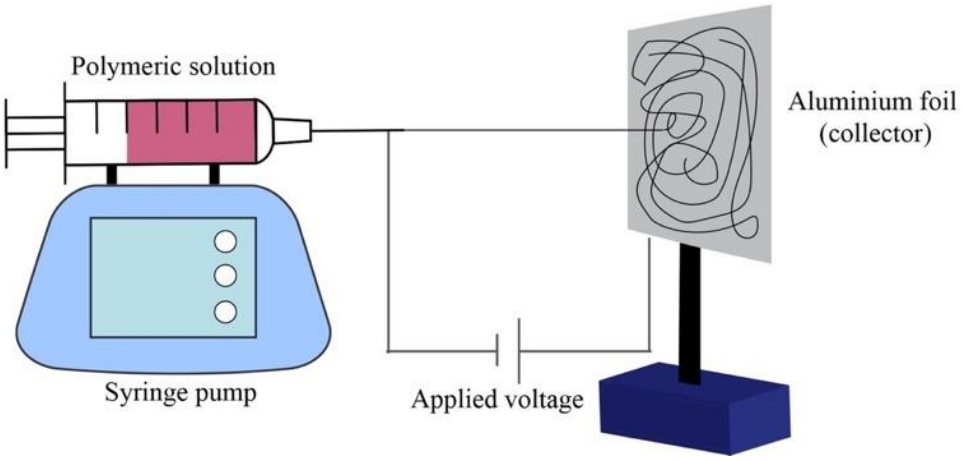

Figure 1-19. Schematic of electrospinning process for preparation of nanofibers. The polymer solution is filled in the needle, pushed with syringe pump and nanofibers are prepared when high voltage is applied between the needle tip and collector [the figure is prepared for this thesis by the author].

The final fiber and its properties depend strongly on different parameters such as polymer solution condition, processing conditions and ambient conditions. These parameters are briefly discussed in following paragraphs.

1.1.1.1 Solution properties

Physical and chemical properties of the solution are important factors contributing to the quality of the final product. Among them polymer molecular weight, viscosity, surface tension, conductivity, temperature and dielectric effect of the solvent can be listed [60]. Viscosity and electrical properties determine the elongation, which is important for the fiber diameter and bead formation. In the cases that the solution electrical conductivity is not appropriate, salt or acid can be added in order to increase the conductivity.

1.1.1.2 Process properties

Instrumental factors are also important for obtaining appropriate fibers. These factors include applied voltage between needle and collector, feed rate, type of collector (static or dynamic), feeding needle diameter and the distance between needle and collector. These parameters can be used to alter the fiber properties [59]. Generally high electrical voltage (>6 kV) should be applied in order to get thinner fibers on the collector. The feeding rate is also critical, too low rate is not enough to obtain consistent fiber with constant diameter, and too high rate can lead to thick fiber or beads. Needle diameter can affect feeding rate and in some cases, small orifices can be easily blocked with viscous solutions [60].

1.1.1.3 Ambient properties

The fiber jet needs to pass the distance between needle and reach the collector in ambient condition, which can influence the fiber structure through drying process. Among different ambient parameters, humidity and temperature are the most important ones. It is observed that high humidity can alter fiber morphology by forming some small droplets in the fibers, that leads to hole formation after drying. Temperature also affects the drying process [59].

1.16 Preparation of gas standard mixture

For studies using needle–trap, in most of the cases gas–phase samples are studied including but not limited to air and exhaled breath samples. In these cases, the optimization and calibration should also be in similar gas phase environments. There are different methods for preparing gas phase standard mixture. Some of these methods can provide a continuous flow of gas sample with constant concentration of analytes in gas–phase, others have a static design and the sample should

be renewed after experiments for constant and reproducible results. In the following paragraphs, some of these methods are explained.

1.16.1 Gas generators instruments – continuous gas stream

Gas generator is an instrument comprised of a glass sample chamber, gas permeation tubes, thermostat, an input and output for carrier gas connected to a gas tank. The gas permeation tubes are filled with pure analytes and left inside the thermostat chamber (Figure 1-20). The temperature is set based on the volatilities of analytes. The permeated analytes through tube walls are transferred to the sampling chamber using carrier gas. The type of carrier gas depends on the application and can be nitrogen, helium or any other type of inert gas. The mass of the gas permeation tubes is monitored regularly to calculate the permeation rate. The concentration of the gas phase analytes can be tuned by changing either the temperature or the carrier-gas flow rate. This device is commercially available and has been used for preparing gas–phase formaldehyde [61,62], BTEX [63], etc.

1.16.2 Heating assisted liquid injection – static gas mixture

The simplest method of preparing gas phase sample is injecting a known volume of liquid sample inside a glass sampling bulb and heat the bulb to evaporate the liquid. It is suggested to vacuum the bulb before injection for easier vaporization and reducing the chance of settling compounds in the walls as a result of saturation. The volume of liquid should be as low as possible [64]. For heating the bulb, a normal oven can be used. It is also possible to focus the heat to sample and not the whole bulb by microwave heating. In this case since most microwave instruments radiate a wavelength for water absorption, the sample should include water. To this end, in one

study, a small amount of wet glass wool was inserted inside a glass sampling bulb for heating the sample mixture. This way there is enough water to absorb the heat and evaporate the liquid sample [65].

1.16.3 Liquid injection using syringe pump – continuous gas stream

Another method is to continuously inject the liquid mixture into a heated mixing tee for vaporization. Gaseous mixture is then sent to sampling chamber using a carrier gas. The liquid can be pure analyte or a solution with known concentration of analytes. The concentration of analytes in gas phase can be calculated using the concentration in solution, feeding rate and carrier gas flow

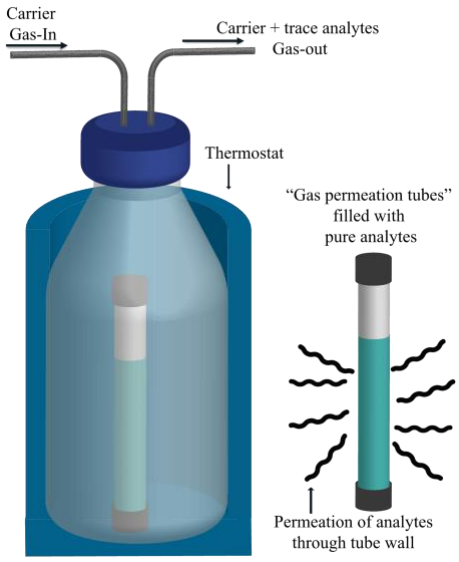

Figure 1-20. Gas generator setup for preparation of gas–phase analytes. Pure analytes are filled in the tube and the permeated gas through the tube wall is transferred to sampling location using carrier gas [with permission from [66]].

rate. This method was previously used for analysis of VOCs in breath samples [67], alkanes and terpenes [68].

1.17 Applications of needle-trap devices

While the application of NTD for active analysis of liquid samples is plausible, high back pressure and fast needle clogging has limited the sample type to the gaseous mixtures. In initial NTD studies, application of NTD was mostly narrowed to the analysis of volatile compounds, which was further extended to polar and less-volatile compounds. In an attempt to apply NTD for analysis of VOCs, Pawliszyn et al. [28] used multi–component (PDMS/DVB/Carboxen) packed needle for analysis of n-alkanes and BTEX from gas samples. In 2006, Jinno et al. [33] packed the needle with polymer beads in order to extract small VOCs such as hexane, acetone and toluene. They showed that samples could be quantitatively recovered up to 7 days after storage of the needle at room temperature with Teflon cap, this characteristic can be used for on-site sampling. The same group later extended the application of NTD to more complex sample matrixes and tobacco smoke samples were analyzed by in 2007 [69]. At the same time analysis of VOCs was extensively studied using NTD with various research groups [31,42,70,71].

To widen the area of application of NTD, Pawliszyn et al. added a gas aspirating pump to enhance the volatility of non–volatile compounds such as acetic acid and formic acid [72]. Extraction of analytes with high polarity and low volatility was a success. Low detection limit and acceptable figure of merits opened a new window for extension of the application of NTD into polar compounds. The application of NTD for analysis of metallic elements was investigated by the same group [73], where they benefited from mercury/gold amalgamation for extracting mercury. A list of various sample types studied with NTD is provided in Table 1-1.

Table 1-1. Types of previous samples, target compounds and extraction/desorption conditions studied with NTD reported in literature.

Sample Matrix	Target Compounds	Sampling mode	Desorption time and temp.	Sorbent
Mosquito coil smoke [74]	BTEX[1]	Active, 1.9 mL min^{-1}	250-300 ºC, 0.5-1.5 min	DVB[2] or Carboxen
Infested indoor air [75]	(E)-2-hexenal, (E)-2-octenal	Active, 5 mL min^{-1}	–	DVB
Exhaled Breath [76]	Aromatic compounds	Active, 25-30 mL min^{-1}	290 ºC, <1 min	PDMS[3]/Carbopack B /Carboxen 1000/
Exhaled Breath [77]	VOCs[4]	Active, 5 mL min^{-1}	265 ºC, 5 min	Graphene /PANI
Pig Breath [78]	VOCs	Active, 60 mL min^{-1}	300 ºC, 1.5 min	Tenax/ Carbopack X/ Carboxen 1000
Environmental air [70]	BTEX	Passive	300 ºC	Carboxen 1000
Water [71]	BTEX	Active, 2L	280 ºC	Carbopack X
Air, Breath [79]	hydrocarbons, ketones, aldehydes, aromatics, and sulphurs	Active, 5 mL min^{-1}	300 ºC, 20 s	DVB/Carbopack X/ Carboxen 1000 and Tenax GR
Car exhaust [48]	Free and total Formaldehyde	Active, 10 mL	270 ºC, 10 s	Tenax/Carboxen 1001/ Carboxen 1003
Snow [72]	Acetic acid and formic acid	Active, ~8 mL min^{-1}	220 ºC, 15 s	DVB
River water [80]	PAHs[5]	Active, 2.5 mL min^{-1}	290 ºC, 6 min	CNT/Silica
Wastewater [81]	VOCs	Passive and Active, 6 mL min^{-1}	300 ºC	Tenax TA/Carboxen 1000

[1] Benzene, toluene, ethylbenzene, xylenes
[2] Divinyl benzene
[3] Poly dimethylsiloxane
[4] Volatile organic compounds
[5] Polycyclic aromatic hydrocarbons

Pine tree emission [30]	α-pinene, β-pinene, limonene	Active, 5 mL min^{-1}	-	DVB
Soil [82]	PAHs	Active, 21 mL min^{-1}	280 ºC, 4 min	Amino-silica/graphene oxide
Whole blood [83]	VOCs	Active, 2 mL min^{-1}	300 ºC, 1 min	Tenax TA
Soil [84]	BTEX	Active, 7.9 mL min^{-1}	280 ºC, 5 min	Silica/PANI nanofiber
Air [85]	Organohalogen	Active, 3 mL min^{-1}	300 ºC, 2 min	MWCNTs/silica
Seawater [86]	VOCs	Purge and trap, 40 mL min^{-1}	310 ºC, 30 s	PDMS/Carbopack X/Carboxen 1000/
E-coli and Pseudomonas aeruginosa [87]	Microbial VOCs	Active, 5 mL min^{-1}	-	DVB/Carbopack X/ Carboxen 1000
dry-cleaning shop air [88]	perchloroethylene	Active, 3 mL min^{-1}	290 ºC, 3 min	Graphene
Urine [89]	VOCs	Active, 10 mL min^{-1}	250 ºC, 30 s	DVB/Carbopack X/ Carboxen 1000
Pen ink [90]	VOCs	Active, 4 mL min^{-1}	270 ºC, 4 min	ZIF-8-derived nano porous carbon
Urine [91]	BTEX	Active, 1.8 mL min^{-1}	250 ºC, 1 min	MIL-100(Fe)@Fe_3O_4@SiO_2
Ambient air [92]	Aromatic amine	Active	280 ºC, 3 min	Amberlite XAD-2
Ambient air [73]	Mercury	Active	350 ºC, 2 min	Au-wire
Aqueous sample [93]	Formaldehyde, Acrolein	Active, 3 mL min^{-1}	280 ºC, 2 min	Silica aerogel
Urine [94]	BTEX	Active, 30 mL min^{-1}	~270 ºC, 3 min	MOF
Workplace air [95]	TEX	Passive, up to 12 h	-, 30 s	DVB
Indoor air [28]	BTEX and alkanes	Passive, up to 24 h	300 ºC, 2 min	PDMS/DVB/CAR and Carboxen 1000

1.18 Potential applications of filter-incorporated needle-trap devices

After considering various aspects of filter and NTD and appropriate filters for NTD, it is important to study potential application of filter-packed NTD. There are numerous aerosol environments, in which, filter-incorporated NTD can play a crucial role for comprehensive study of droplet/particle-bound and gas-phase components. Among these, breath sample and air pollutant particles are among the most critical ones as a result of their role in clinical and health related studies. In the following paragraphs, the importance of aerosol samples and the necessity of an integrated method for comprehensive study of aerosols will be discussed.

1.18.1 Breath analysis

NTDs have also been applied for the study of biological samples. Based on their design, most applications of NTDs in this area have focused on breath samples. Although, breath analysis and the connection between breath composition and health status dates back to the work of Hyppocrates in ancient Greece, modern breath analysis began with Pauling's seminal work in 1971 wherein he was able to detect 200 VOCs in breath samples [96]. Thus far, researchers have detected at least 3500 VOCs in breath samples [97], that are either produced inside the body (endogenous) or enter the body from the external environment (exogenous). Endogenous compounds can be used as biomarkers in studying the health status of human subjects, while exogenous compounds serve as indicators of exposure patterns and internal concentrations of various analytes.

There are some challenges regarding breath sampling. One of the issues is the amount of dead volume during sampling. It is estimated that in 500 mL of exhaled breath, 150 mL is dead volume sample that is from upper air tract and does not include analytes and only acts as diluent.

To solve this issue, new breath sampling bags contain a discard bag. During blowing into the sampling bag, initially dead volume sample fill the discard bag and the sample from lower tracts can fill the sampling bag through a one–way valve. The other challenge is the exogenous nature of some VOCs in breath sample. To resolve this problem, breath composition should be compared with air inhaled samples. An important drawback in breath sampling is the variation in breath component depending on age, gender, food habit and etc. It should be noted that the lack of a standard method for sampling method and lack of a universal library for "normal" concentration of VOCs in breath, adds to these difficulties. In the case of analysis of biomarkers, usually the concentration of these analytes is very low and direct analysis of the biomarkers is generally impossible which highlights the importance of an extraction method for preconcentration and introduction of analytes into analytical instruments.

NTDs have been widely used to investigate endogenous VOCs for the purpose of studying disease status. Indeed, prior studies have demonstrated a correlation between exhaled breath composition and diseases such as heart failure [98] and lung disease [99] . An automated NTD protocol has also been designed for the study of breath composition in clinical conditions, and the application of GC×GC-TOF has been shown to improve the detection limits of this method [100]. To introduce a standard procedure for breath analysis, the volunteers in one study were instructed to swallow a capsule containing peppermint. The results of the study showed that the NTD was able to accurately quantify the composition of the capsule and define reference values for a panel of compounds [101]. Humidity has always been a challenge in breath analysis, and some studies have tried to investigate how it influences extraction. The results of such work showed that humidity cannot affect extraction efficiency when a multiple bed NTD and strong sorbents such as Carboxen are used [102].

Notably, nearly all prior applications of NTDs for breath analysis have exclusively focused on the gas phase of the breath samples. The term, "breath analysis" is generally considered to be the analysis of small VOCs in the gas phase of breath samples, also referred to as "exhaled breath vapor" (EBV). However, this description can be ambiguous, as breath is actually an aerosol that contains large numbers of various-sized droplets that carry various compounds. A cold tube can be used to collect these droplets in liquid phase after multiple breaths; these droplets are known as "exhaled breath condensate" (EBC) [103]. It is also possible to trap droplets in their aerosol form, which is known as "exhaled breath aerosol" (EBA) [104].

Each breath component can be distributed between the gas and droplet phase depending on its polarity and volatility; thus, the study of the gas and droplet phases can provide information about different aspects of a breath sample. While the significance of droplets and their composition has been recognized by scientists, the use of NTDs to study breath samples has been limited to the gas phase [76,77]. The importance of aerosol droplets—and the compounds they may contain—in breath samples highlights the need for a device that is able to trap them and extract/preconcentrate gas-phase components, as such a device would offer a solution to the problems of cost and time associated with total breath analysis. A list of previous microextraction techniques applied for breath analysis is provided in Table 1-2.

Table 1-2. A list of previous reports on the application of extraction methods for biomarker determination in breath samples.

Method	Sorbent	Analytes	Ext. time	LOD	Ref.
SPME[1]	PDMS[2], Carbowax/DVB[3], PDMS/DVB	Ethanol, acetone, isoprene	10 s	1.7–12.8 nmol L^{-1}	[105]
SPME	CAR[4]/PDMS	55 VOCs	15 min	0.32–0.75ppb	[106]
NTD	MAA-EGDMA[5]	Isoprene, acetone, pentane, toluene	–	–	[102]
NTD[6]	Graphene/polyaniline	8 aldehydes	10 min	2–3 ng L^{-1}	[77]
NTD	DVB/Carbopack X/ Carboxen1000	22 VOCs	10 min	–	[98]
NTD	Carboxen 1000/Carbopack X/ Tenax	13 VOCs	5 min	1.9–33.9 ng L^{-1}	[78]
NTD	PDMS/Carbopack B/ Carboxen 1000	Benzene, toluene, 1,2,4-TMB	10 s	27.4–30.3 ppb	[76]
TFME[7]	Graphene/PS	6 aldehydes	4 min	4.2–19.4 nmol L^{-1}	[107]
SPME	Carboxen/PDMS	36 VOCs	20 min	–	[108]
SPME	PDMS-DVB	C1-C10 aldehydes	8 min	0.009–0.052 nmol L^{-1}	[109]
SPME	CAR/PDMS	43 VOCs	5 min	1.7–17.2ppb	[110]
NTD	PDMS/Carbopack B/DVB/ Carboxen 1000	19 VOCs	–	1.8–103 ng L^{-1}	[111]
SPME	CAR/PDMS/DVB	propofol	5 min	0.006 nmol L^{-1}	[112]

1.18.2 Analysis of fragrances

Fragrances are a group of emerging organic air pollutants. In contrast to PAHs and BTEX, which are commonly found outdoors, fragrances should be studied in indoor environments, as they

[1] Solid phase microextraction
[2] Poly dimethylsiloxane
[3] Divinylbenzene
[4] Carboxen
[5] Methacrylic acid and ethylene glycol dimethacrylate
[6] Needle–trap devices
[7] Thin–film microextraction

are found in a myriad household item, including toiletries, cosmetics, cleaning products, shampoos, and even foods and beverages. This can be problematic, as long-term exposure and bioaccumulation of fragrances can lead to heightened irritation and skin allergies [113]. Another problem on daily application of fragrances is that people may not detect the fragrances shortly after applying it, so they increase their consumption amount which can enhance their exposure over time. However, the problems associated with fragrances are not limited to their impact on humans; indeed, they can also have a deleterious effect on the environment.

The fragrance industry is self–regulating and the governmental regulations in this area are either limited or unclear. In US, Food and Drug Administration (FDA) and the Consumer Products Safety Commission (CPSC) are responsible for the safety of fragrances. Cosmetics do not require safety check, however if the safety is not confirmed, it should be mentioned in the product label. The individual chemical compound used as fragrance, do not have to be mentioned in the label. EPA considers fragrances as indoor air pollutants since they can exacerbate asthma. In Canadian law, any avoidable hazard should be mentioned in the label. In EU, the Scientific Committee on Cosmetic Products and Non-Food Products (SCCNFP) [114] asked the companies to add the name of potential skin allergens on the label, so people avoid these products if they have allergy.

Fragrances are a complex mixture including a large group of different chemicals and most commonly create air pollution when they are sprayed (e.g., as air fresheners or perfumes), and the aerosol nature of these samples makes it difficult to study such matrices. When a fragrance mixture is sprayed, compounds can be distributed between the gas phase and droplets; however, most studies only analyze exposure concentrations in the gas phase and neglect the droplet portion. Such approaches provide an incomplete picture, as the fragrance-containing droplets in aerosols can also

enter human body through respiratory system. It means the analysis of fragrances is challenging. This problem is worsened when there is a time gap between administration of the sprays and the sampling time. This time decreases the concentration of fragrances in air exponentially, by diffusion. The low concentration and high complexity complicate the procedure of sampling, sample introduction and analysis. Development of a representative sample–preparation method for sampling and pre–concentration of fragrances in both phases is critical and mostly two separate methods are required. A list of previously reported extraction methods for determination of fragrances can be found in Table 1-3.

1.18.3 Analysis of air pollutants

One of the most important NTD applications is air monitoring, and this technology has been shown to provide high accuracy and sensitivity for the detection of BTEX [70], alkanes [28], organohalogens [39], aromatic amines [92], and mercury [73] in air samples. Furthermore, NTDs have also been applied to determine (E)-2-hexenal and (E)-2-octenal in indoor air containing *Cimex lectularius* L.[75] and perchloroethylene in dry-cleaning shop [88].

Table 1-3. A list of previous reports on the application of extraction methods for determination of fragrance compounds

Method	Sorbent	Analytes	Ext. time	LOD	Ref.
SPME[1]	PDMS/DVB[2]	25 fragrances	20 min	0.05–10 ng m^{-3}	[115]
MSPD[3]	Florisil	10 fragrances	5 min	2E-6 w/w	[116]
SPME	DVB/CAR/PDMS	46 fragrances	30 min	0.9–13 μg L^{-1}	[117]
SPME	Carboxen/PDMS	6 fragrances	60 min	–	[118]
SPME	PDMS	42 fragrances	30 min	–	[119]

[1] Solid phase microextraction

[2] Polydimethylsiloxane/divinyl benzene

[3] Matrix solid-phase dispersion

SPME–arrow	DVB/PDMS, PA[1]	8 fragrances	45 min	0.2–2.5 ng g^{-1}	[120]
SPME	CW[2]/DVB	5 fragrances	10 min	–	[121]
NTD	DVB	23 fragrances	30 min	–	[122]

The main challenge in the study of air pollutants, specifically large and heavy hydrocarbons, is their low volatility, as this increases their tendency to attach to particles. Indeed, prior findings have shown that, depending on the characteristics of the compounds under study, up to 70% of heavy PAHs may become attached to the suspended air pollution particles [123]. This reveals the importance of particle-bound analytes in determining the total concentration of pollutants in a sample. Although NTDs have been applied in numerous air pollution studies, most of these studies do not provide a comprehensive analysis, as their results are limited to the gaseous components in the sample. As a result of this limitation, it is necessary to employ two separate methods in order to obtain an accurate picture of the air samples under study. However, NTDs eliminate the need for two methods, as they are able to capture both free and particle-bound air pollutants in a single device. The possibility of trapping particles via NTDs has been reported previously and will be explained below.

There are defined regulations for the concentration of air pollutants. For indoor air quality assessment, occupational exposures to gaseous pollutants, such as threshold limit value (TLV), recommended exposure limit (REL), and permissible exposure limit (PEL) are typically defined in 8h intervals. Occupational short-term exposure limits (STEL) are based on a “15-min TWA

[1] Polyacrylate
[2] Carbowax

concentrations". The US Environmental Protection Agency (EPA) has promulgated 16 unsubstituted PAHs (EPA-PAH) as priority pollutants [124].

Occupational Safety and Health Administration (OSHA) has set a permissible exposure limit (PEL) of 0.2 mg m^{-3} for benzo[a]pyrene, anthracene, pyrene, chrysene, and phenanthrene and 10 mg m^{-3} for naphthalene. Table 1-4 shows some of small VOC air pollutants and their recommended concentrations.

The standard method for study of small air pollutants is NIOSH 2549, based on the extraction of compounds on sorbent tubes, which is further desorbed and analyzed. For particle-bound PAHs, NIOSH 5515 is applied. in this method, air samples are drawn through a filter, which trap particles from air sample. These particles are then washed with solvent and analyzed with analytical instruments.

Among different methods for sampling and sample preparation of air pollutants, SPME can be the method of choice [125]. With all the advantages for SPME, the concentration obtained with SPME is limited to the concentration of components in the vapor–phase. In order to provide a complete view of the sample, it is required to determine the concentration of target compounds in both vapor and particle phase.

Table 1-4. A list of some of air pollutants and their recommended concentration

Substance	Regulatory Limit	Recommended Limits
	OSHA PEL[1]	NIOSH REL[2]

[1] Occupational Safety and Health Administration (OSHA) Permissible Exposure Limits (PELS)

[2] National Institute for Occupational Safety and Health (NIOSH) Recommended Exposure Limits (RELs) (Up to 10-hour TWA)

	mg m^{-3}	
Acetaldehyde	360	
Acetone	2400	250 ppm
Acetonitrile	70	20 ppm
benzene	10 ppm	0.1 ppm
heptane	2000	85
toluene	200 ppm	100 ppm
hexane	1800	50
butyl acetate	710	150 ppm
ethyl benzene	435	100
o-xylene	435	100

To obtain concentrations in particle phase, trapping the particles is the first step. To this end, NTD can be a suitable method. The dynamic sampling and porous structure can make the trapping of particles possible. The trapping efficiency of the NTD packed with sorbent particles is limited. To increase the trapping efficiency, in this work a filter was added and packed inside the needle. Table 1-5 summarizes some of the previous methods on the extraction of air pollutants using microextraction techniques.

Table 1-5. A list of previous reports on the application of extraction methods for determination of indoor air pollutants.

Method	Sorbent	Analytes	Ext. time	LOD	Ref.
SPME	PDMS/DVB	8 VOCs	1 min	1–3 ppb	[126]
SPME	PDMS	BTEX	15 min	0.002–0.005 mg m^{-3}	[127]
SPME	Carboxen/PDMS	22 VOCs	4 min	–	[128]
SPME	PDMS	BTEX	3 min	0.05–2 ppbv	[7]
SPME	CAR/PDMS	16 PAHs	90 min	0.09–0.27 ng mL^{-1}	[129]
SPME	PDMS	16 PAHs	60 min	0.02–1 ng	[130]
NTD	$Zn_3(btc)_2$	5 PAHs	–	0.01–0.02 mg m^{-3}	[131]
TFME	EVA, LDPE	16 PAHs	–	–	[132]

NTD	Sol–gel CNTs	5 PAHs	30 min	0.001–0.01 ng mL^{-1}	[80]
NTD	rGO	5 PAHs	20 min	0.09–0.2 ng mL^{-1}	[133]
NTD	DVB	19 semiVOCs	–	0.005–2.9 ng	[134]
NTD	PDMS/CarbopackX/ Carboxen 1000	11 VOCs	5 min	0.002–0.3 mg m^{-3}	[135]
SPME/TFME/ NTD	DVB/CAR/PDMS, PDMS, DVB	22 VOCs	–	–	[75]
TFME	HLB	6 VOCs	10 min	–	[17]
TFME	Porous carbon/PDMS	6 VOCs	1.5 min	–	[16]
SPME	PDMS/CAR	11 VOCs	45 min	0.3–5 μg m^{-3}	[136]

1.18.4 Beverage analysis

One less studied field of aerosol sample is the importance of droplets in carbonated beverages. The emergence of sparkling beverages had a revolutionary effect on soft drink industry. The feeling and smell of aroma compounds in the beverages is the initial experience of consumer and the product, while it is believed that the presence of droplets is responsible for the enhanced flavor and sense of refreshment that are characteristic to carbonated drinks.

Most of the studies related to the study of beer and other aroma-containing beverages is limited to the study of gas-phase or liquid-phase determination of aroma compounds to improve consumer's gratitude. In these studies, the degassing process is performed to remove bubbles or dissolved CO_2 prior to the experiments. It can be insufficient as the refreshing sense in the moment of bottle opening can be the combination of gaseous and droplets containing aroma compounds and reaching nasal cavity.

All of these explanations clarify the importance of a method for considering the droplet-phase concentration of aroma components.

1.19 Thesis Objectives

The main objective of this thesis is to improve and optimize the packing material of NTD for aerosol samples. To achieve this goal, initially it was required to find appropriate material and preparation method that suits the requirements of a filter as a packing material for NTD (including: high filtration efficiency, low pressure drop, thermal stability, inertness, etc.). The preparation method, packing procedure and filter behavior required to be studied and optimized.

After successful preparation and implementation of the filter for NTD, the next goal was to apply the designed device for real aerosol environments analysis. Additionally, based on the fact that the designed NTD was capable of reporting total concentrations, it was important to apply another microextraction method (i.e., TFME and SPME) for study of gas-phase. The gaseous concentration and its comparison with total concentration could provide a more comprehensive view of the sample, by distinguishing free and total compounds.

Considering the above-mentioned explanations, the filter-incorporated NTD and one or multiple SPME methods were applied for study of breath samples, air pollutant particles, household sprays and sparkling beverages. The goal was to compare free and particle/droplet-bound compounds. The developed method is green, fast and cheap compared to alternative methods and combine multiple methods of aerosol analysis into one. It was believed that the designed device can open a new window on the potential applications of the needle-trap devices.

Filter-Incorporated Needle-Trap Devices (FI-NTD): Development and Optimization

2.1 Preamble

This chapter contains sections that have already published as an article in Analytical Chemistry. All subchapters are included in the article entitled *Needle-trap device containing a filter: a novel device for aerosol studies* by Shakiba Zeinali and Janusz Pawliszyn, *Analytical Chem*istry, 2021, 93, 43, 14401–14408. The contents of the articles are herein being reprinted with permission of the American Chemical Society, in compliance with both publishers and the University of Waterloo policies.

2.2 Introduction

Aerosols are the suspensions of solid particles or liquid droplets in a gas medium. These small particles can have deleterious effects on the health of humans or the environment due to their small size and physiochemical properties. In addition, aerosol particles are capable of carrying other species such as pollutants, biomarkers or microorganisms (coronavirus, E. coli, etc.). For example, the airborne transmission of respiratory diseases generally occurs due to small droplets, which can remain suspended in the air for a long time [137]. These features of aerosols underscore the importance of developing effective methods of analyzing them.

Most methods of analyzing aerosol are based on the chemical analysis of particles or their size distribution [138]. However, since most analytical methods are capable of measuring concentrations of analytes in free format, particle–bound analytes often remain hidden in measurements [139]. This is a significant omission, as particle–bound species are responsible for

transmission of airborne diseases. Thus, it is highly critical that researchers have access to an effective method for determining the types and concentrations of these particle–bound analytes. In particular, any such method should be capable of capturing aerosol particles in order to further identify and quantify analytes that have been adsorbed onto the particle's surface. Most standard methods for studying particle–bound analytes are either expensive or time–consuming. Polycyclic aromatic hydrocarbons (PAHs) attached on the surface of soot in polluted air is an example of particle–bound analytes and the EPA method for analyzing these PAHs includes passing air through filter, Soxhlet extraction, preconcentration with evaporator, clean up with silica gel and finally injection in GC instrument [140]. This method is time–consuming and expensive due to large volume of solvent consumption. In the case of biomarkers dissolved in breath droplets, exhaled breath condensate is the method of choice for sampling, which requires sophisticated cooling instrument and the final liquid sample needs sample preparation prior to injection [141] due to low concentration and incompatibility with some analytical instruments. All these limitations highlight the importance of a simple, integrated method for combining sampling and sample preparation for studying samples with droplets and particles.

Since particle–bound analytes tend to be present in low concentrations, it is vital to develop a sample preparation method that not only preconcentrates the analytes in extraction media, but also facilitates the introduction of samples into analytical instruments. Needle–trap devices (NTD) possess several characteristics that make them a good candidate for capturing aerosol particles and introducing particles–bound analytes into the analytical instruments. For instance, one issue related to the trapping of particles is their low diffusion (compared to molecular analytes) which prevents most of them from reaching the extraction medium in static modes. NTD overcomes this problem by using pumps to allow for the dynamic sampling of aerosols. Furthermore, since NTD requires

the whole sample is forced to pass through a sorbent bed, analytes are generally exposed to higher surface areas than in equilibrium–based extraction methods. As a result, NTD provides enhanced analytes and particle trapping, and thus, a higher chance of exhaustive extraction.

As discussed here, a NTD packed with sorbents composed of spherical particles can act as a filter for aerosol samples. For instance, Niri et al. [47], measured the concentration of allethrin in mosquito–coil smoke and gas from microwave–assisted gas generator using NTD and solid–phase microextraction (SPME). Their results showed that the smoke sample captured via NTD had significantly higher concentration of allethrin compared to SPME, while the concentrations in the gas generator samples (without aerosol particle) were statistically similar for both methods. This difference is attributable to the fact that allethrin molecules bind to smoke particles, which can be captured and analyzed by NTD, while SPME is only able to extract free analytes. Similar results were obtained for an analysis of formaldehyde in car exhaust [48]. In this case, larger differences in the results for NTD and SPME were obtained when the temperature of engine was lower; however, this gap shrunk as engine temperature was increased, as particle-bound formaldehyde molecules tend to be released in gas at higher temperatures.

Although NTD is capable to capture particles, its trapping efficiency is rather low when compared to air filters, mainly due to its use of large sorbent particles to maintain acceptable flow rate during sampling. Ideally, filters appropriate for trapping and analyzing particles, will be capable of capturing as many particles as possible without compromising flow rate and analyte extraction efficiency.

In general, filter designs utilize one of two different structural configurations: porous membranes or fibrous filters. Prior research into the use of porous membranes [30] found that their

low flow rate limited their applicability in NTD. As such, the present research seeks to design a fibrous structure that meets all of the requirements for particle filtration in NTD.

Several prerequisites must be met if a filter is to be appropriate for NTD. In fibrous filters, when bulk density remains constant, the use of smaller fiber diameters increases trapping efficiency, lowers permeability, and limits sampling flow rate. Conversely, the use of shorter packing lengths results in higher flow rates. Therefore, it is necessary to determine a logical balance between fiber diameter and packing length in order to achieve an acceptable flow rate [142]. Consequently, the use of smaller-diameter fibers and shorter packing lengths appear to be optimal for achieving appropriate filtration efficiency and flow rate. Additionally, commercial sorbents can also be incorporated into the final needle design for the extraction of free analytes. Although filters can extract analytes to some extent, lower extraction capacity is preferable, as it avoids interference with the sorbent's extraction behavior. Moreover, stable structure and reproducible extraction/filtration behavior are mandatory for attaining reliable analytical data.

Although there are several previous reports on the application of polymer–based fibrous filters, prepared by electrospinning [143], their application for NTD remains limited due to specific requirements of a proper packing material for NTD. A good filter candidate for NTD should be also thermally stable, as desorption will take place under the high–temperatures of a GC injector. Another important factor to consider in designing an appropriate NTD filter is to ensure that it can be easily and reproducibly packed inside the needle. However, preparing a fibrous structure that possesses the desired physiochemical properties and that can be reproducibly packed is a challenging task. One potential solution to this problem is to utilize an aerogel structure based on electrospun fibers, as it creates a stable porous structure with high particle trapping capacity [144].

Furthermore, aerogel's physical properties would make the packing procedure easier and enable higher flow rates without losing much particle capturing efficacy.

The present research focused on developing an NTD incorporating filter that satisfies all of the above-discussed requirements. Initially, fibers were prepared by electrospinning polyacrylonitrile (PAN). The fibers were then soaked in dispersion liquid and cut with a blender's chopping blade. Once the fibers had been cut, the dispersion media was removed via a freeze–drying method, thus producing the fibrous aerogel. The aerogel was then heated (H-PAN) for stabilization and packed inside the needle. Once the H-PAN-filled NTD had been assembled tests were run to examine the device's filtration efficiency, extraction properties, and stability. Finally, a needle packed with commercial sorbent and an H-PAN filter were applied to analyze aerosol breath samples to demonstrate the developed device's suitability for this application.

2.3 Experimental

2.3.1 Materials and instrument

Polystyrene (Mw= 280,000 g mol^{-1}), polyacrylonitrile (PAN, Mw= 150,000 g mol^{-1}), dimethylformamide (DMF) (99.8%), tetrahydrofuran (THF) (99.8%), 1,4-dioxane (99.8%), carboxen (60/80 mesh size), benzene (>99.9%), 2-pentanone (99.5%), 1-nitropropane (98.5%), pyridine (99.9%), 1-pentanol (>99%), octane (>99%), toluene (>99.8%), ethylbenzene (99.8%) and o-xylene (>99%) were purchased from Sigma-Aldrich (Mississauga, ON, Canada), while DVB (HayeSep Q® 60/80 mesh size), Tenax TA (60/80 mesh size) were obtained from Supelco (Oakville, ON, Canada).

2.3.1.1 Electrospinning

The electrospinning instrument was constructed in-lab, and consisted of a syringe pump from Harvard Apparatus (Pump 11 Elite Infusion/Withdrawal Programmable (Massachusetts, USA) and a high voltage supplier from Spellman (New York, USA). All experiments used a 10 mL BD plastic syringe (New Jersey, USA) with an 18 G syringe tip. A 10×10 cm piece of aluminum foil was used as collector, and high voltage was applied between needle tip and collector. The instrument was set inside a large plexiglass box to prevent any damage from the high voltages.

3% carboxen loaded TFME devices (3×20 mm) were prepared using an Elcometer 4340 film applicator (Elcometer Inc., Manchester, UK) in accordance with the procedure developed by Grandy et al. [145].

2.3.1.2 SMPS instrument

Trapping efficiency was analyzed using a scanning mobility particle sizer (SMPS) (TSI, Minnesota, USA), which featured an extra dry air tank connected to a constant output atomizer (TSI, 3076) with an atmospheric pressure output of less than 10 psig. The atomizer's output was connected to a diffusion dryer to remove humidity; the particles produced by the atomizer were directed into an electrostatic classifier (TSI, 3080) equipped with a neutralizer and an operating sheath flow of 15 L min^{-1}. Finally, the sorted particles were sent to a condensation particle counter (TSI, 3787) in 1.5 L min^{-1} mode. For the tests involving solid particles, the atomizer solution was made up of 0.1 g NaCl dissolved in MiliQ water; for the oil aerosol experiments, 0.1 mL of linalool was dissolved in methanol. Under these normal conditions, the instrument should have a nominal generation rate of 2×10^6 particles per cm^3 (10^8 particles per second).

Sampling was conducted using a 1-L glass bulb (2-2144) from Supelco (Oakville, ON, Canada), and the flow rate measurements were obtained using a flowmeter from Aalborg (New York, USA). The aerogels were heated for 2 h under atmospheric pressure in an Isotemp™ Model 281A Vacuum Oven set to 280 ºC. A Vitamix 7500 blender (Cleveland, Ohio, USA) was used to cut the fibers, which were subsequently visualized via field emission-scanning electron microscopy (FE-SEM, Zeiss UltraPlus; Carl Zeiss Meditec AG, Jena, Germany). Quintron 750-mL breath bags with mouthpieces and 400 mL discard bags were purchased for the breath sampling tests. Solvent removal was conducted using a freeze–dryer (Labconco, Missouri, USA) with a collector temperature set to below –40 ºC and a pressure of ~0.1 Torr. The freeze–milling instrument used in this research was a SPEX™ SamplePrep Freezer/Mill 115 (Toronto, Canada) that used liquid nitrogen as the main cooling source. 3-layered face masks (EnerPlex, Vietnam) and 100% silk face masks were used for breath sampling. The characteristics of the 3-layered face masks were as follows: shell layer, 100% polyester; middle layer, 65% polyester and 35% cotton; inner layer, 65% polyester and 35% cotton with Agion® antimicrobial agent. Pressure drop was measured using an Em201Spkit from UEI instruments (IN, USA).

2.3.1.3 Gas Generator

The gas generator used in this research was fabricated in-lab, and consisted of a heating chamber and a flow regulator. Permeation tubes for each analyte were made by encapsulating pure analyte inside a 100 mm long (1/4 in) Teflon™ tube sealed with 20 mm (1/4 in) solid Teflon™ Swagelok caps. Emission rates for each permeation tube were verified by periodically monitoring weight loss in the individual analyte tubes. Both McReynolds and BTEX compounds were

prepared in gas phase for this study, and temperature was kept constant at 75 ºC with a 300 mL min^{-1} air flow rate as a carrier for analytes.

With the exception of the analysis of real samples, all other data were obtained via chromatographic separations on the HP 5890 gas chromatography–flame ionization detector GC-FID (Hewlett-Packard company, CA, USA). GC-FID was performed using a Rxi-5Sil MS (30 m × 0.25 mm × 0.25 μm) fused silica column from Restek with a nitrogen flow rate of 1 mL min^{-1}. The desorption temperature was set to 280 °C in split–less mode, and FID was held at a constant temperature of 300 °C during analysis.

2.3.1.4 GC-MS for thin–film analysis

TFME analysis was performed using an Agilent 6890A/5973C GC/MS (Agilent Technologies, CA, U.S.A.) coupled with a GERSTEL cooling injection system 4 and a TDU (GERSTEL, Mülheim an der Ruhr, GE). A GERSTEL multipurpose system 2 autosampler was utilized to perform automated injections into the membranes. Separation was conducted using a DB-5.625 capillary column (30 m × 0.25 mm × 0.25 μm) (Agilent J&W, Santa Clara, U.S.A), with helium (99.999%) at a flow of 1.2 mL min^{-1} being used as the carrier gas. The TDU desorption temperature program was initially set at 40 °C (30 s) and increased at 700 °C min^{-1} to a final temperature of 280°C. The analytes desorbed from the membranes were cryo-focused in the CIS 4 at −80 °C with liquid nitrogen; once desorption had been completed, the CIS was heated to 280 °C at 12 °C s^{-1} in order to transfer the analytes to the column, and mass spectrometry detection was performed in scan mode with a mass range of 50–250 m/z using electron impact ionization at 70 eV.

2.3.1.5 GC-MS for needle–trap analysis

Analytes were separated using a Hewlett Packard 6890/5973 GC/MS equipped with a split/splitless injector and a SLB^{TM}-5MB (30 m × 0.25 mm × 0.25 μm) fused silica column from Sigma-Aldrich. Helium at a flow rate of 1 mL min^{-1} was used as carrier gas. MS was conducted using the following parameters: electron ionization (EI) of 70 eV; an ion source temperature of 230 °C; a quadrupole temperature of 150 °C; and a transfer line temperature of 280 °C. The instrument was run in full scan mode with mass range of 50–250 m/z. GC temperature programs are provided in Table 2-1.

Table 2-1. GC temperature programs for the analysis of McReynolds, BTEX and breath studies.

Groups under study	Ramp (ºC min^{-1})	Temperature (ºC)	Time (min)
McReynolds		40	1
	5	50	3
	20	170	2
BTEX		42	1
	25	150	0.2
	45	250	0
Breath		40	2
	10	100	0
	20	200	0

2.3.2 Optimization procedure for preparation of H-PAN aerogel

In order to prepare the aerogel, it is necessary to first generate its constituent fibers. To this end an appropriate polymer was selected and electrospun under optimized conditions. The resultant fibers were then cut into small pieces, placed in an appropriate dispersion media, and frozen. The final aerogel structure is obtained by removing the dispersion media via freeze–drying.

The final product of this procedure is a highly porous aerogel that can be applied for further studies. The schematic of the process steps is provided in Figure 2-1.

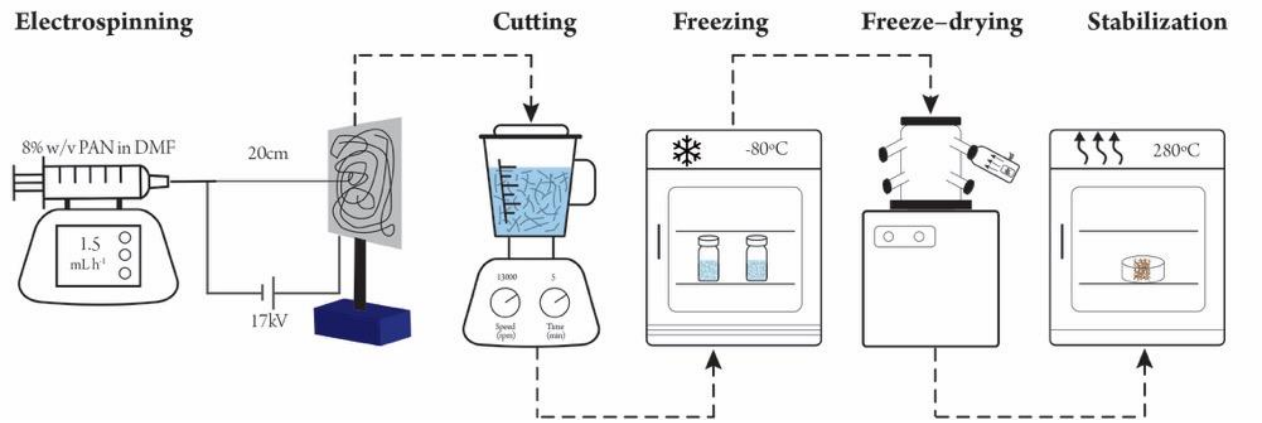

Figure 2-1. Schematic of H-PAN aerogel filter preparation steps including electrospinning, cutting by blender, freezing, solvent removal by freeze-drying and thermal stabilization in oven.

2.3.2.1 Electrospinning

Initially, the electrospinning procedure had to be optimized to obtain a constant flow of fiber from the needle to the collector. The optimal electrospinning conditions were determined by testing different concentrations of PAN (8,10,15%) and various ratios of DMF and THF (0:1, 1:1, 2:1, 1:2, 1:0). All other influential parameters were kept constant during electrospinning. These tests revealed that the optimum electrospinning condition utilized 8% PAN concentration w/v in DMF, an applied voltage of 17 kV, a flow rate of 1.5 mL h^{-1}, and needle–to–collector distance of 20 cm. It should also be noted that a 10 mL BD plastic syringe with a luer–lock tip (I.D. 14.5 mm) and an 18 G needle tip were used in these tests. An image of the obtained fiber can be seen in Figure 2-2.

Figure 2-2. Electrospun fibers from PAN on the aluminium foil (as the collector).

2.3.2.2 Cutting

Two different fiber-cutting procedures were tested: freeze–milling and blending. In the freeze–milling method, the fibers were cooled with liquid nitrogen and then ground to small pieces by the fast back and forth movement of the container inside the instrument. The freeze–milling instrument was set to pre-cool for 2 min, followed by a 1 min run time with different (2, 4, and 6) cycle repetitions at a rate of 15 cpm. Three different conditions were tested for the freeze-milling method: fibers without any solvent, fibers with methanol, and fibers with water (0.02 g fibers and 4 mL solvent).

The other cutting procedure utilized a kitchen blender and the addition of a liquid dispersion media. The selected dispersion liquid should allow the fibers to be suspended for a rather long time in order to ensure homogeneous cutting procedure. After cutting in the blender, the suspension must be frozen; the final aerogel's homogeneity and porosity is highly dependent on the properties of the suspension. As such, different dispersion media (methanol, 1,4-dioxane and water) were tested to determine which one yielded the most stable suspension (Figure 2-3).

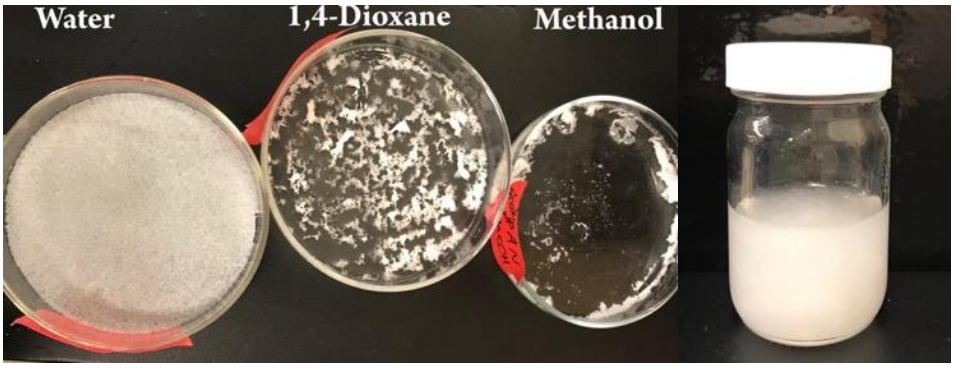

Figure 2-3. Homogeneity of remaining fibers after evaporation of dispersion media (left), and stable PAN in water (250 mg/100 mL) suspension after 6 months (right).

Since the fiber-to-dispersion media ratio (w/v) can also affect both cutting efficiency and the porosity of the final aerogel, this ratio was also optimized. To this end, the blender was set to level 6 (around 13000 rpm) for one or two 5-minute blending cycles. Table 2-2 shows the aerogel preparation under the eight tested conditions.

Table 2-2. Blending conditions for optimization of aerogel cutting procedure for aerogel (numbers are for further reference in next section).

		Cutting Time	
		5 min	10 min
Fiber to dispersion liquid ratio	800 mg/100 mL	1	5
	600 mg/100 mL	2	6
	400 mg/100 mL	3	7
	200 mg/100 mL	4	8

To check the quality of the final product, the aerogel's structure (flexibility/fragility/homogeneity) was tested visually, and its filtration efficiency was tested using SMPS instrument. Based on the aerogel's physical properties (Figure 2-4) lower ratios (aerogel number 4 and 8) enable more flexibility and uniformity, while blending time does not seem to have influence.

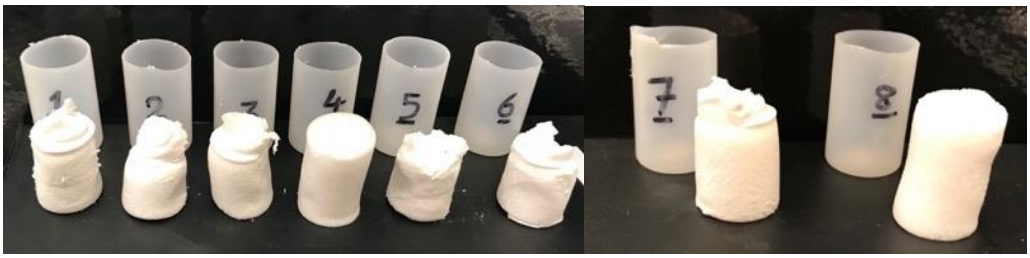

Figure 2-4. Aerogels obtained under different preparation conditions (numbers are based on the conditions explained on Table 2-2).

Furthermore, as shown in Figure 2-5, the results of the filtration efficiency tests showed no significant differences. Ultimately, blending 200 mg fiber/100 mL water for 5 minutes at ~13000 rpm was identified as the optimum blending conditions.

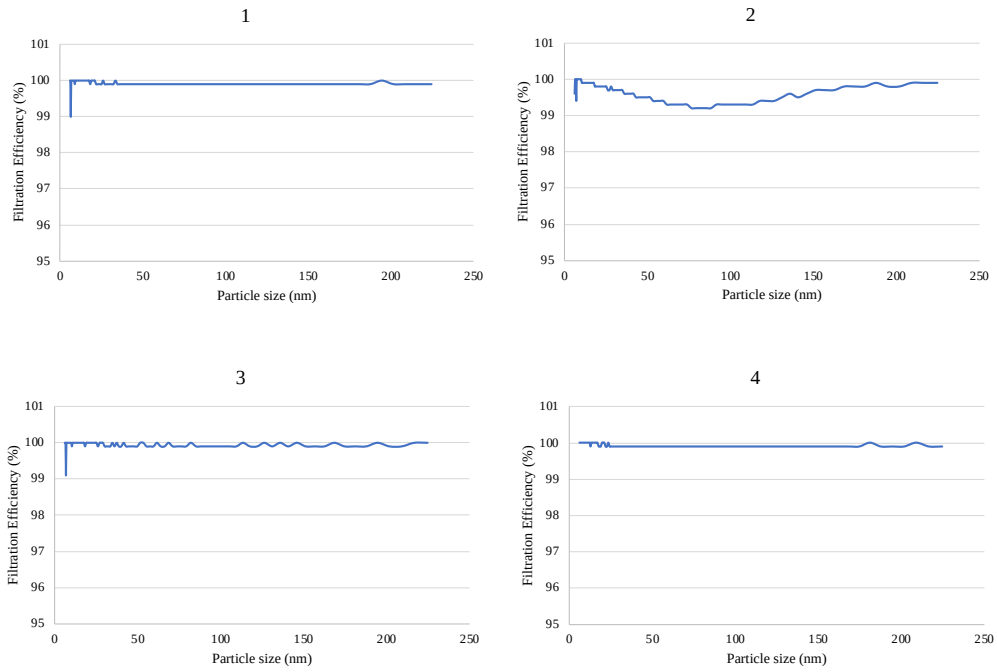

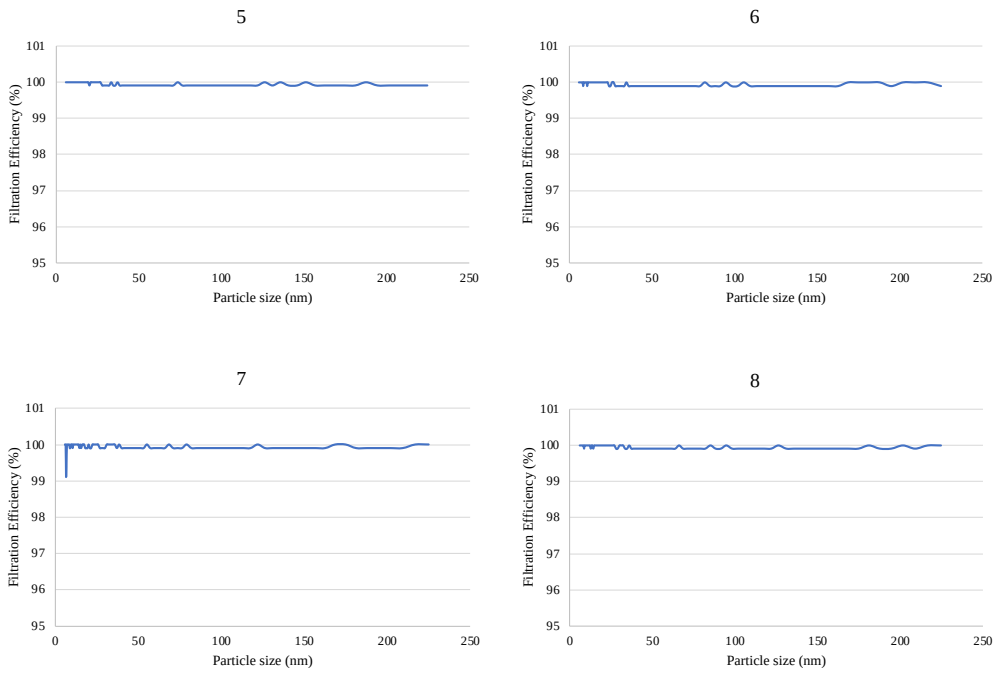

Figure 2-5. Filtration efficiencies obtained from filter (based on preparation conditions listed in Table 2-2).

2.3.2.3 Freeze–drying

To remove the dispersion liquid and obtain the final aerogel, the fiber/dispersion agent suspension must be frozen. After cutting the fibers in a blender, the suspension was transferred to plastic vials. The vials were frozen using both instant freezing with liquid nitrogen and storing them in a freezer at –80 ºC to determine whether the freezing conditions influenced the physical properties of the final aerogel. The frozen suspensions were then transferred to the freeze-drying instrument and left for 24 h. Solidification in freezer resulted in better physical structure.

2.3.2.4 Heating

After choosing the optimal aerogel-preparation conditions, it was necessary to examine the heating procedure that was used. Heating is mandatory because the final aerogel filter would be

packed into the NTD, which would in turn be heated inside the GC injector during desorption. Additionally, heating the aerogel will stabilize it and avoid melting. This transformation can occur as a result of the PAN aerogel shrinking after heating in an air atmosphere, as this will reduce the fiber's diameter, or it can also occur as a result of a chemical reaction (Figure 2-6). Heating also causes the white-colored PAN fibers to become brown in color.

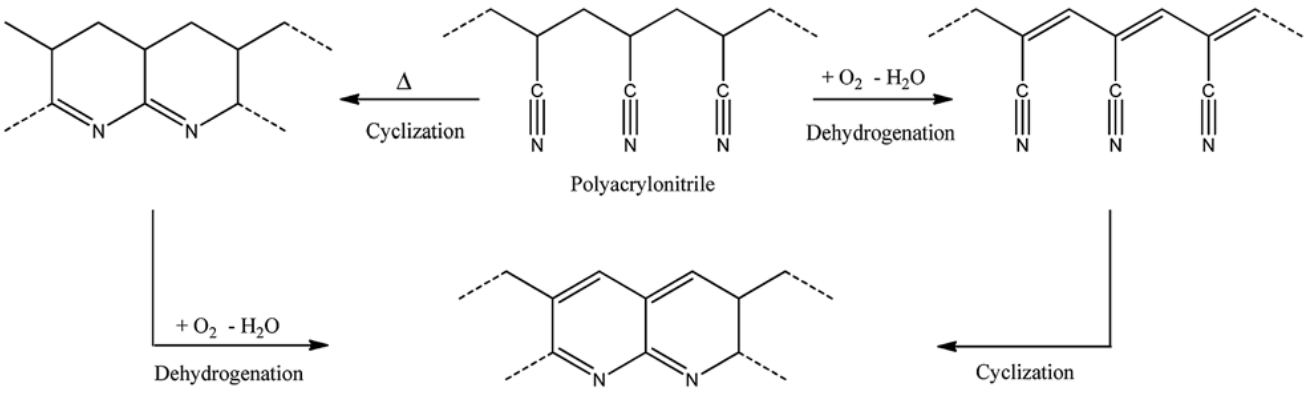

Figure 2-6. Chemical reaction of PAN at high temperature (<300 ºC) under (a) air atmosphere and (b) nitrogen atmosphere (b) [146].

To find the optimum heating conditions two approaches were studied: heating right after electrospinning, and heating after freeze–drying. The first batch of electrospun fibers were heated in an oven at 280 ºC for 2 h prior to cutting in the blender. Once again, different fiber-to-solvent ratios (200, 400, 600, and 800 mg PAN fiber per 100 mL dispersion media) and blending times (5 and 10 minutes) were investigated. The second batch of fibers was heated in an oven at 280 ºC for 2 h after freeze–drying in order to obtain heated brown-colored PAN aerogel (H-PAN). Since heating the fibers after electrospinning did not successfully produce aerogel (Figure 2-7), it was decided that the best approach was to heat the aerogels after freeze–drying.

Figure 2-7. Aerogels prepared from heated fibers (when the fibers were initially heated and then cut, the aerogel structure was not formed).

2.3.3 Needle Packing

The needles used in this study can be categorized into two groups: those packed with aerogel filter (with and without other commercial sorbent particles) (Group I), and those packed only with sorbent particles (Group II). For Group II, extended-tip needles were used to pack particle sorbents into the needles, and springs were inserted before and after the sorbent inside the needle to ensure that the particles remained in place.

The tips of the needles in Group I were initially sharpened to hypodermic tip to facilitate packing procedure (Figure 2-8-a, b). The sharp tips were inserted into the aerogel to extract a small piece, which was then pushed into the needle with small plunger. This procedure was repeated until the filter had reached its desired length. In the conditions where sorbent particles were added into the needle, the needle was first packed with one plug of filter and then sorbent particles were poured into the needle until the desired length had been achieved. Once the desired length had been achieved, another filter plug was packed into the needle. Thus, the sorbent particles are

sandwiched between two filter plugs, which act both as filters and as plugs that keep the sorbent particles inside of the needle. After packing was completed, the sharpened tip was cut and removed, and a cone–shaped tip was fabricated using a metallic grinder (Figure 2-8-c), as this geometry can improve the desorption efficiency of NTDs with narrow–neck liners in the GC injector. A schematic of the final needle structure can be found in Figure 2-8-d.

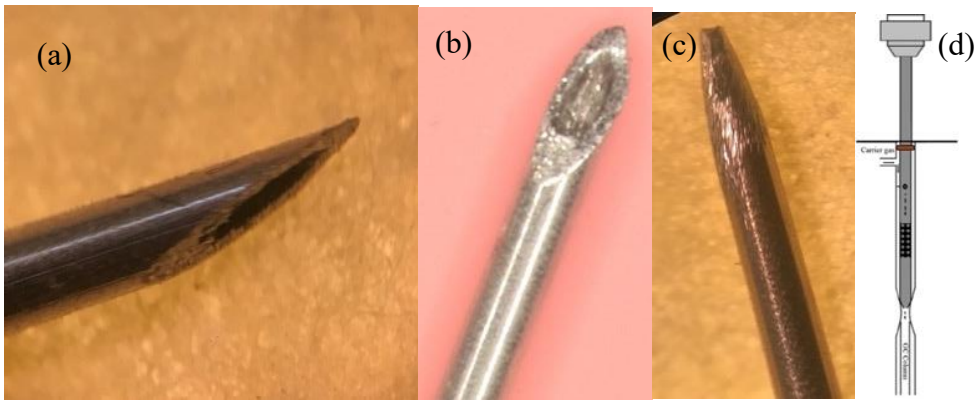

Figure 2-8. (a) Hypodermic needle tips during packing from side and (b) top view, and (c) cone–shaped tip for improved desorption in the final design, and (d) improved desorption by blocking carrier gas passage through narrow-neck liner with cone–shaped needle tip.

The following procedure was used to prepare the filter: electro-spinning of PAN; dispersion and cutting; freezing; freeze-drying; and stabilizing the PAN fibers (Figure 2-1). In brief, the PAN fibers were prepared by electrospinning dissolved PAN in DMF under optimum conditions. For the cutting step, several dispersion liquids and fiber–to–dispersion liquid ratios were tested, with the optimal condition being determined based on the aerogel's final physical properties and/or filtration efficiency. The frozen fiber/dispersion media suspension was freeze-dried to remove dispersion liquid without compromising the structure of the aerogel. Next, the fiber was heated at 280 ºC to stabilize it and prevent any shrinkage and melting inside the needle. For the initial studies, the H-PAN filter was packed inside the needle; in the aerosol analyses, an H-PAN filter with commercial sorbent particles was packed inside the NTD (Figure 2-9). The needle tip was

sharpened to hypodermic shape during packing and then after needle preparation, it was cone–shaped to improve its desorption capabilities during the NTD's final application (Figure 2-8).

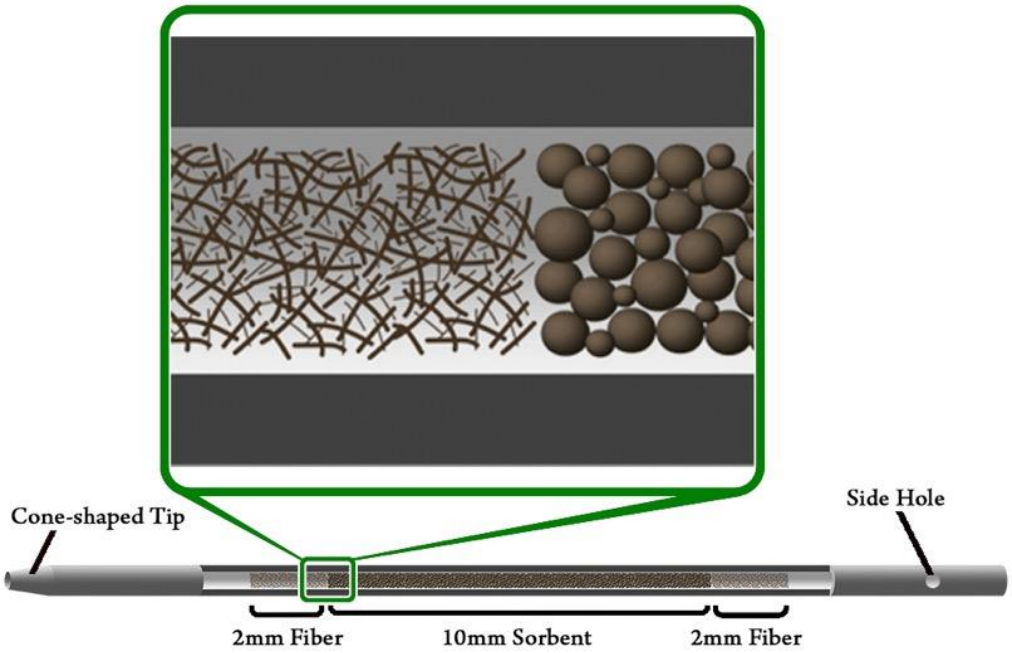

Figure 2-9. Schematic of the final NTD design with stainless steel luer–lock needle packed with extraction phase particles sandwiched between two plugs of aerogel H-PAN filter, equipped side-hole and cone-shaped tip for improved desorption.

2.3.4 Characterization

In order to investigate the properties of the prepared filter, scanning electron microscopy (SEM) was employed to visualize the fiber. Thermogravimetric analysis (TGA) was applied to analyze the thermal behavior of the PAN and H-PAN fiber. The fibers were heated to between 25–600 ºC at 10 ºC min^{-1} in an N_2 atmosphere, with weight loss being measured as a function of temperature.

2.3.5 Background analysis

A freshly prepared needle was packed with 2 mm of H-PAN filter in order to assess the background from the H-PAN filter. The packed needle was then conditioned in a GC injector at 280 ºC for 30 min, at which point the temperature was increased to 300 ºC while the conditioning continued for another 30 min. To study the background from filter, the injector temperature was set to 320 ºC, the needle was inserted into the GC inlet (without sampling), and desorption was performed for 3 min. This procedure was repeated several times at different temperatures. To ensure a robust comparison, system background was assessed by running the instrument in the same conditions and without any injection. The GC column temperature program began at 40 ºC and was increased to 300 ºC in order to cover all possible temperature ranges.

2.3.6 Quality of filter

With the fiber having been prepared, it was then necessary to study the quality of the filter. Optimal performance is achieved by maximizing particle trapping and minimizing pressure drop across the filter. Given these factors, quality factor (Q_f) is defined as:

$$Q_f = -\frac{\ln(1-E)}{\Delta p} \qquad \text{Eq. 2-1}$$

In this equation, E refers to collection efficiency and Δp is the pressure drop across the filter. To calculate the quality factor and study how it changes over time, prepared H-PAN filter was cut into cylinders in accordance with ASTM D6830-02(2016). The filtration efficiency was calculated based on detector particle count before and after inserting the filter into the instrument, while the pressure drop was measured by connecting fittings on either side of the filter holder. Pressure drop

was monitored and recorded during the experiment. To study how filtration efficiency changes over long sampling times, a particle generator was used to continuously introduce particles into the filter bed, with filtration efficiency being measured every 2 h, and pressure drop being recorded accordingly. This procedure was conducted for 12 h, and was repeated 3 times.

2.3.7 Filtration efficiency studies

The filtration efficiency of the prepared filters was evaluated using a scanning mobility particle sizer (SMPS). In this instrument, particles (5-225 nm) are generated in particle generator and then transferred into an electrostatic classifier to be sorted based on size. After being sorted, the particles are counted by a condensation particle counter. Filtration efficiency was determined by inserting a filter into the instrument (after the particle generator and before the particle classifier), with the difference in particle count before and after insertion into the system being taken as the measure of filtration efficiency.

To optimize filter preparation, fibers were packed in rather large tubing (I.D.= 4 mm, Length= 90 mm), which was in turn packed (10 mm) with prepared filter aerogel. The particles were then counted and compared to the blank particle count obtained prior to inserting the filter.

To check if small needles provided the same filtration efficiency, prepared aerogels were packed (packing length= 2 mm) of commonly used gauge size in NTD: 19 G (with O.D.= 1.067 mm) and 22 G (O.D.= 0.717 mm applicable inside normal GC injectors). The main problem with using small packed tubing in conjunction with an SMPS is that small needles are incapable of providing the high flow rate required by the instrument. To solve this problem, multiple needles were packed in parallel to compensate for the low flow rate afforded by single tubing. Specifically,

4 of the larger needles (19 G) and 6 of the smaller needles (22 G) were packed in parallel to this end (Figure 2-10). The same procedure was employed to investigate the filtration efficiency of the final needles, which were packed with both aerogel filter plugs and sorbent particles. To this end, multiple needles were prepared by packing both filter plugs (2×2 mm) and 20 mm of sorbent particles between them (Figure 2-9). Their filtration efficiency was then measured using both solid NaCl particles and oil droplets as analogues for solid and liquid droplets in aerosol samples.

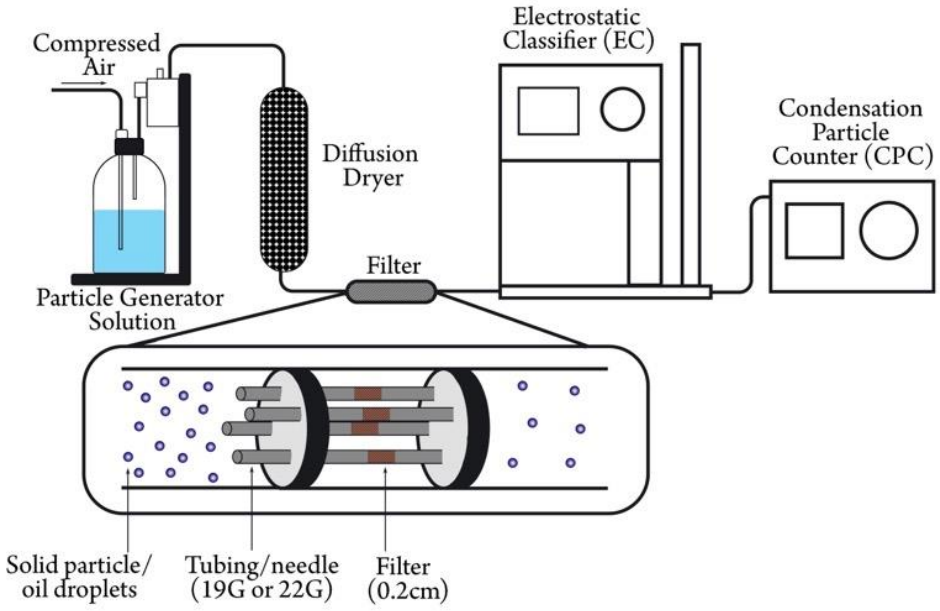

Figure 2-10. SMPS instrumentation setup for particle analysis. The particles are produced in the required size range, sorted by size and counted by the counter. The difference in particle count in the absence and presence of filter is considered as filtration efficiency.

2.3.8 Flow rate measurement

An appropriate filter for an NTD should offer permeability that is sufficient to enable acceptable flow rate and dynamic sampling. To compare the performance of the prepared aerogel with commercially available sorbent particles, different NTDs were prepared with 20 mm of Carboxen (CAR), divinylbenzene (DVB), Tenax (TNX), and hydrophilic-lipophilic balance

(HLB) particles, and two additional NTDs were prepared with either 2 or 20 mm of H-PAN. Nitrogen was passed through the needle at a constant pressure, and the output flow rates were measured and compared.

2.3.9 Filter extraction efficiency and breakthrough volume

The prepared H-PAN aerogel's primary function is as a filter that traps particles; however, its polymeric structure also allows it to function as an extraction substrate. To investigate the H-PAN aerogel's extraction efficiency and breakthrough volume (BTV), McReynolds compounds with different chemical properties (benzene, 2-pentanone, 1-nitropropane, pyridine, 1-pentanol, and octane) were selected. For this study, needles packed with 20 mm of CAR, TNX, DVB, HLB, and H-PAN, as well as 2 mm of H-PAN (2 mm was found to be the optimum packing length for needle preparations, which will be discussed later) were used to extract McReynolds compounds, with constant gas concentration and flow rate being provided by a gas generator system. The permeation tubes were filled with McReynolds compounds and left in the heating chamber of the gas generator, and the generator's output was passed through a 1-L gas sampling bulb. An extraction time of 20 min was selected to assess extraction efficiency. For BTV, different volumes of sample were drawn through the NTD using a pump (flow rate= 10 mL min^{-1}). To determine break-through volume, sample volume was increased until the extraction signal remained constant.

2.3.10 Minimum stable packing length

This study sought to find the minimum packing length that could be used while still maintaining optimum flow rate and filtration efficiency. To this end, the stability of needles packed at different lengths (1, 2, 4, 6 mm) was tested by performing extractions of toluene, ethylbenzene,

and o-Xylene (TEX). Sampling was performed in an aquatic headspace using a 5 mL min^{-1} flow rate for 10 minutes and an analyte concentration of 200 µg L^{-1}. The same procedure was repeated for 12 days over a 2 months span while monitoring the extraction efficiency. In total, 94 extractions were performed with filter over this time period in order to assess its stability over time.

The same gas generator system was employed to determine whether the presence of the particles altered the filter's extraction efficiency/stability, but the tubes in these tests were filled with benzene, toluene, ethylbenzene, o-xylene, and (BTEX). The SPMA particle generator added particles at a rate of 10^8 particles per second. Both the aerosol particles and generated gas were connected to a 100-L plexiglass box equipped with a fan to mix the particles and gas samples prior to sampling. The output from the plexiglass box was passed through a 1-L gas sampling bulb for sampling via the septa (Figure 2-11). Sampling was conducted at 5 mL min^{-1} for 2 h, with a total of 15 extractions (total of 9 L sample was drawn to needle) being performed.

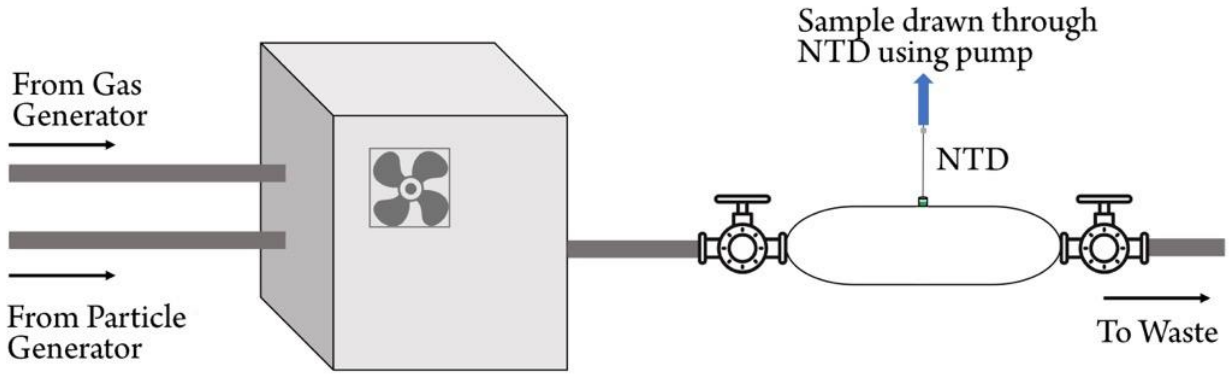

Figure 2-11. Sampling setup from glass bulb with plexiglass box for pre–mixing particles and gases and then transferring the mixture into the glass bulb for sampling with NTD.

To ensure that the particle and gas samples were both present inside the gas sampling bulb, the waste output was connected to the SMPS, and the particle counts were compared to those obtained under normal instrumental conditions. No significant signal drop was observed, confirming that there was no leak in the connection. In addition, no significant difference was observed when the BTEX signal was compared to the expected standard concentration signal.

2.3.11 Proof of concept and applications

In brief, eucalyptol was chosen as a model analyte, and was analyzed by subjecting breath samples from a healthy volunteer who had been chewing eucalyptus gum to NTD and TFME. Sampling was performed in breath bags and the concentration of eucalyptol was measured with two methods (NTD and TFME). To check whether the measurements were influenced by the presence of droplets, sampling was repeated while the participant was wearing a silk mask or a 3–layered mask. These masks were chosen based on previous findings related to particle trapping efficiency, which identify them as exemplars of strong and weak masks.

2.4 Results and discussion

2.4.1 Optimization of filter preparation conditions

The optimum concentration for the PAN fibers was found to be 8% w/v in DMF. PAN fibers were cut with and without solvent using a freeze–milling instrument; however, the resultant fibers were not uniform in structure, and appeared to be crushed rather than cut. So, fibers were then sliced in a blender at ~13000 rpm for 5 and 10 minutes using different fiber-to-dispersion liquid ratios (methanol, 1,4-dioxane, and water). The findings indicated that water was the most appropriate dispersion media, as it offered uniform and stable suspension up to several months

(Figure 2-3). The use of 5 or 10 min cutting times (even in different fiber to dispersion liquid ratios) did not considerably influence the final physical structure of the aerogel (Figure 2-4), and the filtration efficiency data demonstrated that all aerogels are able to provide sufficient filtration (>99%) for such applications (Figure 2-5). Before freezing, the suspension was shaken for 1 min to obtain a homogenous suspension.

Liquid nitrogen and a freezer set to –80 ºC were tested for solidifying the dispersion media, with the results showing that aerogel frozen with liquid nitrogen was physically less rigid and had a tendency to break during application. Given these results, the freezer set to –80 ºC was used to freeze water in suspension.

Furthermore, the fibers were heated in two steps, prior to cutting or after freeze–drying, with results indicating that the aerogels from the heated fibers (before cutting) did not provide a stable physical structure (Figure 2-7). For further investigations, fibers were heated after freeze–drying.

After optimizing different steps, several fiber–to–dispersion media ratios were investigated (10, 50, 250, 500, and 1000 mg PAN in 100 mL water). The results of these tests indicated that the optimal ratio was 250 mg/100 mL water (Figure 2-12). Lower fiber-to-dispersion media ratios resulted in the structural collapse of the aerogel, while higher ratios also seemed to provide less physical stability.

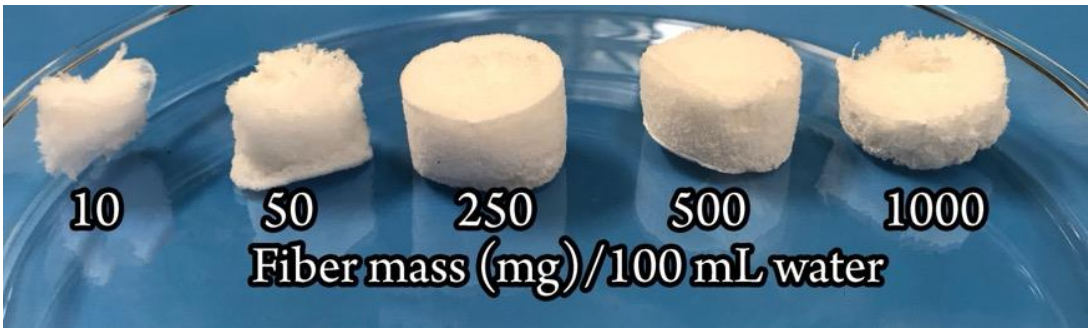

Figure 2-12. Aerogels with different fiber–to–dispersion media ratios.

2.4.2 Optimized Filter Preparation Condition

8% w/v PAN in DMF with a 1.5 mL h^{-1} flow rate was identified as the optimal electrospinning conditions, while an 18 G needle, and a distance of 20 cm from needle to collector were identified as the optimal condition. The aerogel was fabricated by first slicing (level 6 or 13000 rpm) 250 mg PAN/100 mL H_2O for 5 minutes, and then shaking the suspension in a shaker for 1 minute. After shaking, the suspension was left in a freezer at –80 ºC until completely frozen, and then transferred to the freeze–dryer where it was left for at least 24 h to obtain PAN aerogel (Figure 2-13 a). After 24 h in the freeze-dryer the PAN aerogel was removed and heated at 280 ºC for 2 h. The resultant brown H-PAN aerogel (Figure 2-13 b) was then packed in the NTD for extraction studies.

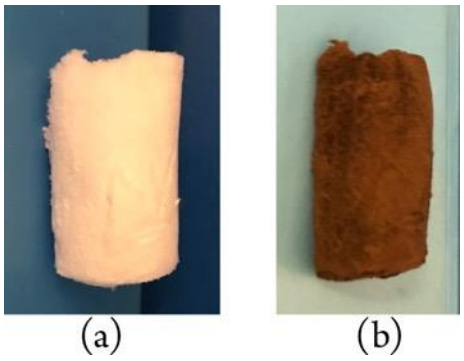

Figure 2-13. PAN aerogels in optimized conditions before (a) and after (b) thermal treatment (H-PAN) in oven at 280 ºC for 2 h.

2.4.3 SEM and TGA results

After the fibers had been prepared, it was necessary to characterize their physical properties. The electrospun PAN aerogel was visualized using an SEM micrograph before and after heating (Figure 2-14). The SEM micrographs indicate that the diameters of PAN and H-PAN are around 300-400 nm. Generally, the structures of the fiber and aerogel do not change after heating, which shows that the fiber is thermally stable at high temperatures.

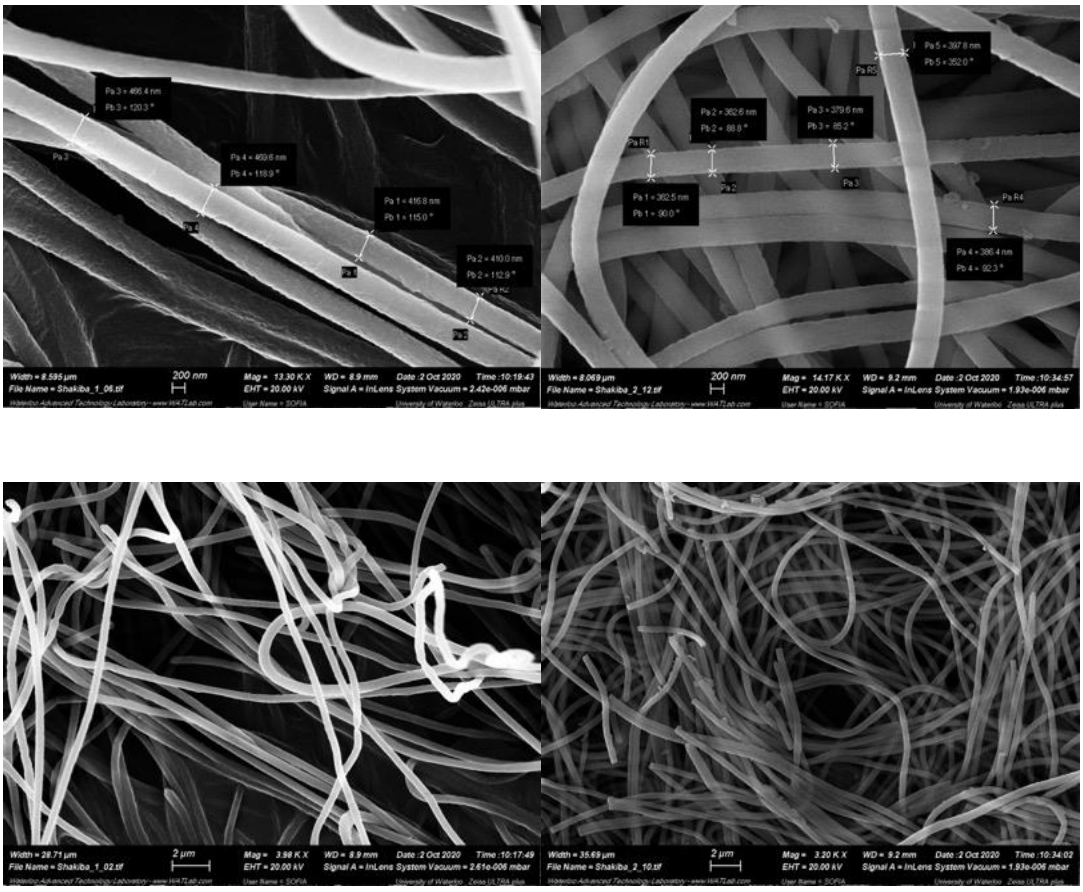

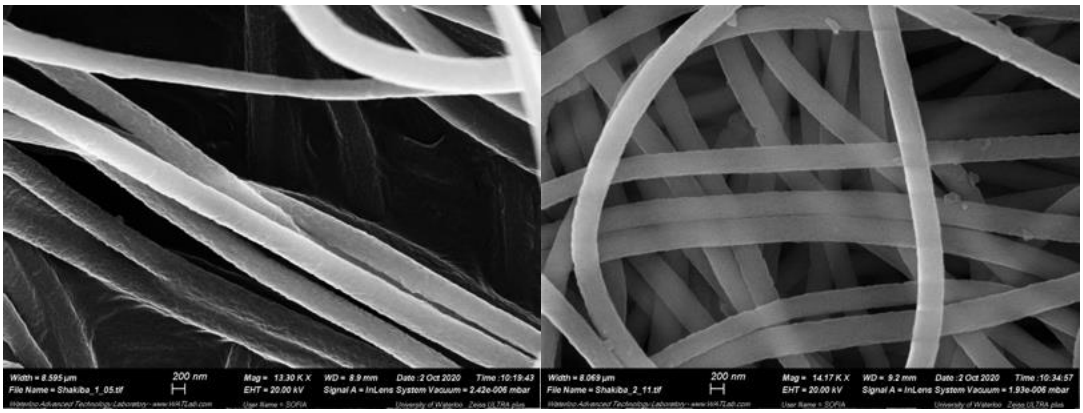

Figure 2-14. SEM micrographs from electrospun PAN fibers (left column) and H-PAN (right column).

Previous data [140,141,139] for the thermal treatment of PAN fibers indicates that heating the fibers to 300 ºC will improve their physical strength due to a stabilization/cyclization process, which will in turn prevent them from melting during desorption in the injector of the GC. This transformation is based on a chemical reaction (Figure 2-6-a) that occurs at high temperatures in an air environment. These data, along with the aerogel preparation procedure, enables the conclusion that the proposed filter can be used in a GC injector with temperatures as high as 300 ºC.

The thermal stability of PAN and H-PAN were further studied using TGA. The results of the TGA analyses for both aerogels (Figure 2-15) were obtained under an N_2 atmosphere, which causes PAN fibers to undergo cyclization (Figure 2-6-b). This reaction is the result of a side-chain rearrangement that does not change the polymer mass. In brief, while PAN chains undergo a chemical reaction, the resultant changes cannot be captured by TGA data because the molecular weight of polymer remains unchanged.

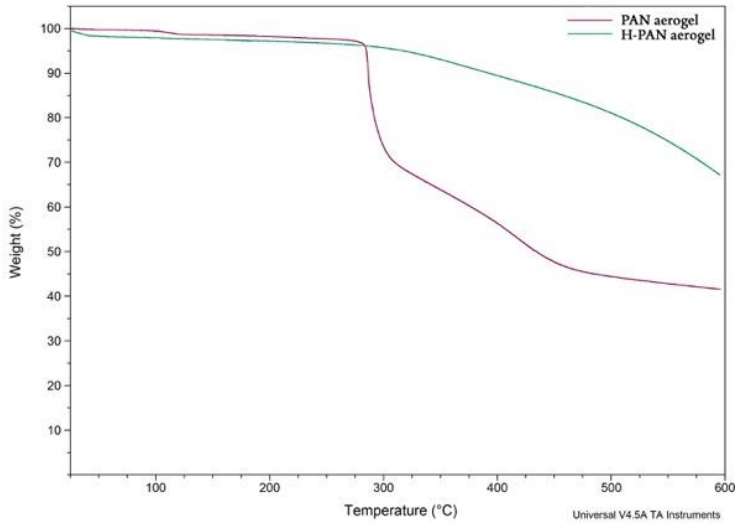

Figure 2-15. TGA analysis thermogram obtained from heating PAN aerogel (purple) and H-PAN aerogel (green). The fibers were heated to between 25–600 ºC at 10 ºC min^{-1} in an N_2 atmosphere and the weight loss was measured accordingly.

The obtained results indicate that both aerogels are relatively stable up to 300 ºC under these conditions. At higher temperatures the PAN fiber starts to lose mass at a higher rate; however, this weight loss occurs much more slowly for H-PAN as a result of undergoing a stabilization process. Both aerogels maintain a large percentage of their weight up to 600 ºC, as carbon fiber, which is highly thermally stable, forms at these temperatures.

2.4.4 Filter background

To test whether the filter was releasing analytes during desorption and adding background peaks to the chromatogram, the needle was packed with an H-PAN filter and desorbed in a GC injector at 320 ºC without sampling. The results showed no additional peaks (Figure 2-16-a). For comparison, a chromatogram was obtained from the instrument in similar conditions without any injection (Figure 2-16-b). The results of this test indicated that the prepared H-PAN filter provided a clean background for analysis and did not produce any interfering peaks during desorption.

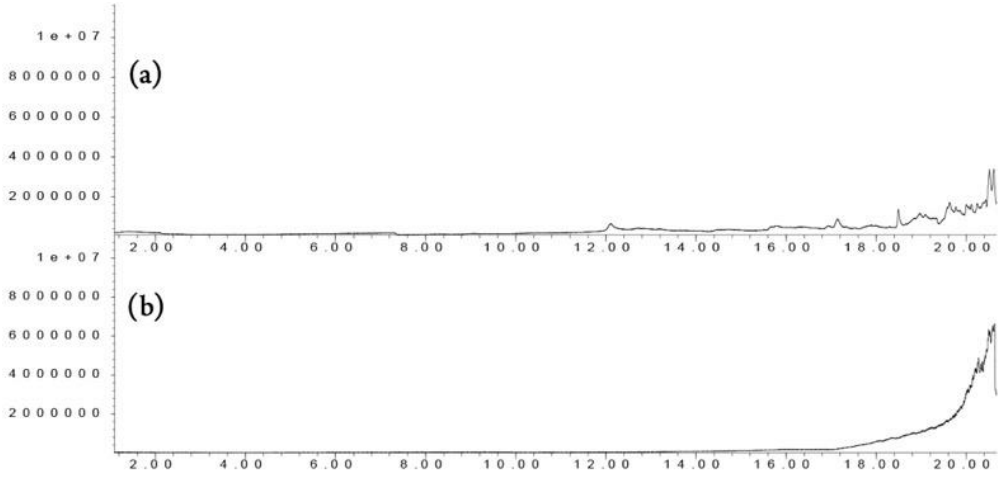

Figure 2-16. (a) Filter-packed NTD GC chromatogram background from injection of needle packed with H-PAN filter in GC injector at 320 ºC without sampling and (b) instrumental GC chromatogram background in similar conditions without any injection.

2.4.5 Filter quality factor over time

To assess the quality and stability of the filter over prolonged exposure to particles, the filter bed was fed with particles for 12 h, with filtration efficiency and pressure drop being measured every 2 h. The obtained results (Figure 2-17) showed that the filter's quality factor was acceptable in comparison to previously reported values (~0.07-0.1 Pa^{-1})[150,151].

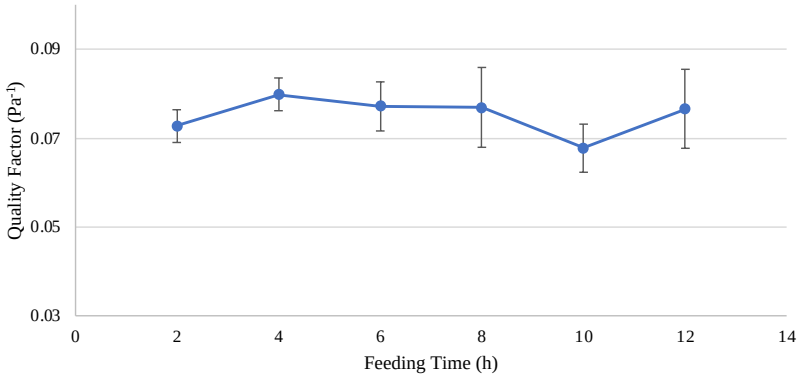

Figure 2-17. Quality factor (in Pa^{-1} with standard deviations) of H-PAN filter over 12 h, for each point, filtration efficiency and pressure drops were measured every 2 h.

Furthermore, the filter's quality factor did not decrease substantially after being fed with solid particles for 12 h, thus confirming its high capacity. These results confirm that the developed filter can be used to trap particles over a long period of time. The filter's high capacity is especially important when working with samples with low concentrations of analytes that require high sampling volume. Raw average data for particle trapping efficiency and pressure drop across the filter are provided in Table 2-3.

Table 2-3. Quality factor of H-PAN and pressure drop across the filter over time (average values are provided here).

Feeding Time (h)	E	Δp (Pa)	Qf (Pa^{-1})
2	0.99	99	0.073
4	0.99	99	0.080
6	0.99	106	0.078
8	0.99	109	0.077
10	0.99	123	0.068
12	0.99	119	0.077

2.4.6 Minimum packing length for NTD

A series of extractions were performed using various filter packing lengths in order to determine the minimum stable packing length. The results of these tests revealed that a length of 1 mm was unstable in extraction/desorption conditions, but lengths of 2, 4, and 6 mm provided repeatable results. Since the goal of this experiment was to find the minimum stable packing length, 2 mm was selected. Next, a needle packed with 2 mm of aerogel H-PAN filter was used to extract TEX over a period of 12 days. This needle was reused 94 times over the course of this experiment. The extraction signals in Figure 2-18 show the H-PAN filter's high stability at high

temperatures and sample flows. An arbitrary unit is employed for easier comparison and visualization of the data; however, the RSD values were obtained from the original data.

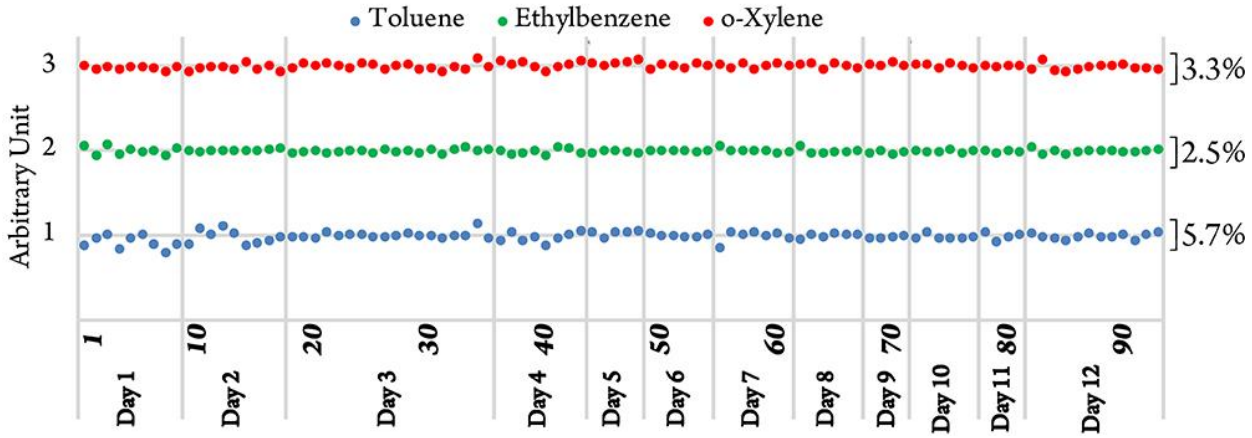

Figure 2-18. Extraction signals (in arbitrary units) from multiple extraction of TEX using an NTD packed with 2 mm of H-PAN. Extraction was performed in an aquatic headspace using a 5 mL min^{-1} flow rate for 10 minutes in 200 µg L^{-1}. The procedure was repeated for 12 days over a 2 months span.

2.4.7 Filtration efficiency

Given the SMPS's flow rate limitations, large-diameter tubing was used in the initial filtration efficiency studies. The results showed that the particle count decreased significantly in both the PAN- and H-PAN-packed filters, with both showing filtration efficiencies of more than 99% (Figure 2-21-a). This result exemplifies the prepared aerogel's high filtration capacity, and confirms that high temperature treatment does not affect filtration efficiency. Reference background particle counts (Figure 2-19) and particle counts after inserting the filter–packed tubing into the instrument (Figure 2-20) are provided.

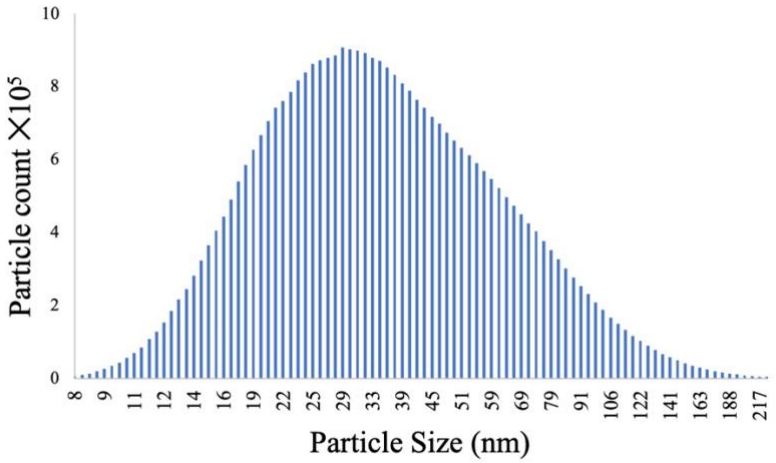

Figure 2-19. Instrumental background particle counts from instrument (without filter).

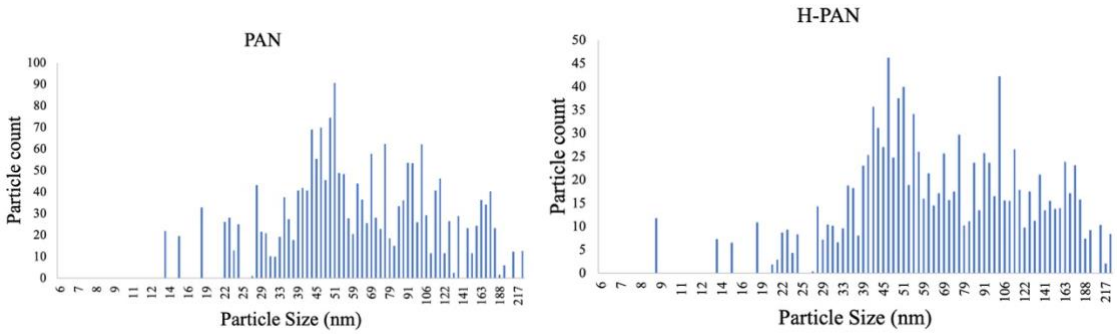

Figure 2-20. Particle count from instrument after insertion of PAN and H-PAN filters into SMPS instrument.

Since the experiments using H-PAN meets the requirements of a high-quality factor, this aerogel will be used henceforth. 22 G and 19 G needles packed with 2 mm of H-PAN were inserted into the SMPS to evaluate filtration efficiency. For this reason, the particle generator was set to generate 5-225 nm NaCl solid particles. As the data in Figure 2-21-b shows, aerogel packed into NTD needles also yields high filtration efficiency. The same procedure was also repeated for oil droplets (Figure 2-21). The only difference between these experiments was the particle generator source, which was set to generate oil particles of the same size.

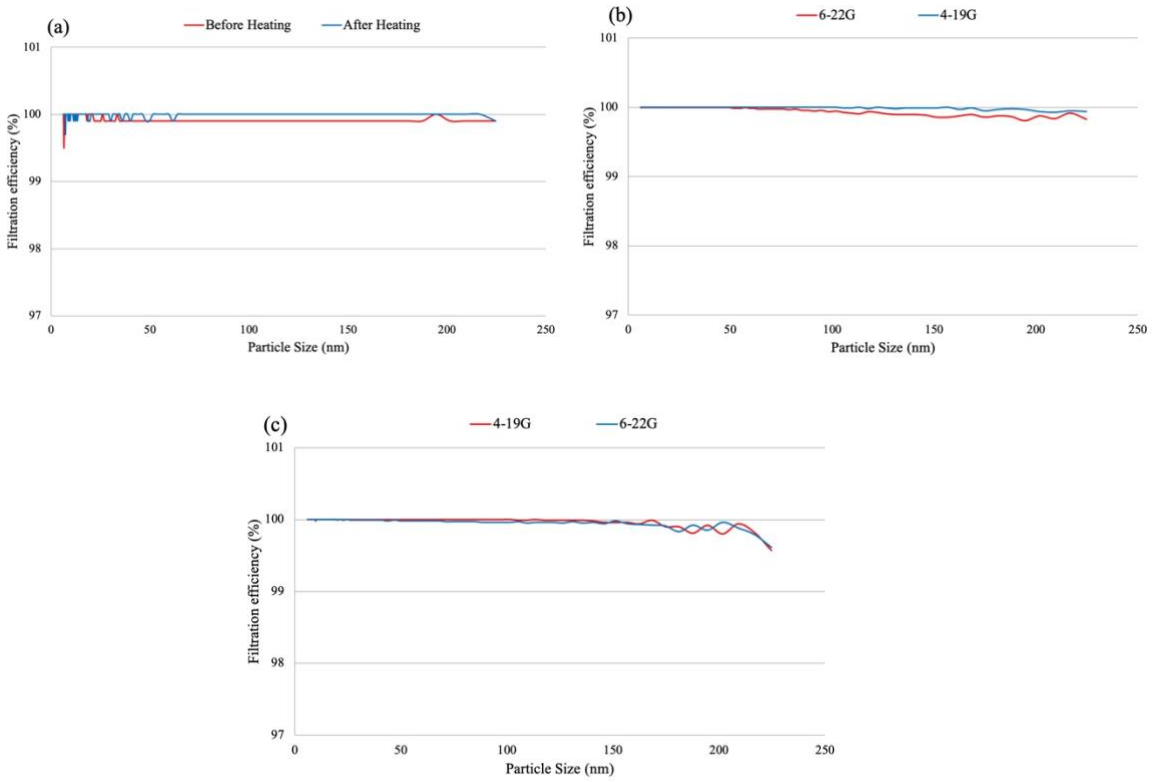

Figure 2-21. (a) Filtration efficiency of large tubing packed with PAN and H-PAN filter, (b) Filtration efficiency of needles packed with H-PAN filter for trapping solid NaCl particles, (c) Filtration efficiency of needles packed with H-PAN filter for trapping liquid oil droplets.

The results confirmed that the prepared H-PAN aerogel filter provided high filtration efficiency (>99%) for both solid particles and liquid droplets. The filtration efficiencies illustrated in Figure 2-22-a were obtained using needles packed with commercial sorbent (20 mm). As can be seen, the filtration efficiency can be as low as 50% in the absence of a filter, but >99% when filter is inserted (Figure 2-22-b), thus making the aerogel filter suitable for filtration applications. The aerogel filter provided filtration efficiency that was > 99.9% the same as commercial filters [152]. An enlarged version of graph is provided in Figure 2-22-b, in order to clarify the values above 99%.

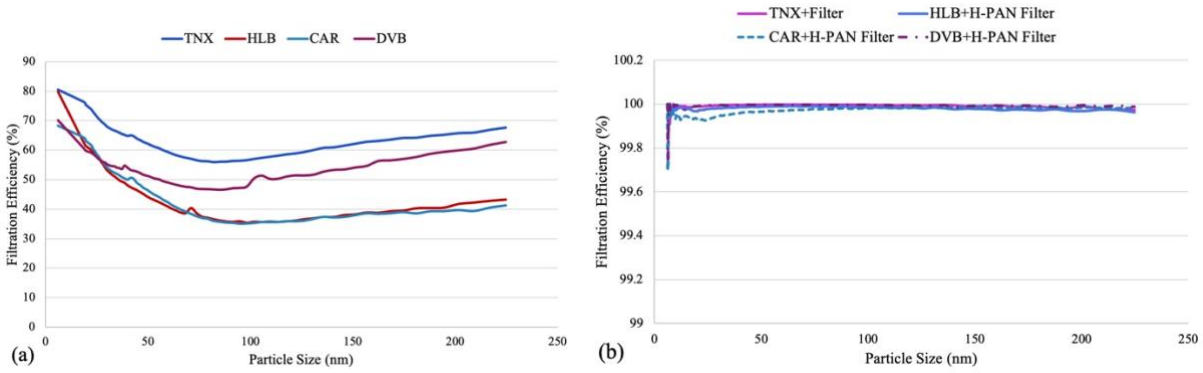

Figure 2-22. (a) Filtration efficiency of needles packed with commercial sorbent particles with and without H-PAN filter, (b) filtration efficiency for needles packed with sorbents and H-PAN filter (for improved visualization, y-axis in chart b was zoomed).

2.4.8 Flow rate measurements

To compare the aerogel filter's permeability to that of commercially available sorbent particles, needles were packed with 20 mm of different commercial sorbent particles, as well as 20 mm and 2 mm of aerogel H-PAN. Output flows were measured using a flowmeter under similar conditions for all needles. A list of these conditions is provided in Table 2-4. The resultant flow rates indicate that the aerogel's permeability is comparable to previously developed sorbents at similar lengths. As expected, the flow rate was higher at the optimum packing length (2 mm), and therefore cannot be a limiting factor for extraction purposes.

Table 2-4. Flow rates obtained from needles packed with 20 mm of commercial sorbents and H-PAN aerogel and 2 mm packed H-PAN.

Packing Material	Flow rate (mL min^{-1})	Packing Material	Flow rate (mL min^{-1})
20 mm CAR	17.5	20 mm DVB	13.2
20 mm HLB	15.6	20 mm H-PAN	13.5
20 mm TNX	14.7	2 mm H-PAN	45.2

2.4.9 Extraction efficiency

Although the goal of this research was to develop an aerogel that would function as an ideal filter in NTDs, it was still essential to investigate its extraction efficiency. Filter plugs with high filtration efficiency and low extraction capacity are desirable, since in the final NTD, sorbent particles are responsible for extraction purposes, and lower extraction by the filter prevents interference with sorbent function. To assess the filter's extraction efficiency, McReynolds compounds were chosen based on their chemical properties and their potential inter–molecular interactions during extraction. In Figure 2-23, the extraction capacity of the 20 mm H-PAN filter is approximately 7-21% of commercial sorbents at a similar length. The extraction efficiency of the small plug packing size of H-PAN (2 mm) decreases to 0.6 - 4% of the commercial sorbents. These low extraction capacities are appropriate for filtration applications.

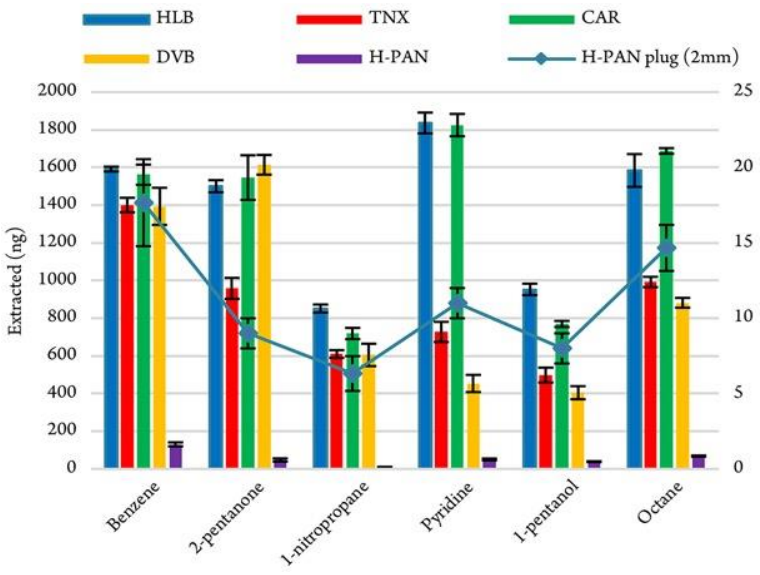

Figure 2-23. Comparison of extraction efficiencies obtained using needles packed with 20 mm of commercial sorbents and H-PAN aerogel as well as needle packed with 2 mm of H-PAN. As a result of difference in the scale for extracted nanograms for needle packed with 2 mm of H-PAN, this data is shown on the secondary (right) axis. Extraction was performed 20 min with flowrate = 10 mL min^{-1} from gas generator.

Breakthrough volume (BTV) measurements are another important factor to consider during NTD development. To assess BTV, a stable flow of gas–phase analytes was pumped into the NTD bed at varying sampling volumes until the BTV was reached. For NTDs with filters, low extraction efficiency, and consequently low BTV, is desirable. Table 2-5 presents the BTV results for the needles packed with 2 mm and 20 mm of H-PAN, as well as those for various commercial sorbents.

Table 2-5. Breakthrough volume (mL) of McReynolds compounds with different commercial sorbents and H-PAN filter

Analytes	20 mm TNX	20 mm CAR	20 mm DVB	20 mm HLB	20 mm H-PAN	2 mm H-PAN
Benzene	573	509	593	575	105	41
2-pentanone	531	1198	585	1020	66	37
1-nitropropane	568	540	590	498	75	34
pyridine	536	1176	587	1267	76	23
1-pentanol	581	502	603	658	82	39
octane	553	1087	584	1094	51	30

According to the obtained results (Figure 2-24), the BTV value for the H-PAN filter was much lower than the value for the commercial sorbents at the same packing length. Similarly, the H-PAN plug packed to 2 mm also returned lower BTV values, which indicates that it does not effectively retain free volatile analytes. Rather, these analytes are extracted by the sorbent, while particles are trapped in the filter.

2.4.10 Particle trapping behavior

While the data for multiple extraction point revealed the filter stability in extraction/desorption conditions, its functional stability must be demonstrated in the presence of particles in aerosol samples. This is especially important because particle trapping can clog the

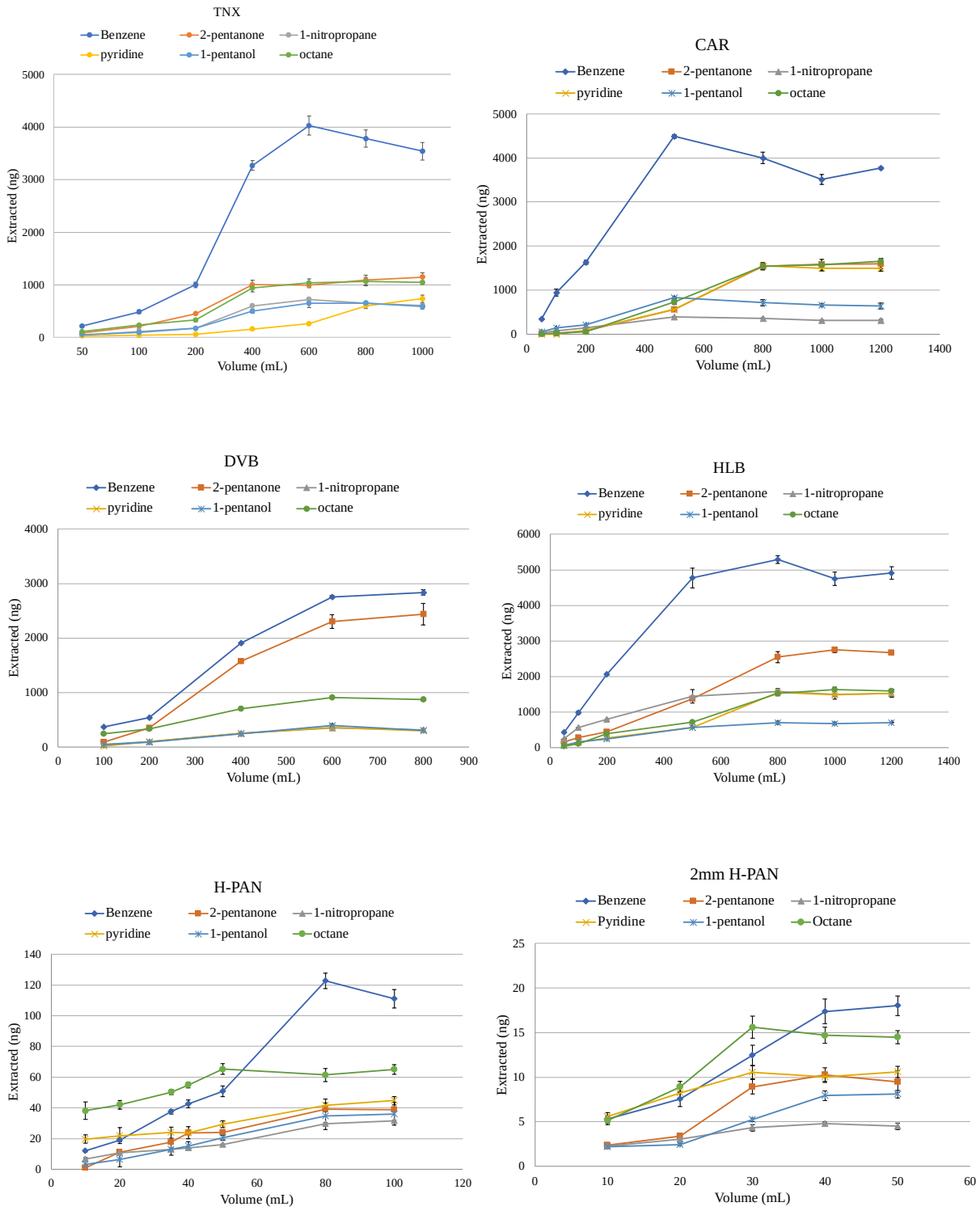

Figure 2-24. BTV from needles packed with 20 mm of commercial sorbents, H-PAN or 2 mm of H-PAN. Extraction was performed with flowrate = 10 mL min^{-1} from gas generator by increasing the sampling volume.

filter input, which can result in decreased extraction due to the resultant reduction in the sampling flow rate. Multiple BTEX extractions in the presence of NaCl nanoparticles provided repeatable results (Figure 2-25). These data confirm that multiple cycles of particle trapping via desorption will not clog the filter, thus allowing it to produce reproducible data in aerosol environments. Arbitrary units were used to enable easier comparison and visualization of the data; however, the RSD values were obtained from original data.

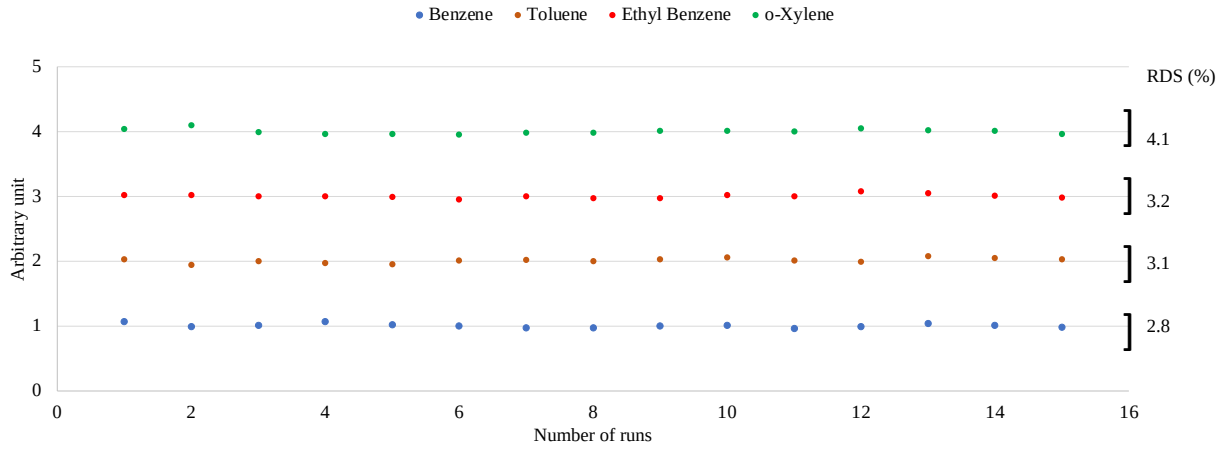

Figure 2-25. Extraction signals (in arbitrary units) from multiple extraction of BTEX in the presence of solid particles in the sampling matrix. The extraction for each point was conducted at 5 mL min^{-1} for 2 h, with a total of 15 extractions.

2.4.11 Proof of concept and application of filter

NTD and TFME were employed to analyze breath samples to verify the above-reported findings, and to showed that these methods produce different results due to their different filtration properties. Breath samples were chosen as the matrix for this study, as they provide an aerosol environment consisting of abundant small droplets generated in the human respiratory system. One health volunteer who had been chewing eucalyptus gum provided samples in a number of different conditions: without a face mask, with a 3-layer face mask, and with a silk mask. Samples were analyzed separately by NTD and TFME. For breath analysis, a healthy volunteer was asked to

chew a piece of eucalyptus gum (purchased from local market) for 30 minutes, and then to provide a breath sample by blowing into a breath-sampling bag. Additionally, samples were acquired while the volunteer was not wearing a mask, or was wearing either a 3-layered mask or a silk mask. A standard gas sample was prepared in a 1L glass gas sampling bulb for calibration. The bulb was washed with methanol, dried, and then vacuumed with a pump. After vacuuming, 1 μL pure standard of eucalyptol was injected into the glass bulb to obtain 146 ppm standard. Different volumes of standard gas sample were drawn with a gas–tight syringe and spiked into blank breath samples to produce the desired eucalyptol concentrations. A linear dynamic range of 1.2– 490 μg L^{-1} was calibrated with each method separately. For NTD, breath samples were drawn through a needle with a flow rate of 10 mL min^{-1}. For TFME, extraction film was inserted and maintained inside the breath bag for 30 minutes in order to reach equilibrium. After extraction, the devices were transferred into the GC desorption inlet and separated using the temperature program detailed in Section I. It is worth noting that the retention times (depicted in the following chromatograms) for TFME and NTD were slightly different for eucalyptol, as each of them were analyzed in separate instruments. The results of these experiments are shown in Figure 2-26.

Eucalyptol was selected as a model analyte for proving the concepts and claims documented in this paper. The obtained results indicated that NTD detected significantly higher concentrations of eucalyptol compared to TFME in the no-facemask samples, the difference between the two methods decreases for the data obtained when the volunteer wore a silk mask, as silk masks are considered to be weak shields against droplets with filtration efficiencies around 50% [153].

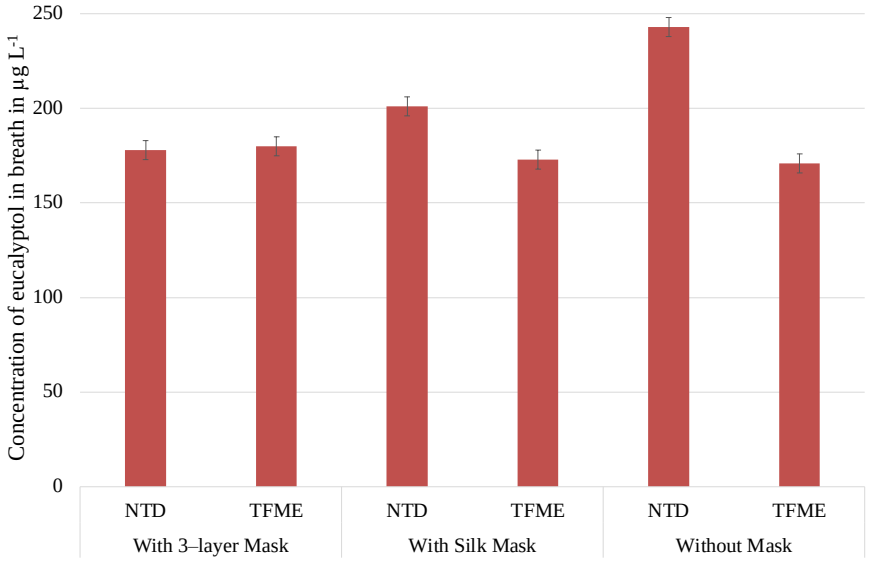

Figure 2-26. Concentrations of eucalyptol analyzed with NTD and TFME for samples given with and without a face mask from a healthy volunteer.

However, the concentrations detected by both methods for the samples captured through highly efficient masks were quite similar. It can be explained as follows; this result indicates that the higher concentration of eucalyptol extracted by NTD in the "no-mask" breath sample was the result of capturing droplets that contained dissolved eucalyptol. This is the reason for similar concentrations when breath samples were obtained using a 3–layered face mask (filtration efficiency > 99%), as the droplets are blocked in face mask and were not present in sampling bag. In contrast, the weak silk face mask was able to block approximately half of these droplets, which is reflected in the results. Based on the results, it is safe to say that the 3–layered face mask successfully blocked all of the droplets, which further indicates that eucalyptol is only present in breath samples in free format. In this case, only free gas–phase eucalyptol is available for extraction with NTD; however, in all cases, TFME is only capable of extracting free analytes (regardless of presence or absence of aerosol droplets). This explains the similarity between the eucalyptus concentrations obtained by TFME in all conditions.

To check the statistically significance of the obtained results, t-test in Microsoft Excel was used. Initially, the results of TFME and NTD for breath sample obtained 3-layered face mask was studied (one-tailed, homoscedastic) and p-value was calculated as 0.4016. When samples obtained though silk mask and without mask were studied, p-values were calculated as 0.0223, and 0.0020 were found, respectively. As p-values shows, for samples with highly efficient face mask, the results of TFME and NTD are statistically similar, while in the case of low efficiency mask and without mask, the concentrations obtained with NTD are statistically higher compared to TFME.

The chromatograms obtained from breath analysis with NTD and TFME with and without face mask are shown in Figure 2-27 and Figure 2-28.

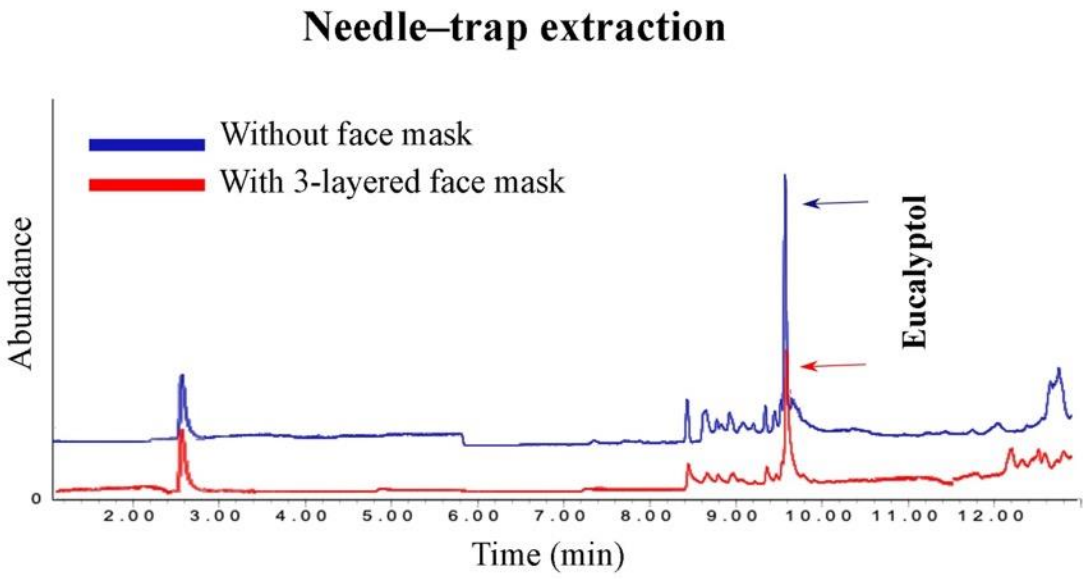

Figure 2-27. Chromatogram from analysis of healthy volunteer breath sample after chewing eucalyptol gum with NTD; sampling conducted either with or without 3-layered face mask.

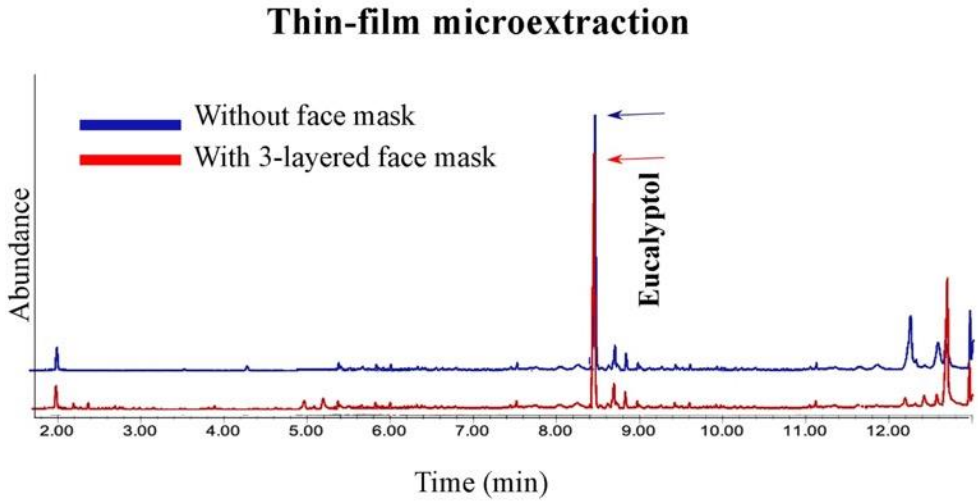

Figure 2-28. Chromatogram from analysis of healthy volunteer breath sample after chewing eucalyptol gum with TFME; sampling conducted either with or without 3-layered face mask.

2.5 Conclusion

This project sought to develop a needle-trap device that can simultaneously adsorb free analytes and capture suspended particles to collect total analytes in free and bound forms. The developed NTD was intended to feature seven key characteristics: 1) high filtration capacity; 2) high adsorption capacity; 3) no interference between adsorption and filtering; 4) high permeability; 5) thermal and mechanical stability; 6) repeatability; and 7) reproducibility. To satisfy these requirements, commercial particle sorbents were packed inside the NTD and sandwiched between 2 filter plugs that had been developed to have high (>99%) filtration capacity for both solid particles and liquid droplets. The developed filter showed high stability (sampling cycle >94) under normal NTD sampling conditions, as well as the high temperature conditions of a GC injector. Notably, quality factor data revealed that the H-PAN filter is usable for up to 12 h of continuous sampling time. The aerogel H-PAN filter features a highly porous structure that makes it an ideal candidate for NTD applications, as it does not limit the sampling flow rate. In addition

to the above–mentioned properties, the H-PAN aerogel plug can hold sorbent particles inside the filter without causing any channeling or flow rate blockages. Furthermore, the breath sample results provided satisfactory data that confirmed the developed NTD's applicability for the investigation of aerosol samples. Additionally, the aerogel filter provided similar trapping performance to the commercial filter. The results of this research indicate that the developed NTD can be coupled with TFME devices to characterize both free components and those present in breath droplets. We believe that these results demonstrate that the developed NTD can replace traditional standard methods for analyzing aerosol samples such as EPA method for determination of PAHs in air quality monitoring studies or EBC method for studying droplets in breath samples.

Filter-Incorporated Needle-Trap Device (FI-NTD) Application: Fragrances

3.1 Preamble

This chapter contains sections that have already published as the cover art and article in Journal of Agriculture and Food Chemistry. All subchapters are included in the article entitled *Determination of droplet-bound and free gas-phase fragrances using a filter-incorporated needle-trap device and solid-phase microextraction technologies* by Shakiba Zeinali and Janusz Pawliszyn, *Journal of Agriculture and Food Chemistry,* 2021, 69, 45, 13657–13667. The contents of the articles are herein being reprinted with permission of American Chemical Society and in compliance with both publisher's and the University of Waterloo policies.

3.2 Introduction

Advances in technology have resulted in the emergence of more office-based jobs, which means that more and more people are spending most of their working hours in indoor environments. Consequently, it is becoming increasingly critical to understand the volatile makeup and the quality of the air in these indoor spaces. Indeed, the recent COVID-19 pandemic, which has confined people around the world to their homes for over a year, has highlighted the significance of fresh air in indoor spaces [154,155]. One common method of creating the perception of improved air quality in indoor spaces is to use scented air fresheners and candles, which introduce fragrances into the air. In addition to candles and air fresheners, fragrances are also used in toiletries, cosmetics, cleaning products (fabric softener, etc.) and a wide variety of

daily consumer products. These compounds can be found as aroma also in food and beverage products.

Unfortunately inhalation of fragrances due to long-term exposure can result in health issues and chronic diseases in people who are highly sensitive to these compounds [156]. In addition, the by-products of fragrances, such as their oxidized form (which can be formed or added to the mixture), can be concerning [149,150].

Fragrances can be allergens [159], photosensitizer, or phototoxins, and they can enter the body through the lung and skin, which can cause systemic problems [160]. Most regulations relating to the use of fragrances focus on how they affect the skin, with little consideration given to how they impact the respiratory and nervous systems. For example, findings have shown that exposure to (±)–limonene can cause an increase in systolic blood pressure, while exposure to (–)–carvone can increase diastolic blood pressure [161]. This is a significant oversight, as airborne fragrant compounds can negatively affect anyone in the general vicinity of the consumed product [162].

From an environmental point of view, fragrances are considered to be air pollutants that deteriorate the quality of air. Furthermore, research has shown that shampoo fragrances, food flavors and aroma, and other odorous compounds often end up in wastewater and groundwater, which is problematic as synthetic fragrances do not biodegrade easily, and most water treatment methods are not designed to process them [163].

An important factor in the toxicology of fragrance compounds is their concentration; as such, cosmetic compounds are subject to their own set of regulations. In Europe, the Scientific

Committee on Cosmetic Products and Non-Food Products (SCCNFP) has identified 24 fragrances that are regulated or restricted by the International Fragrance Association (IFRA). European Union regulations require manufacturers to note the presence of a compound on the packaging if its concentration exceeds a predetermined level (0.001% w/w for leave-on and 0.01% w/w for rinse-off products), while the fragrance concentration in perfumes and deodorants are not properly regulated [115]. However, the reported fragrance compounds' concentration can sometimes be misleading during the study of aerosol samples, as some of these compounds remain inside the aerosol droplets, which can enter one's body. When sprayed products such as perfumes are concerned, the occurrence of fragrance compounds inside the spray droplets is expected, but the studies in this field are commonly focused on gas phase concentration. Therefore, the obtained free gas-phase concentrations will likely not indicate the whole exposure concentration. In addition, there are some less obvious sources of fragrance-containing droplets from daily life including body wash and detergents, textiles and flavors in food and tobacco [164] resulting in the higher daily exposed concentration to fragrance compounds.

The analysis and determination of the fragrant components in a product can be challenging, as these components are often complex mixtures that are largely comprised of essential oils, with tens of different compounds. Moreover, time gaps between the application of a spray and sampling can allow the airborne concentration of the fragrance to decrease such that it is undetectable via direct injection [165]. All of these challenges highlight the need for a sample-preparation step that not only simplifies sample introduction, but also improves sensitivity by preconcentrating compounds on the extraction phase. Researchers have utilized a variety of different methods to determine fragrances, aroma and flavors in different samples, including matrix stir-bar sorptive extraction [166], solid-phase dispersion [116], liquid–liquid extraction [167,168], ultrasound-

assisted solvent extraction [169,170], chemiluminescence [171], ultrasound-assisted emulsification [172], magnetic solid-phase extraction [173]; nevertheless, all of these studies employed concentration in free gas-phase [166,167] or the concentration of polar analytes in a solution [176] thus failing to capture the total exposed concentration of fragrances in the examined aerosol products.

In this study three extraction methods were chosen and compared for measuring the free and total concentration of fragrance compounds in several sprays. For determination of free concentration, thin-film microextraction (TFME) and solid-phase microextraction (SPME) were chosen. Both of these extraction devices were exposed to the sample environment for a specific amount of time to be equilibrated. The analytes (fragrance compounds) can be physically adsorbed on the surface of TFME or SPME based on the interaction between extraction phase and analytes. The amount extracted is proportional to the concentration in the sample. The difference between these two are the mainly surface area and device designs. Based on the low mobility of large droplets in sprays, these methods can represent the concentration in gas phase only.

In the case of total concentration, needle trap device (NTD) was used. In this device, extraction phase and filter are packed inside a needle. The sample was then drawn through the needle with a pump. Unlike TFME and SPME, in NTD, the extraction is exhaustive, which means all analytes can be adsorbed on the extraction phase as long as the breakthrough volume is not reached.

NTD are the best option for determining the total exposed concentration of fragrant and aroma compounds, as their filtration capability enables the trapping of aerosol droplets and the extraction phase adsorb gas-phase analytes. Additionally, drawing sample through packed needle

enhances the filtration efficiency by increasing the mobility of droplets and forcing them to pass through the packed needle with filter. NTDs' droplet-trapping ability is particularly essential for less-volatile compounds that prefer to remain inside water/alcohol aerosol droplets, as trapping them enables their further analysis, which is not possible in TFME and SPME.

The filtration efficiency of previously reported sorbent-packed NTDs [47,177,178] has been limited due to the large size of the packing particles. In this study, we sought to improve filtration efficiency by adding a porous filter inside the NTD, as this should allow the device to capture the total concentration of compounds, both in the free and droplet phases. In order to provide a more comprehensive view of the sample and to enable comparison, the concentrations of fragrances in gas-phases were also analyzed using TFME and SPME.

3.3 Experimental

3.3.1 Materials and Methods

α–Pinene, β–pinene, limonene, γ–terpinene, citronellol, linalool, benzaldehyde, geraniol, cinnamaldehyde, thymol, indole, eugenol, isoeugenol, benzylbenzoate, benzylsalicylate, diethyleneglycolmonoethylether and isopropylalcohol, polyacrylonitrile (PAN), dimethylformamide (DMF), DVB–based particles (HayeSep® Porous Polymer Adsorbent, 60-80 mesh) in analytical grade were purchased from Sigma-Aldrich (Mississauga, ON, Canada).

For real sample, 7 sprays were purchased, including: one fragrance mist (cherry blossom vibes, Hard Candy), 4 fragrance sampler tests (Calgon), one dry body spray (Secret), one body fragrance spray (pink, Body Fantasies).

Please refer to **2.3.1.2 SMPS instrument, 2.3.1.3 Gas Generator, 2.3.1.4 GC-MS for thin–film analysis** and **2.3.1.5 GC-MS for needle–trap analysis** for details on the instrument.

For needle–trap device and SPME different liners appropriate for each device was used. The temperature programming for both instruments with separation time of 16.5 minutes is provided in Table 3-1.

Table 3-1. Temperature programming for separation of fragrances (total time = 16.5 min)

Ramp (ºC min^{-1})	Temperature (ºC)	Time (min)
	80	2
8	100	0
20	150	0
25	200	5
8	220	0

3.3.2 Extraction devices preparation

Please refer to **2.4.2 Optimized Filter Preparation Condition** section for details on the preparation of filter. PAN and H-PAN aerogel are depicted in Figure 2-13. After preparing the filter, in the 22 G stainless-steel needle, 1 cm of HayeSep DVB particles was sandwiched between the two 2 mm of H–PAN filter (Figure 3-1). The filters were added to trap particles in aerosol samples and to act as a retainer to immobilize the DVB particles, which were responsible for extracting the free fragrances.

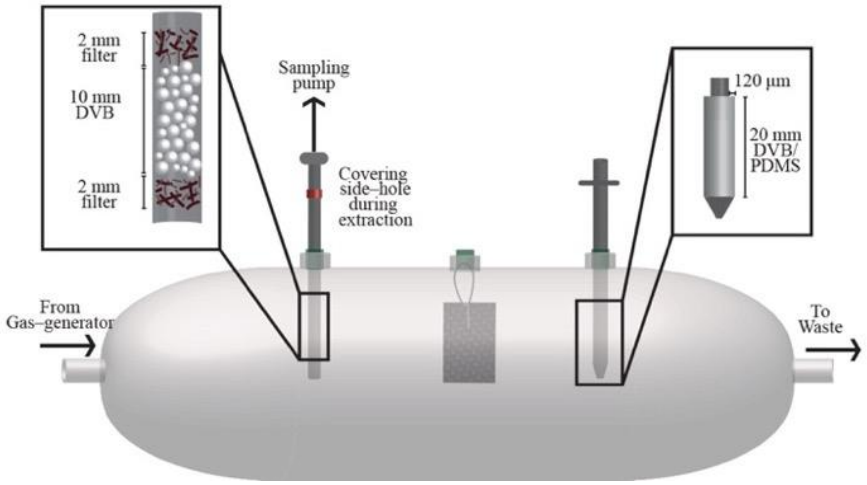

Figure 3-1. Sampling chamber for NTD, TFME, and SPME (each device was used with different bulb and in different times. The combination is shown here for simplified visualization).

The thin films were prepared by using PDMS to adhere DVB particles to carbon mesh thin-film membranes following the procedure detailed by Grandy et al. [145] The thin films were cut into rectangles measuring 4 × 0.5 cm for extraction purposes. The DVB/PDMS-arrow devices (1.10 mm, 20 mm, 120 µm) were purchased from CTC Analytics AG (Zwingen – Switzerland). For simplification for the rest of this chapter, SPME is used instead of SPME-arrow. All extraction devices were conditioned at 280ºC for at least 1h for clean-up and conditioning prior to the extraction step.

3.3.3 Gas mixture preparation

Gas mixtures for the different fragrance compounds were prepared by filling tubes with pure analytes and leaving them in the chamber of a gas-generator instrument. The gas-generator chamber was equipped with a thermostat, which allowed the temperature to be tuned, and it was connected to an input and output, allowing the carrier gas to transfer the gas-phase analytes to the desired sampling container (Figure 1-20).

The weight of the tubes was monitored regularly to calculate their permeation rate. The required concentration of analytes in the gas phase was prepared by altering the temperature and/or flow rate. For the optimization step, the concentration of analytes was set between 40-60 μg L^{-1}. It should be mentioned that due to different permeation rates (depending on the volatility of compounds), it is practically impossible to obtain exactly the same concentrations for all analytes at a definite temperature and flow rate. A complete list of chosen analytes and their physiochemical properties can be found in Table 3-2.

Table 3-2. Full list of fragrances, their retention times and physiochemical properties.

Analyte	Rt (TFME)	Rt (NTD/ SPME)	Boiling point (°C)	Henry Constant (atm m^3 mol^{-1})	CAS	LogP
α–pinene	4.6	4.1	156	1E-1	80-56-8	4.8
β–pinene	5.1	4.7	166	2E-1	127-91-3	4.1
Limonene	5.7	5.4	176	3E-2	138-86-3	3.4
Benzyl alcohol	6.5	5.6	205	2E-5	100-51-6	1.1
γ–terpinene	6.8	5.8	183	3E-2	99-85-4	4.5
Linalool	7.3	6.3	197	2E-5	78-70-6	2.7
Citronellol	8.3	7.7	225	2E-5	7540-51-4	3.2
Geraniol	8.4	7.9	230	1E-5	106-24-1	2.9
Cinnamaldehyde	8.6	8.2	248	3E-6	104-55-2	1.9
Thymol	8.7	8.2	232	3E-6	89-83-8	3.3
Indole	8.7	8.4	254	1E-6	120-72-9	2.1
Eugenol	9.0	8.8	253	1E-6	97-53-0	2.0
Isoeugenol	9.5	9.5	266	3E-6	97-54-1	2.6
Benzyl benzoate	12.2	12.0	323	2E-7	120-51-4	4.0
Benzyl Salicylate	13.7	14.0	320	2E-6	118-58-1	3.2

3.3.4 Filtration efficiency and thermal stability of filter

The filtration efficiency of the designed needle was measured using an SMPS instrument. In this instrument, oil droplets (5–200 nm) are fabricated, sorted based on size, and finally measured on the counter. The needle's filtration efficiency was determined by calculating the ratio of the particles before and after inserting the filter.

3.3.5 Extraction procedures

Three different extraction methods were developed based on the extraction-phase designs. Sampling was performed using a glass sampling bulb with a hole that was connected to the output of the gas generator. For the NTD, the tip of the needle was inserted into the green septa, while the end was connected to a sampling pump, which was turned on during sampling (flow rate = 30 mL min^{-1}) to draw the sample through the sorbent bed. After sampling, the needle was disconnected and inserted into the injector of the GC-MS instrument for desorption.

In contrast, the thin film and SPME were inserted into the sampling glass and left there until extraction time. After extraction, the devices were transferred into the GC–MS instrument for desorption and separation of analytes. A schematic of the sampling chamber for each device is shown in Figure 3-1. While each device was used separately, the combined chamber is shown to simplify the visualization of the sampling procedure. To maximize consistency between the optimization (Figure 3-1) and real sample analysis conditions (Figure 3-2), the sampling flow rate and temperature were controlled to closely replicate the air in a real room.

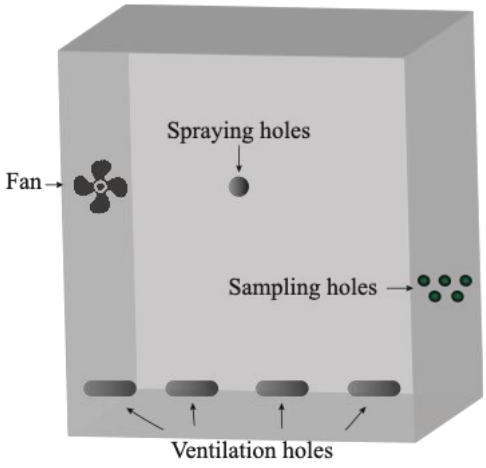

Figure 3-2. Box simulating a real room made from plexiglass, used for sampling fragrances in the breathing zone.

3.3.6 Carry–over

To study the carry-over after each NTD and SPME extraction, the desorption time was varied from 1-5 minutes. After each desorption, the extraction device was then re-desorbed to examine the remaining compounds on the extraction phase. Generally, it is accepted that if the carry-over signal is 5% or less than extraction signal, the desorption conditions can be considered appropriate.

The carry-over effect for TFME was investigated by re-desorbing from the same thin-films after an extraction/desorption cycle. The same procedure was repeated after the application of spray sample.

3.3.7 Breakthrough volume for needle-trap devices

When an extraction system is considered to be exhaustive, it is important to monitor breakthrough volume (BTV). In exhaustive sampling, all analytes are extracted from the sample, which means that the extraction signal can be enhanced by increasing the extraction volume. However, the extraction capacity is not unlimited. When the device reaches its capacity, the

extraction signal becomes constant regardless of further increases to the extraction volume. This volume should be considered, as the loss in linearity between concentration and signal following BTV can affect important parameters such as calibration range. In this study, the BTV for NTD was measured using gas generator. The sampling volume was increased and BTV was defined as the volume at which the signal remains constant despite further increases to the sampling volume.

3.3.8 Equilibrium time for SPME and TFME

Identifying the equilibrium time is vital when using equilibrium-based extraction methods, such as TFME and SPME. For these methods, it is important to make sure that the extraction time is in the equilibrium or pre-equilibrium region, as the monitoring of the exact extraction time becomes more important in decreasing the standard deviations of signals when it is in the pre-equilibrium range. A gas generator was used to prepare the gas-phase samples used to measure the equilibrium times for TFME and SPME. The gas analytes were transferred to a glass with a septum-sealed hole for sampling, and the carrier gas containing the analytes was then sent to the waste. The extraction devices (thin film and arrow) were left inside the sampling glass for a known amount of time, and the extraction signal was monitored until it remained constant despite further increases to the extraction time.

3.3.9 Absolute recovery for TFME and SPME

To provide a more complete comparison of the methods developed in this study, absolute recovery values for the equilibrium-based extraction methods were calculated. To this end, the SPME and thin–film devices were exposed to samples with known analyte concentrations, and the

extracted amounts were calculated in nanograms. Absolute recovery was calculated by finding the ratio between the mass of the extracted analytes and the mass of the analytes in the sample.

3.3.10 Method validation

The three developed methods were validated by finding the linear dynamic ranges using the extraction signals at different concentrations. The limits of detection (LODs) and limits of quantification (LOQs) were also studied based on signal-to-noise ratios of 3 and 10, respectively. The repeatability of the proposed methods was tested by performing extractions of analytes several times on different days to calculate the inter- and intra-day relative standard deviations (RSD). In the case of device-to-device RSD, four thin–films, three SPME, and four needles were prepared separately, and their standard deviations for extractions from similar samples was calculated.

3.3.11 Analysis of home–made and commercial sprays

For the analysis of home-made and commercial sprays, a 100-L plexiglass box was prepared to simulate the conditions of a standard room. Several holes were drilled into the wall of the box at a height corresponding to a "breathing zone." These holes were used for sampling in a similar manner to the hole on the glass sampling bulb. The box also featured a fan and several holes for ventilation, and sampling was conducted with fan both on and off to examine its effect on the concentration of fragrances over time.

To assure the method's applicability for analyzing commercial sprays, a home-made air freshener was prepared based on the instructions provided by the European Patent office [179]. Three fragrances (α-pinene, linalool, and benzyl benzoate) were selected based on their various Henry constants and mixed with diethylene glycol monoethyl ether (DEGMEE), isopropyl alcohol,

and water in a spray bottle. This home-made air freshener was then sprayed into the sampling box (with the fan turned off) and extractions were performed 15 minutes later. To avoid cross-contamination, the inside of the box was covered with aluminium foil, which was changed after each experiment. In addition, the door of the box was left open under a lab fume hood, and the fan was turned on for 5 minutes between samplings to remove gas and particles from previous samples.

Seven different air fresheners and body sprays were applied as real samples to determine the concentration of fragrances in the gas phase and droplets bound in the breathing zone of the box following their application. The fragrance aerosols were sprayed three times for each sampling run, and the concentrations of the fragrances were measured using the three methods (NTD, TFME, SPME). Sampling was performed immediately after administration and at 15, 30, and 60 mins after application.

3.3.12 Comparison of passive and active sampling for studying fragrances in the bathroom

The analysis of indoor pollutants is most often carried out using passive (time weighted averaging) sampling methods. In these methods, the extraction device is left to sit in the environment for a lengthy known period of time; if the diffusion coefficient of the compound is known, the concentration of the sample can then be calculated using [70]:

$$C=\frac{nZ}{DAt} \qquad \text{Eq. 3-1}$$

where C is the analyte concentration (mol cm^{-3}), D is the analyte diffusion coefficient (cm^2 s^{-1}), Z is the length along the diffusion (the distance between the needle tip and the sorbent inside the needle) path in (cm), n is the number of moles in the target analyte (mol), A is the

diffusion path cross-sectional area (needle area) (cm^2), and t is the duration (s) of the sampling period.

To ensure that Z is accurate, a needle was packed with DVB particles (Z=3 mm) without any filter. For comparison, the DVB–SPME was also applied for passive sampling while the fiber was withdrawn inside the needle. Specifically, both devices were used to perform passive sampling of Spray #7, which had been applied inside of a bathroom. The NTD (without pump) and withdrawn SPME were left inside the bathroom for 1 h. After sampling had been completed, the devices were desorbed and the concentration of linalool in the spray was determined based on the D= 0.021 $mm^2\ h^{-1}$ from previous studies [180]. The devices were then compared for their abilities in active sampling, again using Spray #7. For active sampling with the NTD, the bathroom air was drawn through the needle (packed with a filter and DVB) at a rate of 30 mL min^{-1} for 3 minutes; for active SPME, the fiber was exposed to the air inside the bathroom for 3 minutes and then desorbed. This procedure was repeated at 0, 15, 30, and 60 minutes following the application of the spray.

3.4 Results

In perfumes or effervescence (e.g., beer), the fragrance compounds are distributed between gas phase and droplet phase. These droplets can be introduced into the lungs after administration, carrying a portion of the fragrance compounds into one's body. As a result, this portion of analytes is commonly lost during analysis, producing inaccurate results. In an attempt to remedy this limitation and enable a comprehensive sampling of aerosol samples, we designed a novel filter-incorporated NTD that is capable of capturing droplets and extracting free gas-phase analytes via sorbent particles. The obtained data from the analyses using the NTD, TFME, and SPME are provided and discussed in the following sub-sections.

3.4.1 Filtration efficiency and thermal stability of filter–incorporated needle–trap device

The needle-trap device's filtration efficiency was studied using an SMPS instrument. The oil droplets from the SMPS's generator were counted with and without the filter in the SMPS, with the difference being taken as the filtration percentage. The SMPS's initial background particle count and the particle count after inserting the filter-incorporated NTD are reported in Figure 3-3.

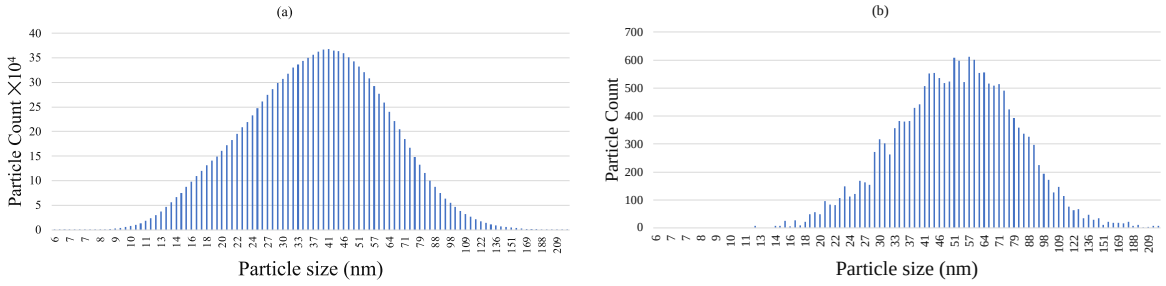

Figure 3-3. Particle count of SMPS instrument before (a) and after insertion (b) of filter–incorporated NTD.

As can be seen in Figure 3-4, the NTD's filtration efficiency exceeded 99.5%, which is acceptable for our application. It should be mentioned that filtration mechanism theory states that the lowest filtration efficiency should occur between 100–200 nm, which was included in the size range chosen for this study. Thus, it can be concluded that, when high filtration efficiency is achieved in this size range (the range with the lowest efficiency), even higher filtration efficiencies can be expected in other ranges. Furthermore, it is also known that larger particles are easier to trap than smaller ones.

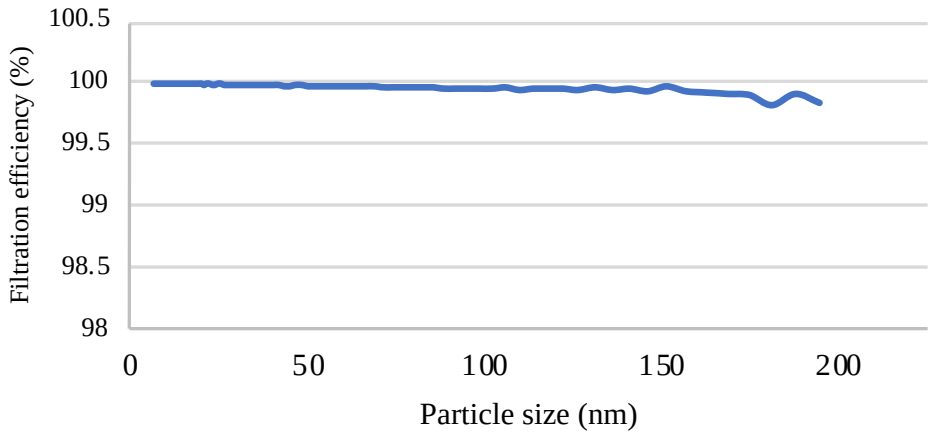

Figure 3-4. Filtration efficiency of the filter-incorporated NTD calculated using SMPS instrument.

3.4.2 Carry–over studies

The carry-over effect was evaluated by varying the desorption time for the SPME and NTD from 5 minutes to 1 minute. The results indicated no carry-over for desorption times of up to 3 minutes; thus, a desorption time of 3 minutes was used for all analyses using these devices. For TFME, the designed desorption method resulted in carry-over of less than 5%; as such, this method was used for all subsequent TFME analyses.

3.4.3 Breakthrough volume measurements for NTD

As explained above, the BTV measurement is important in assessing the capacity of the NTD. The results (Figure 3-5) suggests that BTV is not reached for any of the compounds up to at least 500 mL. Based on these results, it can be concluded that BTV is not reached for any compound after 3 minutes of sampling (flow rate = 30 mL min^{-1}); therefore, 3 minutes was selected as the extraction time for the NTD experiments.

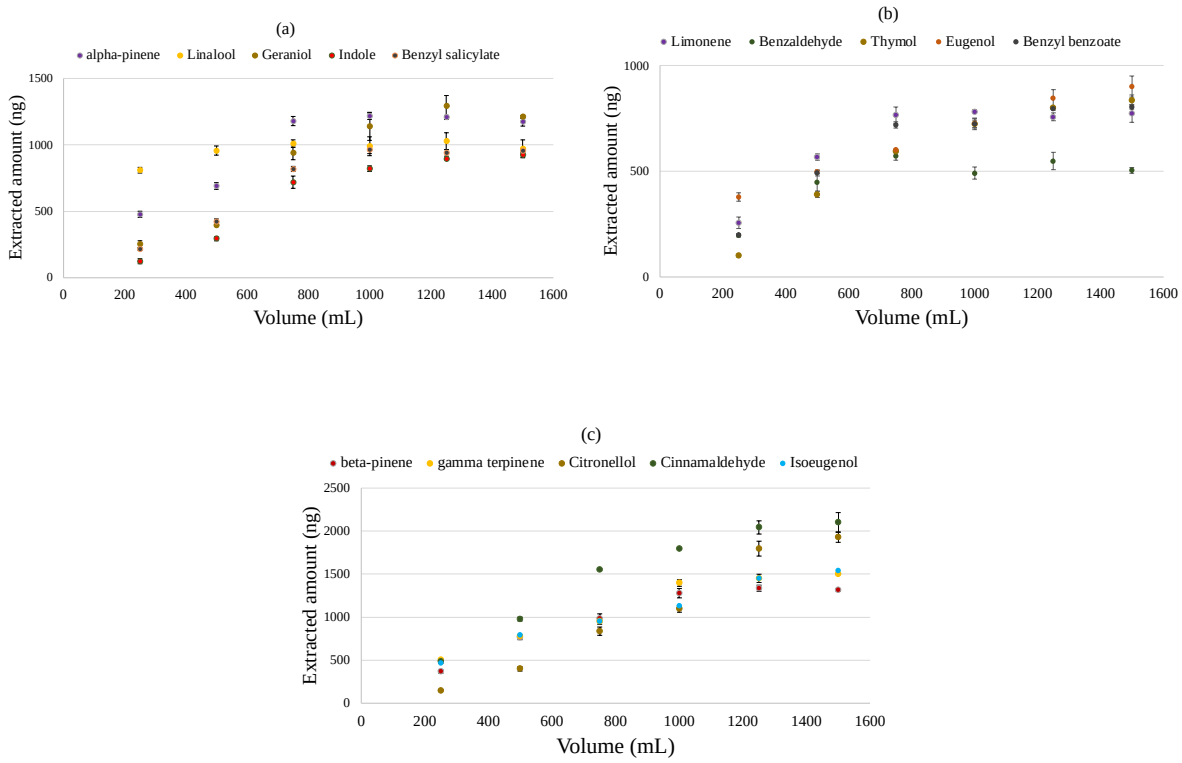

Figure 3-5. BTV for fragrances extracted with NTD using gas generator by increasing sampling volume (flow rate = 30 mL min^{-1}). Plateau shows the breakthrough volume.

3.4.4 Extraction time

For TFME and SPME, equilibrium time was studied by varying the extraction time until equilibrium had been achieved. The results of these tests are shown in Figure 3-6 and Figure 3-7. As can be seen, it took up to 45 minutes for some compounds to reach equilibrium. The final goal of this project was to determine and compare the concentration of fragrances (in gas phase and droplet-bound) in air samples at various time intervals after the application of sprays. The concentration of fragrances after spraying is not constant and decreases over time, which means it is highly impractical to wait until equilibrium after spraying. In addition, it was important to monitor changes of fragrance concentration over time, so if the extraction is conducted until the equilibrium point is reached, the data regarding changes in concentration over time will be lost. To

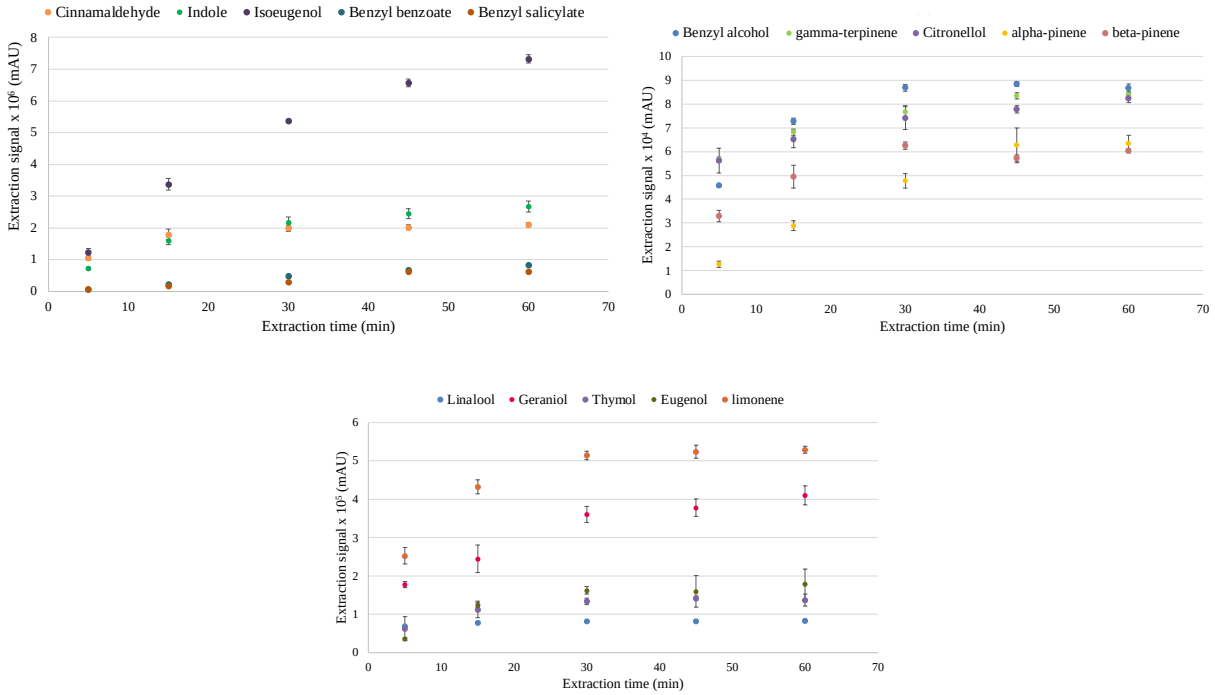

Figure 3-6. Equilibrium time profile for extraction of fragrances with DVB/PDMS SPME.

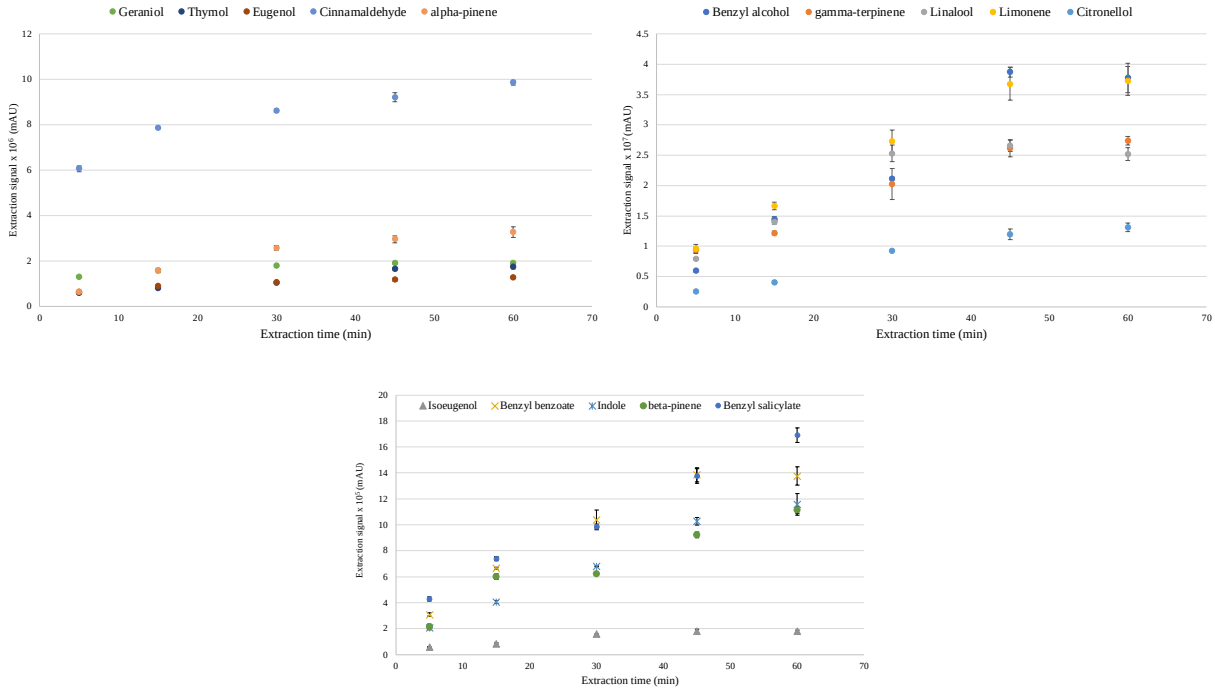

Figure 3-7. Equilibrium time profile for extraction of fragrances with DVB/PDMS TFME.

solve these problems, the pre-equilibrium condition was used for extraction, and a 3-minute extraction time was chosen for calibration and real sample analysis with TFME and the SPME.

3.4.5 Absolute recovery

For TFME and the SPME, which are based on equilibrium, different characteristics such as surface area and analyte-sorbent interaction can influence analyte recovery rates. To ensure a thorough comparison of these two methods, the absolute recovery (AR) values were measured. The results of these measurements are provided in Table 3-3.

Table 3-3. Absolute recovery values of fragrances with DVB/PDMS TFME and DVB/PDMS SPME

Analytes	Absolute Recovery (%)	
	DVB/PDMS–TFME	DVB/PDMS–SPME
α–pinene	25.4	8.2
β–pinene	27.2	8.3
Limonene	76.3	11.8
Benzaldehyde	89.3	6.7
γ–terpinene	75.2	15.4
Linalool	68.8	13.1
Citronellol	86.8	19.6
Geraniol	89.5	25.9
Cinnamaldehyde	85.6	19.3
Thymol	87.9	25.9
Indole	87.4	26.6
Eugenol	84.4	19.9
Isoeugenol	88.3	14.5
Benzyl benzoate	79.5	10.0
Benzyl salicylate	33.2	3.4

Since TFME and SPME use sorbents with similar chemical structures, thus producing similar interactions with fragrances, the higher absolute recovery values recorded for TFME can be attributed to the higher surface area of thin-films compared to SPME.

3.4.6 Method precision

To study the repeatability and reproducibility of the developed methods, inter- and intra-day RSD percentages were measured via repeated extraction/desorption from the sample. The results of these experiments can be found in Table 3-4 and From the final data, it can be concluded that, in general, all three methods provide appropriate repeatability. Additionally, the RSD values for the various extraction setups were generally higher than the inter- and intra-day RSDs, which was expected given that the thin-films and needles had been prepared in the lab.

3.4.7 Method validation

The method was validated by calculating the dynamic linear range using various concentrations of analytes and monitoring the signal until linearity was lost.

Table 3-5.

Table 3-4. Relative standard deviation percentages for inter–day and intra–day variation of fragrance extraction signals with NTD, TFME and SPME.

Analytes	RSD (%)					
	Inter–day			Intra–day		
	NTD	TFME	SPME	NTD	TFME	SPME
α–pinene	4.2	4.2	9.4	2.1	3.2	1.3
β–pinene	3.0	3.4	5.3	3.6	5.2	2.1
Limonene	2.5	3.5	4.6	3.2	4.2	4.2
Benzyl alcohol	6.2	4.4	7.4	1.7	6.3	2.2

γ–terpinene	4.2	2.7	8.5	4.3	5.3	3.1
Linalool	1.4	6.4	6.3	2.7	4.2	4.2
Citronellol	5.3	7.4	5.3	3	2.5	5.2
Geraniol	6.4	6.6	6.6	3.1	1.5	2.4
Cinnamaldehyde	7.3	7.3	7.3	4.2	3.6	2.7
Thymol	5.6	8.9	9.6	5.2	2.4	3.8
Indole	4.0	4.6	4.7	3.8	2.6	1.7
Eugenol	3.5	0.3	8.4	1.9	3.5	3.2
Isoeugenol	2.3	9.4	3.8	2.4	1.9	1.8
Benzyl benzoate	5.4	3.4	8.3	2.1	2.2	2.2
Benzyl salicylate	3.3	3.7	9.4	4.2	3.1	4.3

From the final data, it can be concluded that, in general, all three methods provide appropriate repeatability. Additionally, the RSD values for the various extraction setups were generally higher than the inter- and intra-day RSDs, which was expected given that the thin-films and needles had been prepared in the lab.

3.4.8 Method validation

The method was validated by calculating the dynamic linear range using various concentrations of analytes and monitoring the signal until linearity was lost.

Table 3-5. Relative standard deviation percentages for sorbent–to–sorbent variation of fragrance extraction signals with NTD (n=4), TFME (n=4) and SPME (n=3)

Analytes	RSD (%) Device–to–device		
	NTD	TFME	SPME
α–pinene	10.2	9.5	3.7
β–pinene	9.3	3.0	9.5
Limonene	5.8	6.4	7.5
Benzaldehyde	6.2	7.4	6.4
γ–terpinene	11.1	3.6	3.6
Linalool	3.6	8.5	4.8

Citronellol	8.4	7.3	7.6
Geraniol	7.9	6.5	5.8
Cinnamaldehyde	5.8	7.6	7.5
Thymol	6.3	9.4	8.6
Indole	13.2	10.3	12.1
Eugenol	7.8	12.1	4.8
Isoeugenol	8.8	7.6	7.7
Benzyl benzoate	9.9	8.4	8.3
Benzyl salicylate	10.5	7.7	5.2

In addition, the concentrations were reduced until LOD and LOQ values were obtained based on the criteria of signal-to-noise ratios of 3 and 10, respectively. The method validation results are presented in Table 3-6. As can be seen, TFME and the NTD provided similar limits of detection and quantifications, and the NTD did provide lower LODs in some cases. In contrast, SPME had higher LODs and LOQs for almost all of the analytes.

Table 3-6. Method validation data for limit of detection, limits of quantification and linear dynamic range (in μg L^{-1}) of fragrances obtained with NTD, TFME and SPME

Analytes	Filter/DVB–NTD		DVB/PDMS–TFME		DVB/PDMS–SPME		DVB–NTD & DVB/PDMS–TFME	DVB/PDMS–SPME
	μg L^{-1}							
	LOD	LOQ	LOD	LOQ	LOD	LOQ	Linear range	
α–pinene	0.2	0.7	0.8	2.7	1.2	4.0	2–980	4–980
β–pinene	0.8	2.7	2.9	9.7	4.8	16.0	10–993	17–993
Limonene	0.9	3.0	1.2	4.0	3.8	12.7	4–950	13–950
Benzaldehyde	1.3	4.3	1.5	5.0	9.7	32.3	5–1021	33–1021
γ–terpinene	0.7	2.3	0.9	3.0	2.3	7.7	3–978	8–978
Linalool	0.9	3.0	1.3	4.3	3.4	11.3	4–899	12–899
Citronellol	1.7	5.7	2.0	6.7	4.3	14.3	7–903	19–903
Geraniol	2.7	9.0	3.0	10	5.2	17.3	7–1005	15–1005
Cinnamaldehyde	1.6	5.3	1.9	6.3	4.1	13.7	10–993	18–993
Thymol	0.7	2.3	0.8	2.7	1.4	4.7	6–899	14–899
Indole	0.8	2.7	0.9	3.0	1.5	5.0	2–1025	5–1025
Eugenol	1.4	4.7	1.7	5.7	3.5	11.7	3–928	5–928

Isoeugenol	1.7	5.7	1.9	6.3	5.9	19.7	5–893	12–893
Benzyl benzoate	2.1	7	2.6	8.7	10.5	35.0	7–893	20–893
Benzyl salicylate	2.8	9.3	8.4	28.0	16.7	55.7	8–901	34–901

These disparate results could be explained by these methods' differing extraction mechanisms: NTD is an exhaustive method that can extract all of the analytes from a sample provided the BTV is not reached, while TFME and SPME are equilibrium-based methods with different absolute recovery values. These recovery values are mainly dependent on surface area and the strength of the interaction between the sorbent and analyte. In this case, since the chemical composition of the sorbent—and thus its interaction with the analytes—in both methods was similar, the higher absolute recoveries observed for TFME were undoubtedly due to its greater surface area. Nonetheless, it can be concluded that NTD with full recovery generally provides superior LODs and LOQs.

To find the calibration range, the concentration of analytes was increased until the signal lost its linearity. The tested methods' linear ranges for fragrances can be found in Table 3-6. As the data suggests, the three methods all had similar upper limits, but TFME and NTD provided a wider range due to their lower LOQs.

3.4.9 Home–made air freshener studies

The home-made air freshener was sprayed inside the 100 L plexiglass box and extracted 15 min after administration using the NTD and TFME. The concentrations of the three targeted fragrance compounds (α–pinene, linalool, and benzyl benzoate) are provided in Figure 3-8. As can be seen, α–pinene, which is the most volatile compound with the highest Henry constant, is predominantly present in gas free phase; this is mirrored in the results for the NTD and TFME.

However, the data for benzyl benzoate reveals a significant difference between TFME and the NTD. This difference can be attributed to benzyl benzoate's lower Henry constant, which prevents it from evaporating in the gas phase and largely confines it to the droplets. While it is possible to trap and study these droplet-bound compounds with the NTD, their data is missing in TFME. The results for linalool fell between those of the other two compounds, which possessed extreme properties.

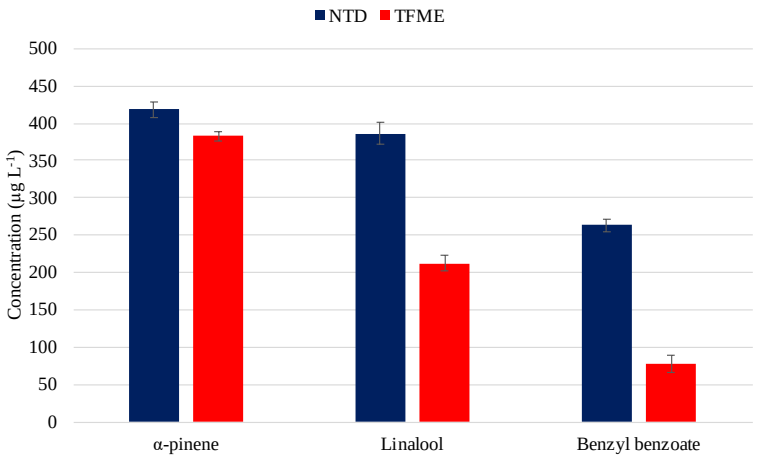

Figure 3-8. Concentration of fragrance compounds 15 min after administration of home-made air freshener in sampling box extracted with the NTD (30 mL min^{-1}, 3 min) and TFME (3 min).

In addition, since a smaller percentage of linalool molecules remained inside of the droplets, the difference between TFME and NTD was also smaller. The chromatogram for these results can be seen in Figure 3-9.

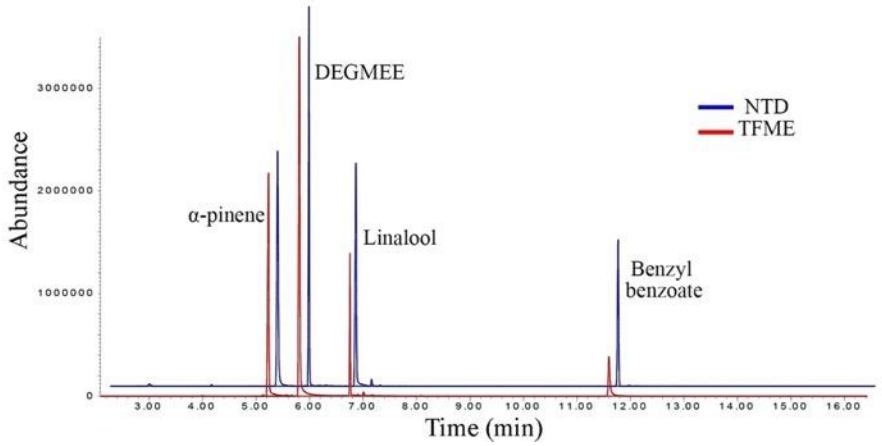

Figure 3-9. Chromatogram from extraction of fragrances from home-made air freshener using the NTD and TFME (sprayed in the simulated box, extracted for 3 min after application).

3.4.10 Spray analysis

To test the developed methods' applicability for determining fragrances in spray samples, a 100 L plexiglass box simulating the conditions of a real room was designed, and the concentration of fragrances was monitored over a "breathing zone" over time in both a "fan on" and "fan off" condition. To monitor concentration over time, an extraction time of 3 minutes was chosen. In all seven sprays, compounds of interest were detected and determined. In addition, many other compounds were detected and identified via GC-MS. The concentrations of the analytes were determined over a 1h period; these figures are presented in Table 3-7.

Table 3-7. Concentration in ng mL^{-1} (relative standard deviation, RSD %) of target fragrance compounds in seven analyzed sprays over a 1 h period (post-application time) with TFME, NTD and SPME (ND=Not detected, below LOQ= below limits of quantification)

Spray #1 (Fan turned off)												
Method	NTD				TFME				SPME			
Analytes	0	15	30	60	0	15	30	60	0	15	30	60
β-pinene	48 (2%)	31 (3%)	10 (10%)	ND	39 (5%)	27 (7%)	Below LOQ	ND	42 (7%)	22 (5%)	ND	ND

Limonene	149 (6%)	83 (4%)	41 (5%)	21 (5%)	148 (3%)	78 (6%)	32 (6%)	14 (7%)	153 (4%)	77 (6%)	42 (5%)	ND
Linalool	361 (4%)	114 (4%)	59 (3%)	33 (6%)	98 (6%)	56 (7%)	30 (7%)	ND	89 (9%)	69 (10%)	27 (4%)	ND
Citronellol	519 (8%)	371 (7%)	167 (3%)	77 (4%)	201 (6%)	94 (7%)	67 (4%)	21 (5%)	197 (2%)	96 (4%)	73 (7%)	19 (5%)
Spray #1 (Fan turned on)												
β-pinene	31 (3%)	ND	ND	ND	28 (4%)	ND	ND	ND	21 (5%)	ND	ND	ND
Limonene	110 (5%)	57 (9%)	23 (4%)	ND	105 (7%)	63 (5%)	ND	ND	107 (4%)	78 (6%)	ND	ND
Linalool	278 (7%)	95 (5%)	31 (6%)	ND	74 (5%)	36 (8%)	ND	ND	79 (3%)	41 (5%)	ND	ND
Citronellol	289 (5%)	105 (6%)	21 (5%)	ND	106 (7%)	46 (9%)	ND	ND	98 (6%)	38 (5%)	ND	ND
Spray #2 (Fan turned off)												
Method	NTD				TFME				SPME			
Analytes	0	15	30	60	0	15	30	60	0	15	30	60
Limonene	68 (4%)	45 (4%)	17 (6%)	8 (13%)	59 (3%)	38 (5%)	12 (3%)	7 (14%)	61 (2%)	40 (5%)	14 (2%)	ND
Benzyl salicylate	123 (8%)	68 (6%)	22 (5%)	ND	41 (5%)	ND	ND	ND	ND	ND	ND	ND
Citronellol	682 (6%)	378 (4%)	107 (6%)	48 (6%)	271 (7%)	115 (6%)	96 (5%)	52 (6%)	269 (6%)	121 (7%)	89 (4%)	48 (4%)
Spray #2 (Fan turned on)												
Limonene	59 (7%)	17 (6%)	ND	ND	49 (4%)	20 (5%)	ND	ND	51 (4%)	18 (6%)	ND	ND
Benzyl salicylate	103 (10%)	31 (32%)	ND	ND	30 (7%)	ND	ND	ND	28 (4%)	ND	ND	ND
Citronellol	618 (4%)	204 (6%)	68 (7%)	ND	199 (5%)	78 (8%)	ND	ND	206 (6%)	83 (13%)	ND	ND
Spray #3 (Fan turned off)												
Method	NTD				TFME				SPME			
Analytes	0	15	30	60	0	15	30	60	0	15	30	60
Limonene	194 (7%)	106 (5%)	21 (5%)	ND	178 (3%)	98 (5%)	24 (4%)	ND	181 (7%)	96 (5%)	21 (5%)	ND
γ-terpinene	451 (3%)	314 (5%)	193 (3%)	69 (6%)	392 (3%)	296 (4%)	164 (6%)	71 (7%)	389 (7%)	278 (7%)	171 (4%)	63 (6%)
Linalool	41 (2%)	15 (7%)	ND	ND	28 (4%)	9 (11%)	ND	ND	31 (3%)	Below LOQ	ND	ND
Benzyl benzoate	841 (3%)	603 (5%)	107 (2%)	56 (5%)	481 (6%)	253 (7%)	88 (5%)	39 (8%)	490 (6%)	261 (8%)	96 (4%)	48 (8%)
Benzyl salicylate	78 (5%)	41 (5%)	ND	ND	45 (4%)	17 (6%)	ND	ND	59 (3%)	ND	ND	ND
Spray #3 (Fan turned on)												

Limonene	142 (4%)	94 (4%)	ND	ND	106 (5%)	74 (5%)	ND	ND	111 (3%)	79 (4%)	ND	ND
γ-terpinene	391 (2%)	106 (4%)	Blow LOQ	ND	279 (3%)	96 (6%)	ND	ND	287 (3%)	79 (5%)	ND	ND
Linalool	18 (6%)	ND	ND	ND	13 (15%)	ND	ND	ND	11 (0%)	ND	ND	ND
Benzyl benzoate	683 (5%)	198 (3%)	69 (4%)	ND	301 (2%)	96 (3%)	41 (5%)	ND	298 (2%)	101 (4%)	48 (4%)	ND
Benzyl salicylate	59 (5%)	ND	ND	ND	33 (6%)	ND	ND	ND	ND	ND	ND	ND

Spray #4 (Fan turned off)

Method	NTD				TFME				SPME			
Analytes	0	15	30	60	0	15	30	60	0	15	30	60
Linalool	367 (5%)	108 (6%)	43 (5%)	9 (11%)	198 (3%)	58 (5%)	6 (2%)	ND	201 (2%)	64 (5%)	9 (11%)	ND
Benzyl benzoate	205 (4%)	79 (6%)	52 (6%)	ND	96 (4%)	43 (7%)	ND	ND	98 (4%)	51 (6%)	ND	ND
Benzyl salicylate	99 (5%)	48 (8%)	13 (8%)	ND	51 (4%)	ND	ND	ND	59 (3%)	Below LOQ	ND	ND

Spray #4 (Fan turned on)

Linalool	161 (3%)	68 (4%)	ND	ND	106 (6%)	41 (7%)	ND	ND	99 (4%)	49 (8%)	ND	ND
Benzyl benzoate	169 (4%)	41 (5%)	ND	ND	79 (3%)	21 (5%)	ND	ND	83 (5%)	26 (8%)	ND	ND
Benzyl salicylate	65 (5%)	17 (6%)	ND	ND	38 (5%)	ND	ND	ND	ND	ND	ND	ND

Spray #5 (Fan turned off)

Method	NTD				TFME				SPME			
Analytes	0	15	30	60	0	15	30	60	0	15	30	60
β πινενε	51 (2%)	16 (6%)	ND	ND	47 (2%)	13 (8%)	ND	ND	49 (2%)	12 (8%)	ND	ND
Limonene	78 (3%)	35 (3%)	12 (8%)	ND	66 (5%)	28 (4%)	11 (9%)	ND	71 (7%)	33 (6%)	ND	ND
Linalool	268 (3%)	114 (5%)	67 (6%)	34 (6%)	105 (5%)	74 (4%)	25 (8%)	ND	98 (4%)	68 (4%)	31 (6%)	ND
Cinnamaldehyde	104 (5%)	61 (3%)	ND	ND	57 (5%)	25 (4%)	ND	ND	61 (7%)	32 (6%)	ND	ND
Indole	86 (3%)	47 (4%)	15 (7%)	ND	38 (8%)	16 (2%)	ND	ND	42 (5%)	21 (5%)	ND	ND
Isoeugenol	194 (3%)	94 (6%)	41 (5%)	ND	67 (7%)	33 (6%)	12 (8%)	ND	72 (3%)	36 (6%)	ND	ND
Benzyl benzoate	278 (8%)	164 (9%)	71 (8%)	37 (8%)	105 (6%)	74 (5%)	38 (5%)	Below LOQ	98 (8%)	67 (7%)	41 (5%)	ND
Benzyl salicylate	241 (7%)	98 (8%)	66 (6%)	31 (6%)	94 (7%)	57 (5%)	15 (13%)	ND	96 (3%)	64 (8%)	21 (5%)	ND

Spray #5 (Fan turned on)

β πινενε	45 (2%)	Below LOQ	ND	ND	37 (3%)	ND	ND	ND	35 (3%)	ND	ND	ND
Limonene	60 (5%)	26 (8%)	ND	ND	51 (6%)	13 (8%)	ND	ND	47 (4%)	Below LOQ	ND	ND
Linalool	181 (5%)	96 (4%)	31 (6%)	ND	89 (3%)	31 (3%)	ND	ND	91 (5%)	42 (7%)	ND	ND
Cinnamaldehyde	78 (3%)	31 (3%)	ND	ND	31 (3%)	Below LOQ	ND	ND	36 (6%)	ND	ND	ND
Indole	71 (6%)	33 (3%)	Below LOQ	ND	21 (10%)	ND	ND	ND	19 (5%)	ND	ND	ND
Isoeugenol	106 (8%)	73 (8%)	21 (5%)	ND	51 (10%)	22 (5%)	ND	ND	54 (7%)	25 (8%)	ND	ND
Benzyl benzoate	121 (8%)	83 (8%)	51 (6%)	ND	72 (6%)	33 (6%)	ND	ND	76 (5%)	41 (5%)	ND	ND
Benzyl salicylate	163 (6%)	67 (7%)	34 (6%)	ND	73 (5%)	31 (6%)	ND	ND	78 (6%)	Below LOQ	ND	ND
Spray #6 (Fan turned off)												
Method	NTD				TFME				SPME			
Analytes	0	15	30	60	0	15	30	60	0	15	30	60
Linalool	418 (3%)	261 (6%)	107 (6%)	78 (6%)	174 (5%)	78 (6%)	ND	ND	181 (6%)	82 (5%)	ND	ND
Citronellol	104 (4%)	51 (6%)	Below LOQ	ND	67 (6%)	35 (3%)	ND	ND	77 (4%)	29 (3%)	ND	ND
Benzyl salicylate	119 (6%)	79 (6%)	51 (4%)	19 (5%)	31 (6%)	Below LOQ	ND	ND	Below LOQ	ND	ND	ND
Spray #6 (Fan turned on)												
Linalool	371 (6%)	104 (7%)	31 (6%)	13 (8%)	103 (7%)	23 (4%)	ND	ND	104 (7%)	38 (8%)	ND	ND
Citronellol	78 (3%)	31 (3%)	ND	ND	56 (4%)	ND	ND	ND	49 (4%)	ND	ND	ND
Benzyl salicylate	98 (3%)	42 (2%)	12 (8%)	ND	20 (5%)	ND	ND	ND	ND	ND	ND	ND
Spray #7 (Fan turned off)												
Method	NTD				TFME				SPME			
Analytes	0	15	30	60	0	15	30	60	0	15	30	60
Linalool	451 (6%)	321 (4%)	204 (5%)	100 (6%)	104 (5%)	78 (6%)	31 (6%)	12 (4%)	98 (5%)	79 (5%)	34 (3%)	Below LOQ
Spray #7 (Fan turned on)												
Linalool	241 (5%)	104 (5%)	41 (5%)	ND	74 (4%)	14 (7%)	ND	ND	69 (6%)	17 (6%)	ND	ND

Given the large amount of data, the data for two compounds (β–pinene and benzyl salicylate) in Spray #5 are provided as charts for simplified visualization. These two compounds were chosen because they served as exemplars of highly volatile and non-volatile fragrance compounds. Based

on their vapor pressure, it was expected that β–pinene would generally prefer to be in the gas phase, while benzyl salicylate would largely remain in the droplet phase.

The data in both charts reveal some common trends. For instance, the concentrations obtained from TFME and SPME are generally similar considering RSD, as these methods are able to determine the concentration of analytes in vapor phases. As expected, the concentration of fragrances decreases exponentially over time, reaching zero for most of the compounds during the sampling time (1 h). Additionally, the concentration of fragrances is lower in the fan-on condition and diminishes faster over time, which reveals the importance, necessity, and efficiency of ventilators when fragrances are applied indoors.

It was also observed that the results for the NTD and TFME (and SPME) begin to converge as time passes. This finding indicates that analytes largely remain in gas phase for some time after the application of sprays before, which can be due to the settling of particles on the walls of the box, which means the remaining fragrance compounds in the air remain in the gas-phase.

The other important finding of this study is the differences in the concentration obtained using the NTD (total concentration) and other two methods (free, vapor phase concentration). The differences between NTD and TFME (and SPME) were larger for lower-vapor-pressure compounds (benzyl salicylate) that prefer to remain in droplets rather than the gas phase (Figure 3-11), which was not the case for volatile compounds with larger vapor pressure values (β–pinene) (Figure 3-10).

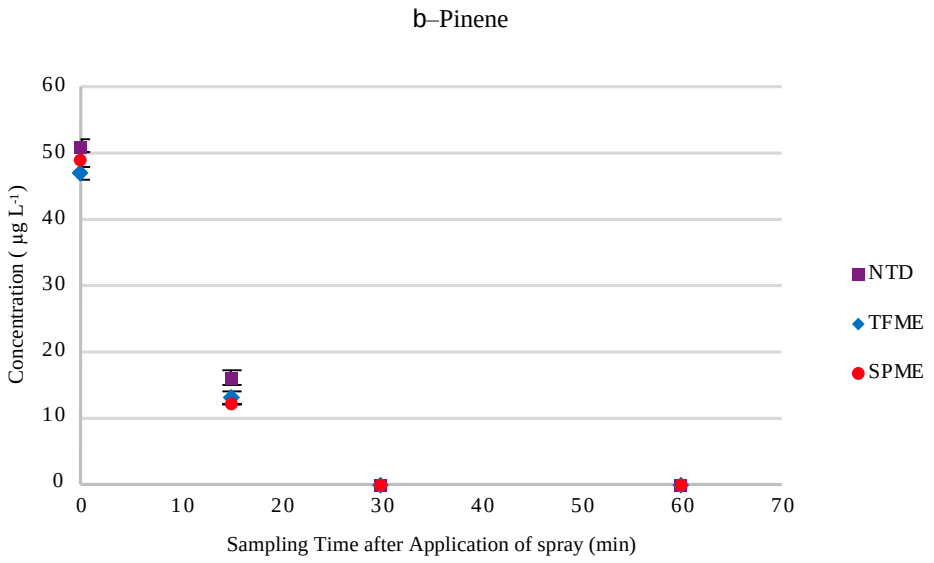

Figure 3-10. Concentration of β–pinene in Spray #1, analyzed over 1 h after application with the NTD, TFME, and SPME.

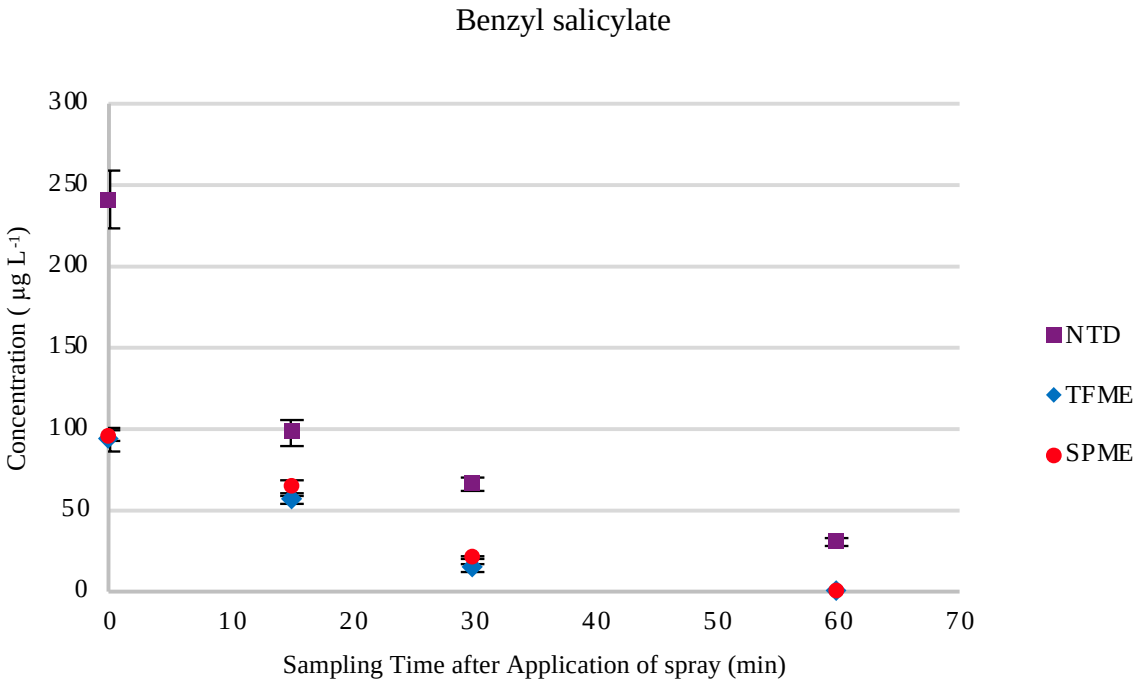

Figure 3-11. Concentration of benzyl salicylate in Spray #1, analyzed over 1 h after application with the NTD, TFME, and SPME.

This difference is due to the NTD's ability to trap particles that cannot be captured by TFME and SPME. Droplets from sprays with less-volatile compounds dissolved in them are trapped by the NTD and can be detected in the GC–MS after desorption, whereas TFME and SPME are only able to extract fragrances present free form in the gas phase. A complete list of these compounds is provided in Table 3-8.

To check if this explanation can be extended to all of the data in this study, the particle-to-vapor phase concentration ratio of the analytes was calculated by $\frac{\text{NTD-TFME}}{\text{TFME}}$, and the analytes were then categorized as either volatile (VP >1 mmHg) or non–volatile (VP<1 mmHg) compounds.

Table 3-8. Full list of compounds (in addition to target compounds) detected and identified in different sprays with NTD and GC–MS instrument.

Retention Time (min)	Compound	Retention Time (min)	Compound
Spray #1		Spray #4	
3.6	Butyric acid, 2-methyl-, ethyl ester	5.6	3,3'-oxybis-2-butanol
3.8	Isopentyl alcohol, acetate	5.8	Oxybis Propanol
5.2	β–pinene	6.3	Linalool
5.4	n-Hexyl acetate	7.2	Ethyl linalool
5.7	Limonene	7.3	p-menth-1-ene-8-ol
5.8	oxybis Propanol	7.8	p-Menthan-7-ol, trans-
6	diethyl ester Malonic acid	7.9	p-Menthan-7-ol, cis-
6.1	2,6-Dimethyl-7-octen-2-ol	9	Thujopsen
6.4	Linalool	9.2	α–Cetone
6.6	Benzene ethanol	9.2	β–Ionone
6.9	β–Terpineol	9.3	3,5-Diisopropenyl-1,1,2-trimethylcyclohexane
7	benzyl ester Acetic acid	9.5	Lilyal
7.1	Heptanoic acid, 2-propenyl ester	10.3	Methyl dihydrojasmonate
7.2	Benzyl alcohol, alpha-methyl-, acetate	10.5	2-(4a,8-Dimethyl-6-oxo-1,2,3,4,4a,5,6,8a-octahydro-naphthalen
7.3	α–Terpineol	11	Dihydro myrcenol
7.3	t-Terpineol	11.4	Benzyl benzoate
7.5	Citronellol	12.2	2-Hydroxycyclopentadecanone

7.7	Linalyl anthranilate
8	Vertenex
8.5	Geraniol acetate
8.9	Indane-1,3-diolmonoacetate
9.1	Cyclamal
9.2	β–Ionone
9.3	Geraniol butyrate
9.4	2-phenoxyethylisobutyrate
9.4	Indane-1,3-diolmonopropionate
9.5	Lilyal
9.7	δ–Undecalactone
10.2	Methyl dihydrojasmonate
10.3	α- pentyl Cinnamaldehyde
10.5	Hexyl salicylate
11.1	α- hexyl Cinnamaldehyde
11.8	Isopropyl myristate
12.3	Galoxolide
12.4	Musk 36A
15	Astratone

Spray #2

5.1	Myrcene
5.6	Limonene
5.7	3,3'-oxybis-2-butanol
5.7	oxybis Propanol
6.1	Dihydro myrcenol
6.4	Linalool
6.5	Benzene ethanol
7	benzyl ester Acetic acid
7.5	Citronellol
7.6	Linalyl anthranilate
8	Vertenex
8.4	α -Terpineol acetate
8.4	Nerol acetate
8.5	Geraniol acetate
9.2	α-Cetone
9.2	β–Ionone
9.3	β– methyl Ionone
9.4	α-N-Methyl ionone
9.4	Indane-1,3-diolmonopropionate
9.5	Lilyal
9.8	Salicylic acid, pentyl ester
10.3	Methyl dihydrojasmonate
10.5	Hexyl salicylate
11.1	α- hexyl Cinnamaldehyde
12.3	Galoxolide
12.7	Benzyl salicylate
13	Musk 36A

Spray #3

12.3	Galoxolide
12.7	Benzyl salicylate
13.1	Musk 36A
15	Musk T

Spray #5

4.6	β–pinene
5	n-Hexyl acetate
5.3	Limonene
5.5	oxybis Propanol
5.6	γ–Terpinene
6.1	Linalool
6.6	Ethyl acetoacetate ethylene ketal
6.7	Benzyl acetate
7	Gardenol
7	n-Dodecane
7.3	Citronellol
7.5	Linalyl anthranilate
7.7	Cinnamaldehyde
7.9	Indole
8.7	Anisyl acetate
8.7	Ananolide
8.8	cis-Ethyl 3-methyl-3-phenylglycidate
8.9	Isoeugenol
9	Cyclamal
9	2,5-Diisopropyl-p-xylene
9.1	α-Cetone
9.3	α-N-Methyl ionone
9.4	Lilyal
10.1	Methyl dihydrojasmonate
10.4	Hexyl salicylate
11.2	Benzyl benzoate
12	Galoxolide
12.4	Benzyl salicylate
12.7	Musk 36A
13.5	Hexadecanoic acid

Spray #6

5.7	Limonene
6.1	Dihydromyrcenol
6.4	Linalool
7.5	1-Methyldodecyl butyrate
7.5	Citronellol
7.7	Guaniol
8	Citronellal hydrate
8.9	Indan-1,3-diol monoacetate
9.1	Cyclamal
9.8	Pentyl salicylate
10.2	Triethyl citrate
10.3	Methyl dihydrojasmonate

5.6	Limonene	10.5	Methyl jasmonate
6	γ–Terpinene	11.1	Cinnamaldehyde, alpha-hexyl-
6.1	Dihydromyrcenol	11.8	Bisomel
6.4	Linalool	12.3	Musk 36A
7	Acetic acid, benzyl ester	12.7	Benzyl salicylate
7.2	Ethyl linalool	15	Musk T
8.2	Dimethylphenethyl acetate		Spray #7
8.8	1-hexen-4-ol,3-methyl-5-phenyl	5.7	oxybis-Propanol,
9.2	β– Ionone	6.4	Linalool
9.2	2,5-Diisopropyl-p-xylene	7.1	Ethyl linalool
9.3	(3-Methyl-4-pentenyl) benzene	7.3	Ethyl maltol
9.7	Dihydrosafrol	7.6	Bergamot mint oil
9.9	Eugenol acetate	8	Vertenex
10.2	Triethyl citrate	9.7	Allyl 2-methoxybenzoate
10.3	Methyl dihydrojasmonate	10.3	Methyl dihydrojasmonate
11.1	α- hexyl Cinnamaldehyde	11.2	n-Octyl benzoate
11.5	Benzyl benzoate	11.8	Bisomel
12.3	Galoxolide	12	Linoleic acid
12.7	Benzyl salicylate	12.5	Undecyl benzoate
12.4	Musk 36A	15.9	Musk T
16	Mono(2-ethylhexyl) phthalate		

A box plot was prepared based on this ratio and VP and can be observed in Figure 3-12. As the data suggest, non-volatile compounds (VP <1 mmHg, blue box) had a wide range of particle-to-vapor phase ratios, including numbers as large as 3.9; in contrast, this ratio was compressed around 1 for the volatile compounds (VP >1 mmHg, orange box). This result suggests that, in the case of non-volatile compounds, a large portion of the fragrance compounds remain in the droplet phase, which can be trapped and detected by the NTD (resulting in large particle-to-vapor phase concentration ratio). Conversely, the results for the NTD and TFME for volatile compounds do not cover a wide range, which implies that most of these volatile compounds are in free vapor phase and can be detected by TFME as well as the NTD.

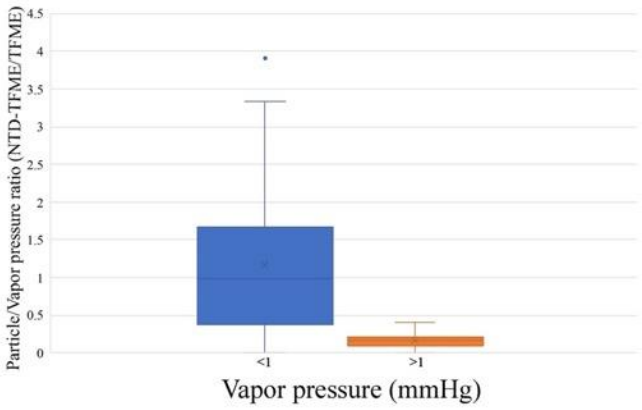

Figure 3-12. Box plot of particle-to-vapor phase concentration ratio vs. vapor pressure (the bars include the whole range of data, with the blue and orange box containing the 2nd and 3rd quartiles).

3.4.11 Passive vs. active sampling of fragrances in the bathroom with NTD and SPME

To compare the devices' abilities for passive and active sampling, Spray #7 was applied inside of a bathroom, and SPME and the NTD were left there to sample for 60 minutes. Active sampling was tested using similar conditions. The results of these tests are listed in Table 3-9.

Table 3-9. Concentrations of linalool found in μg L^{-1} (relative standard deviation, RSD %) in bathroom air after applying Spray #7 using both active and passive NTD and SPME.

Concentration	Active sampling time range (min)				Passive sampling time range (min)
method	0	15	30	60	60
NTD	348 (4%)	251 (7%)	98 (9%)	ND	48 (5%)
SPME	89 (2%)	45 (11%)	22 (14%)	ND	41 (4%)

The values in brackets represents the relative standard deviation percentages. As the data show, the results for both methods were statistically similar when used for passive sampling, likely due to the droplets being unable to reach the NTD nor SPME due to their large size and low diffusion coefficient. It should be noted that the concentrations from passive sampling represent

the average concentration over the sampling period. Based on these explanations, in both methods with passive sampling, only free concentration over 1 h sampling time is measured, which is reflected in similar results obtained by both methods.

As previously noted, the difference between the NTD and SPME for active sampling was due to the concentration of linalool inside of the droplets, which can be determined via NTD, but not SPME. As can be seen, the difference in concentration is quite large, thus demonstrating the necessity of using an NTD equipped with a filter when analyzing aerosol samples.

When compared to SPME and TFME in active sampling mode, the significant concentration of compounds inside the droplets captured by the filter-incorporated NTD is the key factor highlighting its exceptional performance in fragrance analysis. Indeed, while TFME and SPME are only able to capture the free concentration of analytes, the NTD is able to also capture the analytes trapped within the droplets, thus providing the total concentration of analytes.

Unlike other passive sampling methods, which can only reveal the average concentration over a time span, our NTD can determine the total concentration at different times. This is significant, as the ability to monitor the total concentration over time enables us to find the peak concentration after the administration of fragrance containing products. This property is particularly important when considering allergens. For example, while the average and free concentrations of these compounds over time may be lower than the limits set forth by regulatory administrations, they may exceed these limits when their total concentration is considered.

3.5 Conclusion

For analyses of fragrances in spray samples, it is important to develop a sample-preparation method that not only facilitates the injection of samples into the instrument, but that also preconcentrates the fragrances for improved detection sensitivity. In this study, we attempted to fulfill this objective by installing a filter into a needle-trap device to facilitate the capture of droplets in air samples containing sprayed fragrances. Furthermore, we further packed our NTD with sorbent particles to enable the extraction of free fragrances. This combination of filter and sorbent corroborated highly effective at determining the total concentration of fragrances in a given sample. For comparison, TFME and SPME were also applied to the same samples in order to determine the free concentration of fragrances in the gas phase. The results of this comparison revealed that NTD was able to extract a higher concentration of analytes compared to TFME and SPME due to its ability to detect and determine analytes in dispersant (droplets/particles). Notably, this difference was greater for less-volatile and polar compounds with lower vapor pressures, as these compounds tend to remain in droplets. The sampling chamber was equipped with a fan, and the lower concentration of fragrances in the "fan on" condition highlighted the importance and efficiency of good ventilation rooms with a high rate of spray applications, such as hair salons.

The prepared filter showed high repeatability, low flow resistance, and thermal and chemical stability. In addition to filtration efficiency, the filter plugs inside the needle also act as a retainer for sorbent particles. The designed filter-incorporated NTD offers an appealing alternative for exhaustive extractions of spray samples, as it is able to measure the concentration of fragrances in the gas–phase, as well as in droplets. Additionally, NTD technology is compatible with portable instrumentation, which makes it suitable for on-site determinations. The designed NTD can be further applied to other sparkled samples with aroma such as beer, soda, and other beverages which needs further investigation.

Filter-Incorporated Needle-Trap Device (FI-NTD) Application: Sparkling Beverages

4.1 Preamble

This chapter contains sections that have already published as an article in Food Chemistry. All subchapters are included in the article entitled *Free versus droplet-bound aroma compounds in sparkling beverages* by Shakiba Zeinali, Martyna Natalia Wieczorek and Janusz Pawliszyn, *Food Chemistry,* 2022, 378, 131985–131991. The contents of the articles are herein being reprinted with permission of Elsevier, in compliance with both publisher's and the University of Waterloo policies.

4.2 Introduction

For thousands of years, the fermentation process has been one of the main sources of flavour in beverages, as it is a natural method of producing aroma-active components. At present, the ongoing growth in demand for flavored beverages has motivated the development of new flavor-perception enhancements, such as artificial odorants, sweeteners, or CO_2 [181]. Since 70% of flavor is rooted in one's sense of smell, the addition of odorants to beverages would seem to be the most effective approach to influencing consumers' food choices [182].

One of the major innovations in the drink industry has been the introduction of carbonated drinks. It is believed that effervescence is responsible for the enhanced flavor and sense of refreshment that are characteristic to carbonated drinks [183,184]. While several studies have examined how carbonation influences consumers' perceptions of taste and flavor [185–187]

considerably less attention has been devoted to the influence of carbonation and sparkling droplets upon entering the consumer's nasal cavity.

To date, two main approaches have been employed to study aroma compounds in carbonated beverages: the liquid-liquid extraction of aroma from beverages [188,189] and the extraction of volatile organic compounds from the beverage headspace via solid-phase microextraction [190–194]. Additionally, stir-bar sorptive extraction [176,195–197], solid phase extraction [198–201], and thin-film microextraction [202,203] have also been applied to examine aroma in sparkling beverages.

While the above approaches have been successfully optimized to accurately characterize the active odor components in beverages, the majority have involved degassing of the beverage prior to extraction [204]. The effect of degassing is significant, as degassing, and in some cases, the addition of salts, can create a final extraction sample that is completely different from the purchased product. Thus, the results of studies using such samples may not reflect the actual consumer experience. One key issue associated with the above-described approach is its failure to account for the migration of volatiles to the nasal cavity via CO_2 [185,205–207]. Additionally, the degassing process itself may significantly diminish the concentration of volatile organic compounds in the beverage [208]. Another issue associated with such approaches is that the headspace of sparkling beverages comprises two phases: gas phase and droplets. This is important to consider, as the presence of droplets can alter the final concentration of odorants, ultimately influencing flavor perception.

The main goal of the present study is to examine the active odor components in sparkling beverages, both in the gas phase and particle-bound. To this end, polydimethylsiloxane thin-film

microextraction (PDMS-TFME) was applied to perform extractions from the gas phase, and a heated polyacrylonitrile (H-PAN) filter was employed to trap the droplets. The application and properties of this filter have been studied previously. Sampling was conducted without the removal of bubbles or the addition of salt in order to preserve actual consumer conditions. Furthermore, sampling was performed for 3 minutes immediately after opening the bottle, which was sufficient to enable the detection and trapping of droplets before effervescence was completely lost. The results of this research can provide a more accurate understanding of the consumer's experience of flavored beverages in daily life.

4.3 Experimental

4.3.1 Reagents and chemicals

Polyacrylonitrile (PAN) (Mw= 150,000 g mol^{-1}), dimethylformamide (DMF) (99.8%) as well as analytical grade furfural, methional, α–pinene, ethylcaproate, limonene, γ–terpinene, linalool, and citronellol were all purchased from Sigma-Aldrich (Mississauga, ON, Canada).

Lime and orange flavored soda, orange flavored natural carbonated spring water, two lime and lemon-flavored sparkling spring water, and wheat and non-alcoholic beer were purchased from a local market for analysis.

4.3.2 Instruments and conditions

Elcometer 4340 film applicator used for thin-film preparation was from Elcometer Inc., Manchester, UK. Please refer to **2.3.1.4 GC-MS for thin–film analysis** for details on the instrument. GC oven temperature programming is provided in Table 4-1.

Table 4-1 GC temperature programming for separation of aroma compounds.

Rate (ºC min^{-1})	Temperature (ºC)	Hold time (min)
	40	0
20	80	0
8	100	0
20	150	0
25	200	5
8	220	0

4.3.3 Preparation of extraction phases, standards and calibration

Polydimethylsiloxane-loaded thin-film (PDMS-TFME) devices (3×20mm) were prepared according to the procedure developed by [145]. Briefly, 4.54 g of Sylgard 186 PDMS base and 3.8 g of hexane were mixed inside a syringe, followed by the addition of 0.46 g of Sylgard 186 cross-linking agent. Finally, the mixture was spread over a 25 cm × 60 cm carbon-mesh sheet using an Elcometer 4340 motorized film applicator. Once coated, the carbon-mesh sheet was left to dry at 90 ºC at a gauge pressure of -15 mmHg under nitrogen purge for at least half an hour. The coated thin films were then cut into the desired sizes (30 × 4 mm) and conditioned before extraction.

Please refer to **2.4.2 Optimized Filter Preparation Condition** section. 0.5 cm of H-PAN was subsequently packed in the thermal desorption unit (TDU) glass liners with glass frits. The extraction devices are depicted in Figure 4-1.

All experiments were performed in gas phase. For PDMS-TFME calibration, a 1-L glass bulb was initially washed, dried, vacuumed, and injected with 1 μL of pure analytes, which were subsequently evaporated via heating.

Figure 4-1. PDMS-TFME and H-PAN filter packed inside glass liner.

The final concentration of the stock gas mixture was calculated based on the equation provided by Nelson [209] and ranged between 200 and 300 ppm, depending on the analyte properties. A complete list of odorants and their properties are provided in Table 4-2. The stock gas mixture was then diluted in another glass bulb using gas–tight syringes in order to attain the required concentrations of the compounds. The range of calibration is provided in Table 4-2. Another calibration curve (523-2143 μg L^{-1}) was also drawn for limonene to cover the abundant amounts of it found in some samples. The concentration of droplet-bound components trapped by the H-PAN filter was calibrated based on the assumption that trapping was exhaustive due to the small sample volume, and that the breakthrough volume had not been reached. This assumption and the capacity of the filter has been studied previously. To this end, extracted amounts were calculated using a liquid-injection calibration curve (10-1000 ng). The extracted amount (in ng) was divided by the sampling volume (15 mL) to find the concentrations of the compounds in the gas sample.

Table 4-2. List of odor active analytes, their physiochemical properties, and the concentration range for calibration of the method using PDMS-TFME

	Rt (TFME)	Boiling point (°C)	Henry Constant (atm m^3 mol^{-1})	LogP	Calibration concentration range in sampling bulb (µg L^{-1})
Furfural	3.3	161	4E-6	0.4	0.4 – 575
Methional	3.8	165	4E-7	0.3	0.3 – 515
α–pinene	4.2	156	1E-1	4.8	0.2 – 429
Ethyl caproate	4.9	167	4E-6	2.4	0.4 – 433
Limonene	5.3	176	3E-2	3.4	0.1 – 421
γ–terpinene	5.6	183	3E-2	4.5	0.3 – 420
Linalool	6.0	197	2E-5	2.7	0.1 – 432
Citronellol	7.2	225	2E-5	3.2	0.1 - 427

4.3.4 Extraction procedure

Since the main goal of this study was to compare free and droplet-bound concentrations of aroma compounds in sparkling beverages, conventional optimization procedures for improving sensitivity were not performed. Extraction conditions (time and temperature) were selected to mimic the real consumer experience of initial exposure to beverage flavor. As a result, a short extraction time at room temperature was selected. In addition, the short extraction time ensured that the low amounts of water in the H-PAN filter did not cause any problems for the GC instrument.

For the extractions with PDMS-TFME, a pre-equilibrium condition with an extraction time of 3 minutes was chosen. The thin-films were calibrated by exposing them to the gas sample mixture for 3 minutes in a glass bulb, and then transferring them to the TDU liner for desorption.

For H-PAN filter calibration, the concentration of the trapped aroma compounds was calculated by dividing the trapped amount (using liquid injection calibration curve) by the sampling volume (15 mL).

Extraction/trapping was performed immediately after opening the beverage or standard mixture. In cases where the bottle or can did not have enough headspace for sampling, the beverage was transferred to another sampling bottle that provided appropriate extraction conditions. For PDMS-TFME extraction, the thin-films were exposed to the sample headspace for 3 minutes and then transferred for desorption. Droplet trapping via the H-PAN filter involved exposing the packed liner to the sample and drawing the headspace into the liner using a syringe pump (flow rate = 5 mL min^{-1}, volume = 15 mL).

After sampling, the TDU liner was transferred to the GC-MS instrument for desorption. A schematic of extraction procedure is provided in Figure 4-2.

4.3.5 Preliminary studies in standard mixtures

Preliminary studies were conducted to assess the extraction efficiency of PDMS-TFME and the trapping capability of the H-PAN filter in carbonated and non-carbonated samples. To this end, a standard mixture of the analytes was prepared in water (400 μg L^{-1}, 500 mL), with extraction and trapping being performed according to the procedures detailed previously. The same process was repeated for similar mixtures, while the final mixture was carbonated using a Soda Stream machine.

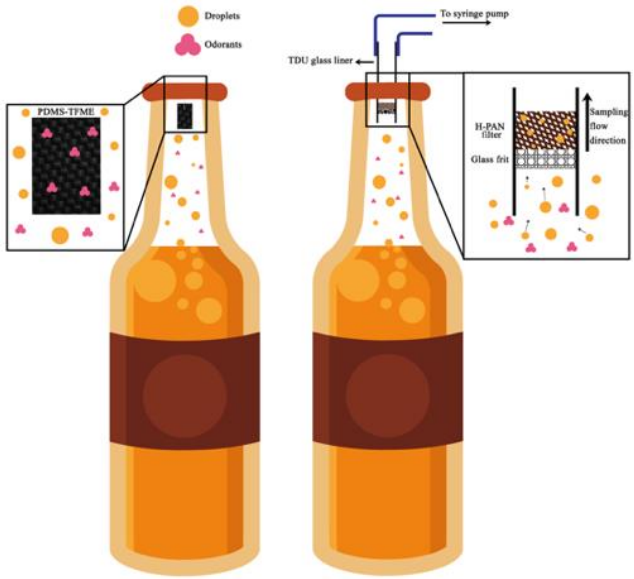

Figure 4-2. Schematic of extraction procedure from sparkling beverages using H-PAN filter and PDMS-TFME for studying aroma compounds in real consumer experience conditions.

4.4 Results and discussion

4.4.1 Comparison of carbonated and non–carbonated mixtures

This study sought to compare the concentration of aromatic compounds present in sparkling beverages in free and droplet-bound format. To ensure distinct results for both phases, it was critical to first design suitable extraction devices. Consequently, an H-PAN filter was designed to only trap droplet-bound analytes, and a PDMS-TFME device was developed to extract compounds from the gas phase. In PDMS-TFME, the available extraction volume can be calculated using surface area and thickness; however, H-PAN is a fibrous, porous filter and the accessible trapping surface is difficult to find. Once sampling had been completed, the analytes from both devices were desorbed in the TDU injection port to obtain the resultant analytical data.

As can be seen in the chromatogram in Figure 4-3, sampling the non-carbonated standard mixture with the H-PAN filter produced peaks with very low intensity. Some polar compounds

(e.g., furfural and methional with logP=0.3-0.4) were not detected by the H-PAN filter, while others non-polar that were detected (e.g., limonene and linalool) had peak-area ratios that were less than 2% of those acquired with PDMS-TFME, thus indicating that the H-PAN filter had very low extraction efficiency for gas phase components. In detail, furfural, methional, α-pinene and citronellol were not detected, while ethyl caproate, limonene, γ-terpinene and linalool had reported concentration ratios 2.1, 0.5, 0.6, 0.6% (vs. PDMS-TFME), respectively. Given the H-PAN filter's low extraction efficiency for gas-phase components, it can be assumed that the obtained results from H-PAN filter are connected to the trapping of the droplets, not from the gas-phase extractions.

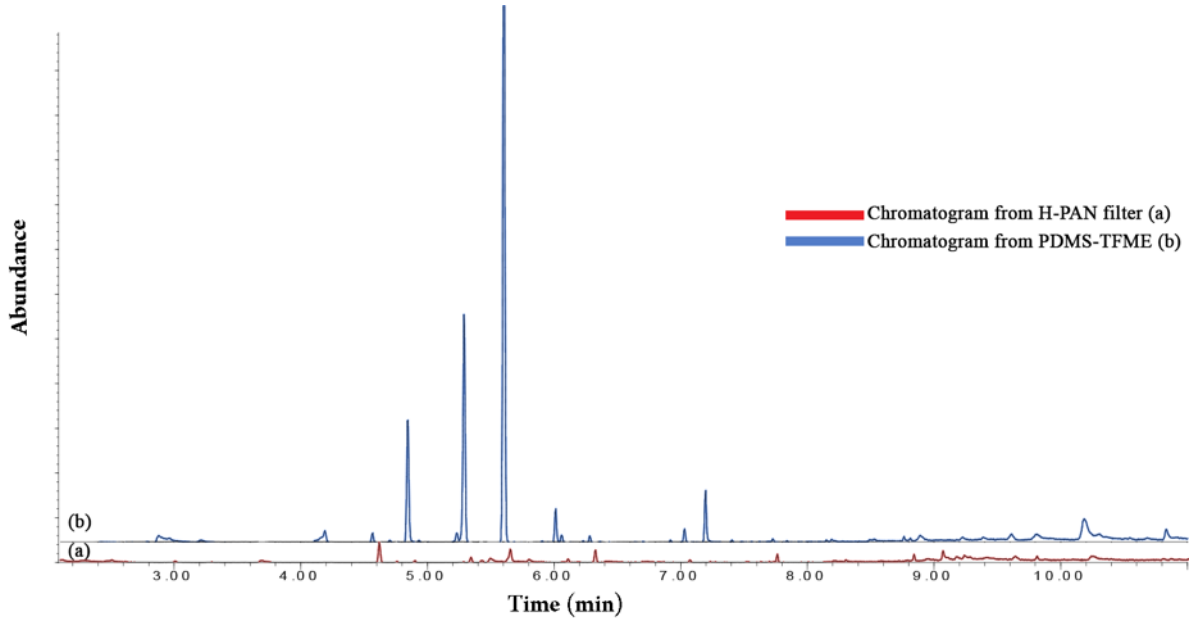

Figure 4-3. Chromatogram from extraction/trapping of non-carbonated standard mixture using H-PAN filter and PDMS-TFME

A comparison of the concentrations of odorants extracted from the carbonated and non-carbonated samples with the H-PAN filter (Figure 4-4), revealed that, with respect to the carbonated sample, the filter was capable of capturing and therefore facilitate quantifying polar compounds with high tendencies to remain in aqueous phase (i.e., furfural and methional with

logP=0.3-0.4). This result was due to the H-PAN filter's ability to trap droplets after carbonation, which was not observed in the non-carbonated sample (without droplets).

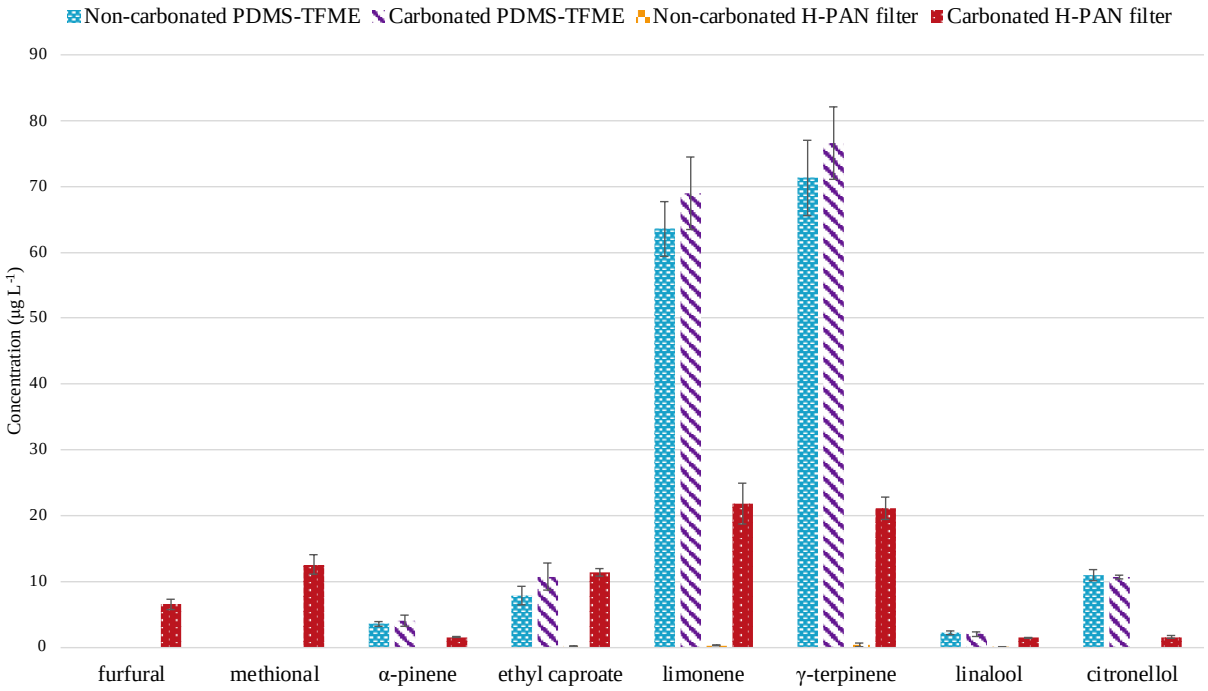

Figure 4-4. Concentration of odorants in carbonated and non-carbonated standard mixtures studied after extraction via H-PAN filter and PDMS-TFME

To ensure that the PDMS-TFME device only extracted analytes from the gas phase, the extractions were performed using carbonated and non-carbonated components. Generally, the PDMS-TFME device extracted similar amounts of analytes from the carbonated and non–carbonated mixtures (Figure 4-4), meaning that the presence/absence of droplets does not play a significant role in extractions with this device. It can therefore be concluded that the PDMS-TFME extractions occurred in the gas phase, and that the slight increase in analytes extracted from the carbonated samples can be attributed to the increased evaporation rate of analytes during bubbling. If this increment was the result of droplet attachment to the PDMS-TFME surface, furfural and methional should have been detected and identified.

4.4.2 Analysis of sparkling beverages

To test the proposed method's applicability for the analysis of sparkling beverages, different types of drinks were studied, including soda and sparkling water with different flavors. As shown in Table 4-3, different compounds, including limonene, γ-terpinene, linalool, citronellol, and ethyl caproate, were detected and quantified in the drink samples. The presence of these compounds is not surprising, as they are the components of lemon oil, lime oil, and orange oil that are commonly added to beverages to introduce the required flavors [210].

Table 4-3. Concentration in μg L^{-1} (relative standard deviation, RSD %) of active aroma compounds in different sparkling beverages determined using PDMS-TFME and H-PAN filter.

Lime-Soda	PDMS-TFME	H-PAN Filter
Limonene	72 (14%)	12 (7%)
γ -terpinene	4 (15%)	0.52 (10%)
Sparkling water-Lime	PDMS-TFME	H-PAN Filter
Limonene	12 (18%)	1.3 (16%)
γ -terpinene	2.4 (13%)	0.26 (8%)
Linalool	0.44 (7%)	0.12 (3%)
Citronellol	1.9 (19%)	0.13 (9%)
Sparkling water-Lemon	PDMS-TFME	H-PAN Filter
Limonene	144 (13%)	52 (11%)
γ -terpinene	10 (18%)	2.9 (15%)
Orange-Soda	PDMS-TFME	H-PAN Filter
Limonene	1665 (11%)	2017 (6%)
Non-alcoholic beer	PDMS-TFME	H-PAN Filter
Ethyl caproate	25 (8%)	12.3 (1%)
Limonene	3.6 (6%)	6.8 (6%)
spring carbonated water-orange	PDMS-TFME	H-PAN Filter
Limonene	823 (3%)	23 (9%)
γ -terpinene	21.6 (4%)	0.61 (12%)
Linalool	7.7 (7%)	0.11 (8%)
Wheat Beer	PDMS-TFME	H-PAN Filter
Ethyl caproate	3.7 (5%)	2.11 (3%)
Citronellol	13.6 (5%)	0.6 (3%)

The concentration of these components varied depending on the type of the drink. Chromatograms obtained after using the H-PAN filter and PDMS-TFME to trap/extract odorants from lime-flavored sparkling spring water and orange-flavored natural carbonated spring water are presented in Figure 4-5 and Figure 4-6. As different approaches were used to calibrate each

method, their detected concentrations cannot be compared using the absolute intensities of the peak areas in the chromatograms. It is worth noting that the odorant concentrations reported herein were detected in the gas phase or droplet-bound portion of the sample headspace; therefore, they cannot be considered as representative of the concentrations of odorants in the liquid phase of the beverage.

It is also important to note that the droplet-bound odorant concentrations reported in Table 4-3 were dependent on different factors, principally physiochemical factors and carbonation type. For physiochemical aspect, the analysis of the standard mixture revealed that polarity also plays an important role, as compounds with higher polarity prefer to remain inside the droplets, which allows them to be trapped and quantified with the filter.

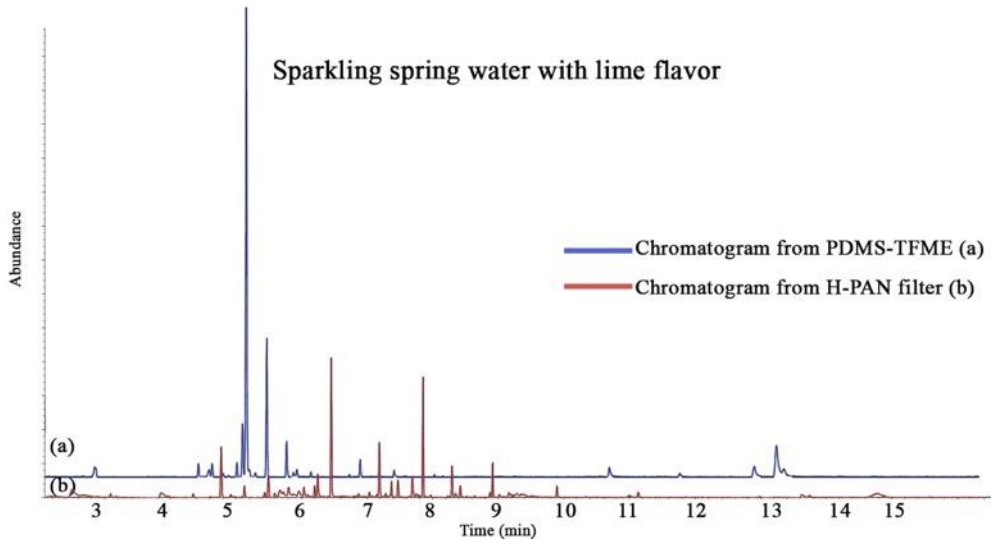

Figure 4-5. Chromatogram from PDMS-TFME and H-PAN filter after analyzing sparkling water with lime flavor

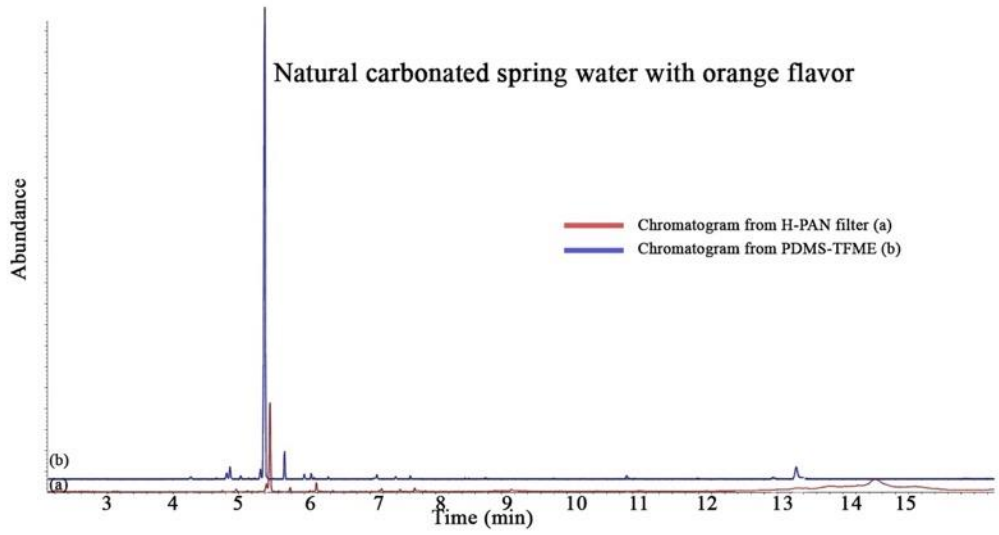

Figure 4-6. Chromatogram from PDMS-TFME and H-PAN filter after analyzing natural carbonated water with orange flavor

Also, the vapor pressure and volatility can determine the tendency of the compounds towards gas or droplet phase. As can be seen in Table 4-3, in most cases, when compound under study is more volatile such as limonene with vapor pressure=1.6 mmHg, the concentration reported with PDMS-TFME is higher, since these compounds are found preferably in gas phase; however, less-volatile components such as linalool with vapor pressure=0.16 mmHg prefer liquid phase.

The findings also showed that the type (pressure and time) of carbonation can influence the final product. Since more carbonation creates more droplets in the headspace, the concentrations reported with filter will increase as well. This phenomenon was evident in the reported concentrations of limonene in orange-flavored soda and lime-flavored sparkling water, where the difference in droplet count was visible to the naked eye. High-pressure carbonation resulted in higher concentrations of limonene being detected in orange-flavored soda by the H-PAN filter compared to PDMS-TFME, whereas for lime-flavored sparkling water with lower number of

droplets, the final reported concentration was much higher for PDMS-TFME compared to H-PAN filter.

Carbonation type also influences the repeatability of the sampling. For beer samples, droplet formation occurs due to biochemical processes which cause a stable foam form after the bottle is opened, rather than a stream of bubbles. This stability effect can be seen in the relative standard deviations of the reported concentrations. The stable foaming observed for beers enables more reproducible results compared to sodas, which have a decaying stream of bubbles and droplets.

In addition to the target compounds, the beverage analysis resulted in the identification of other components using the mass spectrometry library. For example, some compounds such as myrcene and o-cymene were identified with both PDMS-TFME and the H-PAN filter. In contrast, some higher-polarity compounds, such as furfural (below calibration range), 5-hydroxymethylfurfural, and 1,4-anhydro-D-mannitol, were only detected in the droplets captured by the H-PAN filter, while certain non-polar compounds, such as decanal, nonanal, α-humulene, α and β-citral, and β-pinene were detected only with PDMS-TFME.

4.5 Conclusion

This research provided a more comprehensive view of the perception of flavor in sparkling drinks by extracting gas-phase odorants via PDMS-TFME and trapping droplet-bound components with a high-efficiency filter. The results of these tests showed that the PDMS-TFME is best suited to extractions from the gas phase, while the H-PAN filter is appropriate for trapping droplets. In addition, a short extraction time was utilized, not only to mimic the bottle opening experience, but also to minimize the amount of water in the filter, which can be problematic for GC instruments.

As the results suggest, most of the examined odorants can be present in both the gas phase and in droplet-bound form, thus increasing their total concentrations in nasal cavities. This may be a major cause of the sense of flavor enhancement in carbonated beverages. On the other hand, some polar components that could not be detected in the gas phase were detectable when trapped with the filter. This is an important finding, as exclusive study of the gas phase can overlook these compounds' roles in the general perception of flavor. Indeed, their presence inside the droplets is almost certainly an influential factor in shaping the consumer's beverage experience. Additionally, a question arises relating to the utility of odour threshold values of aroma components active in these kinds of beverages. Until now, studies have focused on how factors such as matrix effects impact the release of active aroma components; however, in case of beer/soda, there appear to be no prior studies that have adequately examined the effects of CO_2 content/influence. This is a notable gap, as the present study demonstrates the importance of this parameter to research focusing on odorants. Thus, more attention should be devoted to this area of investigation. If information about non-volatiles in aerosol is desired then the filter can be rinsed with organic solvent followed by LC/MS determination of the wash.

The work presented herein is a preliminary study. As such, it is recommended that future work focuses on optimizing the extraction and particle trapping method to improve sensitivity, as well as testing their performance using different beverages.

Filter-Incorporated Needle-Trap Device (FI-NTD) Application: Breath Analysis

5.1 Preamble

This chapter contains sections that have already published as two articles in Analytica Chimica Acta and Analytical and Bioanalytical Chemistry. All subchapters are included in either the article entitled *Simultaneous determination of exhaled breath vapor and exhaled breath aerosol using filter-incorporated needle-trap devices: A comparison of gas-phase and droplet-bound components* by Shakiba Zeinali, Chiranjit Ghosh and Janusz Pawliszyn, *Analytica Chimica Acta*, 2022, 1203, 339671-339682 and *Effect of household air pollutants on the composition of exhaled breath characterized by solid-phase microextraction and needle-trap devices components* by Shakiba Zeinali and Janusz Pawliszyn, *Analytical and Bioanalytical Chemistry*, special issue" Promising Early-Career (Bio)Analytical Researchers", 2022, 1-11. The contents of the articles are herein being reprinted with permission of Elsevier and Springer, in compliance with both publisher's and the University of Waterloo policies. Subsection 5.3 was the result of a collaboration with University of Waterloo and UHN. The access to the patients was provided by Dr. Liu and with the aid from Mersedeh Pourkar and Khaleeq Khan. The results of this study would be published entitles *Portable microextraction techniques for comprehensive investigation of breath biomarkers from lung cancer patients* by Shakiba Zeinali, Mersedeh Pourkar, Khaleeq Khan, Devalben Patel, Janusz Pawliszyn, as a communication for Green Analytical Chemistry journal.

5.2 Simultaneous determination of exhaled breath vapor and exhaled breath aerosol using filter-incorporated needle-trap devices: A comparison of gas-phase and droplet-bound components

5.2.1 Introduction

Breath analysis has become a popular non-invasive diagnostic approach for obtaining immediate feedback regarding the health of human subjects. Indeed, ancient Greek physicians understood that the sweet smell of breath is the result of diabetes or the attribution of breath smell to kidney failure. Volatile organic compounds (VOCs) in exhaled breath either are the products of metabolism, or are subtracted from inspired air [97]. The non-invasive, cost-effective, and real-time nature of analyzing VOCs in breath samples makes it an ideal approach for disease diagnosis, therapeutic monitoring, and exposure studies. One of the earliest modern breath-analysis studies was conducted by Pauling et al. in 1971, who identified up to 200 compounds in breath [96]. In 1999, Philips et al. attempted to distinguish healthy subjects from lung cancer patients by using breath samples to monitor their metabolic profiles and metabolic-marker concentrations [211]. Furthermore, other researchers have employed breath analysis to diagnose diseases [78,212,213] and to assess environmental exposure [214–219].

Although breath analysis offers many advantages, its routine use to monitor health status is complicated by a number of challenges, including: difficulty in distinguishing exogenous VOCs; variations in breath composition based on age, gender, and diet; a lack of standardized methodology; low VOC concentrations; and the presence of droplets carrying polar and less-volatile components.

The term, “breath analysis” primarily refers to the analysis of VOCs in exhaled breath vapor (EBV); however, less-volatile and polar compounds prefer to remain inside breath droplets known as exhaled breath aerosol [220]. Conventionally, these breath droplets are condensed in a cold container and collected as exhaled breath condensate (EBC) for use in subsequent studies [103,221,222].

Microextraction techniques, which combine preconcentration and sample introduction into a single step, are good candidates for breath analysis and various methods has been applied for breath studies [223]. In particular, thin-film microextraction (TFME) is especially promising for the extraction of free analytes in gaseous phases, as its enhanced surface area enables higher extraction capacities compared to fiber-based solid-phase microextraction. Despite these advantages, only Xu et al. have previously attempted to apply TFME for breath analysis [107]. However, while Xu et al. utilized electrospun polystyrene thin films to extract biomarkers from collected EBC samples, we are unaware of any prior research that has applied TFME to extract free biomarkers from breath vapor.

On the other hand, needle-trap devices (NTD) can extract free VOCs and act as filters, albeit with limited filtration efficiency [47]. However, it is possible to improve filtration efficiency by incorporating a filter into the NTD. The selected filter should provide high filtration capacity, high permeability for dynamic sampling, and thermal stability for thermal desorption. While breath analysis with NTDs has been previously reported [34], these studies exclusively focused on the analysis of free VOCs, with droplet-bound analytes being excluded from the final results.

In this work, we attempt to incorporate a filter and sorbent into an NTD for the simultaneous extraction of VOCs from EBV and EBC. To verify the proposed device’s viability, TFME was

employed to extract VOCs from a gas phase. For this study, we selected VOCs with physiochemical properties associated with various diseases, such as lung cancer [222,224,225] The optimized methods were applied to study the composition of breath samples obtained from volunteers. To study the role of breath droplets, we also analyzed breath samples obtained while the volunteers were wearing a mask. Finally, to assess the effect of inhaled air on VOCs in one's breath, breath samples from a volunteer were analyzed following incidental exposure to various VOCs during routine lab experiments.

5.2.2 Experimental

5.2.2.1 Materials and Instruments

Polyacrylonitrile (Mw=150,000 g mol^{-1}), 2-butanone, methyl cyclopentane, benzene, 2-pentanone, toluene, octane, ethylbenzene, styrene, heptanal, propylbenzene, heptanal, 1,2,4-trimethylbenzene (1,2,4-TMB), decane, undecane, nonanal, methanol and Carboxen (60/80 mesh size) in analytical grade were purchased from Sigma-Aldrich (Mississauga, ON, Canada). For sampling 1-L glass bulb 2-2144 Supelco (Oakville, ON, Canada) was used. For heating aerogels, an Isotemp™ Model 281A Vacuum Oven was heated to 280 ºC under atmospheric pressure and kept in that temperature for 2 h. Vitamix 7500 blender (Cleveland, Ohio, USA) was used for cutting fibers. For sampling with mask, volunteers were wearing 3-layered surgery face mask.

Quintron 750-mL breath sampling bags were purchased with mouthpiece and a 400-mL discard bag. Tee-Mouthpiece Assembly was used for sampling. New mouthpiece was used for every patient. Thin films were prepared by Elcometer 4340 film applicator (Elcometer Inc., Manchester, UK).

Please refer to **2.3.1.2 SMPS instrument, 2.3.1.4 GC-MS for thin–film analysis and 2.3.1.5 GC-MS for needle–trap analysis** for details on the instrument. Mass spectrometry detection was performed in scan mode with a mass range of 50–250 m/z using electron impact ionization at 70 eV for initial studies and for calibration and real sample analysis, selected ion monitoring was used (assigned m/z values and retention times can be found in Table 5-1). For separation with both instruments, Initial temperature was set at 40 ºC for 4 min. Then, the temperature increased to 100 ºC with 5 ºC min^{-1} rate and kept for 1 minute. Finally, temperature increased to 250 ºC with 20 ºC min^{-1} rate.

Table 5-1. List of VOCs and chemical properties

All	Boiling point (ºC)	Henry constant (atm m^3 mol^{-1})	LogP	Rt with TFME (GCMS)	Rt with NTD (GCMS)	m/z	C (ppm) in standard
2-butanone	80	6E-5	0.3	2.6	3.1	43,72	273
Methylcyclopentane	72	3E-1	3.4	2.8	3.5	56,41	218
Benzene	80	1E-2	2.1	3.2	3.9	78,77	275
2-Pentanone	102	8E-5	0.9	3.5	4.4	43,86	230
Toluene	111	1E-2	2.7	5.1	6.7	91,92	230
1-Octene	121	6E-1	4.6	5.8	7.4	55,43	156
Octane	125	3E0	3.9	6.0	7.6	43,57	151
Ethylbenzene	136	1E-2	2.8	7.7	9.9	91,106	199
Styrene	145	3E-3	2.9	8.6	11.2	104,78	213
Heptanal	152	3E-4	2.3	8.9	11.4	70,44	173
Propylbenzene	159	1E-2	3.7	10.5	13.3	91,120	175
1,2,4-TMB	170	1E-2	3.6	11.7	15.1	105,120	178
Decane	174	5E0	5.8	12.0	15.2	57,43	125
Undecane	195	6E0	5.7	15.1	18.7	57,43	116
Nonanal	191	7E-4	3.3	15.2	18.9	57,41	142

5.2.2.2 Preparation of filter included needle–trap device and thin-films

Please refer to **2.4.2 Optimized Filter Preparation Condition** section for details on the preparation of filter. Obtained white PAN aerogel and brown H-PAN aerogel. The resultant aerogel was then heated at 280 ºC for 2 h to increase stabilization and avoidance of melting. Finally, the brown H-PAN aerogel was packed into the NTD for extraction studies. For the filter-incorporated NTD, 1 cm of Carboxen was sandwiched between two 2 mm layer of H-PAN filter (Figure 5-1). H-PAN aerogel acts as a filter that traps particles and as a retainer that sequesters the sorbent particles inside the needle. The final needle tips were cone-shaped for improved desorption. Carboxen-embedded thin film (3×20 mm) was prepared in accordance with the procedure developed by Grandy et al. [145]. Briefly, Carboxen particles were glued onto the carbon mesh using PDMS as an adhesive and an applicator to affix the particles.

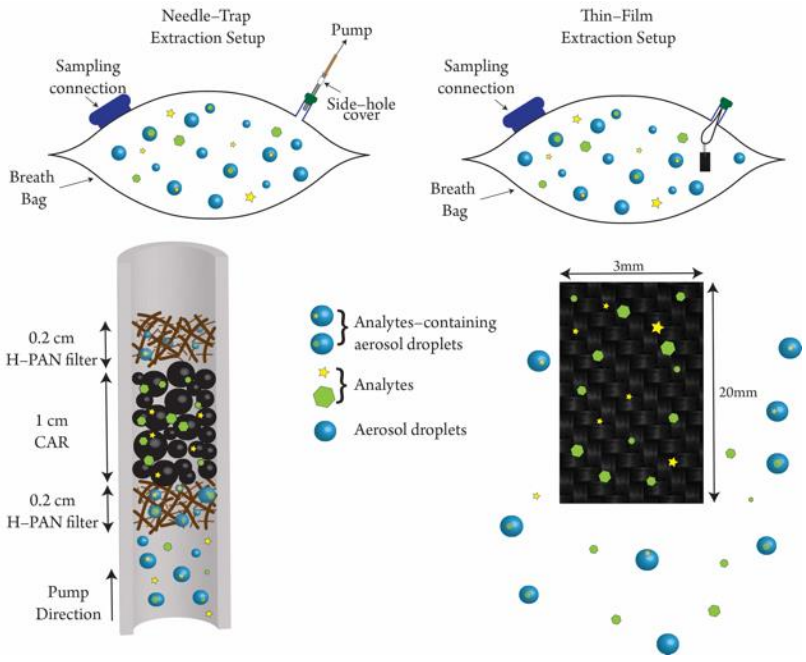

Figure 5-1 Schematic of breath bags used for obtaining breath samples from volunteers and magnified version of the designed extraction devices: NTD and TFME.

5.2.2.3 Preparation of gas standards

To prepare the stock standard in gas phase, a 1-L glass sampling bulb was first washed with methanol, dried, and vacuumed with vacuum pump for 30 minutes. Next, 1 μL of each pure analyte (2-butanone, methylcyclopentane, benzene, 2-pentanone, toluene, octane, ethylbenzene, styrene, heptanal, propylbenzene, heptanal, 1,2,4-TMB, decane, undecane, and nonanal) was injected into the glass bulb and fully evaporated via heating to 200 ºC for 30 minutes. Once the analytes had been evaporated, N_2 gas was added to the bulb to compensate for the difference in pressure between the bulb's interior and the external air. The final concentration of analytes in the standard mixture is provided in Table 5-1. Breath samples with varying concentrations were prepared in breath bags by using gas-tight syringes to inject different volumes of gas standard into the bags and mixing it with appropriate amounts of nitrogen (or breath matrix) to obtain a final volume of 700 mL in each bag.

5.2.2.4 Evaluation of gas mixture stability

To evaluate the concentration of the prepared gas mixtures and to study the stability of the gas-phase standards, the concentration of analytes in the glass bulb was determined by injecting known amounts of gas mixture into a GC instrument using a gas-tight syringe. The injected amounts were calculated via liquid injection. After checking the concentration of VOCs in the glass bulb, the injection from the standard was repeated every 2 h to find the maximum time the gas standard remains stable enough for use in studies.

5.2.2.5 Filtration efficiency

The developed filter's efficiency for trapping solid particles or liquid droplets has been studied extensively in a prior work. However, in this work, the filtration efficiency of the prepared needles was re-measured by inserting the needles into a scanning mobility particle sizer (SMPS) and comparing the particle count before and after insertion.

5.2.2.6 Extraction procedure

The extraction mixture was prepared inside the breath bags by diluting the gas standard mixture with nitrogen gas (or breath matrix). In the case of the NTD, the needle was connected to the bag and used to draw the sample (20 mL min^{-1}). For TFME, the thin films were left inside the bag until equilibrium had been achieved (Figure 5-1). After extraction, both devices were transferred to a GC/MS instrument for desorption and quantification.

5.2.2.7 Effect of humidity

Since breath samples are humid, it was necessary to study how humidity impacted extraction. To this end, two sets of breath bags were prepared, each with an estimate concentration of ~30 ng mL^{-1}. For dry samples, gas-standard mixtures were diluted with dry nitrogen in the breath bags. In contrast, the humid environments were prepared by spiking 40 μL of MilliQ water into a 1-L glass bulb and heated it at 120 ºC for 30 minutes until the water had evaporated, thus creating a saturated humid environment [105]. This humid air was then used to dilute the samples in the glass bulb.

5.2.2.8 Breakthrough volume measurements

The relationship between the extracted amount and sample concentration remains linear in NTD as long as the breakthrough volume (BTV) is not reached. To find the BTV and test how it is impacted by humidity, dry and humid breath bags were prepared with VOC concentrations of ~400 ng mL^{-1}. The sample was drawn through a needle at 20 mL min^{-1} using a pump. Sampling was performed by varying sampling volumes until a plateau had been reached, with BTV having been considered achieved when the extracted amount was 5% (or more) lower than the amount predicted by the linear equation.

5.2.2.9 Equilibrium time

For equilibration-based extractions, it is important to find the equilibrium time in order to reduce uncertainties and maximize the method's sensitivity. To this end, thin-films were placed inside breath bags with ~50 ng mL^{-1} analyte concentrations for 15, 30, 45, 60, and 120 minutes, with equilibrium time being determined by measuring the extracted signals.

5.2.2.10 Absolute recovery values

The absolute recovery values for TFME were determined by performing extractions in optimum conditions from samples with known analyte concentrations. The extracted amounts of analyte were also calculated using liquid injections. The absolute recovery values were calculated by dividing the amounts of analytes extracted by the amount in the sample (in ng).

5.2.2.11 Method validation

To validate the developed methods, different concentrations of samples were prepared in breath bags by diluting appropriate volumes of standard gas mixture with nitrogen. The breath bags containing the samples were then analyzed with NTD or TFME, and the linear dynamic range (LDR) was determined in SIM mode. The limits of detection (LOD) and limits of quantification (LOQ) were measured based on signal to noise ratios of 3 and 10, respectively. To evaluate repeatability of the developed method, inter-day and intra-day relative standard deviations (RSD) were measured by performing repeated extractions from ~50 ng mL^{-1} samples on different days. Device-to-device RSD values were calculated using the results attained from four separate needles and four separate thin films.

5.2.2.12 Stability of breath samples in bags

The NTD and TFME were also applied to examine how long breath droplets can remain suspended inside the breath bags. To this end, breath samples were obtained from a lab member who was working with chemicals during the routine experimental conditions. The samples were collected immediately after the lab work was finished, but the extractions were performed after allowing the sample to sit for different amounts of time to determine how storage time affected the analyte concentrations in the sample. The concentration in the extractions obtained via NTD at 0 storage time were considered to be 100 %, with a decrease in this figure over time being observed accordingly.

5.2.2.13 Real sample analysis

To study the applicability of the proposed method for real sample analysis, breath samples were obtained from seven volunteers (P1-P7) (with ethical clearance approval from University of Waterloo #42853). The volunteers were asked to avoid eating food for at least 3 h prior to sampling, and samples were collected by having them exhale into breath bags. Each volunteer was provided with a sterile new tee mouthpiece. The bags also contained a discard bag to remove any dead-space air and collect the alveolar breath. Additionally, to study the effect of aerosol droplets on extraction signals, three volunteers were asked to blow into breath bags while wearing face masks. After initial screenings, breath samples without any VOCs were then used to obtain the relative recovery (RR) values. The RR% was obtained by spiking these samples with gas standard at two concentration levels (Level I~ 30 ng mL^{-1} and Level II~ 150 ng mL^{-1}).

A breath sample was also obtained from a volunteer who had been working with various chemicals under routine lab conditions for several hours in order to study the effect of exogenous VOCs on the composition of exhaled breath. The breath samples were acquired from the volunteer immediately following exposure to the chemicals, and again at 30- and 60-min post exposure.

5.2.3 Results and Discussions

5.2.3.1 Evaluation of gas standard mixture

The stability of the gaseous mixture was analyzed by directly injecting it into the GC instrument. The GC results (Figure 5-2) revealed that all VOCs (except undecane, decane, and nonanal) showed acceptable stability in the glass bulb up to 6 h, but that concentrations of undecane, decane, and nonanal began to decrease after around 2 h. This decrease can be attributed

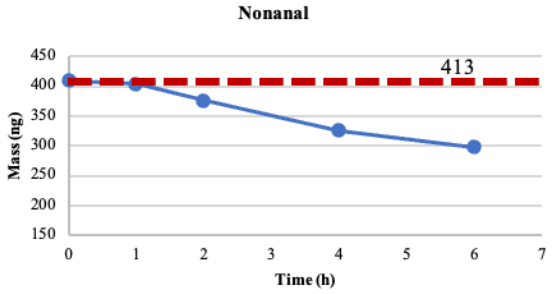
Nonanal
413
Mass (ng)
Time (h)

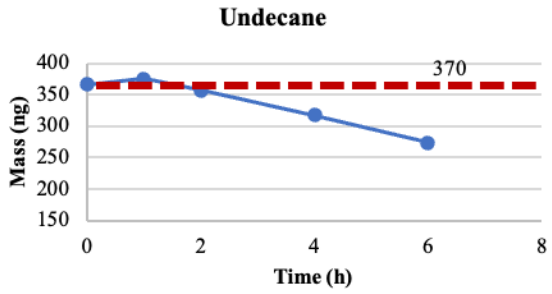
Undecane
370
Mass (ng)
Time (h)

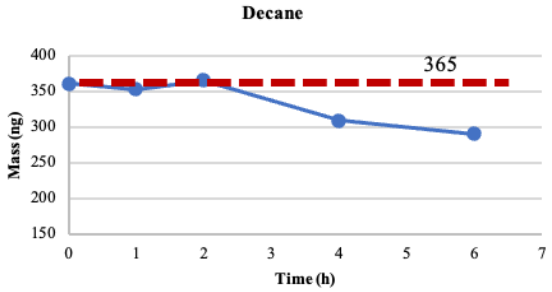
Decane
365
Mass (ng)
Time (h)

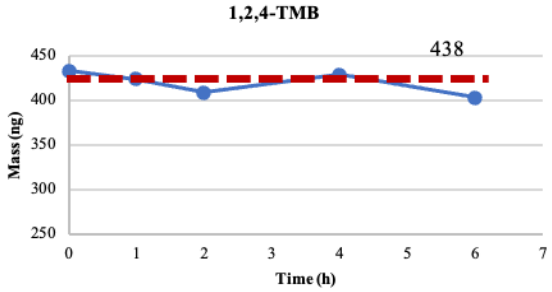
1,2,4-TMB
438
Mass (ng)
Time (h)

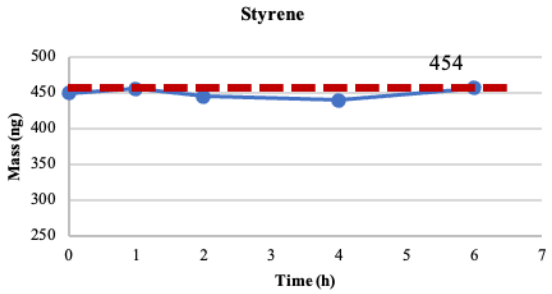
Styrene
454
Mass (ng)
Time (h)

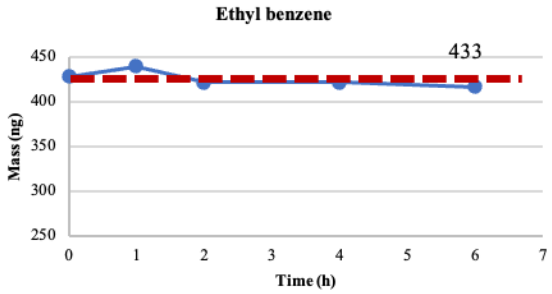
Ethyl benzene
433
Mass (ng)
Time (h)

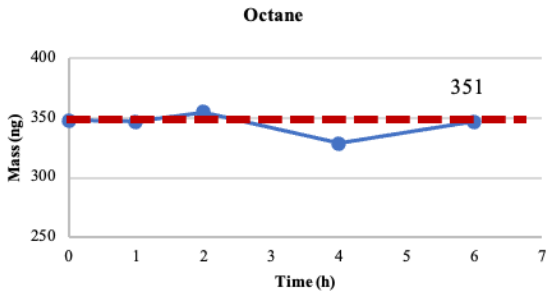
Octane
351
Mass (ng)
Time (h)

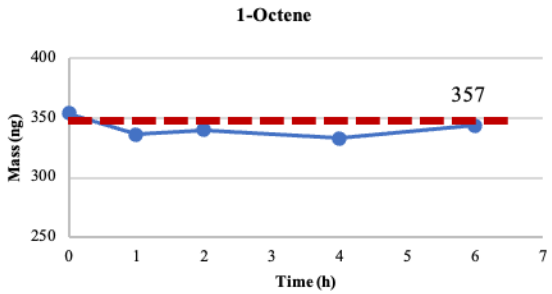
1-Octene
357
Mass (ng)
Time (h)

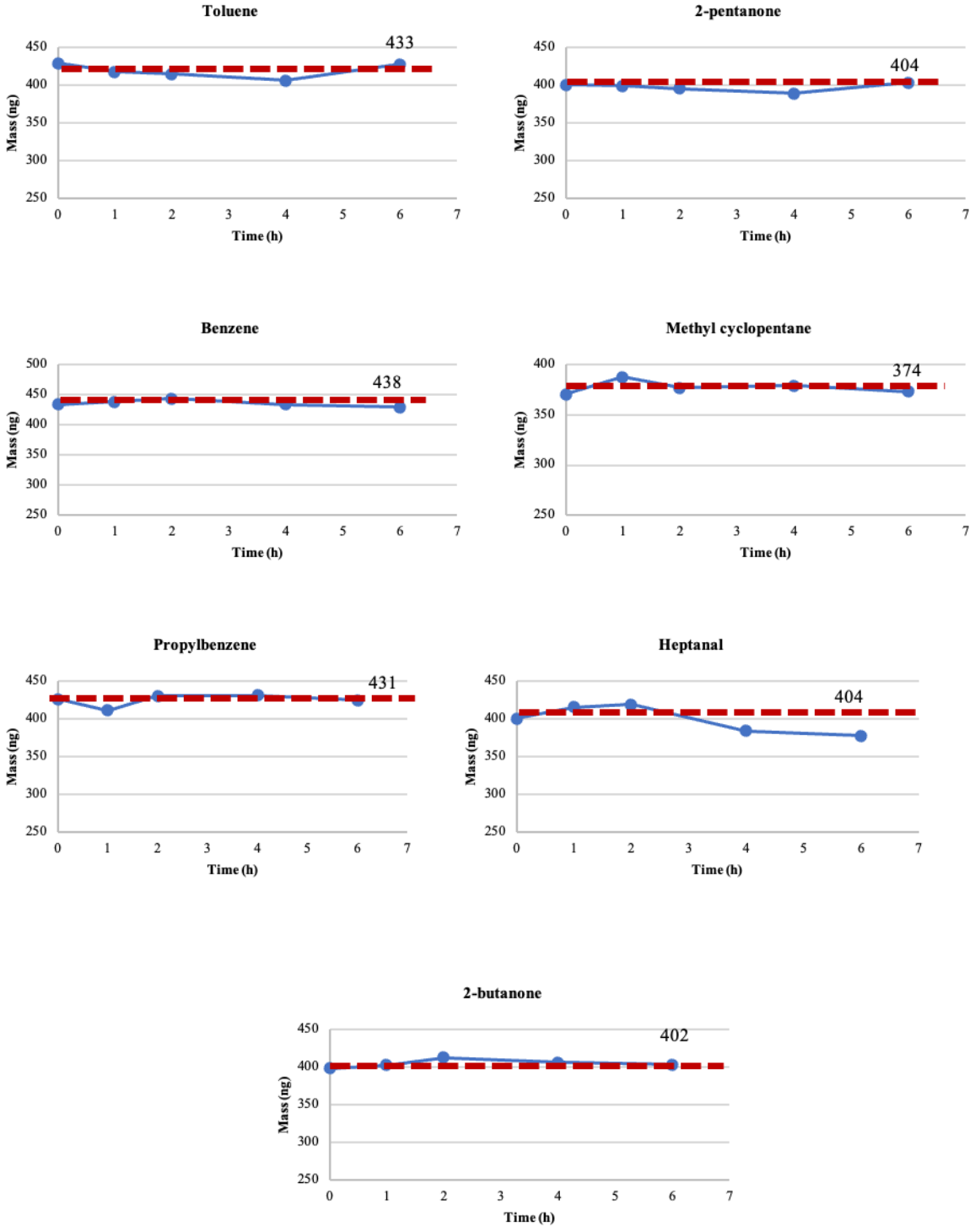

Figure 5-2.Concentration of analytes in gas–phase standard mixture over 6 h after preparation obtained by injection into GC instrument (red dashed line and the number in each chart represents expected concentration of analytes in mixture based on calculations).

to the larger size and lower volatility of these VOCs, which causes them to settle on glass wall rather than remain in the gas phase. Based on these results, the standard sample was renewed every 2–3 h to ensure that reproducible data was being obtained.

5.2.3.2 Filtration capacity

Filtration efficiency was calculated by inserting filter-incorporated NTDs into an SMPS and counting the number of droplets before and after insertion. Under normal conditions, the SMPS generated droplets ranging from 5–225 nm, with a peak count of ~10^6 (Figure 5-3). After inserting the filter, this count decreased to <100 particles (Figure 5-4). The decrease in signal was used to calculate the filtration efficiency percentage, which is shown in Figure 5-5. These data show high filtration efficiencies (>99%) for all particle sizes under study.

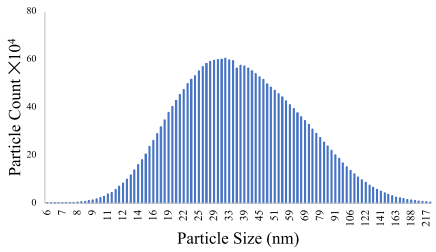

Figure 5-3. Instrumental background particle counts from SMPS instrument before insertion of any filter.

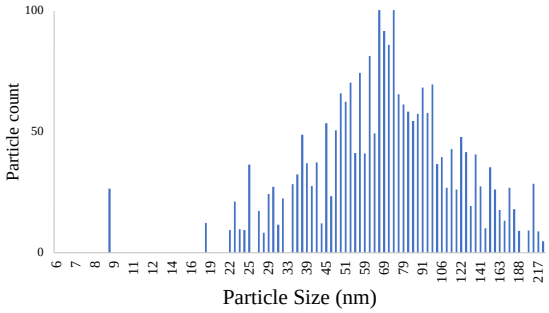

Figure 5-4. Particle count from SMPS instrument after adding needles packed with filter into instrument.

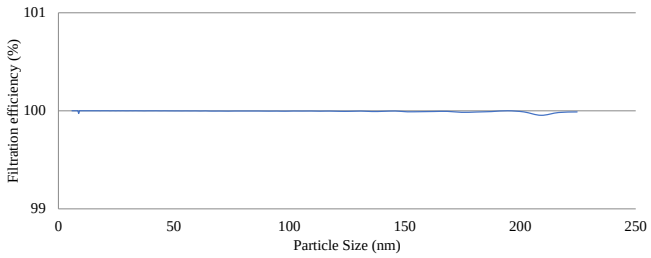

Figure 5-5. Filtration efficiency of filter–incorporated NTD for droplets.

5.2.3.3 Humidity

The results for VOCs extracted with NTD or TFME in humid and dry environment are illustrated in Figure 5-6 and Figure 5-7, respectively. From the obtained signals, it can be concluded that humidity does not significantly influence the extraction efficiency of the NTD or TFME. This result can be ascribed to the hydrophobic nature of the Carboxen sorbent, which prevents water from adsorbing onto the Carboxen surface. It is also worth noting that this result is unsurprising, as Carboxen's inertness towards humidity is the main reason why it is used in most cartridges in purge-and-trap designs with high amounts of water vapor [226].

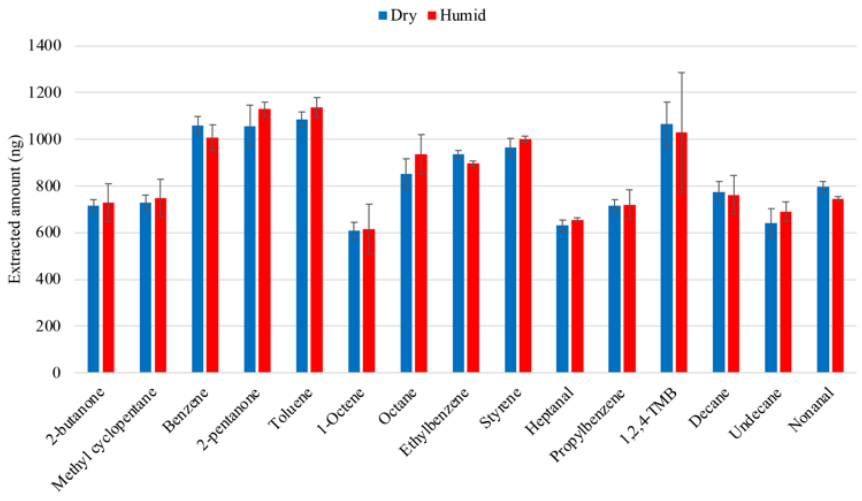

Figure 5-6. Signals from NTD extractions from dry and humid samples containing 30 ng mL^{-1} of VOCs.

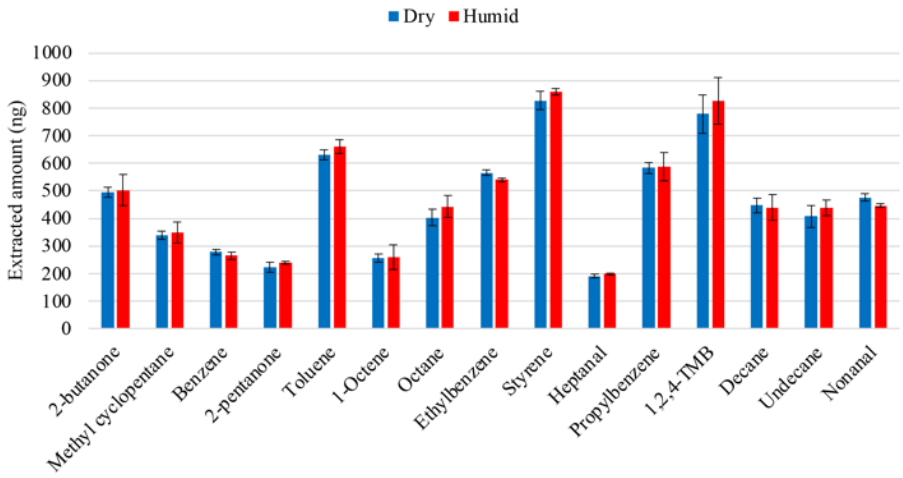

Figure 5-7. Signals from TFME extractions from dry and humid samples containing 30 ng mL^{-1} of VOCs.

5.2.3.4 Breakthrough volume

The BTV was identified by performing extractions from different volumes of breath samples until a plateau had been reached. In addition, tests were also conducted to determine how the BTV is affected by humidity. Based on the filter's trapping capacity, it is possible that water droplets aggregate in the filter after high-volume sampling, thus disturbing the extraction process by clogging the sampling path. The BTVs calculated for the dry and humid (saturated) samples are presented in Figure 5-8. The obtained values indicated that there was no statistically significant difference between the humid and dry samples. This result can be attributed to the high filtration capacity of the designed filter and the evaporation/removal of trapped droplets during each desorption. More importantly, the results showed that the BTV was not reached for any of the compounds during the sampling volume (700 mL).

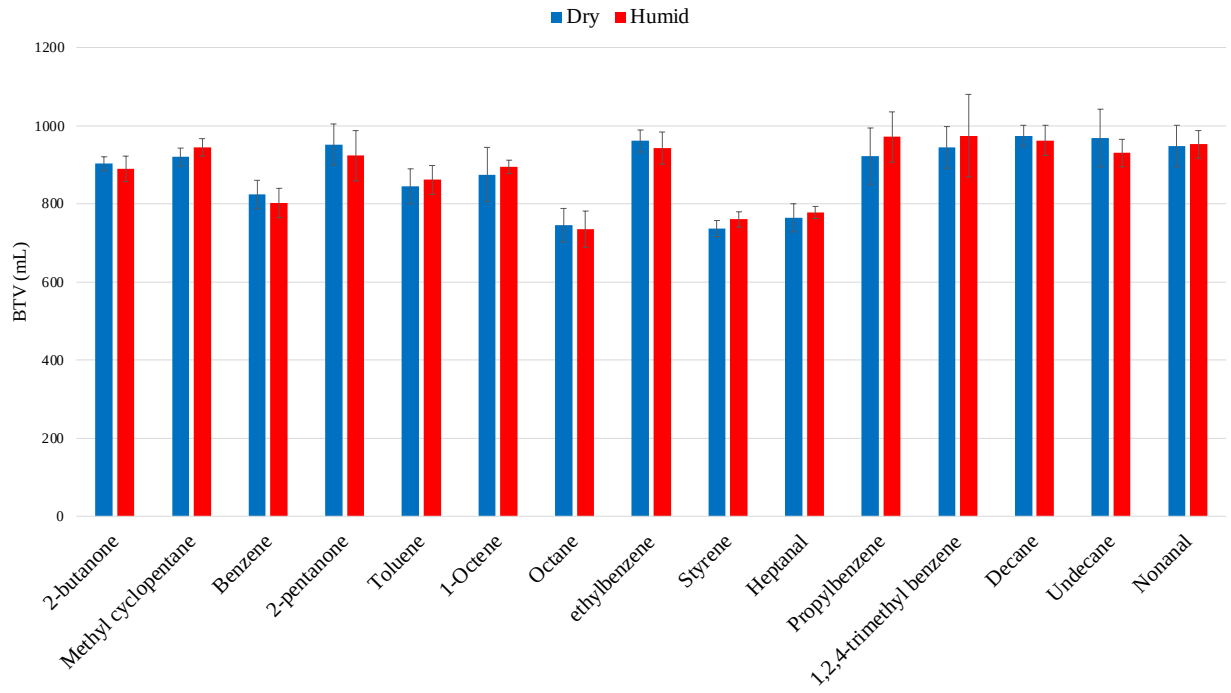

Figure 5-8. BTV obtained from extraction of 400 ng mL^{-1} of VOCs by varying extraction volume.

5.2.3.5 Equilibrium time

Equilibrium time was determined by testing various TFME extraction times, ranging from 15 minutes to 2 hours. The results of these tests revealed that equilibrium is generally reached very quickly, and that the extraction signal remained relatively constant across extraction times. Based on the resultant equilibrium time charts (Figure 5-9), 30 minutes was chosen as the equilibration time, as the extraction signals for most of the analytes remained constant after this time point.

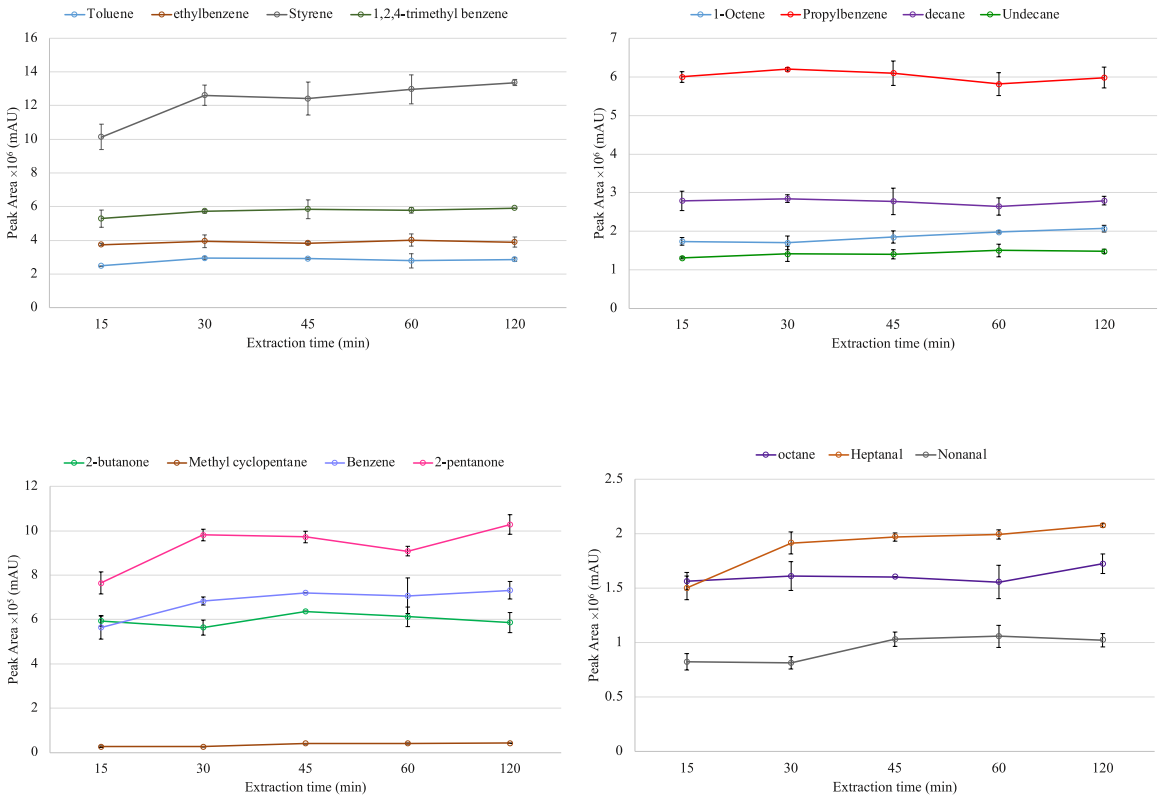

Figure 5-9. Equilibrium time profile for extraction of VOCs with TFME in 50 ng mL^{-1} concentration.

5.2.3.6 Absolute recovery values

As shown in Table 5-2, the obtained absolute recovery (AR) values ranged from 21% for 2-pentanone to 86% for styrene. This wide range of AR values was expected due to the various physiochemical properties of the studied VOCs. For instance, non-polar compounds have higher tendencies towards the Carboxen coating on the TFME device.

Table 5-2. Absolute recovery values for the extraction of VOCs with TFME.

Analyte	AR (%)	Analyte	AR (%)
2-butanone	69	Heptanal	30
Methylcyclopentane	47	Propylbenzene	82

Benzene	26	1,2,4-TMB	73
2-pentanone	21	Decane	58
Toluene	58	Undecane	64
1-Octene	42	Nonanal	60
Octane	47	Styrene	86
Ethylbenzene	60		

5.2.3.7 Calibration

Calibration was performed by mixing different concentrations of analyte standards and nitrogen in breath bags and analyzing them with NTD and TFME. The LOD and LOQ values were obtained by measuring the signal-to-noise ratios. The method validation data is presented in Table 5-3. It should be noted that the LDR range was chosen based on the results of previous studies and the expected concentration of VOCs in the analyzed breath samples [227]. In general, the NTD provided higher sensitivities; however, the detection limits offered by both methods met the requirements for the detection of VOCs and were comparable to those documented in previous reports [78,98,102,111,228].

Table 5-3. Method validation and calibration results for extraction of VOCs with NTD and TFME.

	LOD (ng mL^{-1})		LOQ (ng mL^{-1})		LDR (ng mL^{-1})	
Analyte	NTD	TFME	NTD	TFME	NTD	TFME
2-butanone	0.01	0.03	0.03	0.1	0.06-322	0.1-322
Methylcyclopentane	0.01	0.2	0.03	0.7	0.06-300	0.7-300
Benzene	0.02	0.02	0.07	0.07	0.07-350	0.07-350
2-pentanone	0.02	0.04	0.07	0.1	0.07-350	0.2-350
Toluene	0.01	0.01	0.03	0.03	0.06-345	0.07-345
1-Octene	0.03	0.02	0.1	0.07	0.1-286	0.07-286
Octane	0.03	0.01	0.1	0.03	0.1-281	0.05-281
Ethylbenzene	0.01	0.01	0.03	0.03	0.06-346	0.07-346
Styrene	0.01	0.01	0.03	0.03	0.07-363	0.06-363
Heptanal	0.03	0.2	0.1	0.7	0.1-324	0.6-324

Propyl benzene	0.01	0.01	0.03	0.03	0.06-345	0.6-345
1,2,4-TMB	0.03	0.01	0.1	0.03	0.1-350	0.07-350
Decane	0.04	0.01	0.13	0.03	0.2-292	0.06-292
Undecane	0.03	0.2	0.1	0.7	0.1-296	0.6-296
Nonanal	0.06	0.2	0.2	0.7	0.2-331	0.5-331

A table comparing the figures of merit from this study and previous reports on the application of NTD for the extraction of VOCs from breath samples are provided in Table 5-4.

Table 5-4. Comparison of figures of merit from this study and previous reports.

LOD (ng mL^{-1})	Extraction phase	Flow rate (mL min^{-1})	Sampling volume (mL)	Instruments	References
0.01-0.03	Tenax-Carbopack X-Carboxen 1000	60	40	GC-MS	[78]
11-14	PDMS-Carbopack B-Carboxen 1000	25-30	30	TD-PI-TOFMS	[76]
0.007-0.1	Tenax-Carbopack X-Carboxen 1000	75-100	20	GC×GC-MS	[100]
-	methacrylic acid and ethylene glycol dimethacrylate	10-30	20	GC-MS	[102]
0.02-0.5	DVB-Carbopack X-Carboxen 1000	15	25	GC-MS/MS	[98]
0.5-1	methacrylic acid and ethylene glycol dimethacrylate	~10	50	GC-MS	[34]
0.01-0.2	H-PAN Filter-Carboxen	20	70	GC-MS	Current Study

5.2.3.8 Repeatability

Signal repeatability was studied by performing multiple extractions within a single day and between days. For device-to-device signals, four different extractive media were prepared and

analyzed (Table 5-5). Acceptable inter-day and intra-day RSD values were obtained, with a maximum of 10% for both methods. In general, the NTD had a higher device-to-device RSD, which may have been due to the manual packing procedure.

Table 5-5. Repeatability data obtained from extraction of 50 ng mL^{-1} of VOCs with NTD and TFME

Analyte	Method	RSD (%)		
		Intra–day	Inter–day	Fiber–to–Fiber
2-butanone	NTD	4.1	6.5	10.3
	TFME	3.7	4.7	9.6
Methylcyclopentane	NTD	2.5	5.4	7.9
	TFME	4.6	6.6	9.5
Benzene	NTD	4.2	4.2	11.6
	TFME	5.8	5.8	8.9
2-pentanone	NTD	2.4	3.9	9.9
	TFME	3.1	3.7	5.4
Toluene	NTD	5.3	6.2	12.2
	TFME	3.6	4.2	8.7
1-Octene	NTD	6.6	7.4	13.4
	TFME	4.3	6.8	6.9
Octane	NTD	7.9	10.1	11.5
	TFME	5.2	9.2	9.3
Ethylbenzene	NTD	4.4	8.2	8.9
	TFME	5.9	7.9	5.9
Styrene	NTD	5.1	6.3	10.1
	TFME	3.3	7.4	4.9
Heptanal	NTD	4.7	8.6	13.7
	TFME	6.9	7.9	8.8
Propylbenzene	NTD	5.5	6.3	11.4
	TFME	2.7	3.5	8.6
1,2,4-TMB	NTD	4.1	5.8	12.5
	TFME	6.3	7.1	11.2
Decane	NTD	5.6	5.7	14.6
	TFME	3.7	4.7	9.4

Undecane	NTD	7.5	9.4	8.7
	TFME	8.3	10.4	5.7
Nonanal	NTD	4.4	7.3	13.2
	TFME	6.3	8.8	9.4

5.2.3.9 Relative recovery

Matrix effects were investigated using breath samples from four volunteers that were found to be void of any of the analytes under study. The samples were spiked at two concentration levels, and the results are provided in Table 5-6. The calculated RR values were between 84–108%, which indicates that breath matrix does not interfere with analytical measurement. Thus, the developed methods can be applied for the analysis of VOCs in different breath samples.

Table 5-6. Relative recovery values obtained from spiking breath samples with standard VOCs standard (Level I=30 ng mL^{-1} and Level II= 150 ng mL^{-1})

Analyte	Method	RR (%)			
		P1	P2	P4	P6
		Level I		Level II	
2-butanone	NTD	97	99	101	96
	TFME	101	97	89	103
Methyl cyclopentane	NTD	94	89	94	97
	TFME	89	94	94	98
Benzene	NTD	92	91	92	89
	TFME	106	104	87	87
2-pentanone	NTD	85	100	85	84
	TFME	94	96	103	102
Toluene	NTD	92	96	96	97
	TFME	87	98	98	94
1-Octene	NTD	103	88	92	98
	TFME	99	93	91	100
Octane	NTD	82	103	108	96
	TFME	95	95	99	94

Ethylbenzene	NTD	91	93	84	92
	TFME	93	89	92	94
Styrene	NTD	88	89	91	89
	TFME	84	94	83	104
Heptanal	NTD	104	95	89	103
	TFME	96	93	90	95
Propylbenzene	NTD	99	95	90	96
	TFME	93	92	94	93
1,2,4-TMB	NTD	92	99	93	97
	TFME	94	104	95	93
Decane	NTD	92	106	97	92
	TFME	99	100	92	99
Undecane	NTD	98	98	100	87
	TFME	89	89	104	84
Nonanal	NTD	101	84	97	91
	TFME	100	92	99	99

5.2.3.10 Stability of breath samples in sampling bag

Conducting sampling from aerosol matrices can be tricky due to the settlement of droplets over time. As such, the suspension stability of samples collected in breath bags from volunteers exposed to various chemicals was studied over different storage times. It is known that the sedimentation time of droplets depends on their diameter and evaporation rate. As previous studies have demonstrated [229], while large droplets (tens of microns) can settle within a few seconds, smaller droplets can remain suspended as long as a few hours. The results of this experiment suggest (Figure 5-10), that the concentration of free and droplet-bound 2-pentanone decreases over time, as the free compounds start to attach to the bag walls and the droplets begin to settle. However, the rate of decrement for droplets (obtained by NTD) is much higher compared to gaseous 2-pentanone. These results are consistent with those of previous studies [230] which suggest that only a small portion of breath droplets is large enough to settle within minutes. In

addition, the breath samples create a humid environment inside the bags, which aids the stability of these droplets over a few hours. Based on these results, the breath bags from the volunteers were analyzed immediately after sampling to avoid any droplet loss.

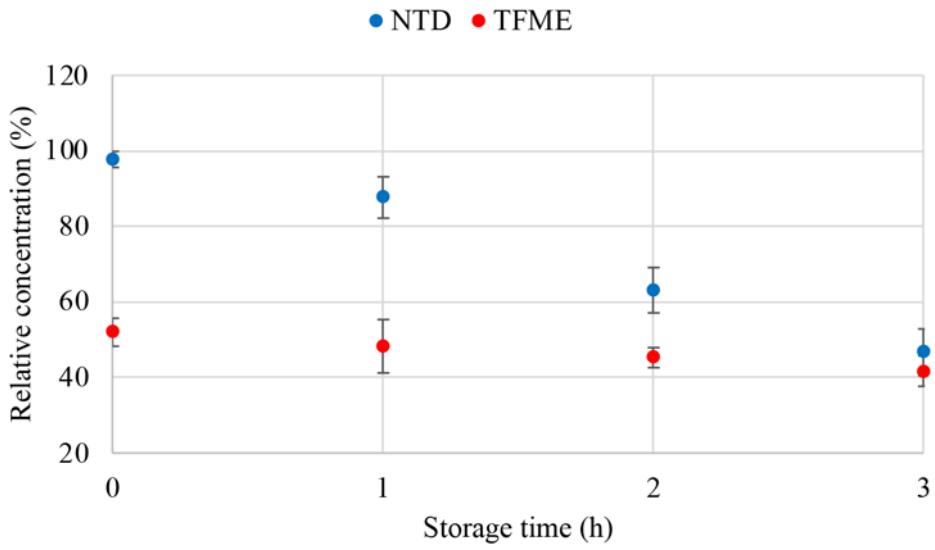

Figure 5-10. relative concentration of 2-pentanone in breath samples from exposed volunteers over 3h storage time in breath bags

5.2.3.11 Analysis of breath samples

VOCs were detected in three of the seven samples obtained from the volunteers. 2-pentanone and propyl benzene were identified in sample P5 (Table 5-7). As the results show, it was possible to detect 2-pentanone with the NTD, but the signal obtained with TFME fell below the LOQ.

Table 5-7. Concentration of VOCs in ng mL^{-1} (relative standard deviations, RSD %) sample P5 with NTD and TFME.

Analyte	Method	Conc. found in sample P5 (ng mL^{-1})
2-pentanone	NTD	15.1 (4%)
	TFME	Below LOQ
Propyl benzene	NTD	57 (8%)
	TFME	45 (6%)

This difference can be attributed to the polarity of 2-pentanone. Based on 2-pentanone's polarity and low Henry constant (LogP=0.9, k_H = 8.36×10^{-5} atm m^3 mol^{-1}), it can be expected to remain inside the droplets rather than the gas phase. This difference in concentration comes from the NTD's ability to trap aerosol droplets, whereas TFME is only able to extract free gas-phase analytes. The concentrations of propyl benzene detected with both methods were statistically similar. These results clearly illustrate the advantages of using the proposed method for the determination of polar compounds in breath samples.

Samples P3 and P7 were acquired from volunteers with and without the use of a facemask. The results for these samples are presented in Figure 5-11 and Figure 5-12.

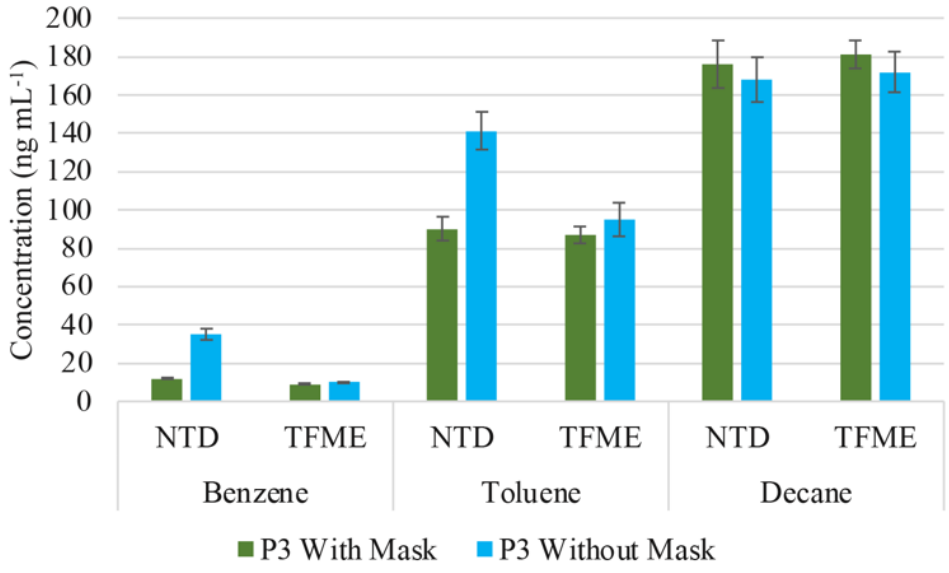

Figure 5-11. Concentration of VOCs in P3 sampled with and without a face mask and analyzed with an NTD and TFME.

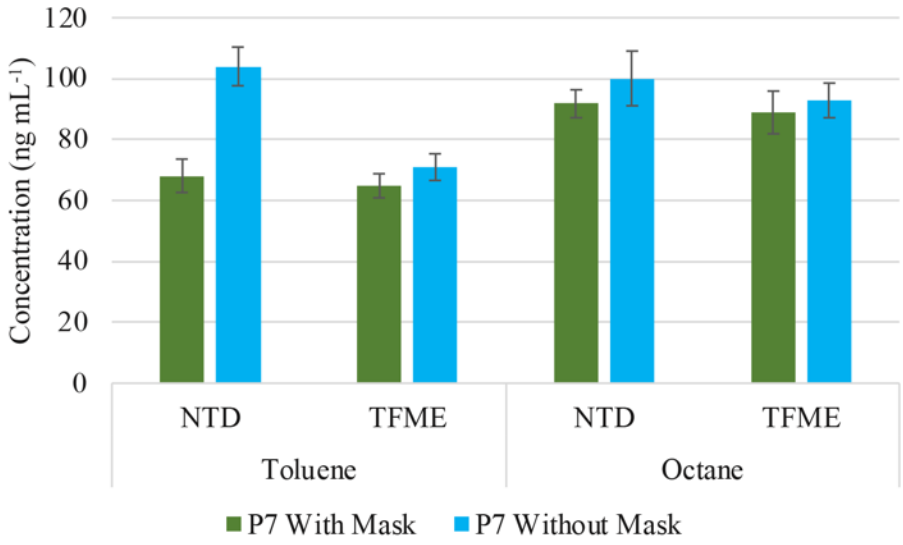

Figure 5-12. Concentration of VOCs in P7 sampled with and without a face mask and analyzed with an NTD and TFME.

The chromatograms for sample P3 (with and without mask) for NTD and TFME analysis are provided in Figure 5-13 and Figure 5-14, respectively.

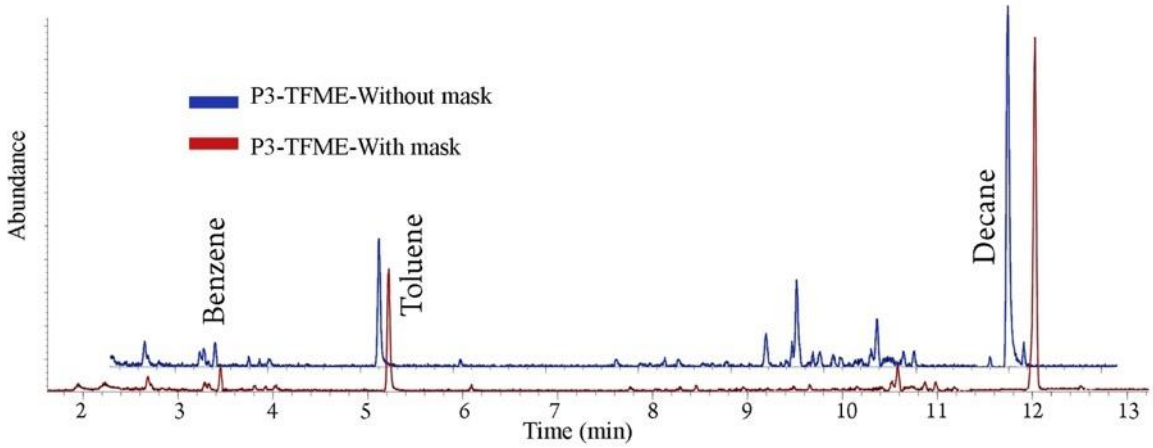

Figure 5-13. Chromatogram for extraction of P3 breath sample with and without face mask using TFME.

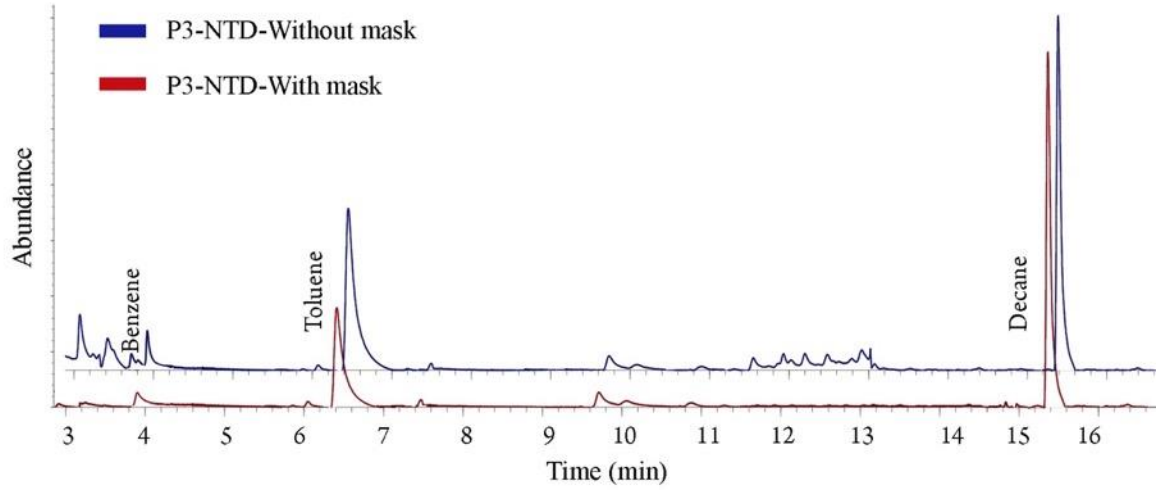

Figure 5-14. Chromatogram for extraction of P3 breath sample with and without face mask using NTD.

As can be seen, both methods were able to quantify benzene and toluene, although the results for the NTD without a mask showed higher concentrations. Notably, the concentrations of these analytes decreased when a mask was used for NTD sampling, but remained unaffected for the TFME extractions. The results for decane and octane did not significantly differ between the mask and no-mask conditions for NTD and TFME. These results can be explained by the physiochemical properties of these components. Benzene and toluene possess lower Henry constants, which means that they are able to remain inside the droplets; in contrast, decane and octane have much higher Henry constants, which makes them more inclined towards the gas phase. This explanation is supported by a comparison of the data obtained with and without a face mask. Since the use of a face mask can prevent breath droplets from reaching the breath bag, the results from the mask-on samples will only cover the concentration of VOCs in the gas phase, as droplets would not have been able to enter the sampling bags. This is the reason why the TFME data for the mask-on and mask-off samples were statistically similar in all cases, as TFME can only extract from the gas

phase, regardless of whether droplets are present. However, compounds with a high affinity towards the liquid phase were detected at higher concentrations by NTD without a facemask compared to the other analytes. The concentrations obtained by NTD and TFME became statistically similar once the droplets were eliminated by the facemask, as both methods were restricted to extracting from similar concentrations of VOCs in the gas phase. It is worth mentioning that the presence of these hydrocarbons in breath samples has been reported previously [231–233].

The data was statistically evaluated by one-tailed homoscedastic t-test. For P7, toluene, the results obtained by NTD with and without mask were compared and p-value was found to be 0.0004. Also, for P3, the concentrations reported for benzene and toluene with NTD for samples obtained through or without face mask was compared and p-values were calculated as 0.0001 and 0.0006, respectively. As the data shows, in all cases, the presence/absence of droplets in sampling bag can result in significantly different reported concentrations.

Next, a breath sample was analyzed from a volunteer who had been working with several chemicals in the lab. The breath samples were studied immediately after collection, as well as 30 and 60 minutes later. The results of this analysis are presented in Table 5-8, and the chromatograms of the exposed breath samples sampled with NTD are provided in Figure 5-15.

As the data suggest, the concentrations obtained with the NTD were higher compared to those obtained with TFME, with this difference being even greater for polar compounds. As explained previously, this difference can be attributed to polar and non-polar compounds' different preferences for liquid phases.

Table 5-8. Concentration of in ng mL^{-1} (relative standard deviation, RSD %) VOCs in volunteer breath sample after exposure to the ambient lab air (ND = Not detected).

Method	NTD		
Time after exposure (min)	0	30	60
2-butanone	45 (4%)	8 (12%)	<LOQ
2-pentanone	38 (3%)	5.5 (9%)	ND
1,2,4-TMB	16 (12%)	7 (14%)	ND
Decane	21 (7%)	9 (11%)	0.54 (6%)
Method	TFME		
Time after exposure (min)	0	30	60
2-butanone	20 (12%)	3.5 (14%)	ND
2-pentanone	18 (6%)	2.5 (22%)	ND
1,2,4-TMB	12 (20%)	3 (33%)	ND
Decane	20 (7%)	10 (10%)	0.45 (3%)

Although concentrations decreased over time, some of the compounds remained detectable up to 60 minutes after the volunteer's exposure. The results of the exposure experiments clearly demonstrate the advantage of the developed needle-trap method for analyzing the total concentration of VOCs in breath samples—especially the improved results for polar compounds, which are always challenging to extract and analyze.

The other important key finding in the data is the different elimination rates for the polar (2-butanone and 2-pentanone) and non-polar components (1,2,4-TMB and decane). For instance, the concentration of ketones was higher immediately after exposure, but diminished much quickly with the passage of time, becoming undetectable after 60 minutes. This finding matches those of previous reports suggesting that exhaled breath is an efficient method of excreting non-polar xenobiotics; however, polar compounds are mostly eliminated through the kidneys [234–236].

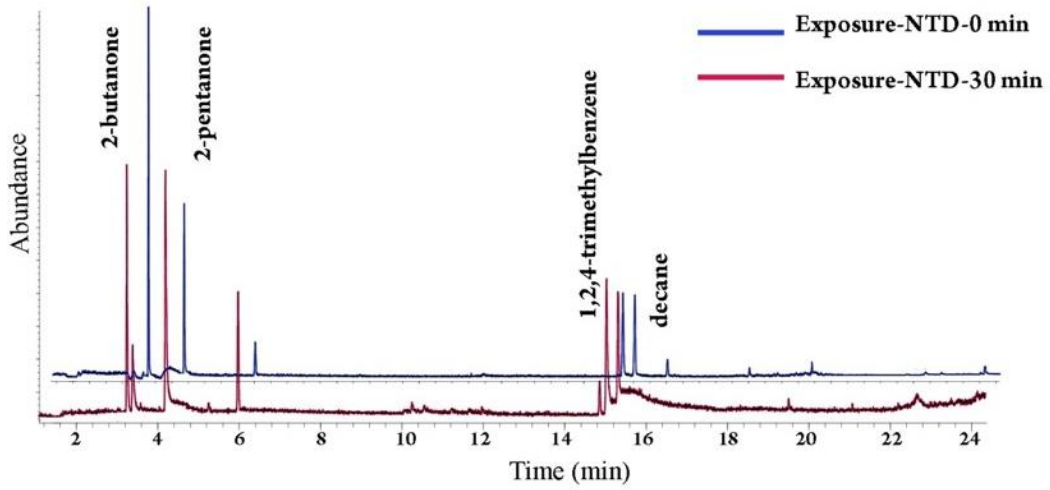

Figure 5-15. Chromatogram for extraction of exposure breath samples using NTD (since each chromatogram has a different Y-axis scale, the scales were removed to avoid confusion).

These results also confirm the important role of exogenous VOCs in breath analysis. The presence of these compounds in breath samples up to an hour after exposure highlights the importance of taking precautionary steps before breath sampling to ensure that the exhaled breath components are not affected by inhaled ambient air.

5.2.4 Conclusion

While breath analysis has always been intriguing to scientists due to its non-invasive nature, low concentrations of VOCs and challenges associated with studying gas phase and droplet-bound components at the same time has limited its widespread use. In this study, a filter-incorporated NTD was developed to enable the simultaneous preconcentration of gas-phase and droplet-bound components. Additionally, for the first time, TFME was used to extract VOCs from the gas-phase. The findings of this work demonstrate that the developed methods are capable of providing high sensitivity. Additionally, the NTD method combines the extraction of exhaled breath vapor and exhaled breath condensate into a single device, which is cheaper and faster than conventional

methods. Furthermore, the designed filter can also act as a retainer to hold sorbent particles in place inside the needle.

The results of the analysis of samples collected from volunteers highlighted the advantages of the developed method for studying droplet-bound compounds, particularly polar analytes. The data from the samples obtained with the use of a face mask revealed the importance of studying droplets in the breath to obtain a complete view of the sample. The results of the exposure study showed how inhaled ambient air can affect the composition of exhaled breath, emphasizing the significance of employing appropriate breath sampling techniques when attempting to determine health status via breath composition.

One issue with the developed technique is the stability of the breath matrix, both gaseous compounds and droplets. In this study, the breath samples were studied immediately after sampling, however, when there is a time gap between sampling and extraction, the compounds can be lost due to the attachment to the wall. The sampling volume should also be chosen carefully. If the breakthrough volume is reached during the sampling, the reported concentrations are underestimating the actual concentrations. This means that the breakthrough volume and the effect of humidity should be studied before choosing the proper sampling volume.

The proposed approach has the potential to become an easy-to-operate bedside method that can be used by the patient or physicians. The results from the NTD and the data from TFME can provide a comprehensive analysis of breath samples by distinguishing the contributions of the analytes in the droplets and the gas phase, which might originate from different sites giving more information about the patient. Furthermore, the exposure results highlight the attractive features of non-invasive breath determinations for the rapid monitoring and determination of exposure levels.

Such an approach can be highly useful in validating safety levels in work environments and evaluating the effectiveness of protective gear.

5.3 Portable microextraction techniques for comprehensive investigation of breath biomarkers from lung cancer patients

5.3.1 Introduction

In this subsection, the method developed in "5.2 Simultaneous determination of exhaled breath vapor and exhaled breath aerosol using filter-incorporated needle-trap devices: A comparison of gas-phase and droplet-bound components" section is applied for study of breath samples from lung cancer patients. Access was granted by Dr. Liu, a member of Princess Margaret cancer center.

5.3.2 Experimental

5.3.2.1 On-site Sampling

Samples were collected from active cancer patients, most of whom were lung cancer patients, using single-patient breath collection bags (QT00830-P, QuinTron^{TM}) with a volume of 750 mL. Active cancer patient was defined as either a patient who was newly diagnosed (before start of treatment) or had a known active cancer that was either being monitored or being treated. Each bag was equipped with tee connector (QT00859-P, QuinTron^{TM}), a Luer-Lock valve, a 400 mL discard bag (QT00843-P, QuinTron^{TM}), and a new single-use mouthpiece. An image of the sampling bags is provided in Figure 5-16-a. Patients were provided with new bags (at least 3) and instructed to blow into them until they were full. The bags were pre-equipped with valves designed for TFME with thin films connected to cotter pins. During the extraction, the valve was closed; after extraction, the valve and connected thin films were removed from the bag, and the thin films were transferred for storage. For the NTD extractions, a valve with a septum was attached to the

bag (Figure 5-16-b). The NTD was connected to the septa, after which the valve was opened and the pump was turned on to begin the extraction. After the extraction, the needle was detached from the pump and bag, capped, and transferred to freezer for storage (Figure 5-16-c).

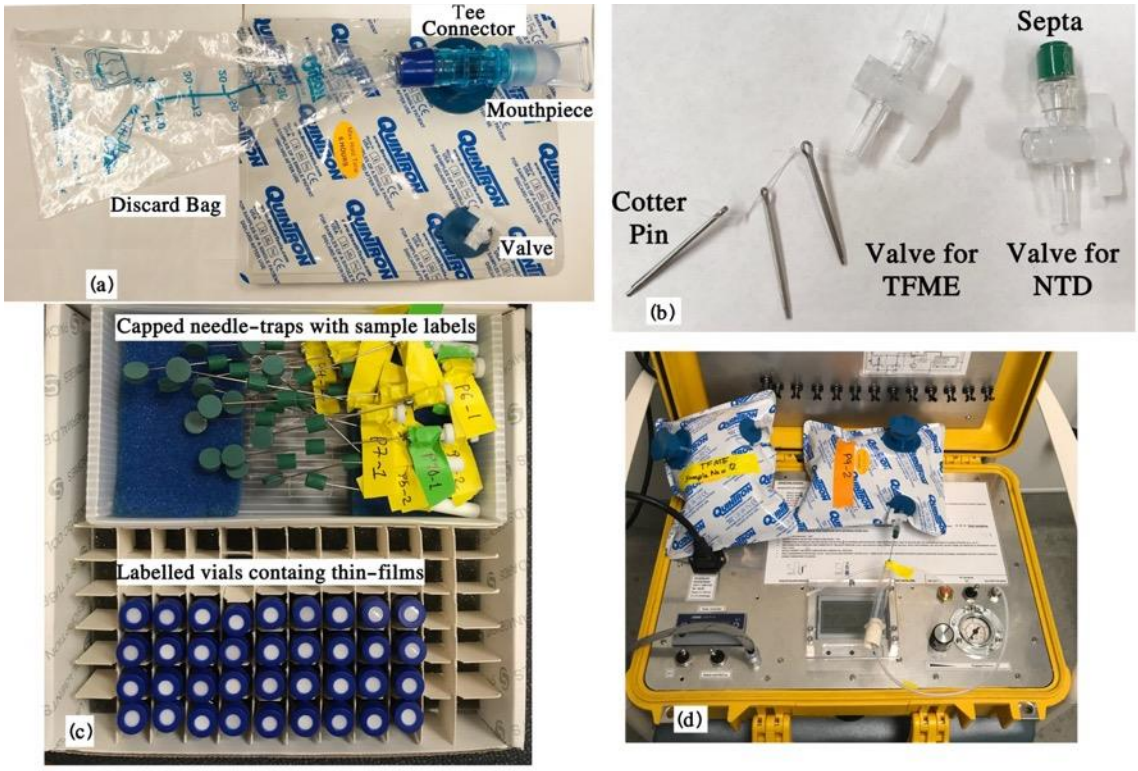

Figure 5-16. image of sampling bag (a), designed valves for extraction with TFME and NTD (b), devices after extraction and prepared for storage (c), on-site sampling devices (yellow box is a pump connected to NTD).

In addition to the exhaled breath samples, inhaled air was also analyzed via TFME and the NTD. This step was critical, as inhaled air is a primary source of exogenous compounds in exhaled breath samples. It should also be mentioned that, while eating or drinking affect breath composition, the conditions of this study made it impossible to control the patients' eating, drinking, or smoking habits prior to sampling.

Multiple TFME and NTD devices were applied to perform extractions from inhaled air samples using the same conditions as applied for the exhaled breath samples. At least 3 of each device was studied in selected ion monitoring (SIM) mode to assess the presence of biomarkers in the ambient inhaled air, while the other devices were studied in TIC mode to check for the presence of other compounds.

5.3.2.2 Extraction procedure

Multiple TFME devices were left inside the bag before sampling. Once the bag was filled with breath, the extraction commenced and continued for 45 minutes until equilibrium had been reached for all analytes For the NTD extractions, the bags were first filled with exhaled breath and the needles were then connected to the sampling pump, which drew 600 mL of the sample into the NTD (flow rate = 20 mL min^{-1}) (Figure 5-16-d). After extraction, the thin films were stored and capped in a 2-mL vial, and the needles were capped on both sides and the side-hole was also covered. The vials containing the needles and thin films were then stored in a freezer until analysis. It is worth noting that previous reports have confirmed that NTDs can provide high recovery (>90%) of VOCs after multiple days of storage at room temperature following extraction [33,78,237]. In this work, sampling was conducted over multiple days, the extraction devices were transferred to the University of Waterloo after the final day. Each device was brought to room temperature, thermally desorbed, and studied using GC-MS.

5.3.2.3 Patients

Access to patients was arranged through Research Ethics Board 06-639 (University Health Network/Princess Margaret Cancer Centre, Toronto, ON, Canada). After patient consent was

obtained, patients were provided with new breath bags and a mouthpiece and were instructed to blow into each bag until it was full. The bags were then immediately labelled and transferred to another room for extraction. A list of the patients and their information is provided in Table 5-9.

Table 5-9. List of lung cancer patients' age, sex (M= male, F= female), state of disease and smoking status.

Patient	Age (in years)	Sex	Disease Stage at time of sampling	Smoking status
1	65	M	IV	Ex-smoker
2	83	M	IVa	Ex-smoker
3	67	F	IVb	Ex-smoker
4	55	M	IVa	Ex-smoker
5	59	F	IVa	Never-smoker
6	65	M	IVb	Ex-smoker
7	79	M	IIIa	Never-smoker
8	63	M	IIIa	Current Smoker
9	64	M	IIIa	Ex-smoker
10	62	F	IVa	Ex-smoker
11	61	M	IIIa	Ex-smoker
12	66	F	IVb	Ex-smoker, light
13	65	M	IVb	Ex-smoker

5.3.3 Results and Discussions

5.3.3.1 Data acquisition and analysis

The temperature program and instrumentation used for the thermal desorption and separation of biomarkers are explained in the Materials and Instruments section. The devices used for the extractions were analyzed in SIM mode for highest sensitivity; however, in cases where multiple extraction device was available for a given sample, one or more device (TFME or NTD) was run in TIC mode to detect other potential biomarkers.

Additionally, inhaled air was simultaneously investigated and none of the target compounds were detected, thus suggesting that all of the targeted biomarkers are endogenous. Due to the small number of samples and the lack of control over the patients' dietary or smoking habits, the results of this study do not lend themselves to medical interpretation. Rather, since the goal of this work was to introduce an analytical method and device for the detection of biomarkers, the results have been interpreted according to this objective. A list of the detected and quantified compounds is provided in Table 5-10.

No biomarkers were detected in 4 of the 13 patients who participated in this study. The most commonly detected biomarker was benzene, which, along with its derivatives, is one of the most highly reported biomarkers of lung cancers. The presence of benzene and its derivatives has also been confirmed in smokers. For instance, findings have shown that smoking can be the reason behind the high concentrations of styrene in P6.

Based on the above results, it would appear that the differences in the results for TFME and NTD are strongly tied to the polarity of the targeted compounds. For comparison, logP was chosen as the criterion of polarity. For instance, compared to TFME, NTD was able to report significantly higher concentrations of polar compounds such as 2-butanone (LogP=0.3) and 2-pentanone (LogP=0.9); however, this difference in reporting was much smaller for non-polar components such as styrene (LogP=2.9) and decane (LogP=5.8). This finding demonstrates the main claim of this paper.

Table 5-10. List of biomarkers detected in breath samples from lung cancer patients and quantified in ng mL^{-1} (± standard deviation) [ND=Not Detected (none of target compounds were detected)].

Sample No.	Compound	TFME	NTD
1		ND	
2	2-butanone	2.4 (±0.4)	4.3 (±0.8)
	Benzene	10.1 (±1.3)	10.9 (±1.4)
3	Methyl cyclopentane	2.4 (±0.6)	2.2 (±0.5)
	Nonanal	7.7 (±1.3)	8.3 (±0.6)
4	Toluene	21.4 (±2.2)	23.5 (±4.3)
	Styrene	0.8 (±0.1)	1.0 (±0.2)
5		ND	
6	Benzene	5.3 (±0.9)	6.5 (±0.9)
	Styrene	101.8 (±7.8)	111.0 (±6.3)
	2-pentanone	5.4 (±0.8)	8.2 (±0.4)
	Toluene	11.5 (±1.3)	16.0 (±2.1)
7	Octane	51.3 (±4.9)	58.0 (±4.8)
8		ND	
9	Benzene	9.1 (±0.8)	14.5 (±1.1)
	Heptanal	1.6 (±0.7)	3.2 (±0.6)
10	2-butanone	7.0 (±0.8)	9.0 (±0.8)
11		ND	
12	Benzene	7.1 (±0.4)	10.3 (±1.3)
	Decane	81.4 (±2.6)	83.1 (±1.7)
13	1,2,4-TMB	34.9 (±4.3)	36.4 (±4.2)

As discussed in the introduction, filter-incorporated NTDs can trap breath droplets, which can dissolve polar compounds. Thus, when NTDs are applied to study breath samples, the results reflect the total concentration targeted compounds (free + droplet bound). Conversely, non-polar biomarkers prefer to remain in the gas phase, which results in similar concentrations of such compounds being reported with NTD and TFME. It is worth noting that the quantified concentrations reported in this study are consistent with previous reports [106,238].

In healthy volunteer samples, out of seven samples, target biomarkers were detected in only three samples. This shows the strong correlation between the biomarkers and disease. On the other hand, the biomarkers detected in three healthy volunteers (benzene, toluene, decane, octane, propyl benzene) are commonly found in smokers as well as lung cancer patients, and these compounds can be the result of smoking. High concentration of decane (~170 ng mL^{-1}) and toluene (60-140 ng mL^{-1}) also confirms the potential exogenous source of these compounds. This explanation highlights the potential of these target biomarkers for early detection of lung cancer disease.

As mentioned earlier, some exhaled breath and inhaled air samples were also studied in the TIC mode of GC-MS. A list of the compounds detected in these breath samples is provided in Table 5-11, with the red entries denoting those that were detected in both sets of samples (breath and air). As can be seen, hydrocarbons were the most common compounds detected exclusively with TFME. In contrast, some aldehydes and ketones were detected only with the NTD, which may be due to their tendency to be droplet-bound. However, the detection of a compound with only one of the applied methods may be due to different limits of detection for each compound caused by the experimental conditions and how the compound interacts with the NTD and TFME. Nonetheless, there are a few interesting exceptions. For example, cyclohexane, hexadecane, and (1-methylethyl)-benzene were only detected by the NTD despite being hydrocarbons with a high affinity towards the TFME. If these compounds are present in free form in amounts consistent with the Henry constant, then they should have also been detected by TFME. Thus, the NTD results indicated that these compounds may be present in the particle phase due to not being fully equilibrated with the gas phase as a result of slow-release kinetics or short time due to immediate sampling. An alternative explanation is that the mucus that comprises the aerosol, releases these compounds during desorption caused by thermal decomposition. In general, while Henry constant

and polarity seems to play the major role on the distribution of compounds in gas and droplet-phase, it seems that other factors such as the source of release and equilibrium state between phases can be also critical. The above observation should be carefully investigated, as it provides an additional interesting characterization of breath samples, which might contribute to more accurate diagnoses. While none of the target compounds were detected in inhaled air samples, the analysis in TIC mode revealed the presence of other small VOCs in hospital air. This is somewhat unsurprising, as the presence of acetone, ethanol, chloroform, and undecane in hospital air has been reported previously [239].

Table 5-11. list of detected compounds with TFME, NTD or both in breath samples studied in TIC mode (red compounds were detected in both air and breath samples)

NTD	Both	TFME
Acetone	Cyclohexane	4-Penten-1-ol
1,3-Pentadiene	Hexane	3-methyloctane
Cyclohexane	Pentane	1,2-Propanediol
Octanal	m-Xylene	Dodecane
m-Ethylstyrene	o-Cymene	Undecane
Nonanal	n-Hexadecanoic acid	Mesitylene
3-methyl-1H-Indene	Ethanol	
Benzaldehyde	Chloroform	
Decanal		
Acetic acid		
2,6,8-trimethylnonanal		
Hexadecane		
(1-methylethyl)-benzene		
Isopropyl Alcohol		

5.3.4 Conclusion and future studies

Breath analysis is a promising alternative for the detection of lung related diseases due to its non-invasive nature and ease of sampling. However, the daily application of breath analysis in medical environments is limited by the low concentration of biomarkers and presence of droplets in breath samples. This study attempted to resolve these issues by employing a filter-incorporated NTD. The filter packed inside the NTD can trap droplets, while the sorbents (in this case, Carboxen

particles) are dedicated to performing extractions from the gas phase. In incorporating sampling and the sample-preconcentration of both phases into a single device, the NTD ensures representative and comprehensive sampling. Comparing the NTD and TFME results is effective at distinguishing between the free and droplet-bound compounds, which may enable the more effective diagnosis of lung cancer and other diseases. Moreover, the developed filter-incorporated NTD is green, portable and cheap.

The cohort of patients studied in this communication was too small to establish a strong correlation between the analytical data and the patients' medical condition. Future investigations should seek to utilize larger cohorts and, ideally, conduct sampling before and after treatment to observe how results vary depending on the treatment and stage of the disease. For total on-site sampling, portable GC-MS can be transported to the sampling site (i.e., hospital) to analyze the extraction devices immediately after extraction. Additionally, comprehensive separation methods such as untargeted GC×GC should be employed to obtain a complete picture of the relationship between the chemical composition of exhaled breath and patients' medical states. Finally, the aerosol trapped by the needle trap can be also desorbed and characterized via LC-MS to characterize the mucus composition.

5.4 Effect of household air pollutants on the composition of exhaled breath gas and aerosol characterized by SPME and NTD

5.4.1 Introduction

The importance of breath composition and its relation to human health has been known for a long time; however, advanced technologies enabling the analysis of breath composition have only emerged over the past few decades. While more than 1000 volatile organic compounds (VOC) have since been detected in breath samples, only a few of these VOCs are common to human samples [240]. The non-invasive nature of breath sampling makes it an excellent candidate for monitoring health status, particularly with respect to clinical diagnosis (endogenous compounds) and exposure analysis (exogenous compounds).

Previously, most breath sample studies have focused on identifying biomarkers that can be used to determine disease stages [97,102,241–248], with little attention being given to the use of breath biomarkers as a tool for the rapid determination of levels of potentially noxious compounds in humans due to exposure, specifically via inhalation [235,249]. According to the National Academy of Sciences, exposure is defined as “an event that occurs when there is contact at a boundary between a human and the environment with a contaminant of specific concentration for an interval of time” [250]. Environmental chemicals can enter the body through a variety of exposure routes, including ingestion, inhalation, and dermal contact. Chemicals with short biological half-lives (nonpersistent chemicals) are removed through the urine and, if volatile, in expired air. Since it is a simpler matrix, expired breath is preferred for measuring exposure to VOCs [214]. Additionally, breath analysis can be used to monitor the decay and degradation of volatile toxic substances in the body in real time.

The use of biomarkers in exposome studies was developed to estimate the relationship between occupational/environmental exposure and its effect on people, with the goal of preventing diseases by reducing exposure through early identification [236]. Since there is an equilibrium between alveolar air and pulmonary capillary blood, breath exposome studies enable the estimation of the internal concentration and distribution of chemicals in the body [251].

Most exposure studies consider industrial environments with high levels of exposure, however, it has been shown that long-term exposure to low concentrations of some VOCs can be carcinogenic or result in allergic reactions [252,253]. Given the increased amounts of time spent indoors inherent to many modern lifestyles, along with greater awareness regarding indoor air quality, it would seem natural to focus greater attention on monitoring indoor air pollution to prevent potentially harmful compounds from entering into people's bodies.

Another issue with breath analysis is the low concentration of VOCs/biomarkers in breath samples and their distribution between the gas and droplet phases. Previously, extraction methods focusing on gas-phase composition of have been reported using solid-phase microextraction (SPME) [108,247,254–256] and solid sorbents [257–259] for preconcentration of breath biomarkers. Nearly all studies in the area of breath analysis have been limited to the investigation of either aerosol/condensate phase [260,261] or gas phase [262], which highlights the need for an integrated and comprehensive method for studying biomarkers in breath samples.

It is possible to trap exhaled breath aerosol and extract exhaled breath vapor using a single needle-trap device (NTD). While the design of commercial NTDs allows them to act as a filter for trapping particles, their filtration efficiency is rather low due to the large size of the packing material. This deficiency can be remedied by adding a proper filter to the NTD. Furthermore,

SPME can be applied to distinguish the aerosol portion of a breath sample from the vapor portion, as it is capable of extracting only from the gas-phase.

To address the aforementioned issues, we packed an NTD with an electrospun heated polyacrylonitrile (H-PAN) filter and commercial divinyl benzene (DVB) and Carboxen (CAR) sorbent particles to enable the trapping of aerosol particles and the extraction of gaseous components, respectively. Additionally, a DVB/CAR SPME fiber was applied to study the gaseous components in breath samples. The developed methods were used to study the relationship between the composition of inhaled air and exhaled breath following exposure to cannabis cigarette/candle/incense smoke and aerosol sprays. To facilitate this study, a breath sampling tube was designed to enable the real-time dynamic monitoring of respiration.

5.4.2 Experimental

5.4.2.1 Materials and Methods

Acetone, methyl acetate, 1-propanol, 2-butanone, chloroform, butyl acetate, benzene, toluene, 1,2,4–trimethylbenzene (1,2,4-TMB), ethylbenzene, o-xylene, benzaldehyde, benzyl alcohol, polyacrylonitrile (PAN, Mw= 150,000 g mol^{-1}), dimethylformamide (DMF) (99.8%), divinylbenzene (DVB) and Carboxen (CAR) particles (60-80 mesh size, HayeSep porous polymer) were purchased from Sigma-Aldrich (Mississauga, ON, Canada). Mosquito repellent candle, normal candle (wood smell), wooden stick incense, fragrance mist, body fragrance spray and fragrance sampler tests were purchased from local stores. Please refer to **2.3.1.2 SMPS instrument and 2.3.1.5 GC-MS for needle–trap analysis** for details on the instrument. The temperature programming: initial temperature was set at 40 ºC for 1 minute, then increased to 100 ºC with 5 ºC

min^{-1} rate, kept for 1 minute, increased to 250 ºC (ramp = 20 ºC min^{-1}). The protocol for breath sampling was based on the ethical clearance approved by University of Waterloo #42853.

5.4.2.2 Preparation of H-PAN filter

Please refer to **2.4.2 Optimized Filter Preparation Condition** section for details on the preparation of filter. A schematic of the filter-preparation process is shown in Figure 5-17.

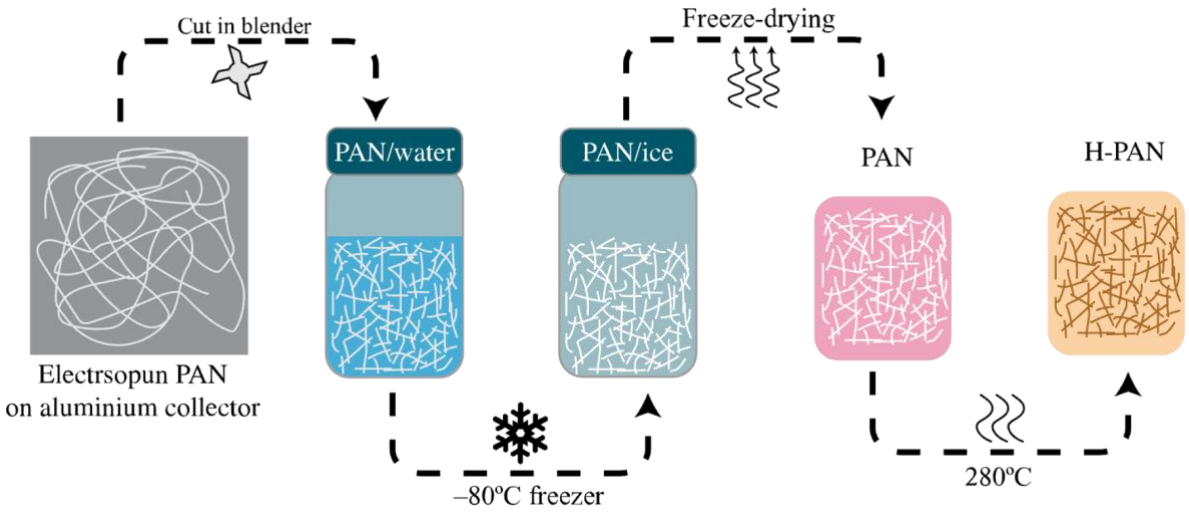

Figure 5-17. Schematic of filter preparation steps, including electrospinning, freeze-drying and heating.

5.4.2.3 Extraction Devices and Procedure

Gas mixtures were prepared via direct injection of the pure liquid analytes into a glass bulb. For this process, A 1-L glass bulb was washed, dried, vacuumed, injected with 1 µL of each analyte, and then heated. Nitrogen gas was added to compensate for the pressure difference between the air in the bulb and the external atmosphere. The concentrations of each analyte in the bulb were calculated according to the equations in [209] and can be found in Table 5-12.

Table 5-12. List of analytes, their physiochemical properties, retention time and concentration in stock mixture

	Rt (min)	Henry Constant (atm m^3/mol)	LogP	m/z	C (μg L^{-1}) in stock mixture
Acetone	1.9	3E-5	-0.2	43,58	791
Methylacetate	2.1	1E-4	0.2	43, 74	934
1-propanol	2.2	7E-6	0.3	42,59	805
2-butanone	2.4	5E-5	0.3	43,72	806
Chloroform	2.7	4E-3	1.9	83,85	1478
Benzene	3.1	1E-2	2.1	78,77	880
Toluene	5.2	6E-3	2.7	91,92	870
Butylacetate	6.7	3E-4	1.7	43,56	880
Ethylbenzene	8.2	8E-3	3.1	91,106	870
o-xylene	9.3	5E-3	3.1	91,106	880
Benzaldehyde	11.9	3E-5	1.5	77, 106	1046
1,2,4-TMB	13.1	6E-3	3.6	105,120	881
Benzyl alcohol	14.9	3E-7	1.1	79,108	1041

For extraction, appropriate amounts of the standard gas mixture were transferred from the 1-L glass bulb to a 125-mL glass bulb using gas-tight syringes in order to obtain the desired concentrations (Figure 5-18).

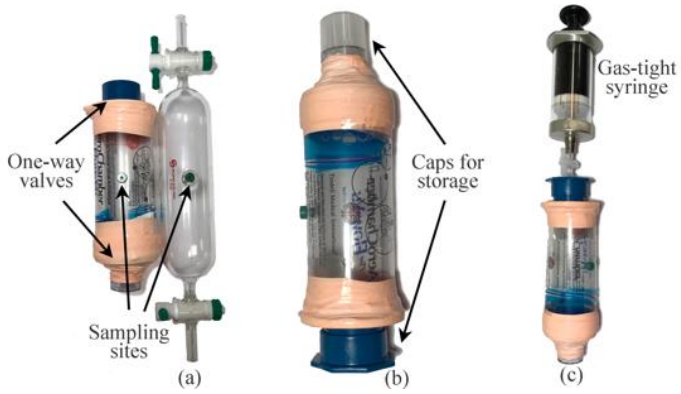

Figure 5-18. 125-mL glass sampling bulb and the sampling tube designed for dynamic breath analysis (a) sampling sites and valves (b) capped device during storage and extraction, (c) devices for injection of gaseous mixture

A DVB/CAR SPME fibre (50/30 µm, SUPELCO) and a home-made H-PAN/DVB/CAR NTD were applied for the extraction of gaseous compounds during the optimization and calibration steps. The NTD was packed with 5 mm of DVB and 5 mm of CAR, which were sandwiched between two filter plugs (2 mm). The SPME fiber was left inside the mixture for a pre-defined time period, while NTD extractions were performed by using a pump to draw the sample through the needle (Flow rate=20 mL min^{-1}). A schematic of the extraction devices is presented in Figure 5-19.

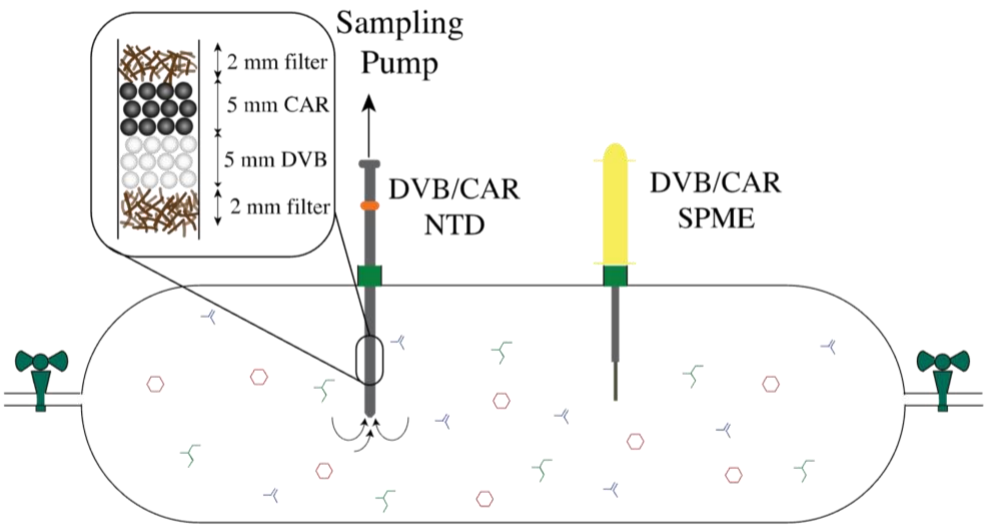

Figure 5-19. Schematic of extraction procedure using SPME and NTD during optimization and calibration.

For the extraction of gaseous compounds from breath samples, a volunteer (with ethical approval from University of Waterloo #42853) was asked to exhale into the sampling tube. As shown in Figure 5-20, the initial exhaled breath sample fills discard bag #1 (pink path #1), which ensures that any stagnant mouth air is removed and that the sample consists entirely of alveolar air. After filling the first discard bag, the breath pressure opens the one-way valve and enters the sampling tube, before being pushed into discard bag #2 (green path #2). The sampling process

continues until discard bag #2 is full. The incorporation of the second discard bag is significant, as it enables the reproducible sampling of alveolar air. Additionally, based on the size of the discard bags (400 mL) and the tube volume (125 mL), it is possible to be sure that the air in the tube has been fully replaced by breath when the second discard bag is full. In addition, the tubes can be cleaned by passing clean nitrogen gas through them for 30 minutes after each sampling run, thus making it possible to reuse the same tube for multiple runs. A full diagram of the sampling device can be found in Figure 5-20. The breath samples were extracted by inserting the developed extraction devices into the sampling portal located on the tube (green septum). Additionally, to control for the inhaled air, the air surrounding the volunteer during the experiment was studied by performing the extraction procedure under optimum conditions with the DVB/CAR SPME fiber.

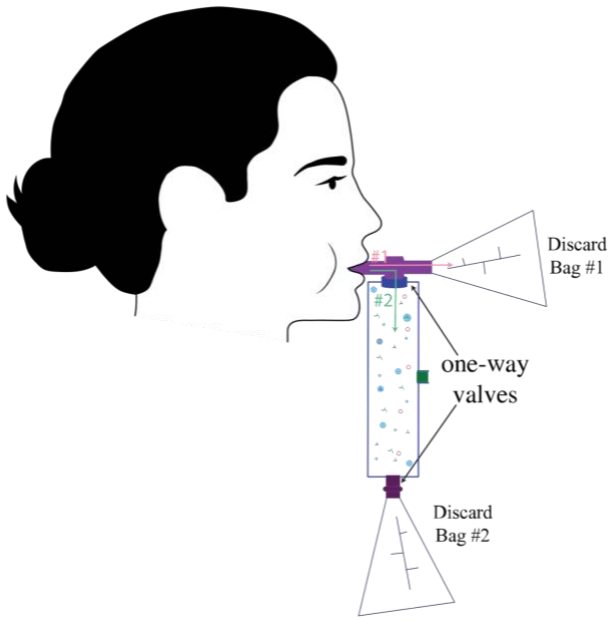

Figure 5-20. Sampling process for breath analysis. first discard bag #1 is filled with mouth air. Then alveolar air pushed air from the sample tube into the discard bag #2.

5.4.2.4 Filtration efficiency

The filtration efficiency of the developed NTD was assessed using a scanning mobility particle sizer (SMPS). Specifically, the H-PAN/DVB/CAR NTD was inserted into the SMPS, with the filtration efficiency being defined as the difference in the instrument's particle count before and after insertion. To make up for the high flow rate required by the SMPS, 6 parallel needles were inserted into it during these tests.

5.4.2.5 Extraction time: gas/droplet stability and equilibrium time

Two important factors were considered in determining the optimum sampling time: the stability of the gas/droplets in the sampling device, and the equilibrium time required for SPME. Ideally, the extraction time for SPME should be long enough to achieve equilibrium, as this will ensure maximum sensitivity; however, in gas mixtures, analytes can be lost due to attachment to the chamber wall, diffusion, or escape through valves/connections. This phenomenon is more significant for low sampling volumes, as they are generally accompanied by high ratios between the container surface area and gas volume. Therefore, it was important to carefully consider equilibrium time and sample stability when determining the optimum sampling time. The stability of VOCs in glass bulbs has been studied previously, with findings showing that a gas mixture can remain stable inside a glass bulb for at least a few hours [263–265].

To check the stability of the gas mixture, home-made sampling tube were spiked with gas mixture and a 1-min extraction by SPME-fiber was applied (Figure 5-18-c). The extraction was performed over 30-min time period after injection while the tube was left capped in room temperature (Figure 5-18-b) and the relative signals of the two volatile components were followed

and reported as an indicator of the stability. The signals were adjusted to compensate for the depletion after each SPME extraction.

Acetone was chosen as the target compound for studying the stability of aerosol droplets in breath due to its polarity and presence in droplet-phase. Multiple breath samples were obtained, and extractions were performed at different time points after sampling using NTD (1 min, 20 mL min^{-1}).

The equilibrium time for the SPME method was determined by exposing an SPME-fiber to the gas mixture for different amounts of time. The equilibrium time was considered to have been achieved when the extraction signal remained constant despite further increases to the extraction time.

Finally, the optimal sampling time was selected by considering the stability of the gaseous mixture and droplets, as well as the equilibrium time profile.

5.4.2.6 Breakthrough volume (BTV)

Breakthrough volume is defined as the sampling volume at which the NTD reaches its full capacity or equilibrium. It is important to study BTV when using NTDs, as the linear relationship between the extracted amount and sample concentration is lost after the BTV has been reached. If two needles are connected in series, the BTV is assumed to have been reached when compounds start escaping from the 1st needle and are detected in the 2nd needle. Therefore, the DVB/CAR NTD under study was connected to a secondary commercial needle to determine the BTV. The signal of the compounds in the secondary needle was monitored while increasing the sample volume up to 250 mL (sample concentration ~ 500 ng mL^{-1}); if no compounds were detected at a

given sample volume, the BTV was not considered to have been reached, as the primary NTD was still functioning as an exhaustive sampler.

5.4.2.7 Method validation

To validate and calibrate the developed DVB/CAR NTD and DVB/CAR SPME methods, gas mixtures with varying concentrations were prepared by spiking the glass bulb with different volumes of stock mixture and humid air. The humid air was prepared in a separate 1-L glass bulb, after injection and heating of 40 μL of MiliQ water. To check the repeatability of the developed method, inter-day and intra-day relative standard deviations (RSD) was investigated. The linear dynamic range (LDR) was chosen based on previous reports detailing the possible concentrations of pollutants in breath after exposure and calculated with external calibration method. The limits of detection (LODs) and limits of quantification (LOQs) were investigated using signal-to-noise ratios of 3 and 10, respectively. All optimization was performed in selected ion monitoring (SIM) mode for optimum sensitivity, and the selected m/z values are provided in Table 5-12.

5.4.2.8 Real sample analysis

Breath samples were obtained from volunteers following exposure to smoke from wooden stick incense, a mosquito repellant candle, and a normal unscented candle to analyze the effect of exposure to household pollutants on exhaled breath. In addition, the composition of breath samples obtained after exposure to air freshener spray, fragrance mists and smoking of cannabis was also investigated. The volunteers were asked to refrain from eating at least 3h and to wash their mouth with water prior to exposure. In addition, the sampling tubes were cleaned with nitrogen gas (Figure 5-21-a), and a control sample was obtained via SPME to assess breath composition pre-

exposure. Each volunteer's breath was obtained once pre-exposure to study the breath composition resulting from exogenous sources.

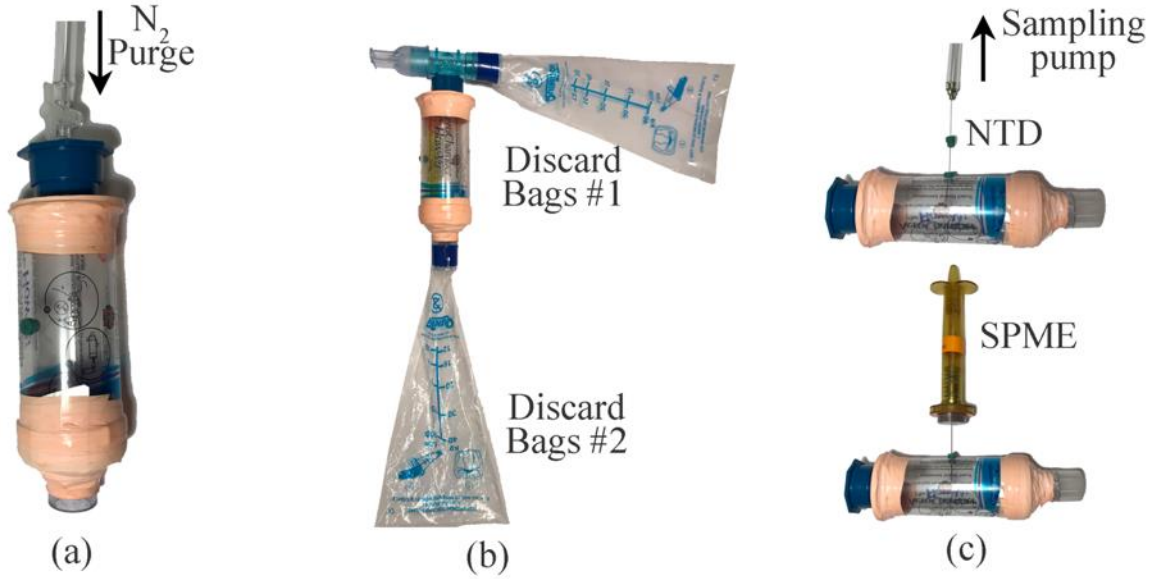

Figure 5-21. Breath sampling procedure (a) nitrogen purge for cleaning the tube, (b) mouth-piece and discard bags for removing mouth air and reproducible sampling, (c) extraction using SPME and NTD.

The exposure environment was created by lighting an incense stick or a candle. A distance of ~ 50 cm was maintained between the source of the smoke and the volunteer nose, and the volunteer was instructed to breathe normally. Each test used an exposure time of 1 h, as this was the time required to completely burn one incense stick. Once the exposure time had elapsed, the incense/candle smoke was removed from the environment, and the breath samples were obtained and analyzed. For sampling after smoking, the breath sample was obtained after the smoking of cannabis in routine conditions.

Exposure to the fragrance mist and air freshener was conducted by releasing five spritzes of the aerosol at a distance of ~ 25 cm from the face of a volunteer who was breathing normally. For these tests, breath samples were obtained and analyzed following an exposure of 5 minutes. During

some of the samplings, to study the effect of breath droplets, the mouthpiece was equipped with a filter during breath sample collection after exposure, in order to prevent breath droplets from reaching the sampling tube. Sampling was repeated 1h after exposure for some of the volunteers. The sampling tube and extraction experiments are shown in Figure 5-21-b and c. During all experiments (except cannabis smoking), DVB/CAR SPME devices were also positioned close to the volunteer's nose to determine the concentration of air pollutants in the inhaled air. Every sample was quantified in SIM mode, but one run per sample was performed in TIC mode to detect any other potential components.

5.4.3 Results

5.4.3.1 Filtration efficiency

The filtration efficiency of the devices was analyzed using the SMPS, with the results being shown in Figure 5-22. As can be seen, the NTD provided a filtration efficiency of > 99%. Since the droplets under study had a very small size range (between 5-225 nm) with theoretically minimum filtration efficiency [51], it can be expected that similar or better filtration efficiency can be obtained in a sample matrix.

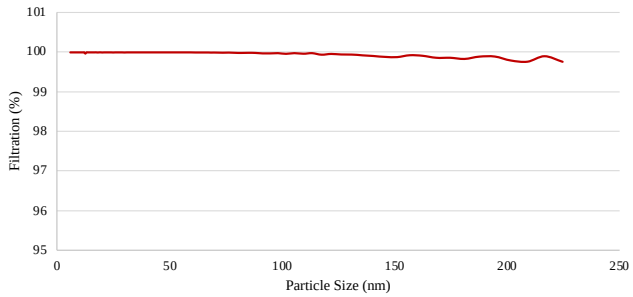

Figure 5-22. Filtration efficiency of the NTD packed with a DVB/CAR/H-PAN filter.

5.4.3.2 BTV investigations

To find the BTV, the sampling volume was increased to 250 mL, and a secondary needle was monitored for signals from the analytes. The results of these tests showed that the BTV was not reached until 250 mL (which covers the sample volume = 125 mL), as desorption of the secondary NTD did not show any peaks associated with the VOCs under study prior to this level. Based on the obtained results, it was concluded that BTV was not reached during breath sampling (sampling volume = 100 mL).

5.4.3.3 Extraction time: gas / droplet stability and SPME equilibrium time

The stability of the gas mixture in the tube was assessed by extracting the sample via SPME (1min) immediately after injection and every 5 minutes for a period of 30 min. The results are shown in Figure 5-23.

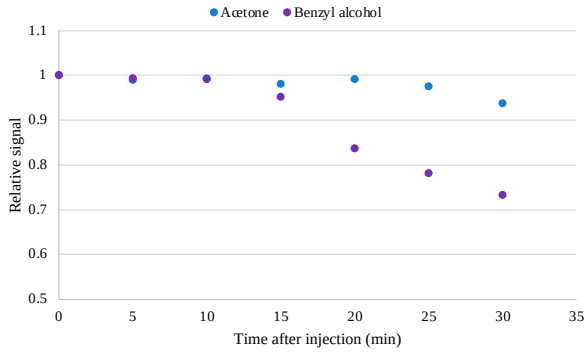

Figure 5-23. Relative signal of acetone and benzyl alcohol in gas mixture over a 30-min period after injection into sampling tube.

As the data suggests, volatiles and non-volatiles remain stable in the gas mixture up to the 15-minute mark, but this stability begins to diminish beyond this point. This loss of stability may be the result of the compounds settling in the walls of the sampling tube or escaping from the

device through connections or valves. Since heavier compounds were found to diminish more rapidly, it can be concluded that this instability is primarily attributable to the settlement of compounds in the walls of the tube.

The gas-phase study showed that acetone remains quite stable for up to 20 minutes in the sampling tube. Significantly, acetone's polar structure allows it to also be present inside breath droplets, which is why it was selected as a marker for monitoring the stability of droplets inside the sampling tube.

A breath sample containing acetone was obtained from a volunteer, with subsequent extractions being performed using the NTD. The concentration reported via the NTD consisted of both gas-phase and droplet-bound acetone. Based on these explanations, and considering the stability of acetone in gas-phase (Figure 5-23), it can be assumed that any decrease in the concentration detected via the NTD during this time range can be attributed to the settlement of droplets in the sampling tube. The stability of acetone (relative signal) is reported in Figure 5-24. Based on these data, breath droplets can be considered stable for up to 10 minutes after sampling.

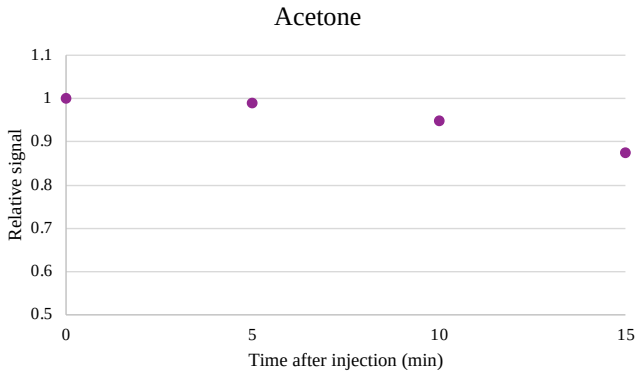

Figure 5-24. Relative signal of acetone in breath samples detected via NTD over 15 minutes following sampling.

To find the best extraction time, it was also important to study the equilibrium time of analytes extracted using SPME. As the equilibrium time profile reveals (Figure 5-25), equilibrium is achieved at around 15 minutes for most of the compounds; however, more hydrophobic characterized by higher distribution constant components required 30 minutes to reach equilibrium.

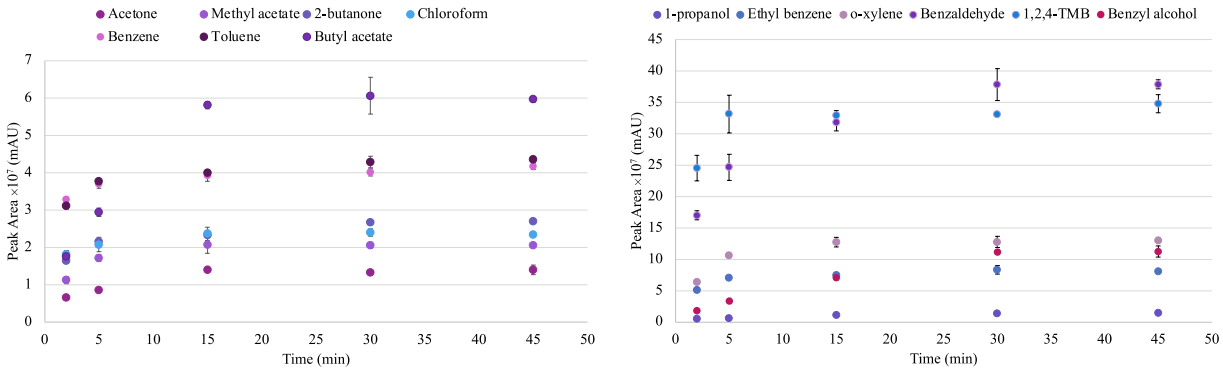

Figure 5-25. Equilibrium time profile of VOCs using DVB/CAR SPME.

As explained earlier, both sample stability and equilibrium time can be considered as limiting factors in finding the optimum extraction time. As the equilibrium time data shows, a 30-minute extraction time is required for full equilibrium to be reached between the analytes and the SPME fiber coating; however, gaseous analytes and droplets can remain stable inside the prepared sampling device for up to 10 minutes. To ensure the reproducibility and stability of the sampling method, and based on the discussed results, a pre-equilibrium condition with a 5-minute extraction time was selected as optimum for this study. That is, extractions were performed by leaving the DVB/CAR SPME fiber inside the tube for 5 minutes; similarly, sampling was conducted with the DVB/CAR NTD for a period of 5 minutes (flow rate = 20 mL min^{-1}).

5.4.3.4 Method validation

The figures of merit, including LODs, LOQs, and LDR, were studied with the DVB/CAR SPME fiber and the DVB/CAR NTD using different concentrations of gaseous mixture in the glass bulb. The inter-day and intra-day RSD can be found in Table 5-13.

Table 5-13. Inter-day and intra-day relative standard deviations

	RSD	
	Inter-day	Intra-day
Acetone	10.1	2.5
Methylacetate	9.4	3.5
1-propanol	3.6	6.2
2-butanone	6.4	5.2
Chloroform	7.8	1.7
Benzene	8.8	4.2
Toluene	7.4	2.1
Butylacetate	15.9	2.7
Ethylbenzene	6.4	3.6
o-xylene	7.4	4.7
Benzaldehyde	11.5	5.3
1,2,4-TMB	13.5	6.1
Benzyl alcohol	12.6	8.1

The results of these tests are provided in Table 5-14. As the data suggests, the method's sensitivity regarding the detection and quantification of the analytes under study was satisfactory, considering the pre-equilibrium condition of the study and the low sample volume. Indeed, the observed sensitivities were similar or better to those reported in previous breath studies using NTD or SPME [34,76,98,105,255,266] and were capable of meeting the concentration limits set forth by health agencies.

Table 5-14. Figures of merit for the study of analytes using the DVB/CAR SPME fiber and DVB/CAR NTD using standard gas with humidity.

Analyte	LOD (ng mL^{-1})		LOQ (ng mL^{-1})		LDR (ng mL^{-1})	
	NTD	SPME	NTD	SPME	NTD	SPME
Acetone	0.2	0.3	0.8	1.0	1.3-316	1.3-316
Methyl acetate	0.2	0.3	0.7	1.0	0.7-374	1.5-374
1-propanol	0.2	0.2	0.7	0.8	1.3-322	1.3-322
2-butanone	0.1	0.2	0.5	0.7	0.6-322	1.3-322
Chloroform	0.1	0.2	0.5	0.8	1.2-591	1.2-591
Benzene	0.09	0.1	0.3	0.4	0.7-352	0.7-352
Toluene	0.09	0.1	0.3	0.3	0.7-348	0.7-348
Butyl acetate	0.1	0.2	0.5	0.7	0.7-352	0.7-352
Ethyl benzene	0.05	0.08	0.2	0.3	0.7-348	0.7-348
o-xylene	0.06	0.07	0.2	0.2	0.7-352	0.7-352
Benzaldehyde	0.1	0.1	0.3	0.5	0.8-418	0.8-418
1,2,4-TMB	0.05	0.09	0.2	0.3	0.7-352	0.7-352
Benzyl alcohol	0.09	0.1	0.3	0.4	0.8-416	0.8-416

5.4.3.5 Real sample results

Some compounds such as acetone were detected before exposure, but are not reported as they were considered to be “endogenous”, not the result of exposure. The analytes are reported in Table 5-15 and considered “exogenous”, only when they were not detected pre-exposure. Additionally, after each sampling and cleaning of sampling tube, the cleanness of tube was tested and no compound was detected. The concentration of the compounds detected and determined in

exhaled breath samples with the DVB/CAR SPME fiber and the DVB/CAR NTD are provided in Table 5-15 and the chromatogram in SIM mode for the study of Spray #1is shown in Figure 5-26.

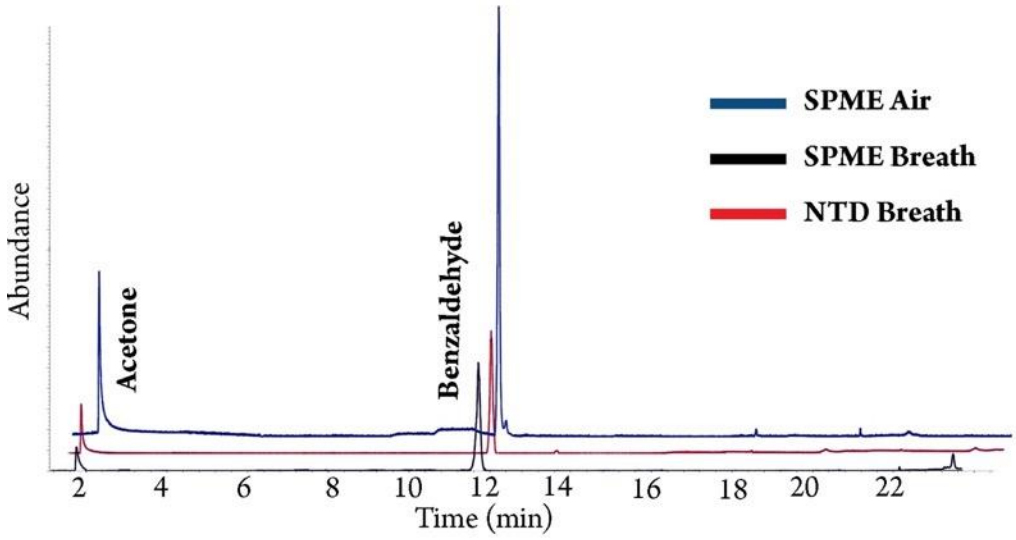

Figure 5-26. Chromatogram from study of inhaled air and expired breath after exposure volunteer to Spray #1.

In addition to studying exhaled breath, air inhaled by the volunteers was also studied to determine the correlation between their respective compositions. As expected, higher concentrations of pollutants were detected in the air samples. However, one notable finding relates to the difference between the concentrations reported with NTD and SPME: whereas both NTD and SPME reported similar concentrations for non-polar pollutants, NTD generally reported higher concentrations for polar compounds (acetone, benzaldehyde and benzyl alcohol), with the largest difference being observed for acetone. This difference can be attributed to the NTD's ability to trap breath droplets, which enables it to report the total concentration of compounds (both in exhaled breath vapor and in exhaled breath aerosol). Non-polar components prefer the vapor phase, while polar and less-volatile analytes tend to remain inside of droplets. This claim is supported by

the data for Spray #3, which was obtained through a filter that prevented aerosol droplets from reaching the sampling tube. In this case, only exhaled breath vapor was available for extraction and, as a result, similar concentrations for acetone and benzyl alcohol were determined by the NTD and SPME fiber (unlike Spray #1).

Table 5-15. Concentration of compounds in ng mL^{-1} (± standard deviation) determined via DVB/CAR SPME and DVB/CAR NTD in ambient air and exhaled breath following exposure and immediate sampling (ND = not detected)

Incense Smoke	Breath		Air
	SPME	NTD	SPME
1,2,4-TMB	5.6 (±0.6)	6.6 (±1.2)	79.3 (±5.5)
o-Xylene	ND	ND	38.3 (±6.1)
Mosquito repellant candle	Breath		Air
	SPME	NTD	SPME
Benzene	ND	ND	15.4 (±1.2)
Ethylbenzene	4.1 (±0.3)	3.8 (±0.5)	28.3 (±1.9)
Candle with wood smell	Breath		Air
	SPME	NTD	SPME
Benzene	ND	ND	8.9 (±1.5)
Cannabis smoke	Breath		Air
	SPME	NTD	SPME
o-Xylene	14.3 (±1.4)	15.4 (±1.6)	-
Spray #1	Breath		Air
	SPME	NTD	SPME
Acetone	2.4 (±0.5)	5.3 (±0.5)	87.0 (±2.6)
Benzaldehyde	11.6 (±1.3)	14.3 (±1.7)	184.0 (±12.0)
Spray #2	Breath		Air
	SPME	NTD	SPME
Benzyl alcohol	5.5 (±0.6)	6.4 (±0.9)	215 (±23)
Spray #3 (sampled through mouth filter)	Breath		Air
	SPME	NTD	SPME
Acetone	4.1 (±0.6)	3.6 (±0.3)	85 (±9)
Benzylalcohol	7.9 (±1.1)	7.5 (±0.5)	194 (±16)

These data clearly suggest that the differences observed for these methods between samples is due to the NTD's ability to trap droplets. Similar concentrations of these air pollutants were reported previously [264,267,268].

In some of the cases, the sampling was repeated 1h after exposure. In most cases, the compound was undetectable after 1h. In the case of incense smoke, 1,2,4-TMB was detected (below LOQ) even after 1 h from exposure. This was a significant finding, revealing how the long-term exposure to these household air pollutants can introduce large concentration of hydrocarbons into human body. It also shows that polar compounds can be removed faster, because in some cases, the concentration of polar compounds detected in breath was higher, however, they were eliminated from body faster and became undetectable earlier than non-polar. This finding is attributed to the elimination of polar compounds through kidney, while non-polar compounds are generally removed via breath [234–236].

Data in TIC mode: As mentioned previously, all air and breath samples were analyzed once in TIC mode to identify any other components that may be present. Overall, the following compounds were detected in the air samples: pyrene, anthracene, para-ethyl styrene, isopropyl benzene, pinane, limonene, pyridine, limonene, linalool, 1,3,5-trimethyl naphthalene, benzofuran, benzyl benzoate, isoeugenol, diethyl phthalate, citronellol, geraniol, cinnamaldehyde, and carvone. The compounds detected via breath analysis in TIC mode included cinnamaldehyde, pyridine, limonene, isoeugenol. It should be mentioned that there were some other tested candles and sprays, however, they are not reported here as there was no compound detected in their associated breath sample after exposure.

5.4.4 Discussion

The term, “air pollution” can be misleading, as mostly people generally think of car exhaust and factory smoke when they hear this term. However, studies conducted by the World Health Organization (WHO) have found that “8 million people die every year globally because of air pollution. Among these, 4.3 million die because of air pollution from household sources.” Some of the main sources of household air pollution include cooking-related smoke, smoking, perfume and deodorants, and building materials. While these types of pollution may seem negligible based on type and amount, long-term exposure has shown to be problematic and, in the worst cases, deadly [269].

Breath analysis is one of the best options for studying exogenous compounds and monitoring exposure patterns, as it is non-invasive, fast, and enables real-time monitoring. The main challenge associated with this form of analysis is that exhaled breath is aerosol in nature. This is problematic, as breath studies that are limited to analysis of the gas-phase will not be able to detect polar compounds hidden inside droplets. Thus, the NTD developed in this work is an important contribution to this area of study, as it enables the gas-phase and droplet-bound components in breath samples to be studied simultaneously.

A comparison of the results obtained with the developed NTD and fiber format of SPME confirmed the NTD’s superior performance, especially for polar components. The NTD allows breath droplets, including polar components, to be trapped, desorbed, and studied, while SPME is only capable of studying exhaled breath gas. The superiority of the values obtained via NTD compared to SPME was demonstrated through an experiment designed to control for the effect of droplets in the other studies. In this experiment, samples were obtained through a mouthpiece

equipped with a filter to remove all droplets from the sample. With the droplets removed, both methods produced similar values for polar compounds.

The compounds detected in the breath samples, as well as the identification of other chemicals in TIC mode, revealed the extent of the types of air pollution that are voluntarily produced inside people's houses. While the concentrations of detected components in breath are low and are removed quickly from body, long-term exposure to smokes and sprays can be problematic and initiators of respiratory diseases and allergies.

In addition, this study also introduced a new device for acquiring breath samples. This device consisted of a sampling tube equipped with valves at either end and a hole (covered with green septum) in the middle to enable sampling with the SPME fiber and NTD. Furthermore, the device's use of discard bags made it possible to completely eliminate pre-existing mouth air and enable reproducible alveolar breath sampling. The one-way valves situated on either end of the sampling tube facilitated dynamic breath sampling over time, or time-weighted averaging studies, by allowing the previous sample to be replaced with freshly exhaled breath. Moreover, the sampling tubes were re-usable; this was enabled by passing clean air or nitrogen gas through them after each application.

5.4.5 Conclusion

This study investigated the potential of using a filter-incorporated NTD for the analysis of breath composition and exposure patterns. The simultaneous application of NTD and SPME provided a comprehensive view of the sample by distinguishing the free and droplet-bound components. The results obtained with developed devices confirmed their tremendous potential

for the investigation of polar components in breath samples, which are often lost due to their affinity for attaching to droplets. Furthermore, the re-usable sampling tubes designed for this research is cheap and enable the possibility of real-time dynamic sampling, and they can also be applied for time-weighted averaging studies wherein sampling is repeated at different time points to find the average concentration of desired compounds in breath samples. The combined use of the designed sampling devices provides a fast and green method for studying breath composition and the effects of inhaled air on expired breath. Some chemicals were detected both in the air samples close to sources of pollution (smokes and sprays) and the acquired breath samples, revealing the potential dangers of exposure to routine household air pollutants. While the analyzed breath samples contained low concentrations of air pollutants, long-term exposure to these chemicals can be hazardous. In this study only direct products of sprays and smokes were studied, it is possible to extend this study to the metabolites of these compounds after entering body. Untargeted determination via GC×GC would enhance the determination of the impact of the exposure as it facilitate monitoring the change in breath of the endogenous compounds, which might indicate subject's health status. The developed devices are simple and can be conveniently adopted to common use. Characterization of compounds carried by aerosol particles and dissolved in gas might have significance leading to correct medical diagnosis.

Filter-Incorporated Needle-Trap Device (FI-NTD) Application: Air Monitoring

6.1 Preamble

This chapter contains sections that have already published as an article in ACS Sustainable Chemistry & Engineering. All subchapters are included in the article entitled *Green portable method for simultaneous investigation of gaseous and particle-bound air pollutants in indoor and outdoor environments* by Shakiba Zeinali and Janusz Pawliszyn, *ACS Sustainable Chemistry & Engineering*, 2022, 10, 12, 3981-3989. The contents of the articles are herein being reprinted with permission of American Chemical Society, in compliance with both publisher's and the University of Waterloo policies.

6.2 Introduction

Human activities introduce a wide range of pollutants into the environment, including volatile organic compounds (VOC) and polycyclic aromatic hydrocarbons (PAH). These compounds do not remain confined to the industrial or pharmaceutical settings from which they originate; rather, they spread over a large area via the wind and waterways, ultimately entering the human body through the food chain, air, or groundwater This can pose a serious problem, as research has demonstrated that some of these organic compounds can be carcinogenic, mutagenic, and teratogenic [275,276]. Although airborne pollutants are generally only detected at low concentrations in indoor and outdoor environments [277], long-term exposure to these compounds can lead to the development of respiratory and cardiovascular disease [278].

While the importance of constantly monitoring the presence of air pollutants is clear, a variety of factors can make it difficult to accurately measure concentrations of pollutants, including: pollutant type, the presence of particles, low concentrations of pollutants, the ventilation system, interaction between the pollutants and environmental compounds, and the absence of appropriate sampling and sample-introduction techniques. The concentrations of particle-bound [279] gaseous [280] and combined particle and gaseous [281] air pollutants have been successfully measured in prior studies, but, in each case, two separate methods were required for the determination of the gas-phase and particle-bound concentrations.

Solid-phase microextraction (SPME) and thin-film microextraction (TFME) have previously been applied to extract VOCs and PAHs from the gas phase [282,283]. Although these methods are solventless and fast, they are only sensitive to gas-phase concentration of aerosol samples including air pollution [7,284,285].

The standard method for analyzing the particle–bound pollutants is NIOSH 5515 [286], which entails trapping the particles on a filter bed and then desorbing them for further analysis. However, this method is time consuming and requires a large amount of organic solvents and equipment. In addition, larger sample volumes and longer sampling times are required to compensate for this method's relatively poor sensitivity and use of large desorption volumes.

Needle-trap devices (NTD) are the best alternative to conventional approaches for studying airborne pollutants, as they are exhaustive and their packed needle enables the dynamic sampling and trapping of solid particles from air samples. Although the filtration efficiency of NTDs packed with commercial sorbents is limited, this can be improved by further incorporating a proper filter. The selected filter should provide high filtration efficiency, permeability, and thermal stability.

In the present work, we attempt to address the challenge of simultaneously extracting particle-bound and gaseous compounds by preparing a needle-trap device packed with a polyacrylonitrile (PAN)-based filter and commercial sorbent. The performance and sustainability of the proposed NTD was then compared to two equilibrium-based methods—SPME and TFME—for the extraction of free concentrations of PAHs and VOCs, respectively. For this purpose, these three methods were assessed according to the principles of Green Analytical Chemistry (GAC) and White Analytical Chemistry (WAC), using dedicated tools, AGREE and RGB 12, respectively. The designed extraction devices were applied to sample air in a parking lot, as well as candle, incense, and cigarette smoke. Finally, the results from benchtop GC/MS were compared to those of portable GC/MS to verify the method's portability.

6.3 Experimental

6.3.1 Materials and Instruments

Benzene, toluene, 1,2,4–trimethylbenzene (1,2,4-TMB), butyl acetate, heptane, ethylbenzene, o-xylene, decane, acenaphthene, fluorene, phenanthrene, anthracene, fluoranthene, pyrene, 1,2-benzanthracene (Benz[a]anthracene), polyacrylonitrile (Mw= 150,000), dimethyl formamide (DMF) (99.8%), divinylbenzene particles (60-80 mesh size, HayeSep porous polymer) were purchased from Sigma-Aldrich (Mississauga, ON, Canada). Hypophilic-lypophilic balance particles were homemade (60-80 mesh size). Cigarette, mosquito repellant candle, normal candle with wood smell, wooden stick incense and cone incense waterfalls were purchased from local stores. Please refer to **2.3.1.2 SMPS instrument, 2.3.1.3 Gas Generator, 2.3.1.4 GC-MS for thin–film analysis and 2.3.1.5 GC-MS for needle–trap analysis** for details on the instrument. The instruments were run in full scan mode with mass range of 50–250 m/z. The initial

temperature for VOC was set at 40 ºC for 1 minutes, then increased to 100 ºC with 5 ºC min^{-1} rate (total time 13 minutes). For PAH, the temperature was set at 40 ºC for 1 minutes, increased to 275 ºC (ramp = 25 ºC min^{-1}) and increased to 300 ºC (ramp = 10 ºC min^{-1}) with a total of 13.9 minutes for each run. For real samples, a combined method was used to assure effective separation in complex mixture: 40 ºC for 1 minutes, then increased to 100 ºC with 5 ºC min^{-1} rate, increased to 275 ºC (ramp = 25 ºC min^{-1}) and increased to 300 ºC (ramp = 10 ºC min^{-1}) with a total time of 23.5 minutes.

Portable GC-MS: Torion Tridion-9 GC- toroidal ion trap MS coupled with a prototype high volume desorption (HVD) module (Torion Technologies Inc. UT) was used. Chromatographic separations on the Tridion-9 were performed using a low thermal mass (LTM) MXT-5 (5 m × 0.1 mm × 0.4 μm) Siltek-treated stainless-steel column (Restek Co. Bellefonte, PA). Helium carrier gas was used at a flow rate of approximately 0.3 mL min^{-1}. For VOC: Initial temperature is 40 ºC holds for 5 s, increased to 150ºC (2ºC s^{-1}) holds for 10s with a total run time of 70 s. injector temperature was kept at 270 ºC with 25 s desorption time. For PAH: Initial temperature is 50 ºC holds for 10 s, increased to 290 ºC holds for 60s with a total run time of 190s. injector temperature was kept at 270 ºC with 25 s desorption time. For NTDs and SPME devices, the desorption was by direct insertion of extraction devices into portable GC-MS instrument. For thin-films, the extracted analytes were initially desorbed and transferred into commercial NTD with high capacity (Figure 6-2). Then the commercial NTD was desorbed and analytes were sent into chromatographic column. Full lists of the compounds and their properties can be found in Table 6-1 and Table 6-2.

Table 6-1. list of studied VOCs with their physiochemical properties.

Name	Portable Rt (SPME and NTD, s)	Benchtop-Rt (SPME and NTD, min)	Boiling point (°C)	LogP
benzene	23.5	2.7	80	2.1
heptane	26.1	3.2	98	4.6
toluene	33.4	4.4	110	2.7
butyl acetate	37.3	5.5	126	1.7
ethyl benzene	42.8	6.6	136	3.1
o-xylene	45.8	7.5	144	3.1
1,2,4-TMB	54.8	10.5	169	3.6
decane	55.7	10.6	174	5.0

Table 6-2. list of studied PAHs with their physiochemical properties.

	Portable-Rt (TFME and NTD, s)	Benchtop-Rt (TFME, min)	Benchtop-Rt (NTD, min)	Boiling point (°C)	LogP
Acenaphthene	95.1	7.9	8.3	279	3.9
Fluorene	102.0	8.1	8.8	295	4.2
Phenanthrene	115.0	8.4	9.8	340	6.1
Anthracene	120.3	9.4	10.2	339	4.4
Fluoranthene	129.8	10.6	11	384	5.2
Pyrene	132.9	10.8	11.3	404	4.9
Benz[a]anthracene	15.2	12.1	12.9	438	5.8

6.3.2 Preparation of the filter

Please refer to **2.4.2 Optimized Filter Preparation Condition** section for details on the preparation of filter, a depiction of the products from each step is shown in Figure 6-1.

Figure 6-1. The process of preparing filter, from left to right, electrospun fiber, fiber-water suspension, PAN aerogel (white) and heated PAH (H-PAN) aerogel (brown)

6.3.3 Experiments with portable GC-MS

Portable instruments can provide the advantage of on-site sampling which can facilitate the procedure and reduce the costs and time of the experiment. In this study, in order to evaluate the applicability of the portable GC-MS, the experiments for real samples were analyzed by both benchtop and portable GC-MS instruments. The same DVB/SPME-fiber and HLB/TFME devices were used for both instruments and the equilibrium time experiments were not repeated with the portable GC-MS. Only in the case of NTD, based on the injection port of portable GC-MS, 19 G needles were used for experiments. Since, the 19 G needles have larger diameter compared to 22 G, they can provide higher capacity (with similar packing length). It can be concluded that by choosing appropriate sampling volumes for extraction using 22 G needles (with lower capacities), it can be assured that the BTV for 19 G needles was not reached. So, the results for BTV studies

of 22 G needles (studied with benchtop GC/MS) were applied to portable GC/MS application as well. The method validation data for thin-film, SPME fiber devices and NTDs (19G needles) were repeated with portable GC/MS for calibration curve calculations.

For desorption with portable GC/MS, the needles of NTDs and SPME could be directly injected into the instrument for thermal desorption. For thin-films a high volume desorber (HVD) was used for thermally desorbing analytes and transferring them to a commercial NTD, which can be further desorbed and analyzed (Figure 6-2).

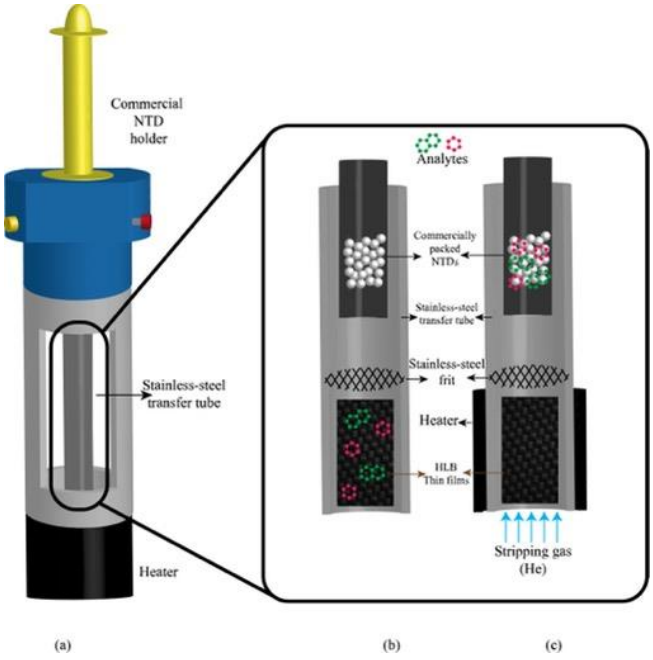

Figure 6-2. Schematic of the high volume desorber (HVD) used for desorption of thin-films for portable GC/MS and transferring the compounds to commercial NTD

6.3.4 Extraction Devices and Procedure

A strong HLB extraction phase was chosen to ensure the efficient extraction of VOCs and some polar compounds from the air pollutants, while DVB was selected for the extraction of PAHs

and to assure proper desorption. The extraction of VOCs was performed using HLB-coated thin-films (HLB/TFME; 5×20 mm) prepared according to the procedure developed by Grandy et al. [145] The NTD used for VOC extraction was packed with two of 2 mm H-PAN filter, as well as 10 mm of HLB particles (HLB/NTD).

The PAH extractions were performed using a commercially available DVB/SPME-fiber (65 mm, SUPLECO) and an NTDs that had been packed with 2×2 mm of H-PAN filter and 10 mm of DVB particles (HayeSep® Porous Polymer Adsorbent**,** 60-80 mesh) (DVB/NTD). For both sets of extractions, the prepared needles were packed inside a 22 G luer-lock stainless steel needle (Figure 6-3).

The same thin-films and SPME fibers were used in the portable GC/MS studies. However, due to the size of the portable GC/MS's injector port, a larger (19 G) luer-lock needle with similar packing length was applied for these studies.

For the TFME and SPME fiber extractions, the devices were exposed to the sample for a pre-defined amount of time until equilibrium had been achieved. For the NTD extractions, the samples were drawn through the needle using a pump (flow rate = 10 mL min^{-1}). After extraction, the devices were transferred to a benchtop or portable GC/MS instrument for thermal desorption and analysis. A schematic of the sampling procedure is provided in Figure 6-3.

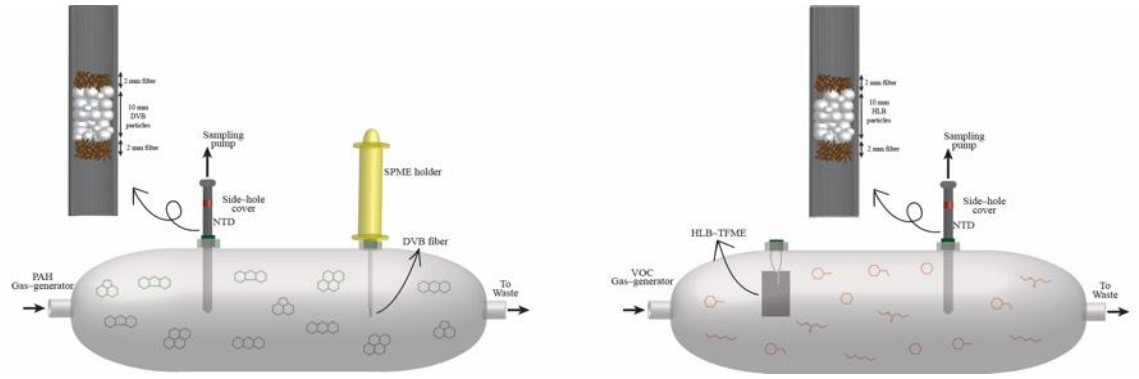

Figure 6-3. Gas sampling bulb for the extraction of PAHs (green) using DVB/SPME and DVB/NTD, also extraction of VOCs (red) using HLB/TFME and HLB/NTD. Each device was used in a different bulb and at different times. The devices are shown together here for simplified visualization.

6.3.5 Gas Mixture Preparation

The gas mixture was prepared by first filling the tubes in a gas generator with pure analytes. In the case of VOCs, the heating chamber temperature was set at 40 ºC and, while it was increased to 150 ºC for PAHs to ensure a constant flow (concentration range of 10-30 ng mL^{-1} for optimization) of the analyte mixture. Next, the gas mixture was transferred to a gas sampling bulb using a carrier gas for extraction. The concentration of the mixture was calculated by constantly monitoring the loss of weight in the analyte tubes and by calculating the permeation rates. To check the stability of the gas system, VOCs and PAHs with different volatilities were extracted via DVB/SPME, and their signal was monitored over a 6-h span.

6.3.6 Study of Filter Performance

The full characterization of the prepared filter has been studied previously. However, for this manuscript, the filtration efficiencies of the needles were studied by using a scanning mobility particle sizer (SMPS) and measuring the particle count before and after inserting the filter-incorporated NTDs into the instrument as filtration efficiency. To make-up for the disparity

between the needle's low flow rate and the relatively higher flow rate required by the SMPS, 6 similarly packed needles were used in parallel.

The extraction/desorption behavior of the prepared filter was assessed by using a filter-incorporated NTD (without sorbent) to extract VOCs from the gas phase. The same needle was also used to trap particles from incense smoke. After trapping, the needle was desorbed multiple times to assess the desorption efficiency and carry-over effect.

6.3.7 Breakthrough Volume (BTV) for NTDs

NTD is an exhaustive method, which means that all of the analytes can be extracted as long as the NTD does not become saturated (i.e., before breakthrough volume (BTV)). After this point, the linearity between signal and the concentration is lost. Therefore, it is important to consider BTV in NTD studies. Since analytes start escaping the needle after the BTV, one way of studying it is to connect two NTDs in a series and monitor the second needle's chromatogram while increasing the sampling volume. The BTV is reached when the analyte peaks start appearing from the desorption of the second NTD (Figure 1-11). In this work, the needle under study was connected to a commercial needle, and the chromatogram from the desorption of second needle was monitored by increasing the sample volume, with the BTV being considered as the volume at which the analyte peaks were detected.

6.3.8 Equilibrium Time for SPME and TFME

TFME and SPME are based on achieving equilibrium between the analytes in the sample matrix and the extraction coating on the device. To find the equilibrium time, the thin-films or SPME fibers were exposed to the sampling gas for progressively longer periods of time (up to 60

minutes). Equilibrium was considered to have been reached when the extraction signal remained constant irrespective of increases to the extraction time.

6.3.9 Absolute Recovery for TFME and SPME

The absolute recovery values for SPME and TFME were evaluated by performing extractions in a gas mixture with a concentration range of 10-20 ng mL^{-1}. Due to different permeation rates, it was not possible to prepare a mixture with the same concentration for all components; however, the exact concentration for each compound in the mixture was known. The absolute recover values were calculated by dividing these extracted amounts by the amounts of compounds in the mixture

6.3.10 Method Validation

To study the reproducibility and repeatability of the method and developed devices, the same experiments were repeated multiple times (minimum n=3) in one day and on multiple days to calculate the inter- and intra-day relative standard deviations (RSDs). Furthermore, the device-to-device RSD was measured by using the 3 extraction devices (thin-film, fiber, or needle) to perform sampling from similar samples (n=3).

For calibration, concentrations of VOCs and PAHs in the gas mixture were altered by changing either the heating chamber temperature or carrier gas flow rate. The limits of detection (LOD) and limits of quantification (LOQ) were reported based on signal-to-noise ratios of 3 and 10, respectively. A wide range of concentrations were studied in determining the linear dynamic range (LDR). To ensure conditions similar to those used in the portable instrument experiments, total ion chromatogram (TIC) mode was used to determine sensitivity; however, the maximum potential sensitivity was also assessed using the benchtop instrument's selected ion monitoring

(SIM) mode to determine the LODs for some of the components. Except the LOD data provided in "method development" section of results and discussion, all other data were obtained in TIC mode.

6.3.11 Green Evaluation

The whiteness and sustainability of three devices studied in this manuscript were compared with EPA method "TO-13A" and CDC method "NIOSH 5515", as the reference standard methods for analysis of air pollutant, using the white analytical chemistry principles [287]. Additionally Analytical Greenness Calculator (AGREE) have been adopted as a tools for greenness measurements [288].

6.3.12 Real Sample Analysis

Different indoor and outdoor environments were chosen for this study. At each sampling site, all extraction devices (HLB/TFME, HLB/NTD, DVB/SPME- fiber, DVB/NTD) were applied in their optimum condition for monitoring possible target compounds. For the parking lot samples, the thin films and fibers were left close to idling cars until equilibrium had been achieved, while NTD sampling was conducted by drawing air into the needle with a pump. For the candle and incense smoke samples, each of these items were lit inside a plexiglass chamber designed to reproduce the conditions of a real room, with sampling being conducted at the height of a simulated breathing zone. The box was also equipped with fan for ventilation. Sampling was conducted by lighting the candles and incense inside the box, and then inserting the extraction devices. For incense, which seemed to produce the highest amounts of particles, a secondary NTD was connected to the primary NTD to assure that the BTV was not reached during the sampling. The

Canadian tobacco regulations routine was applied for the cigarette smoke samples (55 mL puff of 2 s duration, every 30 s) [289], with a pump being used to imitate the inhalation of smoke. As with the candle and incense, a cigarette was artificially smoked inside the box, with the devices being used to analyze the air inside. A schematic of the sampling chamber is provided in Figure 6-4. The inside of the box was covered with aluminum foil, which was changed after each experiment to preclude memory effects from the previous studies. In addition, the box's lid was left open with fan working for 30 minutes after each study to ensure that all particles and components from previous experiments had been completely removed.

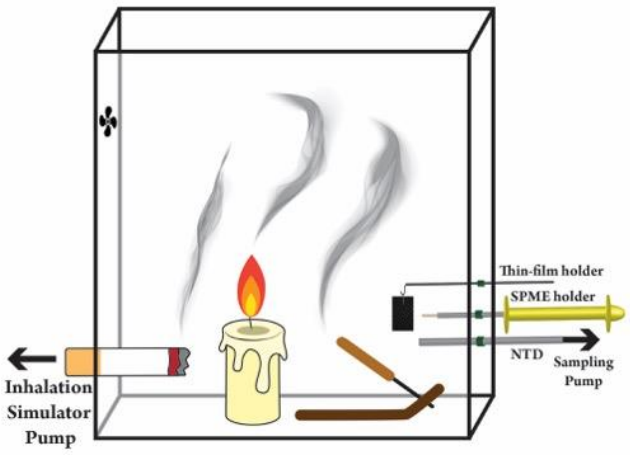

Figure 6-4. Schematic of the plexiglass box sampler used for indoor pollutant studies. The dimensions of the box and objects are not to scale, and each sample was analyzed separately. All sample pollutants are shown together for simplified visualization.

6.4 Results and Discussions

6.4.1 Gas Generation Stability

To check the stability of the gas generator, the gas mixture in the glass bulb was monitored over a 6-h period using DVB/SPME, and the signal stability was reported as the relative signal

(Figure 6-5) The compounds with highest and lowest volatility were chosen to represent all analytes. The findings indicated that the gas mixture was able to provide a stable gaseous composition over a 6-h period (RSD= 1.8-2.9%).

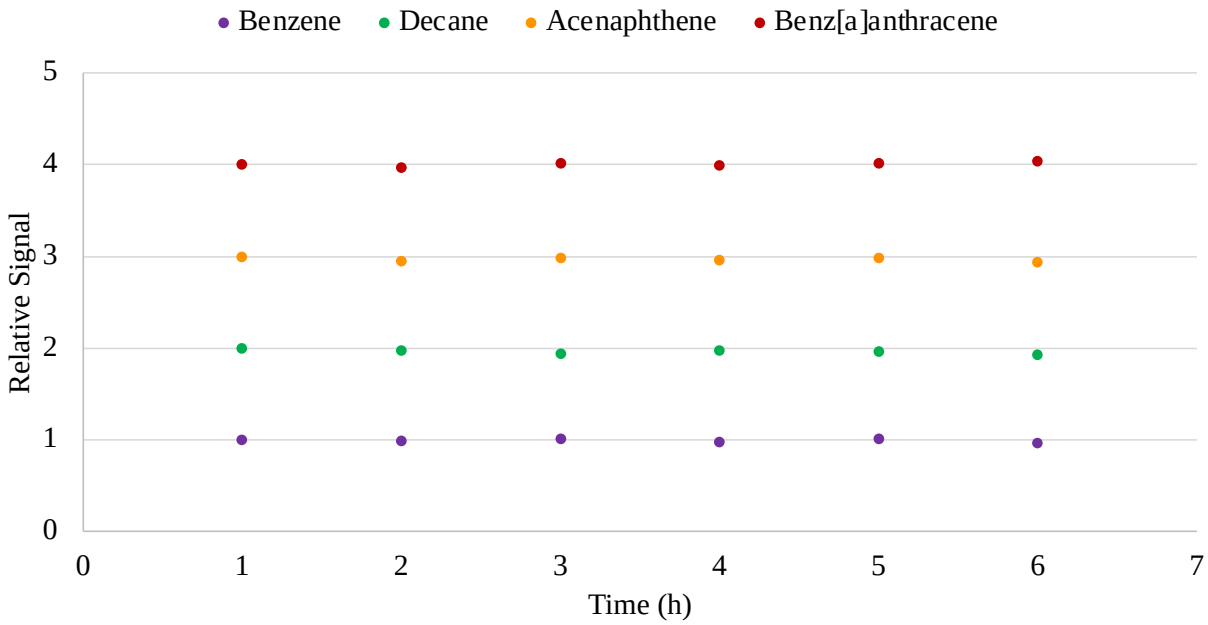

Figure 6-5. Relative signal for VOC and PAH with various volatilities (extracted using DVB/SPME) over 6h.

6.4.2 Investigation of H-PAN Filter Behavior

To provide a device capable of trapping particles in air samples, it was important to ensure that the designed NTDs were able to trap particles efficiently. As can be seen in Figure 6-6, the prepared NTDs provided high trapping efficiency for solid particles in the studied range. Since this size range covers very small particles with minimum filtration efficiency, it can be assumed that the trapping efficiency in air samples can be maintained at this level or higher, as air pollution particles are commonly larger in size.

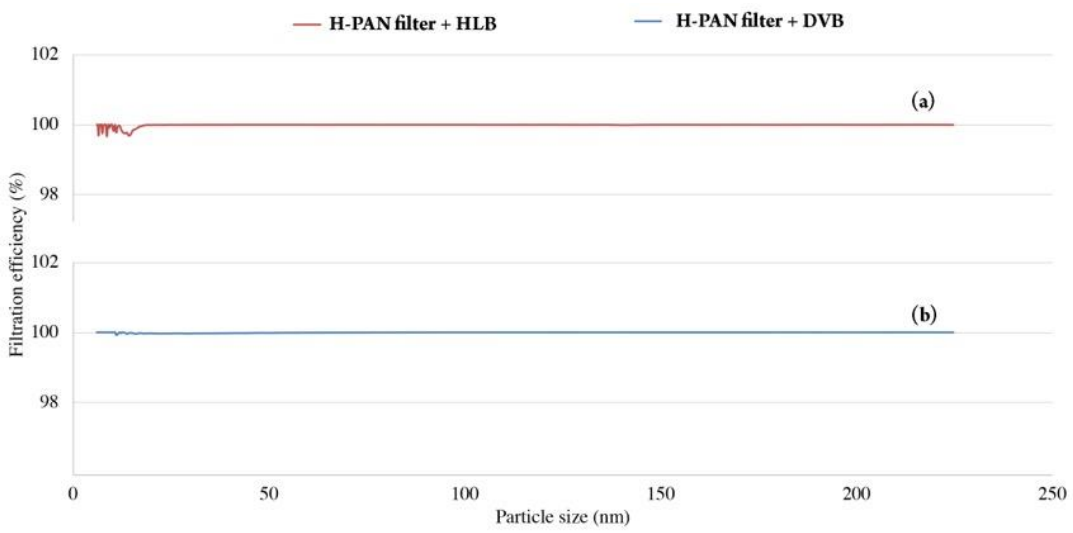

Figure 6-6. Filtration efficiency of needles packed with (a) H-PAN filter and HLB and (b) H-PAN filter and DVB

Next, the filter-packed needles were used to perform extractions from the VOC gaseous mixture and incense smoke to assess the filter's extraction/desorption behaviors. The resultant chromatograms are provided Figure 6-7. As can be seen in Figure 6-7-a, the filter's extraction efficiency with respect to gas analytes is very weak which indicates that it plays a negligible role as an extraction phase for gas components. In addition, the filter's low extraction efficiency with regards to the gas mixture reveals that the peaks from the filter-packed NTD (Figure 6-7-c) are created by the particle phase. Finally, the clean chromatogram for secondary desorption indicates the low carry-over of NTD after efficient desorption (Figure 6-7-b), which guarantees reproducible results.

6.4.3 Breakthrough Volume for NTDs

BTV was studied for VOCs and PAHs using needles packed with H-PAN filter + HLB and H-PAN filter + DVB, respectively. The BTV was considered to have been reached when the peaks of analytes began appearing in the secondary commercial NTD.

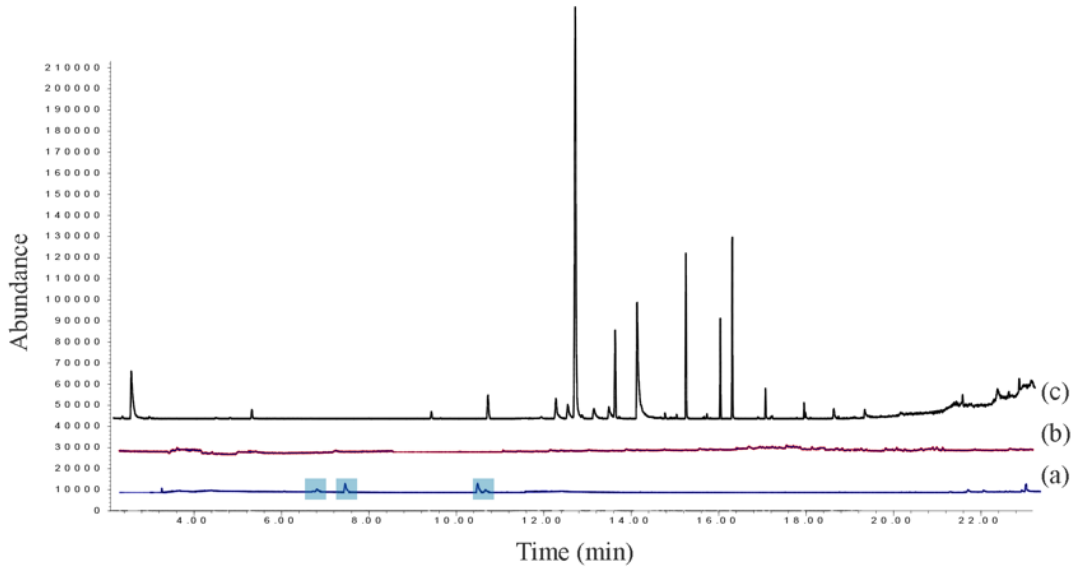

Figure 6-7. Chromatogram of filter-packed NTD (a) after extraction from gas mixture (blue boxes are peaks related to extraction of VOC), (b) from carry over of incense smoke (secondary desorption), (c) after extraction of incense smoke (primary desorption)

The chromatograms from the BTV studies are provided in Figure 6-8 and Figure 6-9. As can be seen, the BTV was reached at around 450 mL for PAH, and around 300 mL for VOC. Based on these results, sampling volumes of 400 and 250 mL were chosen for PAH and VOC, respectively, with a flow rate of 10 mL min^{-1}.

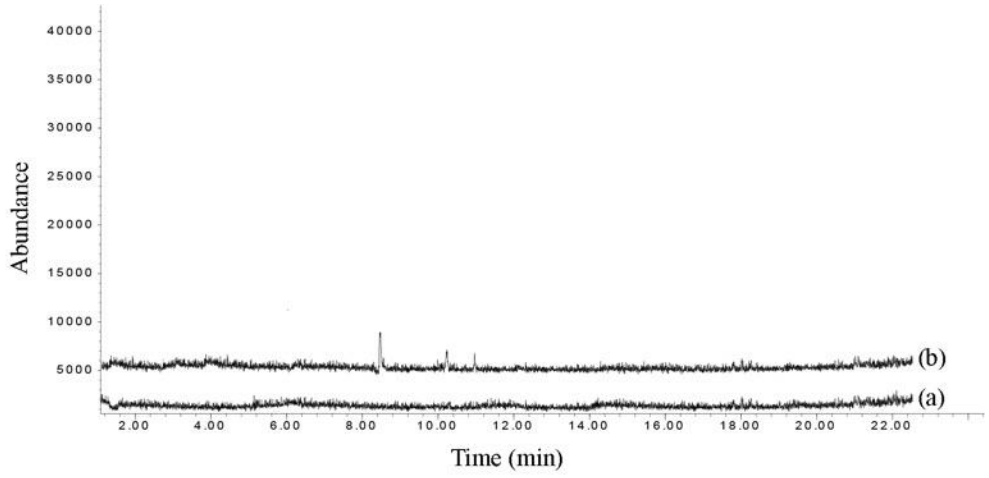

Figure 6-8. Chromatogram from desorption of second commercial NTD after extraction of (a) 400 mL and (b) 450 mL of PAH using DVB/NTD

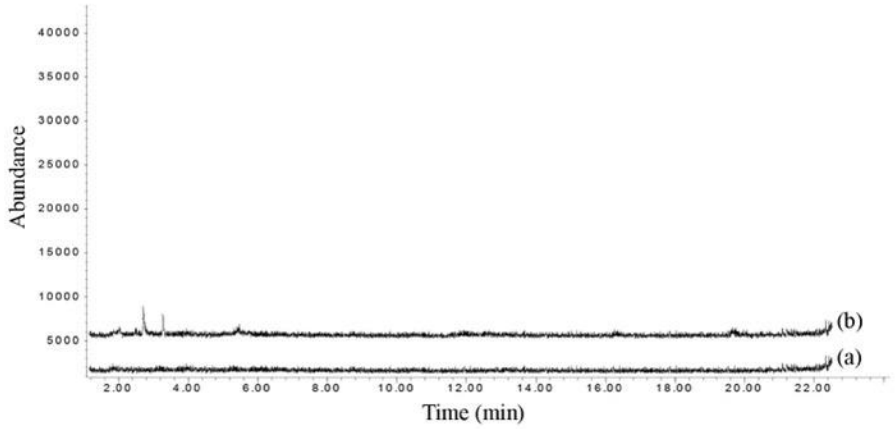

Figure 6-9. Chromatogram from desorption of second commercial NTD after extraction of (a) 250 mL and (b) 300 mL of VOC using HLB/NTD

6.4.4 Equilibrium Time for SPME and TFME

As the equilibrium time data for PAH (Figure 6-10) suggests, equilibrium is achieved rather quickly for some compounds. In the case of VOCs (Figure 6-11), equilibrium was reached in as little as 5 minutes for lighter compounds, while heavier compounds required an equilibrium time of 30 minutes. Based on these results, an extraction time of 45 minutes was chosen for the extraction of PAH via the DVB/SPME-fiber, and 30 minutes was used as the extraction time for VOC using HLB/TFME.

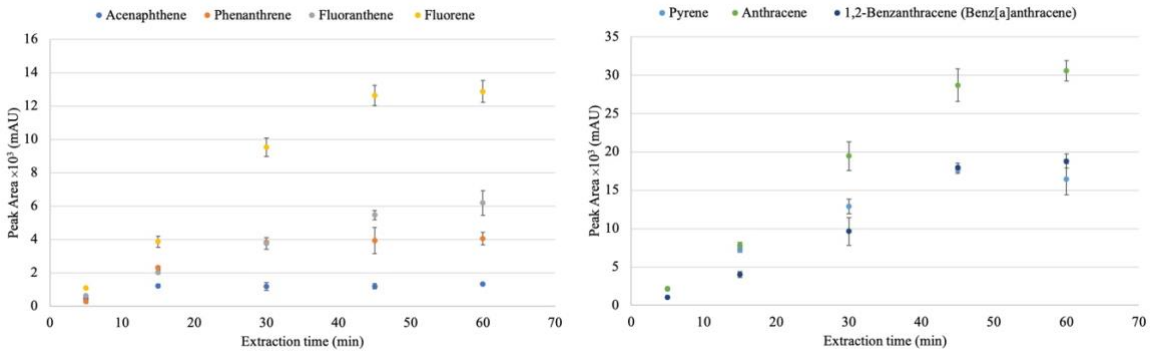

Figure 6-10. Equilibrium time profile for extraction of PAH using DVB/SPME

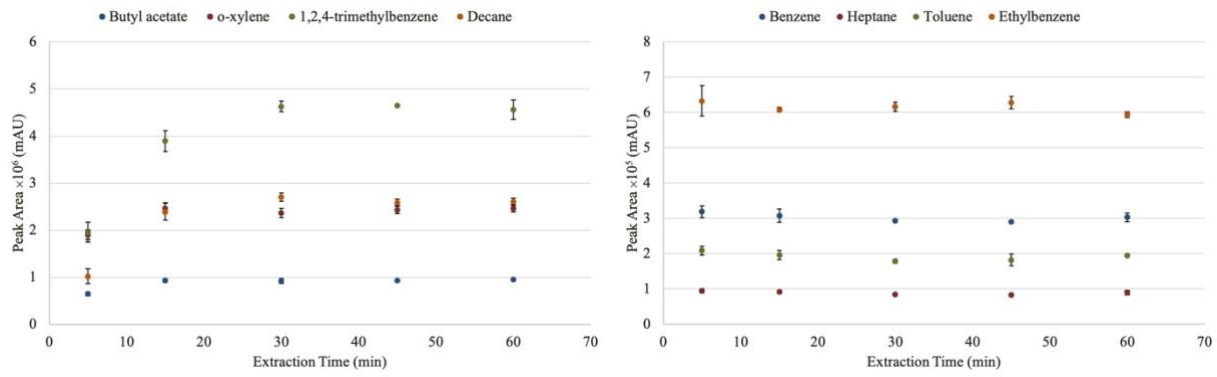

Figure 6-11. Equilibrium time profile for extraction of VOC using HLB/TFME.

6.4.5 Absolute Recovery in Bulb Extraction

Absolute recovery values were calculated for the extraction of VOCs and PAHs with HLB/TFME and the DVB/SPME-fiber, respectively. It should be noted that the NTD is an exhaustive device, which means that it is capable of extracting all of the components in a sample matrix. For this reason, the NTD's absolute recovery values are not reported. As the data in Table 6-3 suggests, TFME generally had higher absolute recovery values compared to the SPME fibers, which can be attributed to the thin-films' relatively higher volume of extraction phase.

Table 6-3. Absolute recovery (AR) percentages for extraction of VOC with HLB/TFME and PAH using DVB/SPME.

DVB/SPME	AR (%)	HLB/TFME	AR (%)	HLB/TFME	AR (%)
Acenaphthene	6.1	Benzene	56.0	Decane	67.3
Phenanthrene	10.1	Heptane	33.6		
Fluoranthene	8.5	Toluene	66.0		
Fluorene	12.8	Butyl acetate	25.4		
Pyrene	16.1	Ethyl benzene	74.7		
Anthracene	19.2	o-xylene	74.0		
Benz[a]anthracene	20.3	1,2,4-TMB	86.9		

6.4.6 Method Development

The repeatability and reproducibility of the proposed methods were assessed by calculating their inter-day, intra-day, and device-to-device RSDs through the repetition of experiments. From the results in Table 6-4, it can be seen that, generally, the RSD values are below 11%, which is appropriate for quantitative analysis. Additionally, the device-to-device RSDs are higher, which was expected as, with the exception of the SPME fibers, all devices used in this work were made manually in the lab.

Table 6-4. Relative standard deviation (RSD) percentages for inter-day, intra-day and device-to-device extraction of VOC using HLB/TFME, HLB/NTD and PAH with DVB/SPME, DVB/NTD.

RSD (%)	Device-to-device		Inter-day		Intra-day	
	HLB/TFME	HLB/NTD	HLB/TFME	HLB/NTD	HLB/TFME	HLB/NTD
Benzene	4.4	6.1	3.0	5.1	1.5	1.2
Heptane	4.1	5.5	3.4	6.3	2.0	4.7
Toluene	3.9	9.2	6.8	6.0	3.0	4.9
Butyl acetate	6.9	5.4	9.5	5.6	6.1	2.2
Ethylbenzene	5.1	8.9	6.5	6.8	2.0	2.7
o-xylene	4.2	9.2	3.4	5.4	4.2	3.2
1,2,4-TMB	5.3	5.0	6.3	10.9	2.5	0.3
Decane	7.0	7.9	4.2	15.3	3.3	6.6
	DVB/ SPME	DVB/NTD	DVB/SPME	DVB/NTD	DVB/SPME	DVB/NTD
Acenaphthene	3.4	2.0	2.1	3.1	2.4	2.9
Fluorene	4.3	7.9	2.1	8.4	3.8	2.9
Phenanthrene	7.3	6.9	2.6	6.3	5.0	3.7
Anthracene	8.3	7.2	8.5	5.9	3.8	0.2
Fluoranthene	7.5	9.1	2.8	3.6	4.2	9.7
Pyrene	6.3	8.4	1.6	5.8	3.6	4.6
Benz[a]anthracene	4.2	6.8	1.2	8.7	2.6	3.1

The extraction devices (DVB/SPME-fiber, DVB/NTD, HLB/TFME, and HLB/NTD) were calibrated by varying the concentration of components and then analyzed using both benchtop and portable GC-MS in TIC mode. Detailed data relating to method development are provided in Table 6-5. For PAHs, a LOD range of 0.10 to 0.35 ng mL^{-1} was obtained with the benchtop instrument, while the range obtained with the portable GC/MS was 0.17 to 0.65 ng mL^{-1}. Similarly, an LOD range of 0.07-0.8 ng mL^{-1} was obtained for VOCs on the benchtop GC/MS, while an LOD range of 0.2-0.75 ng mL^{-1} was obtained with the portable instrument. To further improve sensitivity, LOD values for 4 compounds of interest were also calculated in SIM mode (with NTD/benchtop GC/MS). The results of this analysis were as follows: with DVB/NTD-benchtop GC/MS—phenanthrene = 0.02 ng mL^{-1}, benz[a]anthracene = 0.02 ng mL^{-1}; with HLB/NTD- benchtop GC/MS—o-xylene = 0.01 ng mL^{-1} and 1,2,4-TMB = 0.02 ng mL^{-1}.

As the data suggests, the developed methods have acceptable sensitivity in TIC mode compared to previous studies. Furthermore, these detection limits cover the maximum residual limit of these compounds set by the EPA (0.2 mg m^{-3} for PAHs in air, and less than 0.20 mg m^{-3} for Total Volatile Organic Compounds) and Health Canada (similar with some specific regulations for hazardous compounds: Ethylbenzene = 2000 μg m^{-3}, Xylenes = 100 μg m^{-3}, benzene = as low as possible, toluene = long-term exposure limit (24 hours): 2.3 mg m^{-3}, short-term exposure limit (8 hours): 15 mg m^{-3} for indoor air.

Table 6-5. LOD, LOQ and LDR ranges for extraction of VOC using HLB/TFME, HLB/NTD and PAH with DVB/SPME, DVB/NTD in full scan mode

	LOD (ng mL^{-1})				LOQ (ng mL^{-1})				LDR (ng mL^{-1})			
	Benchtop		Portable		Benchtop		Portable		Benchtop		Portable	
	DVB/SPME	DVB/NTD	DVB/SPME	DVB/NTD	DVB/SPME	DVB/NTD	DVB/SPME	DVB/NTD	DVB/SPME	DVB/NTD	DVB/SPME	DVB/NTD

Acenaphthene	0.35	0.20	0.65	0.37	1.17	0.67	2.17	1.23	1.5–415	1–415	2.2–415	1.5–415
Fluorene	0.25	0.12	0.5	0.24	0.83	0.4	1.67	0.80	1–423	0.5–423	1.7–423	1–423
Phenanthrene	0.16	0.10	0.47	0.29	0.53	0.33	1.57	0.97	0.5–378	0.4–378	1.5–378	1–378
Anthracene	0.24	0.20	0.35	0.29	0.80	0.67	1.17	0.97	1–489	0.7–489	1.2–489	1–489
Fluoranthene	0.35	0.25	0.58	0.41	1.17	0.83	1.93	1.37	1.2–392	0.9–392	2–392	1.4–392
Pyrene	0.27	0.10	0.45	0.17	0.90	0.33	1.50	0.57	1–482	0.4–482	1.5–482	0.6–482
Benz[a]anthracene	0.16	0.10	0.55	0.34	0.53	0.33	1.83	1.13	0.6–514	0.4–514	2–514	1.5–514
	LOD (ng mL^{-1})				LOQ (ng mL^{-1})				LDR (ng mL^{-1})			
	Benchtop		Portable		Benchtop		Portable		Benchtop		Portable	
	HLB/TFME	HLB/NTD	HLB/TFME	HLB/NTD	HLB/TFME	HLB/NTD	HLB/TFME	HLB/NTD	HLB/TFME	HLB/NTD	HLB/TFME	HLB/NTD
Benzene	0.25	0.10	0.75	0.30	0.80	0.33	2.5	1.00	0.9–673	0.4–673	2.5–673	1–673
Heptane	0.45	0.15	0.60	0.20	1.50	0.5	2.00	0.67	1.5–714	0.5–714	2–714	0.7–714
Toluene	0.15	0.08	0.30	0.16	0.50	0.27	1.00	0.53	0.5–693	0.3–693	1–693	0.6–693
Butyl acetate	0.80	0.20	0.90	0.23	2.70	0.67	3.00	0.77	2.7–573	0.7–573	3–573	0.8–573
Ethyl benzene	0.15	0.09	0.45	0.27	0.50	0.30	1.50	0.90	0.5–615	0.3–615	1.5–615	1–615
o-xylene	0.10	0.08	0.30	0.24	0.33	0.27	1.00	0.80	0.4–658	0.3–658	01–658	0.8–658
1,2,4-TMB	0.10	0.07	0.40	0.28	0.33	0.23	1.33	0.93	0.4–748	0.3–748	1–748	1–748
Decane	0.10	0.08	0.45	0.36	0.33	0.27	1.50	1.20	0.4–651	0.3–651	1.5–651	1.5–651

6.4.7 Green Evaluation

Based on the importance and growing demand for air monitoring, it was important to study the sustainability of the developed methods in this study. To this end, the concepts of white analytical chemistry [287] and analytical greenness metric [288] were applied to evaluate the sustainability of the developed methods. Since all methods used GC/MS for separation and quantification, only sample preparation section was considered for this comparison.

The results for white analytical chemistry are provided in Figure 6-12 and Figure 6-13. The red principles are related to analytical performance, green principles are related to the greenness

and environmental friendliness, while blue principles consider practical aspects. The white chart is the average score of the methods.

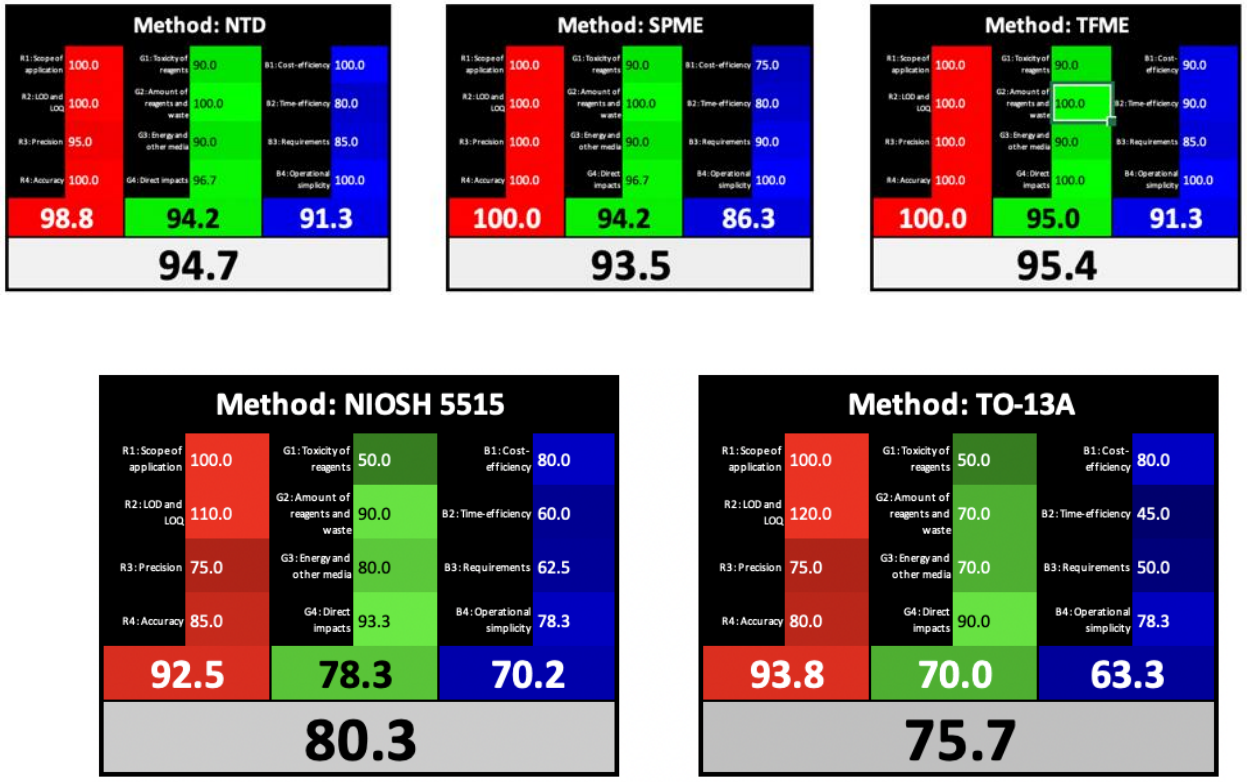

Figure 6-12. Whiteness of the three developed methods and two standard methods

As can be seen, considering the environmental friendliness, analytical performance and practical issues, the developed methods (TFME, SPME and NTD) are greener compared to EPA and CDC approved methods (TO-13A[290] and NIOSH 5515[286]) for analysis of air pollutants. The average score for each method is as follows: NTD = 94.7, SPME = 93.5, TFME = 95.4, NIOSH 5515 = 80.3, TO-13A = 75.7 .

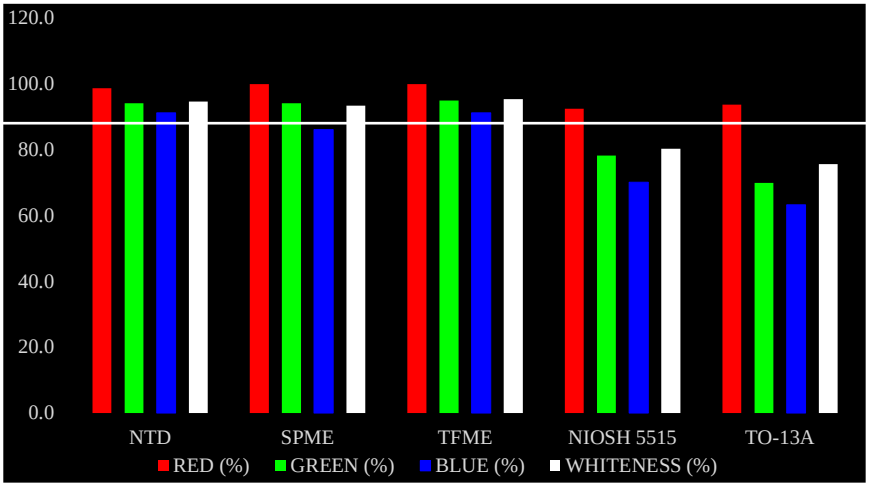

Figure 6-13 . Comparison of the developed methods and 2 standard methods for air monitoring obtained from the RGB 12 analysis, the white line indicates 100%.

As a second criterion, AGREE software was used calculate the score of these methods. Considering the similarity of the extraction process for TFME, SPME and NTD, only one chart is provided to represent the greenness of all three methods. The detailed and final score are provided in Figure 6-15 and Figure 6-14. As the chart shows, the microextraction methods (SPME, TFME, NTD) developed in this study have a high value of 0.64 (scale is 0.0-1.0). This data shows the highly environmentally friendly nature of these devices.

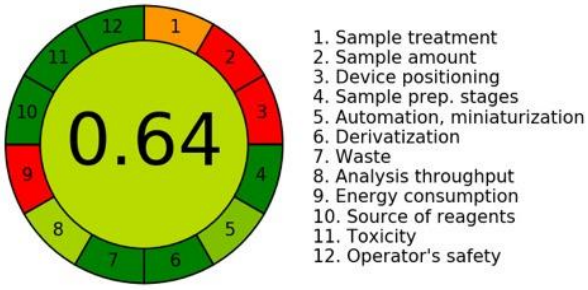

Figure 6-14.Obtained values for SPME, NTD and TFME according to the 12 principles of GAC, performed using the AGREE algorithm.

Criteria	Score	Weight
1. Direct analytical techniques should be applied to avoid sample treatment.	0.3	2
2. Minimal sample size and minimal number of samples are goals.	0	2
3. If possible, measurements should be performed in situ.	0.0	2
4. Integration of analytical processes and operations saves energy and reduces the use of reagents.	1.0	2
5. Automated and miniaturized methods should be selected.	0.75	2
6. Derivatization should be avoided.	1.0	2
7. Generation of a large volume of analytical waste should be avoided, and proper management of analytical waste should be provided.	1.0	2
8. Multi-analyte or multi-parameter methods are preferred versus methods using one analyte at a time.	0.68	2
9. The use of energy should be minimized.	0.0	2
10. Reagents obtained from renewable sources should be preferred.	1.0	2
11. Toxic reagents should be eliminated or replaced.	1.0	2
12. Operator's safety should be increased.	1.0	2

Figure 6-15. Details of the values for greenness of microextraction methods (SPME, TFME and NTD) in this study

6.4.8 Analysis of PAHs and VOCs in indoor and outdoor environments

Several realistic indoor and outdoor environments were chosen to study the developed method's applicability for determining air pollutants in real-world conditions. To this end, air samples were collected from a university parking lot near some idling vehicles and a carport (parking with roof, without walls) spot to investigate outdoor conditions, while a large box outfitted with sampling spots resembling a breathing zone was used to simulate indoor conditions. Mosquito repellent was sprayed, and a cigarette, a candle, and incense were lit inside the box (not

all at the same time), and the air in the box was subsequently analyzed with the fan in on or off mode via benchtop or portable GC/MS.

The results of these studies are provided in Table 6-6. Generally, the concentrations of pollutants in the outdoor samples were lower than those observed in the indoor samples. A comparison of the results obtained with the NTD, TFME, and SPME showed that the devices captured very similar concentrations, particularly in relation to small-molecule VOCs. However, the results also indicated that the NTD captured higher concentrations of larger compounds and PAHs, which was likely due to its particle trapping ability. The designed NTD can measure the combined gaseous and particle-bound concentrations in a sample, as it is packed with both a filter and extraction phase. Conversely, the data for the SPME and TFME extractions only reflects the gas-phase portion of the air pollutants.

In addition to the target compounds reported in Table 6-6, other compounds were also detected and identified using MS. These compounds include: isopropyl benzene, 5-methylhexanophenone, acetophenone, and para-alpha-dimethyl styrene (parking lot); pinane, beta-myrcene, menthol and derivatives, limonene, eucalyptol, meta-divinylbenzene, and para-ethyl styrene (mosquito repellant and candle smoke); pyridine, furfural derivatives, squalene, annulene, phenol, and nicotine (cigarette smoke); limonene, p-ethylstyrene, linalool, m-divinylbenzene, benzyl acetate, beta-ionane, linalool formate, hexyl cinnamaldehyde, benzyl benzoate, and benzyl salicylate (wood-scented candle); m-methyl styrene, furfural, m-cymene, limonene, carvone, 1,3-dimethyl naphthalene, and 1,3,5-trimethylnaphthalene (wooden stick incense smoke); and benzofuran, o-cresol, diethyl phthalate, benzyl benzoate, 3,5-xylenol, and isoeugenol (waterfall incense smoke).

Table 6-6. Concentration of air pollutants obtained with extraction devices in the optimum conditions. Values are expressed in ng mL^{-1} ± standard deviation (ND = not detected, < LOQ = below limit of detection).

Color guide	HLB/TFME	HLB/NTD	DVB/SPME	DVB/NTD

Cigarette Smoke	Fan-off				Fan-on			
	Benchtop		Portable		Benchtop		Portable	
Benzene	18.3 ± 1.3	17.8 ± 0.9	19.2 ± 1.5	18.7 ± 2.1	1.4 ± 0.1	1.4 ± 0.1	ND	1.8 ± 0.1
Ethyl benzene	5.2 ± 0.6	7.7 ± 0.8	4.9 ± 0.7	8.1 ± 0.7	ND	ND	ND	ND
o-Xylene	39 ± 1.3	45.2 ± 2.1	37.3 ± 0.9	47.4 ± 2.7	5.5 ± 0.4	9.4 ± 1.4	6.1 ± 0.5	8.9 ± 1.4
Phenanthrene	24.3 ± 1.6	41 ± 2.4	25.4 ± 1.9	43.6 ± 3.2	3.2 ± 0.4	4.7 ± 0.4	3.3 ± 0.8	5.1 ± 0.8
Benz[a]anthracene	1.3 ± 0.1	6.4 ± 0.4	< LOQ	7.1 ± 0.8	ND	0.5 ± 0.1	ND	< LOQ

Mosquito repellant candle	Fan-off				Fan-on			
	Benchtop		Portable		Benchtop		Portable	
Benzene	4.31 ± 0.3	5.1 ± 0.5	4.5 ± 0.4	5.3 ± 0.4	ND	ND	ND	ND
Ethyl benzene	10.4 ± 0.7	12.3 ± 1.3	11.3 ± 1.4	11.3 ± 1.4	0.3 ± 0.1	0.4 ± 0.1	ND	ND
Pyrene	8.4 ± 0.4	14.3 ± 1.3	9.1 ± 0.5	15.4 ± 1.7	ND	1.4 ± 0.3	ND	1.5 ± 0.4

Wooden stick incense	Fan-off				Fan-on			
	Benchtop		Portable		Benchtop		Portable	
Toluene	45.3 ± 1.4	53.3 ± 1.7	43.3 ± 2.6	55.5 ± 3.2	3.2 ± 0.2	4.7 ± 0.7	4.2 ± 0.7	5.3 ± 1.6
o-Xylene	12.5 ± 2.7	13.3 ± 1.6	11.6 ± 1.7	14.4 ± 1.0	ND	ND	ND	ND
Fluorene	2.6 ± 0.7	4.4 ± 0.3	2.8 ± 0.4	4.8 ± 0.7	ND	ND	ND	ND
Anthracene	21.5 ± 1.7	36.5 ± 3.7	20.8 ± 0.8	38.5 ± 1.7	ND	1.78 ± 0.06	ND	< LOQ

Candle with wood smell	Fan-off				Fan-on			
	Benchtop		Portable		Benchtop		Portable	
Benzene	32.7 ± 1.8	35.4 ± 2.4	31.5 ± 1.5	33.9 ± 3.2	10.5 ± 3.2	9.5 ± 1.2	9.5 ± 1.8	11.4 ± 1.7

Waterfall incense	Fan-off				Fan-on			
	Benchtop		Portable		Benchtop		Portable	
Benzene	9.3 ± 0.4	8.9 ± 0.3	10.4 ± 1.2	9.4 ± 0.7	ND	ND	ND	ND
Toluene	19.3 ± 1.6	23.6 ± 1.9	18.4 ± 2.4	24.4 ± 3.2	1.3 ± 0.78	1.6 ± 0.6	Below LOQ	1.1 ± 0.2
1,2,4-TMB	38.3 ± 3.2	39.7 ± 1.8	37.6 ± 2.7	41.3 ± 2.5	2.4 ± 0.7	4.4 ± 0.4	3.1 ± 0.8	4.8 ± 0.6
Fluoranthene	3.2 ± 0.6	5.5 ± 0.8	2.8 ± 0.7	6.4 ± 1.7	ND	1.3 ± 0.13	ND	Below LOQ
Pyrene	8.3 ± 0.7	14.4 ± 1.5	9.2 ± 1.3	15.3 ± 3.2	ND	2.6 ± 0.5	ND	1.97 ± 0.64

Parking lot/ running cars	Benchtop		Portable	
Benzene	1.3 ± 0.2	2.4 ± 0.3	ND	ND
Toluene	0.7 ± 0.1	0.8 ± 0.5	ND	ND
1,2,4-TMB	15.5 ± 1.2	18.4 ± 0.89	16.2 ± 1.6	19.4 ± 1.4
Anthracene	1.7 ± 0.2	3.2 ± 0.12	1.9 ± 0.5	3.1 ± 0.4
Pyrene	4.3 ± 0.1	8.6 ± 0.4	3.9 ± 0.3	8.1 ± 0.8

Parking lot/ ramada	Portable	
Toluene	ND	0.5 ± 0.1
Benz[a]anthracene	ND	1.6 ± 0.2

Most of the compounds were detected and identified with both the NTD and SPME-based method, but some heavy compounds such as 1,3,5-trimethylnaphthalene, squalene and annulene were only identified with NTD. As such, it can be concluded that these components are only present in the particle-phase.

Next, tests were conducted to assess the role of the fan in the sampling process. As predicted, the concentration of air pollutants was generally higher when the fan was turned off. For some of the samples, the ratio of gaseous to particle-bound particles ($\frac{C_{SPME\ or\ TFME}}{C_{NTD}-C_{SPME\ or\ TFME}}$) remained similar in the fan-on and fan-off conditions; however, this ratio changed for other samples. This phenomenon can be attributed to the different rate of removal or settlement of particles/gases in various samples. Generally, these data reveal the importance of proper ventilation for indoor air quality.

The secondary commercial NTD was examined after sampling the smoke from the two types of incense, with none of the VOCs or PAHs under study being found after the desorption of the secondary NTD. The application of the secondary needle demonstrated that breakthrough did not occur for the compounds under study, which enabled the proper quantification of VOCs and PAHs during the study.

During previous applications of filter-incorporated NTDs, the device could be re-used multiple times when the aerosol sample includes liquid droplets. In this study, however, the flow rate of the NTD began to decrease after multiple extractions from dirty samples with large particles, such as incense smoke. This issue can be attributed to the different fate of droplets and particles during desorption, as liquid droplets trapped in the filter can be vaporized during the thermal desorption. However, the associated peak cannot be observed in the chromatogram, as

water and alcoholic solvents are lost during solvent delay at the beginning of the chromatogram. This vaporization means the filter can being completely cleaned after each desorption. This process will not occur for solid soot particles, as they are not volatile. Thus, the introduction of large amounts of micron-sized particles into the filter can lead to blockage after a few experiments, depending on the number and size of particles in the sample. In this study, a minimum of 3 replicate experiments were performed with the NTD for the dirty waterfall incense smoke. It can be suggested that, since 200 mg of electrospun PAN filter can be used to prepare up to 20 needles, multiple needles should be prepared for studies dealing with dirty smoke, and a new needle should be used for each experiment. It should also be noted that, for standard methods such as NIOSH 5515, filters are to be disposed of after each use.

6.4.9 Benchtop vs. Portable GC/MS

One important aspect of this study was the comparison between benchtop and portable GC/MS. As the method development data suggest (Table 6-5), the detection limits obtained with the portable GC/MS were similar to or higher than those obtained with the benchtop GC/MS. Generally, these detection limits are acceptable for a portable instrument. Furthermore, the portable GC/MS's short desorption (a few seconds) and separation times (3 min) can reduce the total analysis time substantially. In addition, the larger injection port on the portable GC/MC means that larger needles can be used for NTD and SPME, which enables better sensitivity due to the higher capacities associated with these needles. Moreover, the portable GC/MS allows the same injection system to be used for SPME, TFME, and NTD. The use of the same injection system for all extraction devices means that the instruments are less costly, easy to use, and appropriate for on-site sampling. The portable GC/MS was not designed specifically to accommodate the home-made

NTD and do not have exact equivalent of narrow neck liner in benchtop instruments, which can result in less efficient desorption and carry-over effects with home-made NTDs, especially for heavy compounds and samples with higher concentrations. For the desorption of TFME, a separate thermal desorption instrument should be available for on-site sampling, and a 5-minute desorption step should be added to the analysis time. While the portable GC/MS has some disadvantages compared to its benchtop counterpart, its ability to provide short analysis times, acceptable sensitivity, and reliable data makes it a good choice for on-site sampling, specifically, when the sample is unstable, can be lost during the transport, or there is need for immediate results.

6.5 Conclusion

In this study, a NTD packed with sorbent particles and an H-PAN filter was introduced as an alternative method for the simultaneous determination of free and particle-bound air pollutants. SPME and TFME devices were applied to extract only the free concentration of compounds in the studied samples in order to distinguish the differences between the free and particle-bound portions. The results showed that the developed methods were reliable, reproducible, and sensitive for the determination of PAHs and VOCs in air samples. The findings of the tests in outdoor environments, such as a parking lot, revealed that the developed methods can be applied in real-life situations. While the tested devices were able to provide high sensitivity compared to conventional or standard methods [286] the use selected ion monitoring (SIM) mode for GC/MS enhanced the sensitivity even further. Additionally, the sensitivity of the developed method could be further improved by increasing the packing length of the NTD, or by using larger devices in the case of TFME and SPME. The results of the analyses of air samples containing car exhaust, mosquito repellent, and candle, incense, and cigarette smoke all revealed the potential of filter-

packed NTD for the determination of free and particle-bound components in real-life contexts. Furthermore, the comparison of the developed methods showed capable of revealing the concentrations of gaseous and particle-bound portion of the compounds. The experiments were repeated with portable GC/MS, with results proving that portable GC/MS is able to provide reproducible and sensitive on-site sampling with short total analysis times. The portable GC/MS results also revealed that the filter-incorporated NTD is a green, solventless, small, convenient, fast, cheap, and reproducible alternative to conventional methods for determining particle-bound PAHs that provides higher sensitivity compared to NIOSH 5515. Ultimately, the devices and method described in this work can be applied for the rapid on-site investigation of smoke associated with fires, vehicle emissions, smog, and sources of indoor pollution.

The developed methods could successfully determine the concentration of air pollutants and their environmentally friendly nature was presented with principles of white analytical chemistry and AGREE algorithm. This research opens up numerous avenues for future study. For instance, future research may examine whether packing the developed filter into a separate needle and connecting it to a commercially available NTD in series can enable the comprehensive study of airborne compounds. The use of a secondary needle packed with sorbent in real-life sampling contexts is highly recommended, as it can assure proper quantification and the absence of breakthrough during the sampling procedure

Concluding Remarks and Future Trends

7.1.1 Challenges

The previous chapters have detailed the advantages of NTDs, their potential areas of application, and the required characteristics for an appropriate packing material. In this section, we discuss an overview of the challenges associated with these devices.

The packing procedure in NTD has always been challenging and requires some level of expertise for reproducible results. The choice of the type, diameter, and length of packing material are all critical factors that should be carefully considered. In this regard, data from previous studies can be used. One main issue in needle-trap extractions is to ensure that the BTV is not reached, as this will negatively impact the accuracy of quantification studies.

The most important element in the design of a filter-incorporated NTD is the filter capacity. Given the limitations in flow resistance and the small size of the needle, it is important to ensure that the packing length of the filter is as small as possible. However, decreasing the packing length diminishes the filter surface area, which results in limited filter capacity. The mechanism by which particles are filtered is similar to exhaustive samplers; that is, almost all of the particles are trapped by the filter until it reaches full capacity, after which point the particles begin to pass through. For exhaustive studies, it is important to ensure that the filter does not reach its full capacity during sampling. This issue is particularly critical for filters packed inside NTDs, as they are small in size and therefore do not have a large total capacity. The filter capacity depends on the size and number of particles in a sample. Filter capacity can be studied by monitoring filtration efficiency and pressure drop while continuously introducing particles into the filter bed. The filter is considered

to have reached its full capacity when the pressure drop starts to increase, or when the filtration efficiency starts to decrease.

Another critical consideration relating to filter-incorporated NTDs is the possibility of needle clogging during sampling. Such blockages are generally due to one of two phenomena, depending on the type of aerosol under study. First, filters can become wet and lose their porous structure when they are used to trap particularly large quantities of droplets (e.g., fog, spray samples, sparkling beverages, etc.), which can result in needle blockage due to decreased permeability. Second, in applications wherein NTDs are used to trap solid particles (e.g., air pollution, car exhaust, etc.), filter clogging may occur due to large particles or the accumulation of a large number of particles after multiple extractions. Whereas trapped liquid droplets can be vaporized and removed during desorption—leaving the needle completely clean and ready for subsequent extractions—solid particles can remain trapped inside the needle after desorption, leading to blockage. These issues can be mitigated by decreasing the sampling volume to avoid the accumulation of particles/droplets in the filter, or by disposing of the needles after each extraction to prevent the effects of carry-over and blockage.

7.1.2 Summary and conclusion

NTDs are robust, green, and fast sampling devices that are ideal for on-site sampling due to their simple calibration and their ability to eliminate analyte loss during storage. Furthermore, NTDs are flexible, as their capacity and selectivity can be optimized by changing the packing type, packing length, and sampling volume. The active sampling mode and the packed design of NTDs are also suitable for trapping particle- and droplet-bound compounds, followed by desorption and analysis.

Prior studies wherein NTDs were applied to aerosol samples revealed that NTDs packed with sorbent particles alone have low filtration efficiency, but that this can be enhanced by packing the device with an appropriate filter. A suitable filter for use in an NTD should provide:

(1) high filtration capacity; (2) predictable adsorption behavior; (3) no interference between adsorption and filtering; (4) high permeability; (5) thermal and mechanical stability; (6) repeatability and reproducibility; and (7) inertness towards the sample matrix. Fibrous filters are among the best options, as they possess most, if not all, of these characteristics.

Study of fragrances in spray samples revealed that these compounds can be present in gas or droplet-phase, depending on their characteristics. While most studies only consider that gas-phase concentration of fragrances during application, resulting in underestimation of inhaled fragrances. The fragrance compounds are generally considered as harmless; however, this study showed that the real exposure amount of these compounds can be much more than previously thought.

The studies from sparkling beverages and a comparison between gas and droplet-phase aroma components showed that the initial sense of freshness after bottle opening can be a combination of gas-phase and droplet-bound components. It can be a leading study for food chemist, opening a new way of looking at carbonated beverages and possible methods for improvement of the quality and safety of soft drinks.

Among others, the study of breath sample was perhaps the most crucial one. It was known that polar and less-volatile compounds prefer to remain inside the breath droplets, however, separate methods are usually used for study of gas and droplet phase. The proposed methods in this thesis provided a combined method capable of providing a comprehensive overview of the

sample in both phases. The results obtained from breath samples with masks demonstrated previous claims about the entrapment of aerosol droplets with the designed NTD. Both endogenous and exogenous compounds in breath were studied. In addition, the effect of daily household air pollutants such as candle and sprays verified that the exposure to indoor air pollutants can introduce chemicals into human body which can accumulate and cause health issues over time.

For air pollution studies, the proposed NTD device can combine and replace NIOSH 5515 and NIOSH 2549 into one device. This alternative method, unlike standard methods, is solvent-less, portable and fast. The study of air pollution particles showed that analyzing particle-bound components is very critical in air monitoring, especially for heavy and non-volatile compounds as in some cases a large portion of the compound can be detected only in particle-phase. The application of the developed devices enabled the on-site analysis and distinguishing of free and particle-phase components.

A properly designed NTD can be applied to analyze droplet-bound compounds in aerosol samples including, but not limited to breath, air pollution, and sprays. It has been shown previously that droplets/particles in aerosol samples can carry various chemical species, which can be trapped and studied via NTDs.

To date, NTDs have been successfully applied for the study of volatile and semi-volatile compounds. We believe the new generation of NTDs—namely, needles packed with a filter and sorbent—can enable a new range of applications dealing with polar and non-volatile components that may be bound to droplets or particles. Future works could examine the viability of different types of filters with higher capacities, improved desorption efficiency, and greater permeability. In addition, future works could explore new filter-packed needle designs. These new needles could

be applied separately to trap droplets/particles, or they could be connected in series to a commercially available NTD for the comprehensive investigation of aerosols. The desorption of each of these needles would provide valuable information about the matrix under study. The advantage of a needle packed only with a filter is lower pressure drop and the possibility of being combined with commercially available NTDs.

While this thesis has focused on small needle-packed extraction devices, it is possible to use larger tubes for the extraction and entrapment of compounds and droplets/particles. The commercial version of sorbent traps or sorbent tubes has facilitated the study of VOCs in air samples, and a filter-packed thermal desorption unit (TDU) tube can be introduced for the capture and analysis of droplets from sparkling beverages. Larger tube sizes are more conducive to packing and sampling; however, thermal desorption can be problematic due to the requirement of an external injection system for GC instruments.

7.1.3 Future studies

This thesis was focused on fibrous aerogel air filter as the packing material for NTD, however, other filter types can be studied in future. It is possible to investigate all of these aspects and alter the whole preparation procedure to get better filtration efficiency or pressure drop. The whole preparation steps can be changed and other configurations can be deployed for obtaining high efficiency filters. The initial polymer material and experiment conditions can be changed.

As mentioned in previous section, the capacity and the clogging of the needle can be an issue when dirty samples are under study. To solve this issue, creative designs can be introduced to increase capacity or sampling volume without clogging, which can result in improved sensitivity.

From the needle design aspect, changing the packing length, both for filter and extraction phase can be studied. While the variation in filter packing length has been investigated here, the effect of changing packing length of sorbent, filter or both can be studied. For routine applications, a needle only packed with filter can be designed. This needle can be applied for trapping particles from aerosol samples, or it can be connected in a series to another commercially packed needle with sorbent. The desorption from each of these needles can provide some valuable information. The advantage of a needle only packed with filter is lower pressure drop and possibility of combination with commercially available needles. One potential development can be the design of time-weighted averaging devices in the format of diffusive pens for averaged exposure concentration to pollutant concentrations. The developed design and the diffusive pen can be used for on-site sampling. The coupling to portable instruments can provide the chance of fully on-site analysis, otherwise, the NTD can be applied for on-site analysis and brought back to lab for desorption and analysis.

With respect to samples and analytes, future work could apply NTDs to study other samples such as fire smoke, fog, mist, and air humidifiers, as well as other possible conditions for samples that have already been studied. For instance, the effect of food, dermal exposure, working environment, and long-term exposure to chemicals on exhaled breath aerosol could be investigated. In the case of air pollution, the effects of particle size and sampling sites, such as factories, could be explored.

Further work involving NTDs should aim to expand these initial applications into fully developed future standard methods and, hopefully, push the limits of what is possible for aerosol analysis.

Letters of Copyright Permissions

Chapter 1

The evolution of needle-trap devices with focus on aerosol investigations

Author: Shakiba Zeinali,Mehrdad Khalilzadeh,Janusz Pawliszyn
Publication: TrAC Trends in Analytical Chemistry
Publisher: Elsevier
Date: August 2022

© 2022 Elsevier B.V. All rights reserved.

Journal Author Rights

Please note that, as the author of this Elsevier article, you retain the right to include it in a thesis or dissertation, provided it is not published commercially. Permission is not required, but please ensure that you reference the journal as the original source. For more information on this and on your other retained rights, please visit: https://www.elsevier.com/about/our-business/policies/copyright#Author-rights

BACK CLOSE WINDOW

Fig 1-16

If you are **the author of this article, you do not need to request permission to reproduce figures and diagrams** provided correct acknowledgement is given. If you want to reproduce the whole article in a third-party publication (excluding your thesis/dissertation for which permission is not required) please go to the Copyright Clearance Center request page.

Fig 1-17

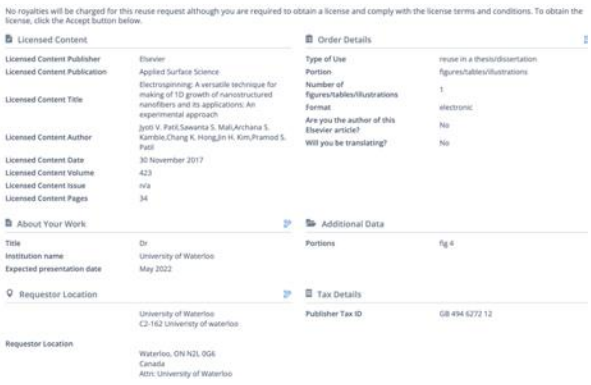

No royalties will be charged for this reuse request although you are required to obtain a license and comply with the license terms and conditions. To obtain the license, click the Accept button below.

Licensed Content

Licensed Content Publisher	Elsevier
Licensed Content Publication	Applied Surface Science
Licensed Content Title	Electrospinning: A versatile technique for making of 1D growth of nanostructured nanofibers and its applications: An experimental approach
Licensed Content Author	Jyoti V. Patil,Sawanta S. Mali,Archana S. Kamble,Chang K. Hong,Jin H. Kim,Pramod S. Patil
Licensed Content Date	30 November 2017
Licensed Content Volume	423
Licensed Content Issue	n/a
Licensed Content Pages	34

Order Details

Type of Use	reuse in a thesis/dissertation
Portion	figures/tables/illustrations
Number of figures/tables/illustrations	1
Format	electronic
Are you the author of this Elsevier article?	No
Will you be translating?	No

About Your Work

Title	Dr
Institution name	University of Waterloo
Expected presentation date	May 2022

Additional Data

Portions	fig 4

Requestor Location

	University of Waterloo C2-162 University of waterloo
Requestor Location	Waterloo, ON N2L 0G6 Canada Attn: University of Waterloo

Tax Details

Publisher Tax ID	GB 494 6272 12

Fig 1-18

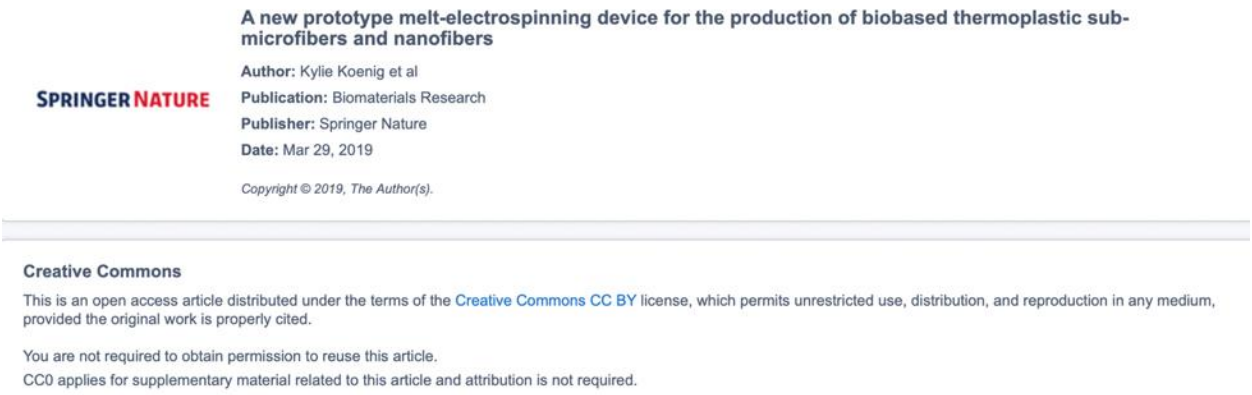

A new prototype melt-electrospinning device for the production of biobased thermoplastic sub-microfibers and nanofibers

Author: Kylie Koenig et al
Publication: Biomaterials Research
Publisher: Springer Nature
Date: Mar 29, 2019

Copyright © 2019, The Author(s).

Creative Commons

This is an open access article distributed under the terms of the Creative Commons CC BY license, which permits unrestricted use, distribution, and reproduction in any medium, provided the original work is properly cited.

You are not required to obtain permission to reuse this article.
CC0 applies for supplementary material related to this article and attribution is not required.

Chapter 2

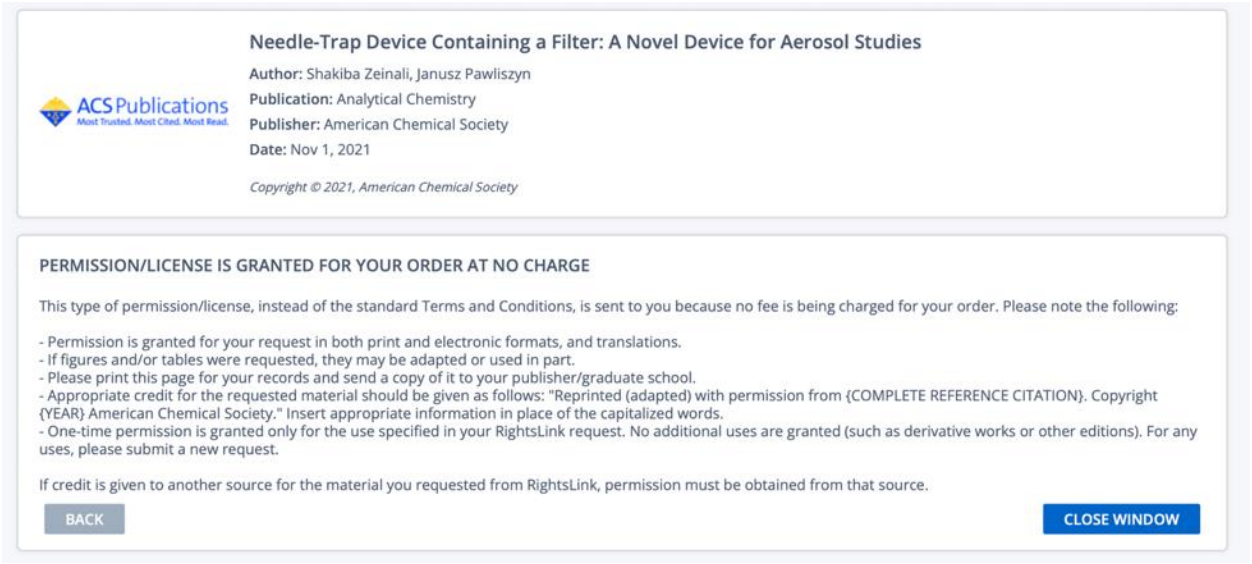

Needle-Trap Device Containing a Filter: A Novel Device for Aerosol Studies

Author: Shakiba Zeinali, Janusz Pawliszyn
Publication: Analytical Chemistry
Publisher: American Chemical Society
Date: Nov 1, 2021

Copyright © 2021, American Chemical Society

PERMISSION/LICENSE IS GRANTED FOR YOUR ORDER AT NO CHARGE

This type of permission/license, instead of the standard Terms and Conditions, is sent to you because no fee is being charged for your order. Please note the following:

- Permission is granted for your request in both print and electronic formats, and translations.
- If figures and/or tables were requested, they may be adapted or used in part.
- Please print this page for your records and send a copy of it to your publisher/graduate school.
- Appropriate credit for the requested material should be given as follows: "Reprinted (adapted) with permission from {COMPLETE REFERENCE CITATION}. Copyright {YEAR} American Chemical Society." Insert appropriate information in place of the capitalized words.
- One-time permission is granted only for the use specified in your RightsLink request. No additional uses are granted (such as derivative works or other editions). For any uses, please submit a new request.

If credit is given to another source for the material you requested from RightsLink, permission must be obtained from that source.

BACK CLOSE WINDOW

Chapter 3

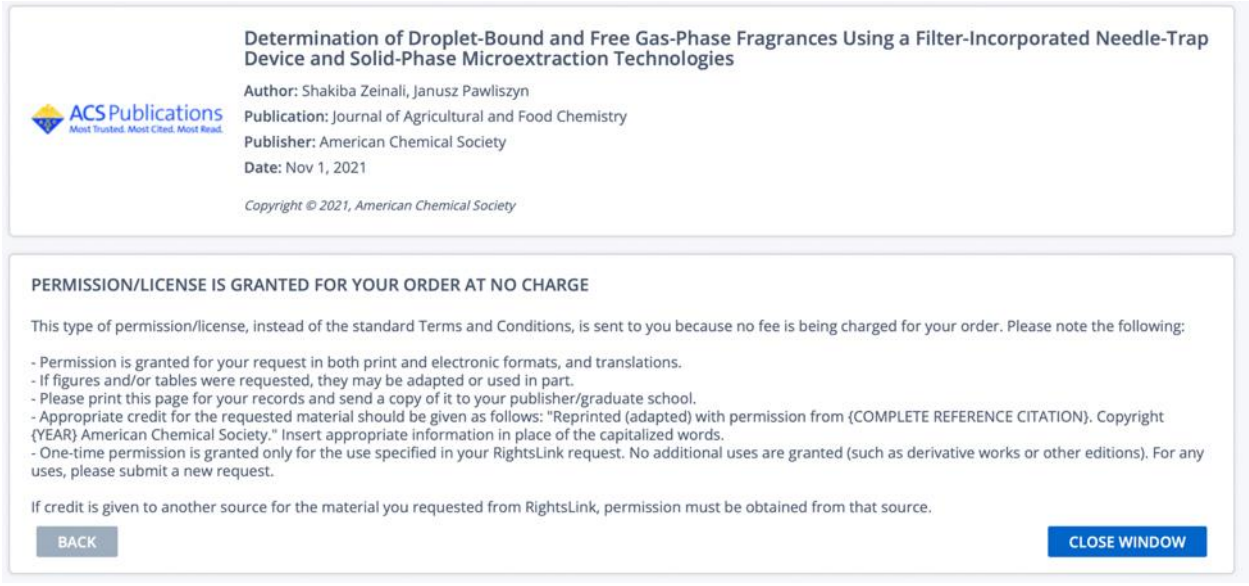

Determination of Droplet-Bound and Free Gas-Phase Fragrances Using a Filter-Incorporated Needle-Trap Device and Solid-Phase Microextraction Technologies

Author: Shakiba Zeinali, Janusz Pawliszyn
Publication: Journal of Agricultural and Food Chemistry
Publisher: American Chemical Society
Date: Nov 1, 2021

Copyright © 2021, American Chemical Society

PERMISSION/LICENSE IS GRANTED FOR YOUR ORDER AT NO CHARGE

This type of permission/license, instead of the standard Terms and Conditions, is sent to you because no fee is being charged for your order. Please note the following:

- Permission is granted for your request in both print and electronic formats, and translations.
- If figures and/or tables were requested, they may be adapted or used in part.
- Please print this page for your records and send a copy of it to your publisher/graduate school.
- Appropriate credit for the requested material should be given as follows: "Reprinted (adapted) with permission from {COMPLETE REFERENCE CITATION}. Copyright {YEAR} American Chemical Society." Insert appropriate information in place of the capitalized words.
- One-time permission is granted only for the use specified in your RightsLink request. No additional uses are granted (such as derivative works or other editions). For any uses, please submit a new request.

If credit is given to another source for the material you requested from RightsLink, permission must be obtained from that source.

BACK CLOSE WINDOW

Chapter 4

Free versus droplet-bound aroma compounds in sparkling beverages

Author: Shakiba Zeinali,Martyna Natalia Wieczorek,Janusz Pawliszyn
Publication: Food Chemistry
Publisher: Elsevier
Date: 1 June 2022

© 2022 Elsevier Ltd. All rights reserved.

Journal Author Rights

Please note that, as the author of this Elsevier article, you retain the right to include it in a thesis or dissertation, provided it is not published commercially. Permission is not required, but please ensure that you reference the journal as the original source. For more information on this and on your other retained rights, please visit: https://www.elsevier.com/about/our-business/policies/copyright#Author-rights

BACK CLOSE WINDOW

Chapter 5-1

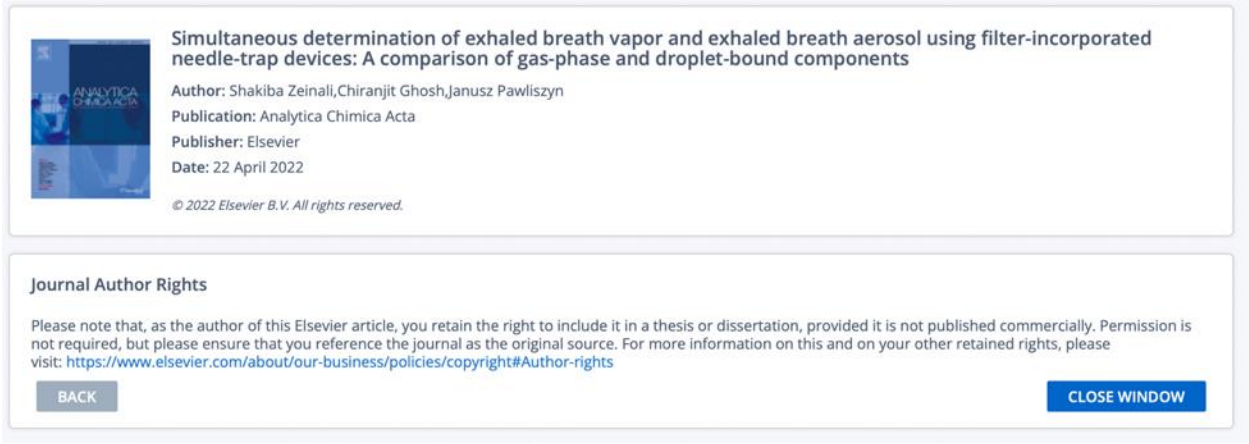

Simultaneous determination of exhaled breath vapor and exhaled breath aerosol using filter-incorporated needle-trap devices: A comparison of gas-phase and droplet-bound components

Author: Shakiba Zeinali,Chiranjit Ghosh,Janusz Pawliszyn
Publication: Analytica Chimica Acta
Publisher: Elsevier
Date: 22 April 2022

© 2022 Elsevier B.V. All rights reserved.

Journal Author Rights

Please note that, as the author of this Elsevier article, you retain the right to include it in a thesis or dissertation, provided it is not published commercially. Permission is not required, but please ensure that you reference the journal as the original source. For more information on this and on your other retained rights, please visit: https://www.elsevier.com/about/our-business/policies/copyright#Author-rights

BACK CLOSE WINDOW

Chapter 6

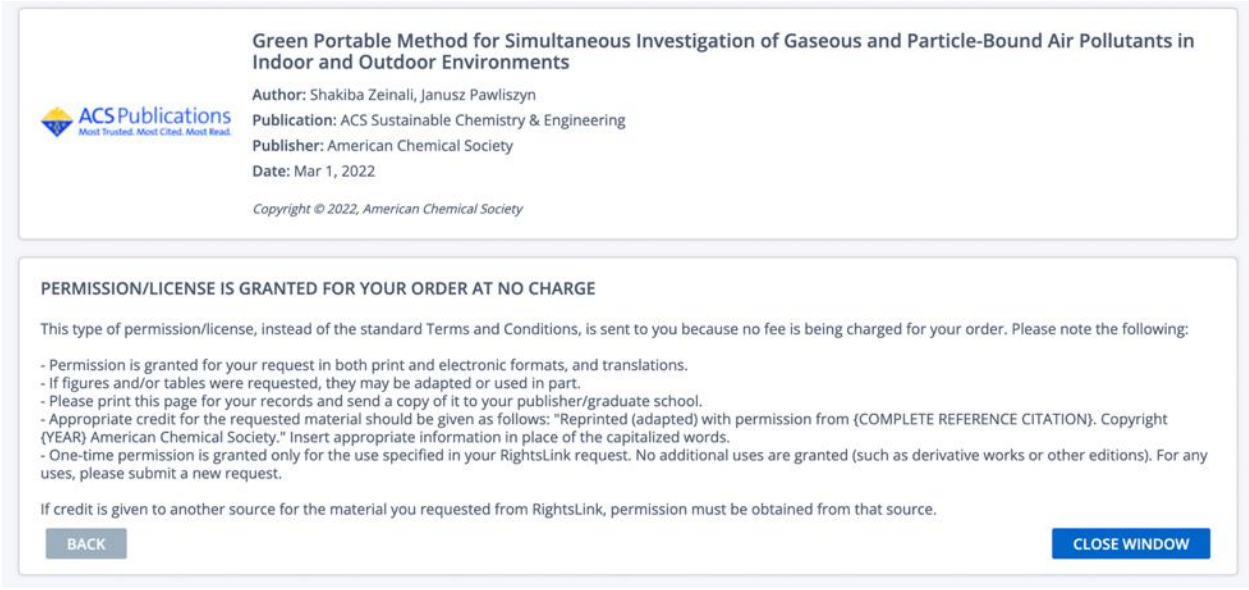

Green Portable Method for Simultaneous Investigation of Gaseous and Particle-Bound Air Pollutants in Indoor and Outdoor Environments

Author: Shakiba Zeinali, Janusz Pawliszyn
Publication: ACS Sustainable Chemistry & Engineering
Publisher: American Chemical Society
Date: Mar 1, 2022

Copyright © 2022, American Chemical Society

PERMISSION/LICENSE IS GRANTED FOR YOUR ORDER AT NO CHARGE

This type of permission/license, instead of the standard Terms and Conditions, is sent to you because no fee is being charged for your order. Please note the following:

- Permission is granted for your request in both print and electronic formats, and translations.
- If figures and/or tables were requested, they may be adapted or used in part.
- Please print this page for your records and send a copy of it to your publisher/graduate school.
- Appropriate credit for the requested material should be given as follows: "Reprinted (adapted) with permission from {COMPLETE REFERENCE CITATION}. Copyright {YEAR} American Chemical Society." Insert appropriate information in place of the capitalized words.
- One-time permission is granted only for the use specified in your RightsLink request. No additional uses are granted (such as derivative works or other editions). For any uses, please submit a new request.

If credit is given to another source for the material you requested from RightsLink, permission must be obtained from that source.

BACK CLOSE WINDOW

Chapter 5-2

SPRINGER NATURE LICENSE
TERMS AND CONDITIONS

Mar 15, 2022

This Agreement between University of Waterloo -- Shakiba Zeinali ("You") and Springer Nature ("Springer Nature") consists of your license details and the terms and conditions provided by Springer Nature and Copyright Clearance Center.

License Number	5270321185517
License date	Mar 15, 2022
Licensed Content Publisher	Springer Nature
Licensed Content Publication	Analytical and Bioanalytical Chemistry
Licensed Content Title	Effect of household air pollutants on the composition of exhaled breath characterized by solid-phase microextraction and needle-trap devices
Licensed Content Author	Shakiba Zeinali et al
Licensed Content Date	Mar 10, 2022
Type of Use	Thesis/Dissertation
Requestor type	academic/university or research institute
Format	electronic
Portion	full article/chapter

References

[1] E.V.S. Maciel, A.L. de Toffoli, E.S. Neto, C.E.D. Nazario, F.M. Lanças, New materials in sample preparation: Recent advances and future trends, TrAC Trends Anal. Chem. 119 (2019) 115633. https://doi.org/10.1016/j.trac.2019.115633.

[2] C.L. Arthur, J. Pawliszyn, Solid phase microextraction with thermal desorption using fused silica optical fibers, Anal. Chem. 62 (1990) 2145–2148.

[3] A. Spietelun, M. Pilarczyk, A. Kloskowski, J. Namieśnik, Current trends in solid-phase microextraction (SPME) fibre coatings, Chem. Soc. Rev. 39 (2010) 4524–4537.

[4] L.B. Abdulra'uf, W.A. Hammed, G.H. Tan, SPME fibers for the analysis of pesticide residues in fruits and vegetables: a review, Crit. Rev. Anal. Chem. 42 (2012) 152–161.

[5] P. Rocío-Bautista, I. Pacheco-Fernández, J. Pasán, V. Pino, Are metal-organic frameworks able to provide a new generation of solid-phase microextraction coatings?–A review, Anal. Chim. Acta. 939 (2016) 26–41.

[6] G. Ouyang, J. Pawliszyn, SPME in environmental analysis, Anal. Bioanal. Chem. 386 (2006) 1059–1073.

[7] M. Chai, J. Pawliszyn, Analysis of environmental air samples by solid-phase microextraction and gas chromatography/ion trap mass spectrometry, Environ. Sci. Technol. 29 (1995) 693–701.

[8] S. Balasubramanian, S. Panigrahi, Solid-phase microextraction (SPME) techniques for quality characterization of food products: a review, Food Bioprocess Technol. 4 (2011) 1–26.

[9] H. Kataoka, H.L. Lord, J. Pawliszyn, Applications of solid-phase microextraction in food analysis, J. Chromatogr. A. 880 (2000) 35–62.

[10] M. Volante, M. Cattaneo, M. Bianchi, G. Zoccola, Some applications of solid phase micro extraction (SPME) in the analysis of pesticide residues in food, J. Environ. Sci. Health Part B. 33 (1998) 279–292.

[11] J. Pereira, C.L. Silva, R. Perestrelo, J. Gonçalves, V. Alves, J.S. Câmara, Re-exploring the high-throughput potential of microextraction techniques, SPME and MEPS, as powerful strategies for medical diagnostic purposes. Innovative approaches, recent applications and future trends, Anal. Bioanal. Chem. 406 (2014) 2101–2122.

[12] B. Bojko, E. Cudjoe, G.A. Gómez-Ríos, K. Gorynski, R. Jiang, N. Reyes-Garcés, S. Risticevic, É.A. Silva, O. Togunde, D. Vuckovic, SPME–Quo vadis?, Anal. Chim. Acta. 750 (2012) 132–151.

[13] W. Filipiak, B. Bojko, SPME in clinical, pharmaceutical, and biotechnological research–How far are we from daily practice?, TrAC Trends Anal. Chem. 115 (2019) 203–213.

[14] J. Pawliszyn, Handbook of solid phase microextraction, Elsevier, 2011.

[15] J. Pawliszyn, Solid phase microextraction: theory and practice, John Wiley & Sons, 1997.

[16] K. Murtada, V. Galpin, J.J. Grandy, V. Singh, F. Sanchez, J. Pawliszyn, Development of porous carbon/polydimethylsiloxane thin-film solid-phase microextraction membranes to facilitate on-site sampling of volatile organic compounds, Sustain. Chem. Pharm. 21 (2021) 100435. https://doi.org/10.1016/j.scp.2021.100435.

[17] J.J. Grandy, V. Singh, M. Lashgari, M. Gauthier, J. Pawliszyn, Development of a Hydrophilic Lipophilic Balanced Thin Film Solid Phase Microextraction Device for Balanced Determination of Volatile Organic Compounds, Anal. Chem. 90 (2018) 14072–14080. https://doi.org/10.1021/acs.analchem.8b04544.

[18] M. Pietrzyńska, A. Voelkel, Optimization of the in-needle extraction device for the direct flow of the liquid sample through the sorbent layer, Talanta. 129 (2014) 392–397. https://doi.org/10.1016/j.talanta.2014.06.026.

[19] M. Ogawa, Y. Saito, I. Ueta, K. Jinno, Fiber-packed needle for dynamic extraction of aromatic compounds, Anal. Bioanal. Chem. 388 (2007) 619–625. https://doi.org/10.1007/s00216-007-1255-6.

[20] L. Yang, R. Said, M. Abdel-Rehim, Sorbent, device, matrix and application in microextraction by packed sorbent (MEPS): a review, J. Chromatogr. B. 1043 (2017) 33–43.

[21] S. Zeinali, M. Khalilzadeh, J. Pawliszyn, The evolution of needle-trap devices with focus on aerosol investigations, TrAC Trends Anal. Chem. 153 (2022) 116643. https://doi.org/10.1016/j.trac.2022.116643.

[22] H.L. Lord, W. Zhan, J. Pawliszyn, Fundamentals and applications of needle trap devices: a critical review, Anal. Chim. Acta. 677 (2010) 3–18.

[23] F. Raschdorf, Quantitative criteria for needle trap device selection, Chimia. 32 (1978) 478–483.

[24] T. Qin, X. Xu, T. Polák, V. Pacáková, K. Štulík, L. Jech, A simple method for the trace determination of methanol, ethanol, acetone and pentane in human breath and in the ambient air by preconcentration on solid sorbents followed by gas chromatography, Talanta. 44 (1997) 1683–1690.

[25] V. Berezkin, E. Makarov, B. Stolyarov, Needle-type concentrator and its application to the determination of pollutants, J. Chromatogr. A. 985 (2003) 63–65.

[26] M.A. Jochmann, X. Yuan, B. Schilling, T.C. Schmidt, In-tube extraction for enrichment of volatile organic hydrocarbons from aqueous samples, J. Chromatogr. A. 1179 (2008) 96–105.

[27] J.A. Koziel, M. Odziemkowski, J. Pawliszyn, Sampling and analysis of airborne particulate matter and aerosols using in-needle trap and SPME fiber devices, Anal. Chem. 73 (2001) 47–54.

[28] A. Wang, F. Fang, J. Pawliszyn, Sampling and determination of volatile organic compounds with needle trap devices, J. Chromatogr. A. 1072 (2005) 127–135.

[29] J.M. Warren, J. Pawliszyn, Development and evaluation of needle trap device geometry and packing methods for automated and manual analysis, J. Chromatogr. A. 1218 (2011) 8982–8988.

[30] S. Asl-Hariri, G.A. Gómez-Ríos, E. Gionfriddo, P. Dawes, J. Pawliszyn, Development of needle trap technology for on-site determinations: active and passive sampling, Anal. Chem. 86 (2014) 5889–5897.

[31] I. Eom, J. Pawliszyn, Simple sample transfer technique by internally expanded desorptive flow for needle trap devices, J. Sep. Sci. 31 (2008) 2283–2287.

[32] Y. Saito, I. Ueta, M. Ogawa, A. Abe, K. Yogo, S. Shirai, K. Jinno, Fiber-packed needle-type sample preparation device designed for gas chromatographic analysis, Anal. Bioanal. Chem. 393 (2009) 861–869.

[33] Y. Saito, I. Ueta, K. Kotera, M. Ogawa, H. Wada, K. Jinno, In-needle extraction device designed for gas chromatographic analysis of volatile organic compounds, J. Chromatogr. A. 1106 (2006) 190–195.

[34] I. Ueta, Y. Saito, M. Hosoe, M. Okamoto, H. Ohkita, S. Shirai, H. Tamura, K. Jinno, Breath acetone analysis with miniaturized sample preparation device: In-needle preconcentration and subsequent determination by gas chromatography–mass spectroscopy, J. Chromatogr. B. 877 (2009) 2551–2556.

[35] P. Přikryl, R. Kubinec, H. Jurdakova, J. Ševčík, I. Ostrovský, L. Sojak, V. Berezkin, Comparison of needle concentrator with SPME for GC determination of benzene, toluene, ethylbenzene, and xylenes in aqueous samples, Chromatographia. 64 (2006) 65–70.

[36] Y. Saito, Y. Nakao, M. Imaizumi, T. Takeichi, Y. Kiso, K. Jinno, Fiber-in-tube solid-phase microextraction: a fibrous rigid-rod heterocyclic polymer as the extraction medium, Fresenius J. Anal. Chem. 368 (2000) 641–643. https://doi.org/10.1007/s002160000574.

[37] M. Alonso, A. Godayol, E. Antico, J.M. Sanchez, Needle microextraction trap for on-site analysis of airborne volatile compounds at ultra-trace levels in gaseous samples, J. Sep. Sci. 34 (2011) 2705–2711.

[38] R. Kubinec, V.G. Berezkin, R. Górová, G. Addová, H. Mračnová, L. Soják, Needle concentrator for gas chromatographic determination of BTEX in aqueous samples, J. Chromatogr. B. 800 (2004) 295–301.

[39] M. Heidari, A. Bahrami, A.R. Ghiasvand, F.G. Shahna, A.R. Soltanian, A needle trap device packed with a sol–gel derived, multi-walled carbon nanotubes/silica composite for sampling and analysis of volatile organohalogen compounds in air, Anal. Chim. Acta. 785 (2013) 67–74.

[40] K. Kędziora, W. Wasiak, Extraction media used in needle trap devices—Progress in development and application, J. Chromatogr. A. 1505 (2017) 1–17.

[41] Z. Bo, L. Dawei, O. Junjie, S. Peigang, W. Lan, Preparation of Formic Acid Molecularly Imprinted Polymer and its Application on Needle Trap Extraction Techniques [J], Mod. Sci. Instrum. 1 (2011).

[42] I.-Y. Eom, V.H. Niri, J. Pawliszyn, Development of a syringe pump assisted dynamic headspace sampling technique for needle trap device, J. Chromatogr. A. 1196 (2008) 10–14.

[43] P. Loevkvist, J.A. Joensson, Capacity of sampling and preconcentration columns with a low number of theoretical plates, Anal. Chem. 59 (1987) 818–821.

[44] K. Bielicka-Daszkiewicz, A. Voelkel, Theoretical and experimental methods of determination of the breakthrough volume of SPE sorbents, Talanta. 80 (2009) 614–621.

[45] W. Zhan, J. Pawliszyn, Investigation and optimization of particle dimensions for needle trap device as an exhaustive active sampler, J. Chromatogr. A. 1260 (2012) 54–60.

[46] F. Raschdorf, Rapid measurements in the ppm and ppb region, Chimia. 32 (1978) 478–483.

[47] V.H. Niri, I. Eom, F.R. Kermani, J. Pawliszyn, Sampling free and particle-bound chemicals using solid-phase microextraction and needle trap device simultaneously, J. Sep. Sci. 32 (2009) 1075–1080.

[48] J.J. Poole, J.J. Grandy, G.A. Gómez-Ríos, E. Gionfriddo, J. Pawliszyn, Solid phase microextraction on-fiber derivatization using a stable, portable, and reusable pentafluorophenyl hydrazine standard gas generating vial, Anal. Chem. 88 (2016) 6859–6866.

[49] S. Asl-Hariri, Development and application of needle trap devices, UWSpace, 2015. http://hdl.handle.net/10012/9848.

[50] D. Thomas, A. Charvet, N. Bardin-Monnier, J.-C. Appert-Collin, Aerosol filtration, Elsevier, 2016.

[51] W. Lindsley, Filter pore size and aerosol sample collection, NIOSH Man. Anal. Methods. 14 (2016).

[52] H.-J. Kim, S.J. Park, D.-I. Kim, S. Lee, O.S. Kwon, I.K. Kim, Moisture effect on particulate matter filtration performance using electro-spun nanofibers including density functional theory analysis, Sci. Rep. 9 (2019) 1–8.

[53] Y. Bian, L. Zhang, C. Chen, Experimental and modeling study of pressure drop across electrospun nanofiber air filters, Build. Environ. 142 (2018) 244–251. https://doi.org/10.1016/j.buildenv.2018.06.021.

[54] P. Bulejko, Numerical comparison of prediction models for aerosol filtration efficiency applied on a hollow-fiber membrane pore structure, Nanomaterials. 8 (2018) 447.

[55] W. Li, S. Shen, H. Li, Study and optimization of the filtration performance of multi–fiber filter, Adv. Powder Technol. 27 (2016) 638–645. https://doi.org/10.1016/j.apt.2016.02.018.

[56] C. He, W. Nie, W. Feng, Engineering of biomimetic nanofibrous matrices for drug delivery and tissue engineering, J. Mater. Chem. B. 2 (2014) 7828–7848. https://doi.org/10.1039/C4TB01464B.

[57] J.V. Patil, S.S. Mali, A.S. Kamble, C.K. Hong, J.H. Kim, P.S. Patil, Electrospinning: A versatile technique for making of 1D growth of nanostructured nanofibers and its applications: An experimental approach, Appl. Surf. Sci. 423 (2017) 641–674. https://doi.org/10.1016/j.apsusc.2017.06.116.

[58] K. Koenig, K. Beukenberg, F. Langensiepen, G. Seide, A new prototype melt-electrospinning device for the production of biobased thermoplastic sub-microfibers and nanofibers, Biomater. Res. 23 (2019) 1–12.

[59] H. Bagheri, O. Rezvani, S. Zeinali, S. Asgari, T.G. Aqda, F. Manshaei, 11 - Electrospun nanofibers, in: C.F. Poole (Ed.), Solid-Phase Extr., Elsevier, 2020: pp. 311–339. https://doi.org/10.1016/B978-0-12-816906-3.00011-X.

[60] H. Bagheri, O. Rezvani, S. Zeinali, S. Asgari, T.G. Aqda, F. Manshaei, Electrospun nanofibers, in: Solid-Phase Extr., Elsevier, 2020: pp. 311–339.

[61] P.A. Martos, J. Pawliszyn, Sampling and determination of formaldehyde using solid-phase microextraction with on-fiber derivatization, Anal. Chem. 70 (1998) 2311–2320.

[62] J.A. Koziel, J. Noah, J. Pawliszyn, Field sampling and determination of formaldehyde in indoor air with solid-phase microextraction and on-fiber derivatization, Environ. Sci. Technol. 35 (2001) 1481–1486.

[63] J. Koziel, M. Jia, A. Khaled, J. Noah, J. Pawliszyn, Field air analysis with SPME device, Anal. Chim. Acta. 400 (1999) 153–162.

[64] L. Müller, T. Górecki, J. Pawliszyn, Optimization of the SPME device design for field applications, Fresenius J. Anal. Chem. 364 (1999) 610–616.

[65] G. Xiong, J. Pawliszyn, Microwave-assisted generation of standard gas mixtures, Anal. Chem. 74 (2002) 2446–2449.

[66] S. Zeinali, J. Pawliszyn, Determination of Droplet-Bound and Free Gas-Phase Fragrances Using a Filter-Incorporated Needle-Trap Device and Solid-Phase Microextraction Technologies, J. Agric. Food Chem. (2021).

[67] H. Lord, Y. Yu, A. Segal, J. Pawliszyn, Breath analysis and monitoring by membrane extraction with sorbent interface, Anal. Chem. 74 (2002) 5650–5657.

[68] P.A. Martos, J. Pawliszyn, Calibration of solid phase microextraction for air analyses based on physical chemical properties of the coating, Anal. Chem. 69 (1997) 206–215.

[69] Y. Saito, I. Ueta, M. Ogawa, M. Hayashida, K. Jinno, Miniaturized sample preparation needle: a versatile design for the rapid analysis of smoking-related compounds in hair and air samples, J. Pharm. Biomed. Anal. 44 (2007) 1–7.

[70] Y. Gong, I.-Y. Eom, D.-W. Lou, D. Hein, J. Pawliszyn, Development and application of a needle trap device for time-weighted average diffusive sampling, Anal. Chem. 80 (2008) 7275–7282.

[71] H. Jurdáková, R. Kubinec, M. Jurčišinová, Ž. Krkošová, J. Blaško, I. Ostrovský, L. Soják, V.G. Berezkin, Gas chromatography analysis of benzene, toluene, ethylbenzene and xylenes using newly designed needle trap device in aqueous samples, J. Chromatogr. A. 1194 (2008) 161–164.

[72] D.-W. Lou, X. Lee, J. Pawliszyn, Extraction of formic and acetic acids from aqueous solution by dynamic headspace-needle trap extraction: temperature and pH optimization, J. Chromatogr. A. 1201 (2008) 228–234.

[73] J. Cai, G. Ouyang, Y. Gong, J. Pawliszyn, Simultaneous sampling and analysis for vapor mercury in ambient air using needle trap coupled with gas chromatography–mass spectrometry, J. Chromatogr. A. 1213 (2008) 19–24.

[74] I.-Y. Eom, A.-M. Tugulea, J. Pawliszyn, Development and application of needle trap devices, J. Chromatogr. A. 1196 (2008) 3–9.

[75] I.-Y. Eom, S. Risticevic, J. Pawliszyn, Simultaneous sampling and analysis of indoor air infested with Cimex lectularius L. (Hemiptera: Cimicidae) by solid phase microextraction, thin film microextraction and needle trap device, Sel. Pap. Present. 12th Int. Symp. Extr. Technol. ExTech 2010. 716 (2012) 2–10. https://doi.org/10.1016/j.aca.2011.06.010.

[76] J. Kleeblatt, J.K. Schubert, R. Zimmermann, Detection of gaseous compounds by needle trap sampling and direct thermal-desorption photoionization mass spectrometry: concept and demonstrative application to breath gas analysis, Anal. Chem. 87 (2015) 1773–1781.

[77] Y. Li, J. Li, H. Xu, Graphene/polyaniline electrodeposited needle trap device for the determination of volatile organic compounds in human exhaled breath vapor and A549 cell, RSC Adv. 7 (2017) 11959–11968.

[78] M. Mieth, S. Kischkel, J.K. Schubert, D. Hein, W. Miekisch, Multibed needle trap devices for on site sampling and preconcentration of volatile breath biomarkers, Anal. Chem. 81 (2009) 5851–5857.

[79] D. Biagini, T. Lomonaco, S. Ghimenti, M. Onor, F.G. Bellagambi, P. Salvo, F. Di Francesco, R. Fuoco, Using labelled internal standards to improve needle trap micro-extraction technique prior to gas chromatography/mass spectrometry, Talanta. 200 (2019) 145–155. https://doi.org/10.1016/j.talanta.2019.03.046.

[80] H. Bagheri, Z. Ayazi, A. Aghakhani, A novel needle trap sorbent based on carbon nanotube-sol–gel for microextraction of polycyclic aromatic hydrocarbons from aquatic media, Anal. Chim. Acta. 683 (2011) 212–220. https://doi.org/10.1016/j.aca.2010.10.026.

[81] M. Alonso, L. Cerdan, A. Godayol, E. Anticó, J.M. Sanchez, Headspace needle-trap analysis of priority volatile organic compounds from aqueous samples: Application to the analysis of natural and waste waters, J. Chromatogr. A. 1218 (2011) 8131–8139. https://doi.org/10.1016/j.chroma.2011.09.042.

[82] N. Heidari, A. Ghiasvand, S. Abdolhosseini, Amino-silica/graphene oxide nanocomposite coated cotton as an efficient sorbent for needle trap device, Anal. Chim. Acta. 975 (2017) 11–19. https://doi.org/10.1016/j.aca.2017.04.031.

[83] M. Alonso, M. Castellanos, E. Besalú, J.M. Sanchez, A headspace needle-trap method for the analysis of volatile organic compounds in whole blood, J. Chromatogr. A. 1252 (2012) 23–30. https://doi.org/10.1016/j.chroma.2012.06.083.

[84] K. Dalvand, A. Ghiasvand, Simultaneous analysis of PAHs and BTEX in soil by a needle trap device coupled with GC-FID and using response surface methodology involving Box-Behnken design, Anal. Chim. Acta. 1083 (2019) 119–129.

[85] M. Heidari, A. Bahrami, A.R. Ghiasvand, F.G. Shahna, A.R. Soltanian, A needle trap device packed with a sol–gel derived, multi-walled carbon nanotubes/silica composite for sampling and analysis of volatile organohalogen compounds in air, Anal. Chim. Acta. 785 (2013) 67–74. https://doi.org/10.1016/j.aca.2013.04.057.

[86] E. Mesarchaki, N. Yassaa, D. Hein, H.E. Lutterbeck, C. Zindler, J. Williams, A novel method for the measurement of VOCs in seawater using needle trap devices and GC–MS, Mar. Chem. 159 (2014) 1–8. https://doi.org/10.1016/j.marchem.2013.12.001.

[87] C. Zscheppank, H.L. Wiegand, C. Lenzen, J. Wingender, U. Telgheder, Investigation of volatile metabolites during growth of Escherichia coli and Pseudomonas aeruginosa by needle trap-GC-MS, Anal. Bioanal. Chem. 406 (2014) 6617–6628. https://doi.org/10.1007/s00216-014-8111-2.

[88] M. Heidari, A. Bahrami, A.R. Ghiasvand, M.R. Emam, F.G. Shahna, A.R. Soltanian, Graphene packed needle trap device as a novel field sampler for determination of perchloroethylene in the air of dry cleaning establishments, Talanta. 131 (2015) 142–148.

[89] P. Porto-Figueira, J.A. Pereira, J.S. Câmara, Exploring the potential of needle trap microextraction combined with chromatographic and statistical data to discriminate different types of cancer based on urinary volatomic biosignature, Anal. Chim. Acta. 1023 (2018) 53–63.

[90] X. Zang, W. Liang, Q. Chang, T. Wu, C. Wang, Z. Wang, Determination of volatile organic compounds in pen inks by a dynamic headspace needle trap device combined with gas chromatography–mass spectrometry, J. Chromatogr. A. 1513 (2017) 27–34. https://doi.org/10.1016/j.chroma.2017.07.030.

[91] N. Saedi, A. Bahrami, F. Ghorbani Shahna, M. Habibi Mohraz, M. Farhadian, S. Alizadeh, A needle trap device packed with MIL-100 (Fe) metal organic frameworks for efficient headspace sampling and analysis of urinary BTEXs, Biomed. Chromatogr. 34 (2020) e4800.

[92] A. Poormohammadi, A. Bahrami, A. Ghiasvand, F.G. Shahna, M. Farhadian, Application of needle trap device packed with Amberlite XAD-2 resin prepared by sol-gel method for reproducible sampling of aromatic amines in air, Microchem. J. 143 (2018) 127–132.

[93] A. Barkhordari, M.R. Azari, R. Zendehdel, M. Heidari, Analysis of formaldehyde and acrolein in the aqueous samples using a novel needle trap device containing nanoporous silica aerogel sorbent, Environ. Monit. Assess. 189 (2017) 171.

[94] R. Rahimpoor, A. Firoozichahak, D. Nematollahi, S. Alizadeh, P.M. Alizadeh, A.A.A. Langari, Bio-monitoring of non-metabolized BTEX compounds in urine by dynamic headspace-needle trap device packed with 3D Ni/Co-BTC bimetallic metal-organic framework as an efficient absorbent, Microchem. J. 166 (2021) 106229.

[95] W.-H. Cheng, W. Zhan, J. Pawliszyn, Extraction of Gaseous VOCs Using Passive Needle Trap Samplers, Aerosol Air Qual. Res. 11 (2011) 387–392. https://doi.org/10.4209/aaqr.2011.01.0001.

[96] L. Pauling, A.B. Robinson, R. Teranishi, P. Cary, Quantitative analysis of urine vapor and breath by gas-liquid partition chromatography, Proc. Natl. Acad. Sci. 68 (1971) 2374–2376.

[97] S. Das, M. Pal, Non-invasive monitoring of human health by exhaled breath analysis: A comprehensive review, J. Electrochem. Soc. 167 (2020) 037562.

[98] D. Biagini, T. Lomonaco, S. Ghimenti, F. Bellagambi, M. Onor, M.C. Scali, V. Barletta, M. Marzilli, P. Salvo, M.G. Trivella, Determination of volatile organic compounds in exhaled breath of heart failure patients by needle trap micro-extraction coupled with gas chromatography-tandem mass spectrometry, J. Breath Res. 11 (2017) 047110.

[99] F. Monedeiro, M. Monedeiro-Milanowski, I.-A. Ratiu, B. Brożek, T. Ligor, B. Buszewski, Needle Trap Device-GC-MS for Characterization of Lung Diseases Based on Breath VOC Profiles, Molecules. 26 (2021) 1789.

[100] M. Mieth, J.K. Schubert, T. Gröger, B. Sabel, S. Kischkel, P. Fuchs, D. Hein, R. Zimmermann, W. Miekisch, Automated needle trap heart-cut GC/MS and needle trap comprehensive two-dimensional GC/TOF-MS for breath gas analysis in the clinical environment, Anal. Chem. 82 (2010) 2541–2551.

[101] F.G. Bellagambi, T. Lomonaco, S. Ghimenti, D. Biagini, R. Fuoco, F. Di Francesco, Determination of peppermint compounds in breath by needle trap micro-extraction coupled with gas chromatography–tandem mass spectrometry, J. Breath Res. 15 (2020) 016014.

[102] P. Trefz, L. Rösner, D. Hein, J.K. Schubert, W. Miekisch, Evaluation of needle trap micro-extraction and automatic alveolar sampling for point-of-care breath analysis, Anal. Bioanal. Chem. 405 (2013) 3105–3115.

[103] G.M. Mutlu, K.W. Garey, R.A. Robbins, L.H. Danziger, I. Rubinstein, Collection and analysis of exhaled breath condensate in humans, Am. J. Respir. Crit. Care Med. 164 (2001) 731–737.

[104] Z.-C. Yuan, W. Li, L. Wu, D. Huang, M. Wu, B. Hu, Solid-phase microextraction fiber in face mask for in vivo sampling and direct mass spectrometry analysis of exhaled breath aerosol, Anal. Chem. 92 (2020) 11543–11547.

[105] C. Grote, J. Pawliszyn, Solid-phase microextraction for the analysis of human breath, Anal. Chem. 69 (1997) 587–596.

[106] J. Rudnicka, T. Kowalkowski, T. Ligor, B. Buszewski, Determination of volatile organic compounds as biomarkers of lung cancer by SPME–GC–TOF/MS and chemometrics, J. Chromatogr. B. 879 (2011) 3360–3366.

[107] J. Huang, H. Deng, D. Song, H. Xu, Electrospun polystyrene/graphene nanofiber film as a novel adsorbent of thin film microextraction for extraction of aldehydes in human exhaled breath condensates, Anal. Chim. Acta. 878 (2015) 102–108. https://doi.org/10.1016/j.aca.2015.03.053.

[108] M. Jalali, M.J.Z. Sakhvid, A. Bahrami, N. Berijani, H. Mahjub, Oxidative stress biomarkers in exhaled breath of workers exposed to crystalline silica dust by SPME-GC-MS, J. Res. Health Sci. 16 (2016) 153.

[109] P. Fuchs, C. Loeseken, J.K. Schubert, W. Miekisch, Breath gas aldehydes as biomarkers of lung cancer, Int. J. Cancer. 126 (2010) 2663–2670. https://doi.org/10.1002/ijc.24970.

[110] M. Ligor, T. Ligor, A. Bajtarevic, C. Ager, M. Pienz, M. Klieber, H. Denz, M. Fiegl, W. Hilbe, W. Weiss, Determination of volatile organic compounds in exhaled breath of patients with lung cancer using solid phase microextraction and gas chromatography mass spectrometry, Clin. Chem. Lab. Med. CCLM. 47 (2009) 550–560.

[111] P. Trefz, S. Kischkel, D. Hein, E.S. James, J.K. Schubert, W. Miekisch, Needle trap micro-extraction for VOC analysis: effects of packing materials and desorption parameters, J. Chromatogr. A. 1219 (2012) 29–38.

[112] W. Miekisch, P. Fuchs, S. Kamysek, C. Neumann, J.K. Schubert, Assessment of propofol concentrations in human breath and blood by means of HS-SPME–GC–MS, Clin. Chim. Acta. 395 (2008) 32–37. https://doi.org/10.1016/j.cca.2008.04.021.

[113] I. Kimber, The role of the skin in the development of chemical respiratory hypersensitivity, Toxicol. Lett. 86 (1996) 89–92.

[114] J.R. Cornelisse-Vermaat, J. Voordouw, V. Yiakoumaki, G. Theodoridis, L.J. Frewer, Food-allergic consumers' labelling preferences: a cross-cultural comparison, Eur. J. Public Health. 18 (2008) 115–120.

[115] J.P. Lamas, L. Sanchez-Prado, M. Lores, C. Garcia-Jares, M. Llompart, Sorbent trapping solid-phase microextraction of fragrance allergens in indoor air, J. Chromatogr. A. 1217 (2010) 5307–5316.

[116] L. Sanchez-Prado, J.P. Lamas, G. Alvarez-Rivera, M. Lores, C. Garcia-Jares, M. Llompart, Determination of suspected fragrance allergens in cosmetics by matrix solid-phase dispersion gas chromatography–mass spectrometry analysis, J. Chromatogr. A. 1218 (2011) 5055–5062. https://doi.org/10.1016/j.chroma.2011.06.013.

[117] D. Wang, C.-Q. Duan, Y. Shi, B.-Q. Zhu, H.U. Javed, J. Wang, Free and glycosidically bound volatile compounds in sun-dried raisins made from different fragrance intensities grape varieties using a validated HS-SPME with GC–MS method, Food Chem. 228 (2017) 125–135. https://doi.org/10.1016/j.foodchem.2017.01.153.

[118] P. Barták, P. Bednář, L. Čáp, L. Ondráková, Z. Stránský, SPME – A valuable tool for investigation of flower scent, J. Sep. Sci. 26 (2003) 715–721. https://doi.org/10.1002/jssc.200301381.

[119] M. An, T. Haig, P. Hatfield, On-site field sampling and analysis of fragrance from living Lavender (Lavandula angustifolia L.) flowers by solid-phase microextraction coupled to gas chromatography and ion-trap mass spectrometry, J. Chromatogr. A. 917 (2001) 245–250. https://doi.org/10.1016/S0021-9673(01)00657-4.

[120] Ó. Castro, L. Trabalón, B. Schilling, F. Borrull, E. Pocurull, Solid phase microextraction Arrow for the determination of synthetic musk fragrances in fish samples, J. Chromatogr. A. 1591 (2019) 55–61. https://doi.org/10.1016/j.chroma.2019.01.032.

[121] C. Deng, G. Song, Y. Hu, Application of HS-SPME and GC-MS to Characterization of Volatile Compounds Emitted from Osmanthus Flowers, Ann. Chim. 94 (2004) 921–927. https://doi.org/10.1002/adic.200490114.

[122] W.-H. Cheng, D.-Y. Tsai, J.-Y. Lu, J.-W. Lee, Extracting Emissions from Air Fresheners Using Solid Phase Microextraction Devices, Aerosol Air Qual. Res. 16 (2016) 2632–2367. https://doi.org/10.4209/aaqr.2016.01.0011.

[123] N.-D. Dat, M.B. Chang, Review on characteristics of PAHs in atmosphere, anthropogenic sources and control technologies, Sci. Total Environ. 609 (2017) 682–693. https://doi.org/10.1016/j.scitotenv.2017.07.204.

[124] V. Samburova, B. Zielinska, A. Khlystov, Do 16 polycyclic aromatic hydrocarbons represent PAH air toxicity?, Toxics. 5 (2017) 17.

[125] D.L. Poster, M.M. Schantz, L.C. Sander, S.A. Wise, Analysis of polycyclic aromatic hydrocarbons (PAHs) in environmental samples: a critical review of gas chromatographic (GC) methods, Anal. Bioanal. Chem. 386 (2006) 859–881.

[126] M. Jia, J. Koziel, J. Pawliszyn, Fast field sampling/sample preparation and quantification of volatile organic compounds in indoor air by solid-phase microextraction and portable gas chromatography, Field Anal. Chem. Technol. 4 (2000) 73–84.

[127] D. Gorlo, B. Zygmunt, M. Dudek, A. Jaszek, M. Pilarczyk, J. Namieśnik, Application of solid-phase microextraction to monitoring indoor air quality, Fresenius J. Anal. Chem. 363 (1999) 696–699.

[128] M.M. Sampson, D.M. Chambers, D.Y. Pazo, F. Moliere, B.C. Blount, C.H. Watson, Simultaneous analysis of 22 volatile organic compounds in cigarette smoke using gas sampling bags for high-throughput solid-phase microextraction, Anal. Chem. 86 (2014) 7088–7095.

[129] R. Doong, S. Chang, Y. Sun, Solid-phase microextraction for determining the distribution of sixteen US Environmental Protection Agency polycyclic aromatic hydrocarbons in water samples, J. Chromatogr. A. 879 (2000) 177–188. https://doi.org/10.1016/S0021-9673(00)00347-2.

[130] H.C. Menezes, Z. de Lourdes Cardeal, Determination of polycyclic aromatic hydrocarbons from ambient air particulate matter using a cold fiber solid phase microextraction gas chromatography–mass spectrometry method, Sel. Pap. 34th ISCC 7th GCxGC Symp. 1218 (2011) 3300–3305. https://doi.org/10.1016/j.chroma.2010.10.105.

[131] S. Soury, A. Bahrami, S. Alizadeh, F. Ghorbani Shahna, D. Nematollahi, Development of a needle trap device packed with zinc based metal-organic framework sorbent for the sampling and analysis of polycyclic aromatic hydrocarbons in the air, Microchem. J. 148 (2019) 346–354. https://doi.org/10.1016/j.microc.2019.05.019.

[132] K.E. Kennedy, D.W. Hawker, J.F. Müller, M.E. Bartkow, R.W. Truss, A field comparison of ethylene vinyl acetate and low-density polyethylene thin films for equilibrium phase passive air sampling of polycyclic aromatic hydrocarbons, Atmos. Environ. 41 (2007) 5778–5787. https://doi.org/10.1016/j.atmosenv.2007.02.033.

[133] K. Kędziora-Koch, I. Rykowska, W. Wasiak, Needle-Trap Device (NTD) Packed with Reduced Graphene Oxide (rGO) for Sample Preparation Prior to the Determination of Polycyclic Aromatic Hydrocarbons (PAHs) from Aqueous Samples by Gas Chromatography–Mass spectrometry (GC-MS), Anal. Lett. 52 (2019) 1681–1698. https://doi.org/10.1080/00032719.2018.1563792.

[134] H. Li, C. Bi, X. Li, Y. Xu, A needle trap device method for sampling and analysis of semi-volatile organic compounds in air, Chemosphere. 250 (2020) 126284. https://doi.org/10.1016/j.chemosphere.2020.126284.

[135] E. Baysal, U.C. Uzun, F.N. Ertaş, O. Goksel, L. Pelit, Development of a new needle trap-based method for the determination of some volatile organic compounds in the indoor environment, Chemosphere. 277 (2021) 130251. https://doi.org/10.1016/j.chemosphere.2021.130251.

[136] L. Tuduri, V. Desauziers, J.L. Fanlo, Dynamic versus static sampling for the quantitative analysis of volatile organic compounds in air with polydimethylsiloxane–Carboxen solid-phase microextraction fibers, ExTech 2001 - Adv. Extr. Technol. 963 (2002) 49–56. https://doi.org/10.1016/S0021-9673(02)00222-4.

[137] V. Stadnytskyi, C.E. Bax, A. Bax, P. Anfinrud, The airborne lifetime of small speech droplets and their potential importance in SARS-CoV-2 transmission, Proc. Natl. Acad. Sci. 117 (2020) 11875. https://doi.org/10.1073/pnas.2006874117.

[138] V.K. Rawat, D.T. Buckley, S. Kimoto, M.-H. Lee, N. Fukushima, C.J. Hogan, Two dimensional size–mass distribution function inversion from differential mobility analyzer–aerosol particle mass analyzer (DMA–APM) measurements, J. Aerosol Sci. 92 (2016) 70–82. https://doi.org/10.1016/j.jaerosci.2015.11.001.

[139] G.C. Pratt, C. Herbrandson, M.J. Krause, C. Schmitt, C.J. Lippert, C.R. McMahon, K.M. Ellickson, Measurements of gas and particle polycyclic aromatic hydrocarbons (PAHs) in air at urban, rural and near-roadway sites, Atmos. Environ. 179 (2018) 268–278. https://doi.org/10.1016/j.atmosenv.2018.02.035.

[140] W.T. Winberry, N.T. Murphy, R. Riggan, Compendium of methods for the determination of toxic organic compounds in ambient air, Atmospheric Research and Exposure Assessment Laboratory, Office of Research …, 1988.

[141] B.R. Winters, J.D. Pleil, M.M. Angrish, M.A. Stiegel, T.H. Risby, M.C. Madden, Standardization of the collection of exhaled breath condensate and exhaled breath aerosol using a feedback regulated sampling device, J. Breath Res. 11 (2017) 047107. https://doi.org/10.1088/1752-7163/aa8bbc.

[142] I.M. Hutten, CHAPTER 6 - Testing of Nonwoven Filter Media, in: I.M. Hutten (Ed.), Handb. Nonwoven Filter Media, Butterworth-Heinemann, Oxford, 2007: pp. 245–290. https://doi.org/10.1016/B978-185617441-1/50021-4.

[143] K.M. Yun, C.J. Hogan Jr, Y. Matsubayashi, M. Kawabe, F. Iskandar, K. Okuyama, Nanoparticle filtration by electrospun polymer fibers, Chem. Eng. Sci. 62 (2007) 4751–4759.

[144] F. Deuber, S. Mousavi, L. Federer, M. Hofer, C. Adlhart, Exploration of ultralight nanofiber aerogels as particle filters: capacity and efficiency, ACS Appl. Mater. Interfaces. 10 (2018) 9069–9076.

[145] J.J. Grandy, E. Boyacı, J. Pawliszyn, Development of a carbon mesh supported thin film microextraction membrane as a means to lower the detection limits of benchtop and portable GC/MS instrumentation, Anal. Chem. 88 (2016) 1760–1767.

[146] M. Maghe, C. Creighton, L.C. Henderson, M.G. Huson, S. Nunna, S. Atkiss, N. Byrne, B.L. Fox, Using ionic liquids to reduce energy consumption for carbon fibre production, J. Mater. Chem. A. 4 (2016) 16619–16626.

[147] X. Zhang, T. Kitao, D. Piga, R. Hongu, S. Bracco, A. Comotti, P. Sozzani, T. Uemura, Carbonization of single polyacrylonitrile chains in coordination nanospaces, Chem. Sci. 11 (2020) 10844–10849. https://doi.org/10.1039/D0SC02048F.

[148] S. Kobayashi, K. Müllen, Encyclopedia of polymeric nanomaterials, Springer Berlin Heidelberg, 2015.

[149] M.S.A. Rahaman, A.F. Ismail, A. Mustafa, A review of heat treatment on polyacrylonitrile fiber, Polym. Degrad. Stab. 92 (2007) 1421–1432. https://doi.org/10.1016/j.polymdegradstab.2007.03.023.

[150] S. Yang, Z. Zhu, F. Wei, X. Yang, Carbon nanotubes / activated carbon fiber based air filter media for simultaneous removal of particulate matter and ozone, Build. Environ. 125 (2017) 60–66. https://doi.org/10.1016/j.buildenv.2017.08.040.

[151] Y.H. Joe, K. Woo, J. Hwang, Fabrication of an anti-viral air filter with SiO2–Ag nanoparticles and performance evaluation in a continuous airflow condition, J. Hazard. Mater. 280 (2014) 356–363. https://doi.org/10.1016/j.jhazmat.2014.08.013.

[152] I.M. Hutten, Chapter 8 - Air Filter Applications, in: I.M. Hutten (Ed.), Handb. Nonwoven Filter Media Second Ed., Butterworth-Heinemann, Oxford, 2016: pp. 451–519. https://doi.org/10.1016/B978-0-08-098301-1.00008-3.

[153] A. Konda, A. Prakash, G.A. Moss, M. Schmoldt, G.D. Grant, S. Guha, Aerosol filtration efficiency of common fabrics used in respiratory cloth masks, ACS Nano. 14 (2020) 6339–6347.

[154] P. Wolkoff, Indoor air humidity, air quality, and health–An overview, Int. J. Hyg. Environ. Health. 221 (2018) 376–390.

[155] J.M. Seguel, R. Merrill, D. Seguel, A.C. Campagna, Indoor air quality, Am. J. Lifestyle Med. 11 (2017) 284–295.

[156] N.B. Goodman, A.J. Wheeler, P.J. Paevere, G. Agosti, N. Nematollahi, A. Steinemann, Emissions from dryer vents during use of fragranced and fragrance-free laundry products, Air Qual. Atmosphere Health. 12 (2019) 289–295.

[157] S.A. Elsharif, A. Buettner, Structure–Odor Relationship Study on Geraniol, Nerol, and Their Synthesized Oxygenated Derivatives, J. Agric. Food Chem. 66 (2018) 2324–2333. https://doi.org/10.1021/acs.jafc.6b04534.

[158] W. Uter, T. Werfel, I.R. White, J.D. Johansen, Contact allergy: a review of current problems from a clinical perspective, Int. J. Environ. Res. Public. Health. 15 (2018) 1108.

[159] H. Leijs, J. Broekhans, L. van Pelt, C. Mussinan, Quantitative Analysis of the 26 Allergens for Cosmetic Labeling in Fragrance Raw Materials and Perfume Oils, J. Agric. Food Chem. 53 (2005) 5487–5491. https://doi.org/10.1021/jf048081w.

[160] P.L. Scheinman, Allergic contact dermatitis to fragrance: a review, Am. J. Contact Dermat. 7 (1996) 65–76.

[161] E. Heuberger, T. Hongratanaworakit, C. Böhm, R. Weber, G. Buchbauer, Effects of chiral fragrances on human autonomic nervous system parameters and self-evaluation, Chem. Senses. 26 (2001) 281–292.

[162] A.C. De Groot, P.J. Frosch, Adverse reactions to fragrances: a clinical review, Contact Dermatitis. 36 (1997) 57–86.

[163] G.G. Rimkus, Polycyclic musk fragrances in the aquatic environment, Toxicol. Lett. 111 (1999) 37–56.

[164] L. He, J. Hu, W. Deng, Preparation and application of flavor and fragrance capsules, Polym. Chem. 9 (2018) 4926–4946.

[165] G. Abedi, Z. Talebpour, F. Jamechenarboo, The survey of analytical methods for sample preparation and analysis of fragrances in cosmetics and personal care products, TrAC Trends Anal. Chem. 102 (2018) 41–59.

[166] Q. Zhou, X. Jia, Y.-Z. Yao, B. Wang, C.-Q. Wei, M. Zhang, F. Huang, Characterization of the Aroma-Active Compounds in Commercial Fragrant Rapeseed Oils via Monolithic Material Sorptive Extraction, J. Agric. Food Chem. 67 (2019) 11454–11463. https://doi.org/10.1021/acs.jafc.9b05691.

[167] T. Karunasekara, C.F. Poole, Determination of descriptors for fragrance compounds by gas chromatography and liquid–liquid partition, J. Chromatogr. A. 1235 (2012) 159–165. https://doi.org/10.1016/j.chroma.2012.02.043.

[168] T.P. Tsiallou, V.A. Sakkas, T.A. Albanis, Development and application of chemometric-assisted dispersive liquid–liquid microextraction for the determination of suspected fragrance allergens in water samples, J. Sep. Sci. 35 (2012) 1659–1666.

[169] J.P. Lamas, L. Sanchez-Prado, C. Garcia-Jares, M. Llompart, Determination of fragrance allergens in indoor air by active sampling followed by ultrasound-assisted solvent extraction and gas chromatography–mass spectrometry, J. Chromatogr. A. 1217 (2010) 1882–1890. https://doi.org/10.1016/j.chroma.2010.01.055.

[170] Z. Wang, Q. Zhang, H. Li, Q. Lv, W. Wang, H. Bai, Rapid and green determination of 58 fragrance allergens in plush toys, J. Sep. Sci. 41 (2018) 657–668.

[171] T. Okabayashi, T. Toda, I. Yamamoto, K. Utsunomiya, N. Yamashita, M. Nakagawa, Temperature-programmed chemiluminescence measurements for discrimination and determination of fragrance, Proc. 5th Eur. Conf. Opt. Chem. Sens. Biosens. 74 (2001) 152–156. https://doi.org/10.1016/S0925-4005(00)00725-5.

[172] J. Pérez-Outeiral, E. Millán, R. Garcia-Arrona, Ultrasound-assisted emulsification microextraction coupled with high-performance liquid chromatography for the simultaneous determination of fragrance allergens in cosmetics and water, J. Sep. Sci. 38 (2015) 1561–1569. https://doi.org/10.1002/jssc.201401330.

[173] K.V. Maidatsi, T.G. Chatzimitakos, V.A. Sakkas, C.D. Stalikas, Octyl-modified magnetic graphene as a sorbent for the extraction and simultaneous determination of fragrance allergens, musks, and phthalates in aqueous samples by gas chromatography with mass spectrometry, J. Sep. Sci. 38 (2015) 3758–3765. https://doi.org/10.1002/jssc.201500578.

[174] Y. Shen, B. Hu, X. Chen, Q. Miao, C. Wang, Z. Zhu, C. Han, Determination of Four Flavorings in Infant Formula by Solid-Phase Extraction and Gas Chromatography–Tandem

Mass Spectrometry, J. Agric. Food Chem. 62 (2014) 10881–10888. https://doi.org/10.1021/jf5013083.

[175] J.P. Rafson, M.Y. Bee, G.L. Sacks, Spatially Resolved Headspace Extractions of Trace-Level Volatiles from Planar Surfaces for High-Throughput Quantitation and Mass Spectral Imaging, J. Agric. Food Chem. 67 (2019) 13840–13847. https://doi.org/10.1021/acs.jafc.9b01091.

[176] N. Ochiai, K. Sasamoto, F. David, P. Sandra, Recent Developments of Stir Bar Sorptive Extraction for Food Applications: Extension to Polar Solutes, J. Agric. Food Chem. 66 (2018) 7249–7255. https://doi.org/10.1021/acs.jafc.8b02182.

[177] J.J. Poole, J.J. Grandy, G.A. Gómez-Ríos, E. Gionfriddo, J. Pawliszyn, Solid phase microextraction on-fiber derivatization using a stable, portable, and reusable pentafluorophenyl hydrazine standard gas generating vial, Anal. Chem. 88 (2016) 6859–6866.

[178] X. Li, G. Ouyang, H. Lord, J. Pawliszyn, Theory and validation of solid-phase microextraction and needle trap devices for aerosol sample, Anal. Chem. 82 (2010) 9521–9527.

[179] Dickerson , Lyndel, Cashman, Donald, Ferguson, John A, Air freshener composition, 1991.

[180] M.A. Teixeira, O. Rodríguez, A.E. Rodrigues, Diffusion and performance of fragranced products: prediction and validation, AIChE J. 59 (2013) 3943–3957.

[181] A. Dunkel, M. Steinhaus, M. Kotthoff, B. Nowak, D. Krautwurst, P. Schieberle, T. Hofmann, Nature's chemical signatures in human olfaction: a foodborne perspective for future biotechnology, Angew. Chem. Int. Ed. 53 (2014) 7124–7143.

[182] C. Gonzalez Viejo, S. Fuentes, D.D. Torrico, A. Godbole, F.R. Dunshea, Chemical characterization of aromas in beer and their effect on consumers liking, Food Chem. 293 (2019) 479–485. https://doi.org/10.1016/j.foodchem.2019.04.114.

[183] B.G. Green, The effects of temperature and concentration on the perceived intensity and quality of carbonation, Chem. Senses. 17 (1992) 435–450.

[184] N.N. Yau, M.R. McDaniel, The power function of carbonation, J. Sens. Stud. 5 (1990) 117–128.

[185] A. Saint-Eve, I. Deleris, E. Aubin, E. Semon, G. Feron, J.-M. Rabillier, D. Ibarra, E. Guichard, I. Souchon, Influence of composition (CO2 and sugar) on aroma release and perception of mint-flavored carbonated beverages, J. Agric. Food Chem. 57 (2009) 5891–5898.

[186] N. Yau, M. McDaniel, F. Bodyfelt, Sensory evaluation of sweetened flavored carbonated milk beverages, J. Dairy Sci. 72 (1989) 367–377.

[187] C. Lederer, F. Bodyfelt, M. McDaniel, The effect of carbonation level on the sensory properties of flavored milk beverages, J. Dairy Sci. 74 (1991) 2100–2108.

[188] T. Kishimoto, A. Wanikawa, K. Kono, K. Shibata, Comparison of the Odor-Active Compounds in Unhopped Beer and Beers Hopped with Different Hop Varieties, J. Agric. Food Chem. 54 (2006) 8855–8861. https://doi.org/10.1021/jf061342c.

[189] D. Langos, M. Granvogl, P. Schieberle, Characterization of the Key Aroma Compounds in Two Bavarian Wheat Beers by Means of the Sensomics Approach, J. Agric. Food Chem. 61 (2013) 11303–11311. https://doi.org/10.1021/jf403912j.

[190] G.C. da Silva, A.A.S. da Silva, L.S.N. da Silva, R.L. de O. Godoy, L.C. Nogueira, S.L. Quitério, R.S.L. Raices, Method development by GC–ECD and HS-SPME–GC–MS for beer volatile analysis, Food Chem. 167 (2015) 71–77. https://doi.org/10.1016/j.foodchem.2014.06.033.

[191] J.M. Jurado, O. Ballesteros, A. Alcázar, F. Pablos, M.J. Martín, J.L. Vílchez, A. Navalón, Characterization of aniseed-flavoured spirit drinks by headspace solid-phase microextraction gas chromatography–mass spectrometry and chemometrics, Talanta. 72 (2007) 506–511. https://doi.org/10.1016/j.talanta.2006.11.008.

[192] H. Mirhosseini, Y. Salmah, S.A.H. Nazimah, C.P. Tan, Solid-phase microextraction for headspace analysis of key volatile compounds in orange beverage emulsion, Food Chem. 105 (2007) 1659–1670. https://doi.org/10.1016/j.foodchem.2007.04.039.

[193] F. Rodrigues, M. Caldeira, J.S. Câmara, Development of a dynamic headspace solid-phase microextraction procedure coupled to GC–qMSD for evaluation the chemical profile in alcoholic beverages, Anal. Chim. Acta. 609 (2008) 82–104. https://doi.org/10.1016/j.aca.2007.12.041.

[194] G.A. da Silva, F. Augusto, R.J. Poppi, Exploratory analysis of the volatile profile of beers by HS–SPME–GC, Food Chem. 111 (2008) 1057–1063. https://doi.org/10.1016/j.foodchem.2008.05.022.

[195] E. Coelho, M.A. Coimbra, J.M.F. Nogueira, S.M. Rocha, Quantification approach for assessment of sparkling wine volatiles from different soils, ripening stages, and varieties by stir bar sorptive extraction with liquid desorption, Anal. Chim. Acta. 635 (2009) 214–221. https://doi.org/10.1016/j.aca.2009.01.013.

[196] O. Geffroy, R. Lopez, E. Serrano, T. Dufourcq, E. Gracia-Moreno, J. Cacho, V. Ferreira, Changes in analytical and volatile compositions of red wines induced by pre-fermentation heat treatment of grapes, Food Chem. 187 (2015) 243–253. https://doi.org/10.1016/j.foodchem.2015.04.105.

[197] C. Ubeda, R.M. Callejón, A.M. Troncoso, A. Peña-Neira, M.L. Morales, Volatile profile characterisation of Chilean sparkling wines produced by traditional and Charmat methods via sequential stir bar sorptive extraction, Food Chem. 207 (2016) 261–271. https://doi.org/10.1016/j.foodchem.2016.03.117.

[198] Y.M. Al Shamari, S.M. Wabaidur, A.A. Alwarthan, M.A. Khan, M.R. Siddiqui, Corncob Waste Based Adsorbent for Solid Phase Extraction of Tartrazine in Carbonated Drinks and Analytical Method using Ultra Performance Liquid Chromatography-Mass Spectrometry, Curr. Anal. Chem. 16 (2020) 924–932.

[199] H. Gallart-Ayala, E. Moyano, M. Galceran, Analysis of bisphenols in soft drinks by on-line solid phase extraction fast liquid chromatography–tandem mass spectrometry, Anal. Chim. Acta. 683 (2011) 227–233.

[200] N. Li, J. Chen, Y.-P. Shi, Magnetic nitrogen-doped reduced graphene oxide as a novel magnetic solid-phase extraction adsorbent for the separation of bisphenol endocrine disruptors in carbonated beverages, Talanta. 201 (2019) 194–203.

[201] Y. Yang, J. Yu, J. Yin, B. Shao, J. Zhang, Molecularly imprinted solid-phase extraction for selective extraction of bisphenol analogues in beverages and canned food, J. Agric. Food Chem. 62 (2014) 11130–11137.

[202] L. Cai, J. Dong, Y. Wang, X. Chen, Thin-film microextraction coupled to surface enhanced Raman scattering for the rapid detection of benzoic acid in carbonated beverages, Talanta. 178 (2018) 268–273.

[203] L. Vernarelli, J. Whitecavage, J. Stuff, Analysis of food samples using thin film solid phase microextraction (TF-SPME) and thermal desorption GC/MS, GERSTEL Application Note 2019, 2019.

[204] P. Perpète, S. Collin, Influence of beer ethanol content on the wort flavour perception, Food Chem. 71 (2000) 379–385. https://doi.org/10.1016/S0308-8146(00)00179-5.

[205] R. Clark, R. Linforth, F. Bealin-Kelly, J. Hort, Effects of ethanol, carbonation and hop acids on volatile delivery in a model beer system, J. Inst. Brew. 117 (2011) 74–81.

[206] C. Gonzalez Viejo, D.D. Torrico, F.R. Dunshea, S. Fuentes, Bubbles, foam formation, stability and consumer perception of carbonated drinks: A review of current, new and emerging technologies for rapid assessment and control, Foods. 8 (2019) 596.

[207] M.Á. Pozo-Bayón, M. Santos, P.J. Martín-Álvarez, G. Reineccius, Influence of carbonation on aroma release from liquid systems using an artificial throat and a proton transfer reaction–mass spectrometric technique (PTR–MS), Flavour Fragr. J. 24 (2009) 226–233.

[208] J. Frasnelli, C. Oehrn, M. Jones-Gotman, Effects of oral irritation on olfaction, Food Chem. 113 (2009) 1003–1007.

[209] G. Nelson, Gas mixtures: preparation and control, 1st Edition, CRC Press, 1992.

[210] S.J. Ameh, O. Obodozie-Ofoegbu, Essential oils as flavors in carbonated cola and citrus soft drinks, in: Essent. Oils Food Preserv. Flavor Saf., Elsevier, 2016: pp. 111–121.

[211] M. Phillips, K. Gleeson, J.M.B. Hughes, J. Greenberg, R.N. Cataneo, L. Baker, W.P. McVay, Volatile organic compounds in breath as markers of lung cancer: a cross-sectional study, The Lancet. 353 (1999) 1930–1933.

[212] S. Kumar, J. Huang, N. Abbassi-Ghadi, P. Španěl, D. Smith, G.B. Hanna, Selected Ion Flow Tube Mass Spectrometry Analysis of Exhaled Breath for Volatile Organic Compound Profiling of Esophago-Gastric Cancer, Anal. Chem. 85 (2013) 6121–6128. https://doi.org/10.1021/ac4010309.

[213] P. Trefz, M. Schmidt, P. Oertel, J. Obermeier, B. Brock, S. Kamysek, J. Dunkl, R. Zimmermann, J.K. Schubert, W. Miekisch, Continuous Real Time Breath Gas Monitoring in the Clinical Environment by Proton-Transfer-Reaction-Time-of-Flight-Mass Spectrometry, Anal. Chem. 85 (2013) 10321–10329. https://doi.org/10.1021/ac402298v.

[214] W. Cao, Y. Duan, Breath Analysis: Potential for Clinical Diagnosis and Exposure Assessment, Clin. Chem. 52 (2006) 800–811.

[215] L.A. Wallace, E. Pellizzari, T. Hartwell, M. Rosenzweig, M. Erickson, C. Sparacino, H. Zelon, Personal exposure to volatile organic compounds: I. Direct measurements in breathing-zone air, drinking water, food, and exhaled breath, Environ. Res. 35 (1984) 293–319. https://doi.org/10.1016/0013-9351(84)90137-3.

[216] H. Vereb, A.M. Dietrich, B. Alfeeli, M. Agah, The possibilities will take your breath away: breath analysis for assessing environmental exposure, Environ. Sci. Technol. 45 (2011) 8167–8175.

[217] J.D. Pleil, A.B. Lindstrom, Exhaled human breath measurement method for assessing exposure to halogenated volatile organic compounds, Clin. Chem. 43 (1997) 723–730. https://doi.org/10.1093/clinchem/43.5.723.

[218] J.D. Pleil, M.A. Stiegel, Evolution of Environmental Exposure Science: Using Breath-Borne Biomarkers for “Discovery” of the Human Exposome, Anal. Chem. 85 (2013) 9984–9990. https://doi.org/10.1021/ac402306f.

[219] M. Locatelli, A. Tartaglia, H.I. Ulusoy, S. Ulusoy, F. Savini, S. Rossi, F. Santavenere, G.M. Merone, E. Bassotti, C. D’Ovidio, E. Rosato, K.G. Furton, A. Kabir, Fabric-Phase Sorptive Membrane Array As a Noninvasive In Vivo Sampling Device For Human Exposure To Different Compounds, Anal. Chem. 93 (2021) 1957–1961. https://doi.org/10.1021/acs.analchem.0c04663.

[220] M. Xu, Z. Tang, Y. Duan, Y. Liu, GC-based techniques for breath analysis: current status, challenges, and prospects, Crit. Rev. Anal. Chem. 46 (2016) 291–304.

[221] A. Peralbo-Molina, M. Calderón-Santiago, F. Priego-Capote, B. Jurado-Gámez, M.L. De Castro, Development of a method for metabolomic analysis of human exhaled breath condensate by gas chromatography–mass spectrometry in high resolution mode, Anal. Chim. Acta. 887 (2015) 118–126.

[222] P. Kubáň, F. Foret, Exhaled breath condensate: determination of non-volatile compounds and their potential for clinical diagnosis and monitoring. A review, Anal. Chim. Acta. 805 (2013) 1–18.

[223] S. Wang, S. Hu, H. Xu, Analysis of aldehydes in human exhaled breath condensates by in-tube SPME-HPLC, Anal. Chim. Acta. 900 (2015) 67–75.

[224] Y. Saalberg, M. Wolff, VOC breath biomarkers in lung cancer, Clin. Chim. Acta. 459 (2016) 5–9.

[225] J. Zhou, Z.-A. Huang, U. Kumar, D.D. Chen, Review of recent developments in determining volatile organic compounds in exhaled breath as biomarkers for lung cancer diagnosis, Anal. Chim. Acta. 996 (2017) 1–9.

[226] C.-W. Lee, C.P. Weisel, Determination of methyl tert-butyl ether and tert-butyl alcohol in human urine by high-temperature purge-and-trap gas chromatography-mass spectrometry, J. Anal. Toxicol. 22 (1998) 1–5.

[227] J. Rudnicka, T. Kowalkowski, T. Ligor, B. Buszewski, Determination of volatile organic compounds as biomarkers of lung cancer by SPME–GC–TOF/MS and chemometrics, J. Chromatogr. B. 879 (2011) 3360–3366.

[228] B. Gruber, T. Groeger, D. Harrison, R. Zimmermann, Vacuum ultraviolet absorption spectroscopy in combination with comprehensive two-dimensional gas chromatography for the monitoring of volatile organic compounds in breath gas: A feasibility study, J. Chromatogr. A. 1464 (2016) 141–146. https://doi.org/10.1016/j.chroma.2016.08.024.

[229] R.R. Netz, Mechanisms of airborne infection via evaporating and sedimenting droplets produced by speaking, J. Phys. Chem. B. 124 (2020) 7093–7101.

[230] R.S. Papineni, F.S. Rosenthal, The size distribution of droplets in the exhaled breath of healthy human subjects, J. Aerosol Med. 10 (1997) 105–116.

[231] H. Yu, L. Xu, P. Wang, Solid phase microextraction for analysis of alkanes and aromatic hydrocarbons in human breath, J. Chromatogr. B. 826 (2005) 69–74. https://doi.org/10.1016/j.jchromb.2005.08.013.

[232] L.I.B. Silva, A.C. Freitas, T.A.P. Rocha-Santos, M.E. Pereira, A.C. Duarte, Breath analysis by optical fiber sensor for the determination of exhaled organic compounds with a view to diagnostics, Talanta. 83 (2011) 1586–1594. https://doi.org/10.1016/j.talanta.2010.11.056.

[233] B. Buszewski, A. Ulanowska, T. Ligor, N. Denderz, A. Amann, Analysis of exhaled breath from smokers, passive smokers and non-smokers by solid-phase microextraction gas chromatography/mass spectrometry, Biomed. Chromatogr. 23 (2009) 551–556. https://doi.org/10.1002/bmc.1141.

[234] L.A. Wallace, Human exposure to volatile organic pollutants: implications for indoor air studies, Annu. Rev. Energy Environ. 26 (2001) 269–301.

[235] M. Alonso, J.M. Sanchez, Analytical challenges in breath analysis and its application to exposure monitoring, TrAC Trends Anal. Chem. 44 (2013) 78–89.

[236] L.C.A. Amorim, Z. de L. Cardeal, Breath air analysis and its use as a biomarker in biological monitoring of occupational and environmental exposure to chemical agents, J. Chromatogr. B. 853 (2007) 1–9.

[237] Y. Saito, I. Ueta, M. Ogawa, K. Jinno, Simultaneous derivatization/preconcentration of volatile aldehydes with a miniaturized fiber-packed sample preparation device designed for gas chromatographic analysis, Anal. Bioanal. Chem. 386 (2006) 725–732. https://doi.org/10.1007/s00216-006-0509-z.

[238] A. Ulanowska, T. Kowalkowski, E. Trawińska, B. Buszewski, The application of statistical methods using VOCs to identify patients with lung cancer, J. Breath Res. 5 (2011) 046008.

[239] V. Bessonneau, L. Mosqueron, A. Berrubé, G. Mukensturm, S. Buffet-Bataillon, J.-P. Gangneux, O. Thomas, VOC contamination in hospital, from stationary sampling of a large panel of compounds, in view of healthcare workers and patients exposure assessment, PloS One. 8 (2013) e55535.

[240] R. Mukhopadhyay, Don’t waste your breath, Anal. Chem. (2004) 273A-276A.

[241] G.B. Hanna, P.R. Boshier, S.R. Markar, A. Romano, Accuracy and methodologic challenges of volatile organic compound–based exhaled breath tests for cancer diagnosis: a systematic review and meta-analysis, JAMA Oncol. 5 (2019) e182815–e182815.

[242] N. Grob, M. Aytekin, R. Dweik, Biomarkers in exhaled breath condensate: a review of collection, processing and analysis, J. Breath Res. 2 (2008) 037004.

[243] Z. Jia, A. Patra, V.K. Kutty, T. Venkatesan, Critical review of volatile organic compound analysis in breath and in vitro cell culture for detection of lung cancer, Metabolites. 9 (2019) 52.

[244] A. Amann, M. Corradi, P. Mazzone, A. Mutti, Lung cancer biomarkers in exhaled breath, Expert Rev. Mol. Diagn. 11 (2011) 207–217.

[245] A.R. Allafchian, Z. Majidian, V. Ielbeigi, M. Tabrizchi, A novel method for the determination of three volatile organic compounds in exhaled breath by solid-phase microextraction–ion mobility spectrometry, Anal. Bioanal. Chem. 408 (2016) 839–847.

[246] G. de Gennaro, S. Dragonieri, F. Longobardi, M. Musti, G. Stallone, L. Trizio, M. Tutino, Chemical characterization of exhaled breath to differentiate between patients with malignant plueral mesothelioma from subjects with similar professional asbestos exposure, Anal. Bioanal. Chem. 398 (2010) 3043–3050.

[247] X. Sun, K. Shao, T. Wang, Detection of volatile organic compounds (VOCs) from exhaled breath as noninvasive methods for cancer diagnosis, Anal. Bioanal. Chem. 408 (2016) 2759–2780.

[248] M. Zhou, R. Sharma, H. Zhu, Z. Li, J. Li, S. Wang, E. Bisco, J. Massey, A. Pennington, M. Sjoding, Rapid breath analysis for acute respiratory distress syndrome diagnostics using a portable two-dimensional gas chromatography device, Anal. Bioanal. Chem. 411 (2019) 6435–6447.

[249] M. Alonso, M. Castellanos, J.M. Sanchez, Evaluation of potential breath biomarkers for active smoking: assessment of smoking habits, Anal. Bioanal. Chem. 396 (2010) 2987–2995.

[250] National Research Council, Human exposure assessment for airborne pollutants: advances and opportunities, National Academies Press, 1991.

[251] World Health Organization, Biological monitoring of chemical exposure in the workplace: guidelines, World Health Organization, 1996.

[252] D.A. Sarigiannis, S.P. Karakitsios, A. Gotti, I.L. Liakos, A. Katsoyiannis, Exposure to major volatile organic compounds and carbonyls in European indoor environments and associated health risk, Environ. Int. 37 (2011) 743–765.

[253] A.P. Jones, Indoor air quality and health, Atmos. Environ. 33 (1999) 4535–4564.

[254] J.D. Pleil, M.A. Stiegel, J.R. Sobus, Breath biomarkers in environmental health science: exploring patterns in the human exposome, J. Breath Res. 5 (2011) 046005.

[255] T. Ligor, M. Ligor, A. Amann, C. Ager, M. Bachler, A. Dzien, B. Buszewski, The analysis of healthy volunteers' exhaled breath by the use of solid-phase microextraction and GC-MS, J. Breath Res. 2 (2008) 046006.

[256] M. Kusano, E. Mendez, K.G. Furton, Development of headspace SPME method for analysis of volatile organic compounds present in human biological specimens, Anal. Bioanal. Chem. 400 (2011) 1817–1826.

[257] M. Alonso, M. Castellanos, J. Martín, J.M. Sanchez, Capillary thermal desorption unit for near real-time analysis of VOCs at sub-trace levels. Application to the analysis of environmental air contamination and breath samples, J. Chromatogr. B. 877 (2009) 1472–1478.

[258] J. Reynolds, G.J. Blackburn, C. Guallar-Hoyas, V. Moll, V. Bocos-Bintintan, G. Kaur-Atwal, M.D. Howdle, E. Harry, L.J. Brown, C. Creaser, Detection of volatile organic compounds in breath using thermal desorption electrospray ionization-ion mobility-mass spectrometry, Anal. Chem. 82 (2010) 2139–2144.

[259] P.T. Scheepers, J. Konings, G. Demirel, E.O. Gaga, R. Anzion, P.G. Peer, T. Dogeroglu, S. Ornektekin, W. van Doorn, Determination of exposure to benzene, toluene and xylenes in Turkish primary school children by analysis of breath and by environmental passive sampling, Sci. Total Environ. 408 (2010) 4863–4870.

[260] Y. Li, H. Xu, Development of a novel graphene/polyaniline electrodeposited coating for on-line in-tube solid phase microextraction of aldehydes in human exhaled breath condensate, J. Chromatogr. A. 1395 (2015) 23–31.

[261] Z.-C. Yuan, W. Li, L. Wu, D. Huang, M. Wu, B. Hu, Solid-phase microextraction fiber in face mask for in vivo sampling and direct mass spectrometry analysis of exhaled breath aerosol, Anal. Chem. 92 (2020) 11543–11547.

[262] J. Zhou, Z.-A. Huang, U. Kumar, D.D. Chen, Review of recent developments in determining volatile organic compounds in exhaled breath as biomarkers for lung cancer diagnosis, Anal. Chim. Acta. 996 (2017) 1–9.

[263] A.J. Scott-Thomas, M. Syhre, P.K. Pattemore, M. Epton, R. Laing, J. Pearson, S.T. Chambers, 2-Aminoacetophenone as a potential breath biomarker for Pseudomonas aeruginosa in the cystic fibrosis lung, BMC Pulm. Med. 10 (2010) 1–10.

[264] C. Prado, P. Marín, J.F. Periago, Application of solid-phase microextraction and gas chromatography–mass spectrometry to the determination of volatile organic compounds in end-exhaled breath samples, J. Chromatogr. A. 1011 (2003) 125–134. https://doi.org/10.1016/S0021-9673(03)01103-8.

[265] I. Devai, R. DeLaune, Changes in reduced gaseous sulfur compounds collected in glass gas sampling bulbs, Anal. Lett. 27 (1994) 2403–2411.

[266] A. Bajtarevic, C. Ager, M. Pienz, M. Klieber, K. Schwarz, M. Ligor, T. Ligor, W. Filipiak, H. Denz, M. Fiegl, Noninvasive detection of lung cancer by analysis of exhaled breath, BMC Cancer. 9 (2009) 1–16.

[267] C. Deng, J. Zhang, X. Yu, W. Zhang, X. Zhang, Determination of acetone in human breath by gas chromatography–mass spectrometry and solid-phase microextraction with on-fiber derivatization, J. Chromatogr. B. 810 (2004) 269–275. https://doi.org/10.1016/j.jchromb.2004.08.013.

[268] L.C.A. Amorim, J.P. Carneiro, Z.L. Cardeal, An optimized method for determination of benzene in exhaled air by gas chromatography–mass spectrometry using solid phase microextraction as a sampling technique, J. Chromatogr. B. 865 (2008) 141–146. https://doi.org/10.1016/j.jchromb.2008.02.023.

[269] K. Apte, S. Salvi, Household air pollution and its effects on health, F1000Research. 5 (2016).

[270] J.J. West, A. Cohen, F. Dentener, B. Brunekreef, T. Zhu, B. Armstrong, M.L. Bell, M. Brauer, G. Carmichael, D.L. Costa, D.W. Dockery, M. Kleeman, M. Krzyzanowski, N. Künzli, C. Liousse, S.-C.C. Lung, R.V. Martin, U. Pöschl, C.A. Pope, J.M. Roberts, A.G. Russell, C. Wiedinmyer, "What We Breathe Impacts Our Health: Improving Understanding of the Link between Air Pollution and Health," Environ. Sci. Technol. 50 (2016) 4895–4904. https://doi.org/10.1021/acs.est.5b03827.

[271] A.H. Goldstein, W.W. Nazaroff, C.J. Weschler, J. Williams, How Do Indoor Environments Affect Air Pollution Exposure?, Environ. Sci. Technol. 55 (2021) 100–108. https://doi.org/10.1021/acs.est.0c05727.

[272] Z. Sun, D. Zhu, Exposure to outdoor air pollution and its human health outcomes: A scoping review, PloS One. 14 (2019) e0216550.

[273] P. Forbes, Monitoring of air pollutants: sampling, sample preparation and analytical techniques, Elsevier, 2015.

[274] I. Manisalidis, E. Stavropoulou, A. Stavropoulos, E. Bezirtzoglou, Environmental and health impacts of air pollution: a review, Front. Public Health. 8 (2020) 14.

[275] M. Kampa, E. Castanas, Human health effects of air pollution, Environ. Pollut. 151 (2008) 362–367.

[276] T. Schikowski, Indoor and Outdoor Pollution as Risk Factor for Allergic Diseases of the Skin and Lungs, (2021).

[277] A.C. Lewis, The changing face of urban air pollution, Science. 359 (2018) 744–745.

[278] B. Wei, D.M. Smith, M.J. Travers, R.J. O'Connor, M.L. Goniewicz, A.J. Hyland, Secondhand marijuana smoke (SHMS): Exposure occurrence, biological analysis and potential health effects, in: Adv. Mol. Toxicol., Elsevier, 2019: pp. 1–30.

[279] R. Ballesteros, Á. Ramos, J. Sánchez-Valdepeñas, Particle-bound PAH emissions from a waste glycerine-derived fuel blend in a typical automotive diesel engine, J. Energy Inst. 93 (2020) 1970–1977. https://doi.org/10.1016/j.joei.2020.04.012.

[280] S. Masri, L. Li, A. Dang, J.H. Chung, J.-C. Chen, Z.-H. (Tina) Fan, J. Wu, Source characterization and exposure modeling of gas-phase polycyclic aromatic hydrocarbon (PAH) concentrations in Southern California, Atmos. Environ. 177 (2018) 175–186. https://doi.org/10.1016/j.atmosenv.2018.01.014.

[281] R.R. dos Santos, Z. de L. Cardeal, H.C. Menezes, Phase distribution of polycyclic aromatic hydrocarbons and their oxygenated and nitrated derivatives in the ambient air of a Brazilian urban area☆, Chemosphere. 250 (2020) 126223. https://doi.org/10.1016/j.chemosphere.2020.126223.

[282] H. Lan, K. Hartonen, M.-L. Riekkola, Miniaturised air sampling techniques for analysis of volatile organic compounds in air, TrAC Trends Anal. Chem. 126 (2020) 115873. https://doi.org/10.1016/j.trac.2020.115873.

[283] V. Jalili, A. Barkhordari, A. Ghiasvand, Solid-phase microextraction technique for sampling and preconcentration of polycyclic aromatic hydrocarbons: A review, Microchem. J. 157 (2020) 104967.

[284] J. Cao, J. Xiong, L. Wang, Y. Xu, Y. Zhang, Transient Method for Determining Indoor Chemical Concentrations Based on SPME: Model Development and Calibration, Environ. Sci. Technol. 50 (2016) 9452–9459. https://doi.org/10.1021/acs.est.6b01328.

[285] D.W. Potter, Janusz. Pawliszyn, Rapid determination of polyaromatic hydrocarbons and polychlorinated biphenyls in water using solid-phase microextraction and GC/MS, Environ. Sci. Technol. 28 (1994) 298–305. https://doi.org/10.1021/es00051a017.

[286] National Institute for Occupational Safety and Health, Polynuclear Aromatic Hydrocarbons by GC-Method 5515, Man. Anal. Methods. (1994).

[287] P.M. Nowak, R. Wietecha-Posłuszny, J. Pawliszyn, White Analytical Chemistry: An approach to reconcile the principles of Green Analytical Chemistry and functionality, TrAC Trends Anal. Chem. 138 (2021) 116223. https://doi.org/10.1016/j.trac.2021.116223.

[288] F. Pena-Pereira, W. Wojnowski, M. Tobiszewski, AGREE—Analytical GREEnness Metric Approach and Software, Anal. Chem. 92 (2020) 10076–10082. https://doi.org/10.1021/acs.analchem.0c01887.

[289] Health Canada, Tobacco reporting regulations, (2000).

[290] D.O.V. Organic, S.-P. Canisters, Compendium of Methods for the Determination of Toxic Organic Compounds in Ambient Air Second Edition, (1999).